ACTA SILVATICA
&
LIGNARIA
HUNGARICA

Acta Silvatica & Lignaria Hungarica

An International Journal in Forest, Wood and Environmental Sciences

Volume 10, Nr. 1
Volume 10, Nr. 2
2014

UNIVERSITY OF WEST HUNGARY PRESS

ACTA SILVATICA ET LIGNARIA HUNGARICA
AN INTERNATIONAL JOURNAL IN FOREST, WOOD AND ENVIRONMENTAL SCIENCES
issued by the Forestry Commission of the Hungarian Academy of Sciences

The journal is financially supported by the
Hungarian Academy of Sciences (HAS),
Faculty of Forestry, University of West Hungary (FF-UWH),
Simonyi Karoly Faculty of Engineering, Wood Sciences and Applied Arts, University of West Hungary (SKF-UWH),
National Agricultural Research and Innovation Center, Forest Research Institute (NARIC-FRI),
Sopron Scientists' Society of the Hungarian Academy of Sciences (SSS).

HU ISSN 1786-691X (Print)
HU ISSN 1787-064X (Online)

Manuscripts and editorial correspondence should be addressed to
MAGDOLNA STARK, ASLH EDITORIAL OFFICE
UNIVERSITY OF WEST HUNGARY,
PF. 132, H-9401 SOPRON, HUNGARY

Phone: +36 99 518 122
Fax: +36 99 329 911
E-mail: aslh@nyme.hu
Information and electronic edition: http://aslh.nyme.hu

The journal is indexed in the CAB ABSTRACTS database of CAB International; by SCOPUS, Elsevier's Bibliographic Database, by EBSCOhost database and by De Gruyter Open Sp. z. o. o., Warsaw

Published by UNIVERSITY OF WEST HUNGARY PRESS,
BAJCSY-ZS. U. 4., H-9400 SOPRON, HUNGARY
Cover design by ANDREA KLAUSZ
Printed by LŐVÉR-PRINT KFT., SOPRON

ACTA SILVATICA ET LIGNARIA HUNGARICA

Vol. 10, Nr. 1

Contents

ACTA SILVATICA ET LIGNARIA HUNGARICA

Vol. 10, Nr. 2

Contents

ACTA SILVATICA ET LIGNARIA HUNGARICA

Vol. 10, Nr. 1

Tartalomjegyzék

Vol. 10, Nr. 2

DE GRUYTER OPEN DOI: 10.2478/aslh-2014-0001 Acta Silv. Lign. Hung., Vol. 10, Nr. 1 (2014) 9–21

Understory Development in an Oak Forest in Northern Hungary: the Subcanopy Layer

Tamás MISIK[a*] – Imre KÁRÁSZ[a] – Béla TÓTHMÉRÉSZ[b]

[a] Department of Environmental Science, Eszterházy Károly College, Eger, Hungary
[b] Department of Ecology, University of Debrecen, Debrecen, Hungary

Abstract – Structural changes in the shrub layer were analysed in a Hungarian oak forest after the oak decline pandemics. This paper focuses on the following questions: (1) which of the woody species tolerated better the forest conditions after oak decline? (2) What are the ecological factors that explain the successful response of woody species to changes in light and thermal conditions? In the monitoring plot, the structural condition of specimens only above 8.0 m was observed. After the appearance of oak decline some *Acer campestre*, *Cornus mas* and *Acer tataricum* specimens appeared that reached between 8.0-13.0 m in height. Significant differences were revealed between top canopy density and foliage cover of the subcanopy and between top canopy density and mean cover of field maple. The findings of the study indicate that the forest responded to oak decline with significant structural rearrangement in the shrub layer and that three woody species compensated for the remarkable foliage loss in the top canopy. These species formed a second crown layer directly below the canopy formed by oaks.

shrub community / woody species / *Acer campestre* L. / cover / dead oaks

Kivonat – A cserjeszint fejlődése Észak-Magyarországon egy tölgyes erdőben: az alsó lombkoronaszint. Egy magyarországi tölgyerdő cserjeszintjének a tölgypusztulás utáni strukturális változásait vizsgáltuk. Ez a dolgozat a következő kérdésekre fókuszál: (1) melyik fásszárú fajok reagáltak jobban a tölgyek pusztulását követően az erdő kondíciójára? (2) Milyen ökológiai tényezők magyarázhatják a fásszárú fajok sikeres válaszát a megváltozott fény- és hőviszonyokra? A monitoring területen a 8,0 m feletti egyedeknek a strukturális kondícióját vizsgáltuk. A tölgypusztulás kezdete után néhány *Acer campestre*, *Cornus mas* és *Acer tataricum* egyed jelent meg elérve a 8,0-13,0 m közötti magasságot. Szignifikáns eltérést találtunk a felső lombkorona denzitása és az alsó lombkorona borítása, illetve a felső lombkorona denzitása és a mezei juhar átlagos lombvetülete között. A kutatásunk megállapításai azt jelzik, hogy az erdő a cserjeszint jelentős strukturális átrendeződésével válaszolt a tölgypusztulásra, és három fásszárú faj pótolta a felső lombkorona jelentős lombveszteségét. Ezek a fajok második lombkoronaszintet hoztak létre közvetlenül a tölgyek alkotta lombkorona alatt.

cserjeközösség / fásszárú fajok / *Acer campestre* L. / borítás / kipusztult tölgyek

* Corresponding author: misiktom@gmail.com; H-3300 EGER, Leányka utca 6.

1 INTRODUCTION

Biotic factors such as climate change and extreme weather conditions (Bolte et al. 2010, Kotroczó et al. 2012), pathogens such as root diseases (Jung et al. 2000, Szabó et al. 2007), and insect gradations (Csóka 1998, Bruhn et al. 2000, Moraal – Hilszczanski 2000) and abiotic factors, such as human influence, climate change, fires and air pollution (Mészáros et al. 1993, Signell et al. 2005, Kabrick et al. 2008) lead to a modified functioning of the whole forest ecosystem and may lead to forest decline. Tree decline has heavily affected oak species, and especially *Quercus petraea* Matt. L. (sessile oak) trees in European countries (Freer-Smith – Read 1995, Thomas – Büttner 1998). Oak death has been described as a widespread and complex phenomenon (Klein – Perkins 1987, Bruck – Robarge 1988). An increase in the death of oak forests has been observed in many regions of Hungary since 1978 (Igmándy 1987). In 1976, oak decline began in Slovakia, found its way to former Yugoslavia by 1979, and finally reached Austria in 1984 (Hämmerli – Stadler 1989). Many papers have reported that increased oak mortality is leading to changes in forest dynamics (Moraal – Hilszczanski 2000, Woodall et al. 2005).

Relatively few studies deal with shrub communities and shrub layer dynamics after oak death and the relationship between the tree and shrub layer (Légaré et al. 2002). Shrub dynamics is linked to the ecological functioning of forest ecosystems (McKenzie et al. 2000, Brosofske et al. 2001, Augusto et al. 2003). The shrub layer is affected by light availability when the canopy is closed (Légaré et al. 2002), leading to negative correlations of shrub layer species richness and/or cover with tree basal area (Hutchinson et al. 1999). Shrubs may provide important indications of site quality, overstory regeneration patterns and conservation status (Hutchinson et al. 1999). Tree species diversity had a positive relationship to shrub cover because a diverse overstory generally created more canopy gaps (Gazol – Ibáñez 2009). The tree layer structure strongly influences shrub species cover by altering microsites, resources and environmental conditions (Oliver – Larson 1996, Stone – Wolfe 1996). The variability in below tree layer light availability and canopy openness strongly influence individual performance and community composition of shrub and herb plants in temperate forest (Hughes – Fahey 1991, Goldblum 1997).

Most papers only used changes in structural conditions in the tree layer to monitor the ecological process in the forest community after tree decline (Bussotti – Ferretti 1998, Brown – Allen-Diaz 2009). The studies of shrub species performed have mostly focused on the static population structure (age and size structures); these parameters have been described by a negative exponential model (Tappeiner et al. 1991, Stalter *et al*. 1997). Other studies have focused on the cover and diversity of shrubs (e.g. Kerns – Ohmann 2004, Gracia et al. 2007). In this paper we used frequency, size and cover variables complemented with basal area to obtain a more complete picture of shrub layer dynamics.

The species composition of the canopy layer was stable until 1979 and the healthy *Q. petraea* and *Quercus cerris* L. (Turkey oak) also remained constant in the mixed-species forest stand (*Quercetum petraeae-cerris* Soó 1963) of Síkfőkút. Serious oak decline was first reported in 1979–80 and by 2012, 62.4% of the oaks had died; this decline resulted in an opening of the canopy. The decline affected both forest stands; however it affected sessile oak considerably more. The mortality rate of Turkey oak trunks was lower, only 16% over the last three decades (Kotroczó et al. 2007). The canopy species composition has changed little, only some trees of *Tilia cordata* Mill. and *Carpinus betulus* L. lived as new codominant species on the site. The regeneration of oak species is rather poor and the cover of the herb layer is low. The possible biotic and abiotic factors of oak decline and the effect of decline on the structural condition of the forest community on the Síkfőkút plot have also been studied in many papers (e.g. Jakucs 1985, 1988). Jakucs'results (1988) show that the soil acidification

induced by the disappearance of mycorrhizal fungi and the air pollutants that promote water and nutrient absorption, have been evaluated and identified as primary causes of deciduous forests' decline. *Q. petraea* suffered a more drastic decline than *Q. cerris* trees in Hungarian woodlands. Later this theory was bought into question by further research (in particular, drought impact). The results of Mészáros et al. (2011) suggest that magnitude of tree water deficit variation (ΔW) was always smaller in *Q. cerris* than in *Q. petraea*. In contrast, *Q. cerris* trees exhibited larger daytime averages and maxima of sap flow density. Béres et al. (1998) state that the bright – i.e. water filled - outer layer can be considered as the active new xylem. This layer is considerably thicker in the case of *Q. cerris* than in the case of *Q. petraea*. The inner compartment of *Q. petraea* contains a very small amount of water and there is no difference between heartwood and sapwood. On the other hand, *Q. cerris* is clearly different, with higher density heartwood and low density sapwood compartments.

Specifically, we address the following questions: (1) What are the most important structural changes in the forest interior after serious oak decline? (2) What kind of woody species in the understory have the most successful response to oak death? (3) What are the ecological factors that explain the successful response of the woody species to changes in light and thermal conditions? (4) Can the forest make up for the significant losses of leaf canopy by means of new structural foliage formation? (5) Finally, what is the interaction between the woody species of the subcanopy layer?

2 MATERIAL AND METHODS

2.1 Study site

The 27 ha reserve research site is located in the Bükk Mountains of northeast Hungary (47°55' N, 20°46' E) at a distance of 6 km from the city of Eger at an altitude of 320–340 m a.s.l.. The site was established in 1972 by Jakucs (1985) for the long-term study of forest ecosystems. Mean annual temperature is 9.9 °C and mean annual precipitation ranges typically from 500 to 600 mm. The mean annual temperature and precipitation are based on measurements at the meteorological recording tower of the site. Description of the geographic, climatic, soil conditions and vegetation of the forest was undertaken in detail by Jakucs (1985, 1988). The most common forest association in this region is *Quercetum petraeae-cerris* with a dominant canopy of *Q. petraea* and *Q. cerris*. Both oak species are important dominant native deciduous tree species of the Hungarian natural woodlands. It was detected on subcanopy layer of the most sessile oak-Turkey oak stand in Hungary with *Acer campestre* L., *Sorbus torminalis* L. Crantz, *Pyrus pyraster* L. Burgsd, *Ulmus procera* Salisb. and *T. cordata* species. Other codominant tree species of the study site included *Ca. betulus*, *Prunus avium* L. and *T. cordata*. The plot under study is made up of evenly-aged trees, is at least 95–100 years old temperate deciduous forest and has not been harvested for more than 50 years.

2.2 Sampling and data analysis

Conditions in the shrub layer were monitored at regular intervals on a 48 m × 48 m plot at the research site, which was subdivided into 144 permanent subplots, each 4 m × 4 m in size. The investigations were performed during the growing seasons. Monitoring activities started in 1972 and repeated shrub layer inventories took place in 1982, 1988, 1993, 1997, 2002, 2007 and 2012. In 2012 three 10 m × 10 m new fixed plots were selected for vegetation sampling to confirm the detected shrub layer development of the site. Orientation of these extra plots was randomly determined. These plots were subdivided into 16 2.5 m × 2.5 m subplots to

determine species occurrence of the understory. Canopy trees were classified as sessile oak and Turkey-oak tree species > 13.0 m in height and ≥ 10.0 cm in diameter at breast height (DBH). Trees were classified as subcanopy trees when between 8.0–13.0 m in height.

In each of the subplots and new plots the following measurements were carried out: species composition, frequency (occurrence % in subplots), species density, height, diameter, basal area and cover of each subcanopy species. The species' density was also determined in plots and the data was extrapolated for one hectare. In stand No. 18 (1982) – 69 (2012) individuals of subcanopy species were sampled in the last decades and then subjected to mean height, mean diameter and mean cover analysis. Plant height was measured with a scaled pole and shoot diameter at 5.0 cm above the soil surface in two directions (if the shape of the shoot of shrub individuals was not regular) with a digital caliper in a field study and the measurement results were averaged.

Within each plot the stand basal area (BA, m^2 ha^{-1}) of subcanopy woody species was calculated from the measured diameters of all subcanopy specimens. Location and percentage cover of the subcanopy trees and high shrubs was also mapped together every 4 to 5 years, beginning in 1972. Many studies included the method of creating a foliage map from the shrubby vegetation (e.g. Jakucs 1985). The foliage map was built in a GIS environment. Based on the digitized map we estimated the foliage area of subcanopy trees and shrub individuals with the Spatial Analysis Tools - Calculate Area function of the GIS. The correlation analysis was used to determine and quantify the connection between stand density and subcanopy layer condition on the monitoring plot from 1982, by using the following structure variables as dependent variables: (1) frequency (2) mean height and diameter (3) mean cover (4) mean and total basal area of subcanopy species. One-way ANOVA with the Tukey's HSD test was used as a post-hoc test if necessary to determine the significant differences among subcanopy species by occurrence frequencies, mean cover and mean basal area. Statistical analysis was performed using PAST statistical software and significant differences for all statistical tests were evaluated at the level of $P \leq 0.05$ or $P \leq 0.01$.

3 RESULTS

Once oak decline had set in, 3 native woody species were identified across the entire study area from 1982 in the new subcanopy layer; *A. campestre* (field maple), *Cornus mas* L. (European cornel) and *Acer tataricum* L. (Tatar maple) were present as subcanopy species in the sample site. In the new plots only some *A. campestre* individuals and single *C. mas* composed this layer. The average number of subcanopy woody specimens per one hectare has varied from 73 to 238 over the past 2 decades. The total top canopy density decreased from 651 to 305 trees ha^{-1}. In contrast, *A. campestre* increased in density (from 56 to 204 specimen's ha^{-1}) and density of *A. tataricum* and *C. mas* did not change in importance (*Figure 1*).

The correlation analysis did show a non-significant association between living oak tree density and occurrence frequency of the subcanopy tree species ($r = 0.75$, $P > 0.05$). The species with the highest occurrence in subplots was *A. campestre* with rates of 6.3–25.7% (*Table 1*). A significant relationship between oak tree density and *A. campestre* occurrence frequency ($r = 0.77$, $P \leq 0.05$) was observed between 1982 and 2012, this relationship was not significant in the cases of *A. tataricum* and *C. mas* ($r = 0.21$ and 0.47, $P > 0.05$) between 1982 and 2012 was observed. The one-way ANOVA indicated significant differences among occurrence frequencies of woody species (*Table 2*).

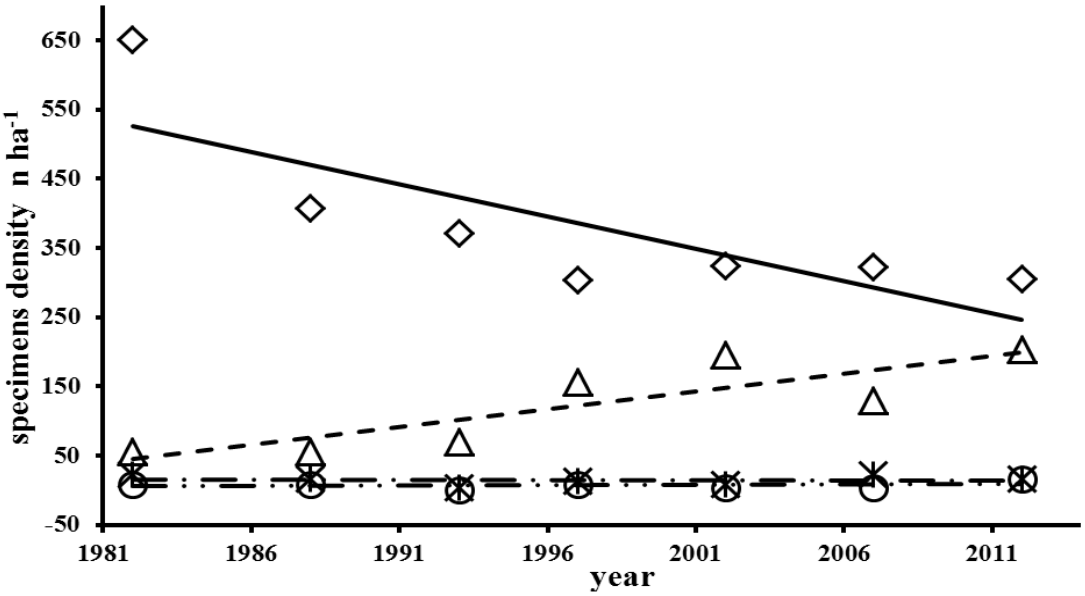

Figure 1. Density trend of oak canopy species and subcanopy woody species for the period from 1982 to 2012 on the monitoring plot.
Notation: ———, deltoid – living oak trees; – – –, triangle – A. campestre; – · · –, circle – A. tataricum; – · –, asterisk – C. mas

Table 1. Frequency condition of the subcanopy woody species on the monitoring and new plots over the period 1982–2012 (N = 144 subplots; N = 48 subplots)*

subcanopy species	occurrence frequency (%) in subplots							
	1982	1988	1993	1997	2002	2007	2012	2012*
A. campestre								
8–13 m	6.3	6.3	12.5	23.6	25.7	20.1	25.0	27.8
> 13 m	0.0	0.0	2.1	0.7	2.1	13.2	7.6	0.0
A. tataricum								
8–13 m	1.4	1.4	0.0	2.1	2.1	0.7	2.8	0.0
C. mas								
8–13 m	1.4	1.4	0.7	4.2	1.4	3.5	2.8	5.6

*mean frequencies of new plots

Frequency distribution of *A. campestre* and *C. mas* woody species between 1993 and 2012 with height and diameter classes is shown in *Figure 2*. Most stems belonged to the 8.0-10.0 m height and 11.6–16.6 cm diameter classes, which contained almost 75% and 55% of these woody species. The height and diameter frequency distribution of subcanopy species had a corresponding two-peak-pattern in 2012 with a first peak at 901–1000 cm height and 11.6–16.6 cm diameter and a second at 800–900 cm and 8.1–11.5 cm class.

Table 2. Results of one-way ANOVA and Tukey's HSD test (p = significance level, F = variance of the group means) for mean basal area, occurrence frequencies and mean cover of dominant woody species on the monitoring plot. Significant differences are shown in bold

	p / *F* values		
	A. campestre	*A. tataricum*	*C. mas*
Mean basal area			
A. campestre	1	–	–
A. tataricum	**0.0204** / 7.1560	1	–
C. mas	0.0648 / 4.1370	0.3451 / 0.9664	1
Occurrence frequencies			
A. campestre	1	–	–
A. tataricum	**0.0006** / 22.650	1	–
C. mas	**0.0008** / 20.450	0.2730 / 1.3210	1
Mean cover			
A. campestre	1	–	–
A. tataricum	0.8827 / 0.0230	1	–
C. mas	0.3033 / 1.1780	0.4737 / 0.5547	1

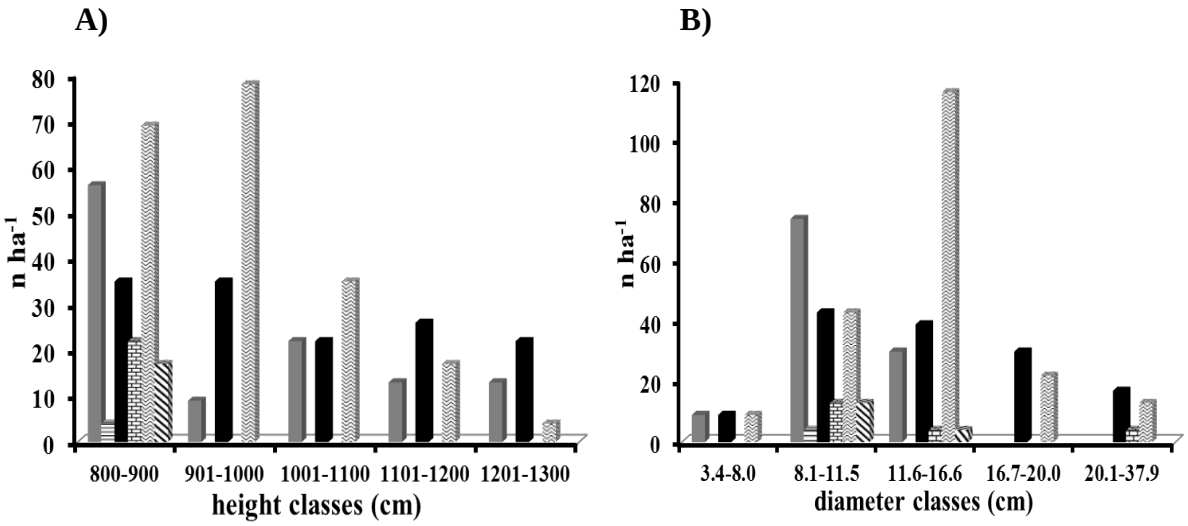

Figure 2. Frequency distribution of A. campestre and C. mas woody species in 1993, 2007 and 2012 considering height (A) and diameter (B) classes on the monitoring plot. Notation: dark gray - A. campestre, 1993; black - A. campestre, 2007; wavy - A. campestre, 2012; ruled - C. mas, 1993; brick - C. mas, 2007; slant line - C. mas, 2012 (N = 499)

Three woody species responded positively to foliage gaps. Box-plots showed the height and diameter changes and distribution of subcanopy species over the period 1982–2012. The median values of *A. campestre* increased considerably, but the minimum and maximum values of height decreased in the last measuring. The *A. tataricum* and *C. mas* boxes did not show unambiguous tendency in height and diameter distribution, but the height decreased considerably between 1982 and 1997. The correlation analysis recorded that after large-scale oak decline, the mean height and shoot diameter of some woody species had increased remarkably but not significantly during the last surveys (height: *A. campestre* $r = 0.78$; *A. tataricum* $r = 0.28$; $P > 0.05$) (diameter: *A. campestre* $r = 0.79$; *A. tataricum* $r = 0.82$; *C. mas* $r = 0.67$; $P > 0.05$). A highly significant relationship between oak tree density and mean height of *C. mas* ($r = 0.99$, $P \leq 0.001$) was confirmed (*Figure 4*).

Stand density and mean and total basal area of subcanopy species were found to have a negative and non-significant relationship (r = 0.43–0.65, $P > 0.05$). The basal area estimates by woody species show that the total basal area of subcanopy layer varied between 0.33 and 2.75 m^2. The mean basal area of woody species increased continually from 1982 and varied between 0.24^{-2} and 1.84^{-2} m^2 on the monitoring plot. The total basal area of woody species increased after the commencement of oak decline and the greatest values were recorded by maple species in 2012 and by *C. mas* in 2007 (*Table 4*). The ANOVA analysis indicated significant differences among the mean shoot's basal area of maple species (*Table 2*).

We found a negative correlation between top canopy density and total foliage cover of the subcanopy layer (r = 0.95, $P \leq 0.05$). The GIS analysis confirmed that after serious oak death the percentage cover of subcanopy layer increased considerably and was at its maximum in 1997 with 969.9 m^2. Mean cover increment of *A. campestre* negatively correlated to oak tree density (r = 0.85, $P \leq 0.05$). Mean cover of *C. mas* (r = 0.71, $P > 0.05$) and *A. tataricum* (r = 0.54, $P > 0.05$) specimens increased, but non-significantly after tree decline. This value increased continually with European cornel individuals, but the mean cover of maple species fluctuated between 11.2 and 18.3 m^2 between 1993 and 2007 (*Table 3*). The ANOVA indicated non-significant differences among mean cover of woody species (*Table 2*).

Table 3. Relationship between oak tree density and mean cover of subcanopy woody species and total foliage cover of subcanopy layer on the monitoring plot over the period 1982–2007

year	oak tree density (n ha^{-1})	mean cover (m^2) ± SD.			total foliage cover of subcanopy layer (m^2)
		A. campestre	*A. tataricum*	*C. mas*	
1982	651	4.8 ± 1.2	3.4 ± 0.8	3.6 ± 0.9	81.2
1988	408	7.8 ± 8.8	4.5 ± 4.0	8.5 ± 7.0	150.0
1993	372	11.7 ± 3.4	–	10.4 ± 0.0*	313.8
1997	304	18.3 ± 6.1	11.2 ± 1.6	19.0 ± 2.2	969.9
2002	324	12.0 ± 2.9	18.2 ± 0.0*	27.0 ± 1.9	612.4
2007	323	14.6 ± 2.8	31.7 ± 0.0*	34.8 ± 6.0	671.6

*on the basis of a single individual

Table 4. Relationship between oak tree density and mean and total basal area of subcanopy woody species on the monitoring plot over the period 1982–2012

year	oak tree density (n ha^{-1})	mean basal area (m^2) ± SD. / total basal area (m^2)		
		A. campestre	*A. tataricum*	*C. mas*
1982	651	$4.8^{-3} \pm 1.9^{-3} / 0.07$	$2.5^{-3} \pm 6.0^{-4} / 4.9^{-3}$	$2.4^{-3} \pm 8.8^{-4} / 4.8^{-3}$
1988	408	$5.2^{-3} \pm 2.0^{-3} / 0.11$	$2.3^{-3} \pm 1.1^{-3} / 6.1^{-3}$	$3.8^{-3} \pm 1.7^{-3} / 4.1^{-3}$
1993	372	$5.9^{-3} \pm 2.2^{-3} / 0.15$	–	$4.1^{-3} \pm 0.0 / 4.1^{-3}$*
1997	304	$8.8^{-3} \pm 4.0^{-3} / 0.40$	$3.8^{-3} \pm 5.6^{-4} / 1.1^{-2}$	$4.5^{-3} \pm 2.6^{-3} / 2.7^{-2}$
2002	324	$1.3^{-2} \pm 1.2^{-2} / 0.60$	$5.6^{-3} \pm 3.0^{-3} / 1.7^{-2}$	$5.1^{-3} \pm 2.1^{-3} / 1.5^{-2}$
2007	323	$1.2^{-2} \pm 7.6^{-3} / 0.39$	$6.1^{-3} \pm 0.0 / 6.1^{-3}$*	$1.0^{-2} \pm 8.7^{-3} / 5.1^{-2}$
2012	305	$1.8^{-2} \pm 1.8^{-2} / 0.87$	$7.6^{-3} \pm 5.2^{-3} / 3.1^{-2}$	$7.4^{-3} \pm 2.3^{-3} / 3.0^{-2}$

*on the basis of a single individual

4 DISCUSSION

Three types of factors should be examined as possible causes of the shrub layer dynamics observed: (1) Changes in the light and thermal regime resulting from changes in canopy structure, particularly gaps; (2) changes in the species composition and density of canopy trees; and (3) other environmental factors such as changes in forest management or human activities. The last factor can be excluded, because the forest community has not been disturbed by forest management for more than 50 years. The second possible factor is only partially relevant to the study site; a significant proportion of sessile oak trunks ($P \leq 0.01$) died on the site and the percentage foliage cover of the tree layer decreased. Despite this ecological process new and/or invasive species could not establish themselves in the oak forest, because some native species of the understory would respond positively to various sizes of canopy gaps. So our study is in agreement with Dunn (1986) who found that the species composition of the shrub layer to density of dead *Ulmus americana* L. trees was not significant in lowland forests of the USA.

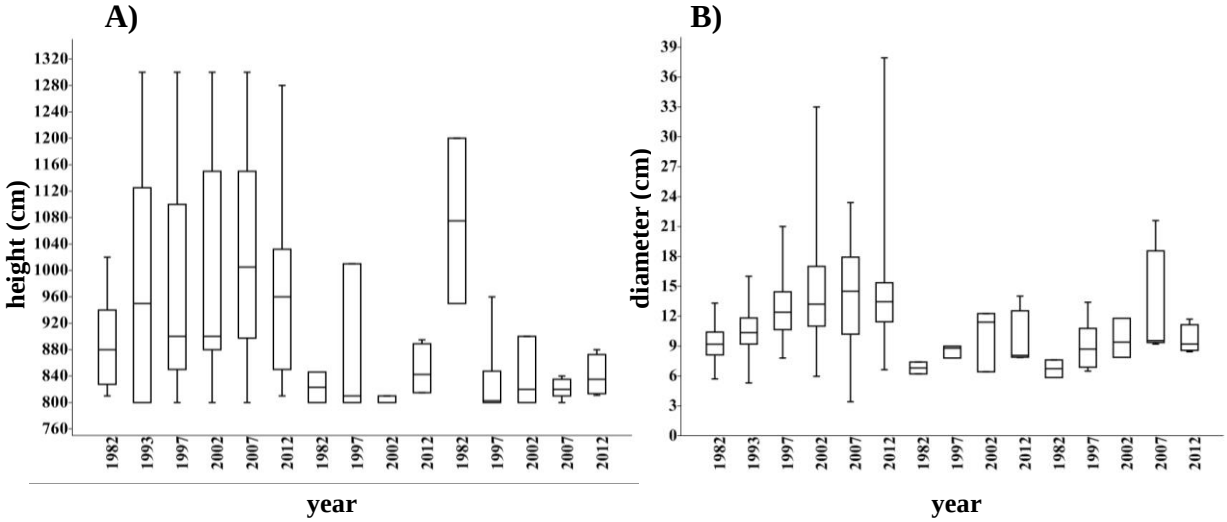

Figure 3. Statistical summary of height (A) and diameter (B) changes of subcanopy woody species (sequentially: A. campestre, A. tataricum and C. mas) on the monitoring plot over the period 1982–2012. Boxes shown are the 25–75% percentile, median, minimum and maximum values (N = 250). Includes only single individual of A. tataricum in 2007 and C. mas in 1993

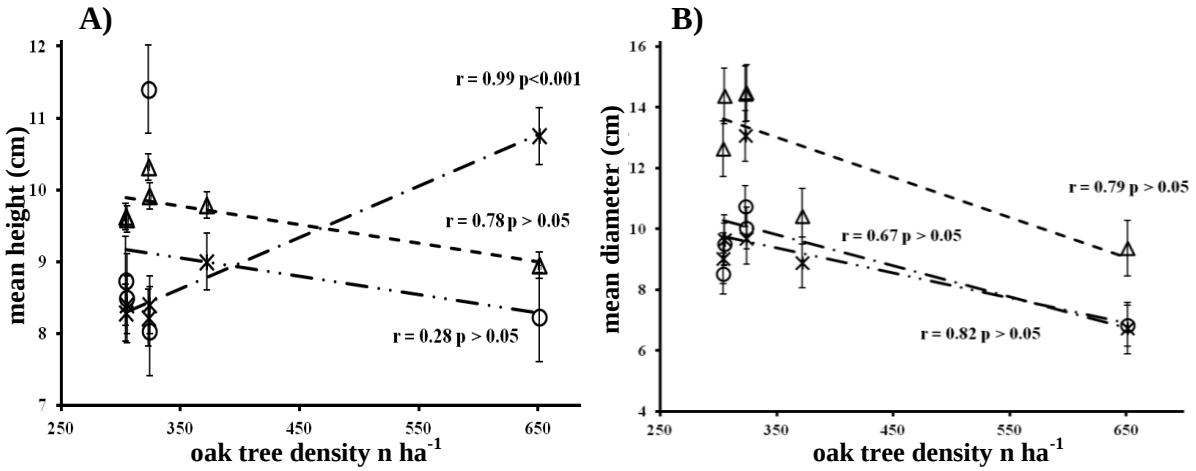

Figure 4. Correlation relationship between oak tree density and average height (A) and diameter (B) ± SE. changes of subcanopy woody species on the monitoring plot over the period 1982–2012 (N = 250).

Notation: – – –, triangle – A. campestre; – · · –, circle – A. tataricum; – · –, asterisk – C. mas

A significant association was not detected between oak canopy density and the density of the subcanopy layer ($P > 0.05$) on the site (*Figure 1*). A non-significant increase in the density of *A. campestre* in the new layer and in the overstory after the oak decline ($P > 0.05$) was recorded, because increasing numbers of *A. campestre* grew out from the subcanopy layer from 1993. This process is coincident with the height increment of the maple specimens (*Figure 4*). The species occurrence frequencies in the subcanopy layer did not change significantly over the past 3 decades. In the USA the total shrub density showed a relationship to dead elm density. The density of shrub layer increased significantly and predictably, when dead elm density was greater than 5 stems/ha (Dunn 1986). Observations from mature *Quercus*-dominated forests throughout the eastern United States suggest that many of these forests are undergoing significant compositional transformation. *Quercus* spp. are being replaced in the understory by species such as *Acer rubrum* L. and *A. saccharum* Marshall, and these mesophytic, relatively shade-tolerant species are likely to become canopy dominants if current trends continue (Shotola et al. 1992, Galbraith – Martin 2005, Nowacki – Abrams 2008). On the other hand, according to Röhrig and Ulrich (1991) *A. campestre* is a relatively drought tolerant species. Oak species cannot successfully compete with these species (McDonald et al. 2002, Zaczek et al. 2002). Our results support these statements, because in Síkfőkút maple specimens showed an increase in size and cover, and a low regeneration potential of oaks due to drought and detected shading effects (*Figure 3, 4*, *Table 3, 4*). A considerable shifting to the larger height and diameter classes in the subcanopy layer under 15 years has been noted from the monitoring (*Figure 2*). In the canopy gaps these species grew up from the shrub layer into the new foliage layer 8.0–13.0 m in height, below the canopy layer of the sessile oak and Turkey oak species. High drought tolerance of *A. campestre* confirms the results of Kotroczó et al. (2012) in Síkfőkút. The mean leaf-litter production of this species was nearly 110.0 kg ha^{-1} between 1972–76 and was five times higher between 2003–10, these differences are significant ($P = 0.001$).This can be explained by the fact that *A. campestre* formerly occurred in the shrub layer, while presently it forms a part of the canopy-layer, where it has become the second most common tree species, representing 28.2% of the total number of trees in the canopy.

We found a negative correlation between oak tree density and total cover of the subcanopy layer ($P \leq 0.05$). A similar connection between top canopy density and mean cover of the species in the subcanopy was detected (*Table 3*). In 2002 we found an important recidivation in total cover of the subcanopy layer, but the individual density of this layer increased further. The reason being that the mean cover of *A. campestre* individuals decreased by 26.0% compared to 1997. Results from different forest types show that the canopy openings modify light, thermal and moisture conditions (Nakashizuka 1985, Holeksa 2003). After large-scale oak decline, different sized gaps were formed in the foliage of the tree layer in the sample site and the shrub species in these gaps could be increased considerably due to the higher light levels. Concerning trees cover its purported influence on the composition of understory species by through it controlling ecosystem processes such as light transmittance and nutrient cycling (Légaré et al. 2001); we cannot support such a statement with our results. The decreasing total top canopy cover led to changes in the structural condition of the shrub layer, but consistent and directional changes in the shrub species composition has not been reported. The dense tree layer can inhibit regeneration of trees and high shrubs (Tappeiner et al. 1991, Stein 1995, Knowe et al. 1997). At our site, oak decline decreased top canopy cover and led to the notable height growth of three species from the shrub layer; this phenomenon is called the "Oskar"-strategy (Silvertown 1982). The *Acer* species is a genus that displays this characteristic in such circumstances. The results, from a mixed forest stand in France, of Caquet et al. (2010) suggest that the new trees in the gaps at the end of the regeneration phase were dominated by *Fagus sylvatica* L. and *Acer pseudoplatanus* L. Two other species,

A. campestre and *Acer platanoides* L., are present in high numbers in the seedling bank, but are totally absent at the end of the regeneration phase in the gaps. 3 years later canopy opening seedlings in the gaps displayed significantly greater diameter and height than those under canopy in *Acer* sp. and *F. sylvatica* L. species ($P < 0.001$). All maple and European beech species responded positively and rapidly to canopy openings. Diameter increment was similar across four species, and height increment was greater for *A. platanoides* and for *A. pseudoplatanus* seedlings (Caquet 2010).

Tree decline substantially increases the resources (e.g. light and nutrients) available to other organisms (naturally to shrub species) in the ecosystem. The amount of resources made available depends on the scale of the oak decline (Franklin et al. 1987). At our site 493 specimens of oak trunks died in the last decades so initially this process guaranteed suitable light for the growing of shrub specimens. In the gaps some woody species (especially *A. campestre*) grew quickly, therefore they were the limiting factor for the natural regeneration and growing of other shrub and oak species by restricting the light supply in the forest. Dense cover of two *Acer sp*. and *C. mas* can inhibit regeneration of other trees and shrubs in our site. *Acer* species are considered very important among the hardwoods of Europe and North America, because of their ecological and economic significance (Morselli 1989). These species provide a considerable source of food and foliage cover for wildlife (Morselli 1989).

5 CONCLUSIONS

Our study suggests that (1) the vertical foliage distribution changed in the understory and a new secondary subcanopy layer appeared below the oak canopy layer, 8–13 m in height. (2) *A. campestre* was the most common shade-tolerant woody species in this new layer. Additionaly, some *C. mas* and *A. tataricum* specimens composed the subcanopy layer. (3) The response of these shade and relatively drought tolerant woody species is strong and rapid once oak decline has set in, the so-called "Oskar"-strategy. (4) The total foliage cover of this layer per hectare was substantially higher in 2012 than in 1982; the new layer can makes up for the significant losses of leaf canopy. (5) *A. campestre* has a strong influence on the frequencies of other subcanopy species and on the mean basal area of *A. tataricum*. The study demonstrated that the forest community compensated for the dead oak trees by forming a subcanopy layer. The woody species of this layer responded successfully to the foliage gaps. Archival data from 1982 allowed us to quantify long-term changes in forest structure and to better understand the impacts of a changing top canopy density and foliage cover rate over the past 30 years. Furthermore, understanding understory development and possible interaction between the understory shrub layer and the canopy is critical to achieving forest management goals in the Hungarian oak forest stands, as this knowledge helps explain stand developmental patterns and predict future stand structures. As the decline in the current oak population continues, and with oak seedlings taking so long to reach sufficient height, more *A. campestre* specimens will grow into the canopy which will lead to the formation of mixed oak forest.

Acknowledgements: The authors were supported during the manuscript preparation by the TÁMOP 4.2.1./B-09/1/KONV-2010-0007 project. We would like to thank our colleagues at the University of Debrecen, Department of Ecology-Debrecen and Eszterházy Károly College, Department of Environmental Science, Eger for help with our field-work until 2002.

REFERENCES

AUGUSTO, L. – DUPOUEY, J.L. – RANGER, J. (2003): Effects of tree species on understory vegetation and environmental conditions in temperate forests. Ann For Sci 60: 823–831.

BÉRES, CS. – FENYVESI, A. – RASCHI, A. – RIDDER, H.W. (1998): Field experiment on water transport of oak trees measured by computer tomograph and magnetic resonance imaging. Chemosphere 36: 925–930.

BOLTE, A. – HILBRIG, L. – GRUNDMANN, B. – KAMPF, F. – BRUNET, J. – ROLOFF, A. (2010): Climate change impacts on stand structure and competitive interactions in a southern Swedish spruce–beech forest. Eur J For Res 129: 261–276.

BROSOFSKE, K.D. – CHEN, J. – CROW, T.R. (2001): Understory vegetation and site factors: implications for a managed Wisconsin landscape. For Ecol Manag 146: 75–87.

BROWN, L.B. – ALLEN-DIAZ, B. (2009): Forest stand dynamics and sudden oak death: Mortality in mixed-evergreen forests dominated by coast live oak. For Ecol Manag 257: 1271–1280.

BRUCK, R.I. – ROBARGE, W.P. (1988): Change in forest structure in the boreal montane ecosystem of Mount Mitchell, North Carolina. Eur J For Pathol 18: 357–366.

BRUHN, J.N. – WETTEROFF, JR. J.J. – MIHAIL, J.D. – KABRICK, J.M. – PICKENS, J.B. (2000): Distribution of *Armillaria* species in upland Ozark Mountain forests with respect to site, overstory species composition and oak decline. Eur J For Pathol 30: 43–60.

BUSSOTTI, F. – FERRETTI, M. (1998): Air pollution, forest condition and forest decline in Southern Europe: an overview. Environ Pollut 101: 49–65.

CAQUET, B. – MONTPIED, P. – DREYER, E. – EPRON, D. – COLLET, C. (2010): Response to canopy opening does not act as a filter to *Fagus sylvatica* and *Acer* sp. advance regeneration in a mixed temperate forest. Ann For Sci 67: 105–115.

CSÓKA, GY. (1998): Oak defoliating insects in Hungary. In: McManus M.L. – Liebhold, A.M. (eds.): Proceedings: Population Dynamics, Impacts, and Integrated Management of Forest Defoliating Insects. USDA Forest Service General Technical Report NE-247. 334–335.

DE VRIES, W. – REINDS, G.J. – POSH, M. – SANZ, M.J. – KRAUSE, G. – CALATAYUD, V. – RENAUD, J.P. – DUPOUCY, H. ET AL. (2003): Intensive monitoring of forest ecosystems in Europe, 2003. Technical Report, EC-UN/ECE, Brussels. Geneva.

DUNN, C.P. (1986): Shrub layer response to death of *Ulmus americana* in southeastern Wisconsin lowland forest. Bull Torrey Bot Club 113: 142–148.

FRANKLIN, J.F. – SHUGART, H.H. – HARMON, E.M. (1987): Tree death as an ecological process. The causes, consequences, and variability of tree mortality. BioSci 37 550–556.

FREER-SMITH, P.H. – READ, D.B. (1995): The relationship between crown condition and soil solution chemistry in oak and Sitka spruce in England and Wales. For Ecol Manag 79: 185–196.

GALBRAITH, S.L. – MARTIN, W.H. (2005): Three decades of overstory and species change in a mixed mesophytic forest in eastern Kentucky. Casta 70: 115–128.

GAZOL, A. – IBÁÑEZ, R. (2009): Different response to environmental factors and spatial variables of two attributes (cover and diversity) of the understorey layers. For Ecol Manag 258: 1267–1274.

GOLDBLUM, D. (1997): The effects of treefall gaps on understory vegetation in New York State. J Veg Sci 8: 125–132.

GRACIA, M. – MONTANÉ, F. – PIQUÉ, J. – RETANA, J. (2007): Overstory structure and topographic gradients determining diversity and abundance of understory shrub species in temperate forests in central Pyrenees (NE Spain). For Ecol Manag 242: 391–397.

HÄMMERLI, F. – STADLER, B. (1989): Eichenschäden - Eine Übersicht zur Situation in Europa und in der Schweiz. Schweiz Z Forstwes 140: 357–374.

HOLEKSA, J. (2003): Relationship between field-layer vegetation and canopy openings in a Carpathian subalpine spruce forest. Plant Ecol 168: 57–67.

HUGHES, J.W. – FAHEY, T.J. (1991): Colonization dynamics of herbs and shrubs in a disturbed northern hardwood forest. J Ecol 79: 605–616.

HUTCHINSON, T.F. – BOERNER, R.A.J. – IVERSON, L.R. – SUTHERLAND, S. – KENNEDY, S.E. (1999): Landscape patterns of understory composition and richness across a moisture and nitrogen mineralization gradient in Ohio (USA) *Quercus* forests. Plant Ecol 144: 177–189.

IGMÁNDY, Z. (1987): Die Welkeepidemie von *Quercus petraea* (Matt.) Lieb. in Ungarn (1978 bis 1986). Österr Forstz 98: 48–50.

JAKUCS, P. (ed.) (1985): Ecology of an oak forest in Hungary. Results of „Síkfőkút Project" I. Akadémia Kiadó, Budapest.

JAKUCS, P. (1988): Ecological approach to forest decline in Hungary. Ambio 17: 267–274.

JUNG, T. – BLASCHKE, H. – OBWALD, W. (2000): Involvement of soilborne *Phytophthora* species in Central European oak decline and the effect of site factors on the disease. Plant Pathol 49: 706–718.

KABRICK, J.M. – DEY, D.C. – JENSEN, R.G. – WALLENDORF, M. (2008): The role of environmental factors in oak decline and mortality in the Ozark Highlands. For Ecol Manag 255: 1409–1417.

KERNS, B.K. – OHMANN, J.L. (2004): Evaluation and prediction of shrub cover in coastal Oregon forests (USA). Ecol Indic 4: 83–98.

KLEIN, R.M. – PERKINS, T.D. (1987): Cascades of causes and effects of forest decline. Ambio 16: 86–93.

KNOWE, S.A. – STEIN, W.I. – SHAINSKY, L.J. (1997): Predicting growth response of shrubs to clear-cutting and site preparation in coastal Oregon forests. Can J For Res 27: 217–226.

KOTROCZÓ, ZS. – KRAKOMPERGER, ZS. – KONCZ, G. – PAPP, M. – BOWDEN, R.D. – TÓTH, J.A. (2007): A Síkfőkúti cseres-tölgyes fafaj összetételének és struktúrájának hosszú-távú változása. [Long term changes in the composition and structure of an oak forest at Síkfőkút, North Hungary] Természetvédelmi Közlemények 13: 93–100. (in Hungarian)

KOTROCZÓ, ZS. – VERES, ZS. – FEKETE, I. – PAPP, M. – TÓTH, J.A. (2012): Effects of climate change on litter production in a Quercetum petraeae-cerris forest in Hungary. Acta Silv Lign Hung 8: 31–38.

LÉGARÉ, S. – BERGERON, Y. – LEDUC, A. – PARÉ, D. (2001): Comparison of the understory vegetation in boreal forest types of southwest Quebec. Can J Bot 79: 1019–1027.

LÉGARÉ, S. – BERGERON Y. – PARÉ D. (2002): Influence of forest composition on understory cover of boreal mixedwood forests of western Quebec. Silva Fenn 36: 353–366.

MCDONALD, R.I. – PEET, R.K. – URBAN, D.L. (2002): Environmental correlates of oak decline and red maple increase in the North Carolina Piedmont. Castanea 67: 84–95.

MCKENZIE, D. – HALPERN, C.B. – NELSON, C.R. (2000): Overstory influences on herb and shrub communities in mature forests of western Washington USA. Can J For Res 30: 1655–1666.

MÉSZÁROS, I. – MÓDY, I. – MARSCHALL, I. (1993): Effects of air pollution on the condition of sessile oak forests in Hungary. Stud Environ Sci 55: 23–33.

MÉSZÁROS, I. – KANALAS, P. – FENYVESI, A. – KIS, J. – NYITRAI, B. – SZŐLLŐSI, E. – OLÁH, V. – DEMETER, Z. – LAKATOS, Á. – ANDER, I. (2011): Diurnal and seasonal changes in stem radius increment and sap flow density indicate different responses of two co-existing oak species to drought stress. Acta Silv Lign Hung 7: 97–108.

MORAAL, L.G. – HILSZCZANSKI, J. (2000): The oak buprestid beetle, *Agrilus biguttatus* (F.) (Col., Buprestidae), a recent factor in oak decline in Europe. J Pest Sci 73: 134–138.

MORSELLI, M.F. (1989): Maple (*Acer* spp.). In: Bajaj, Y.P.S. (ed.): Biotechnology in Agriculture and Forestry Vol. 5. Trees II.

NAKASHIZUKA, T. (1985): Diffused light conditions in canopy gaps in a beech (*Fagus crenata*) forest. Oecol 66: 472–474.

NOWACKI, J.G. – ABRAMS, D.M. (2008): The demise of fire and "mesophication" of forests in the Eastern United States. Biosci 58: 123–138.

OLIVER, C.D. – LARSON, B.C. (1996): Forest stand dynamics. Wiley, New York. 520 p.

RÖHRIG, E. – ULRICH, B. (1991): Ecosystems of the world 7: Temperate deciduous forests. Elsevier, London. 402 p.

SHOTOLA, S.J. – WEAVER, G.T. – ROBERTSON, P.A. – ASHBY, W.C. (1992): Sugar maple invasion of an old-growth oak–hickory forest in southwestern Illinois. Am Midl Nat 127: 125–138.

SIGNELL, S.A. – ABRAMS, M.D. – HOVIS, J.C. – HENRY, S.W. (2005): Impact of multiple fires on stand structure and tree regeneration in central Appalachian oak forests. For Ecol Manag 218: 146–158.

SILVERTOWN, J.W. (1982): Introduction to plant population ecology. Blackwell Scientific, Oxford. UK.

STALTER, A.M. – KRASNY, M.E. – FAHEY, T.J. (1997): Sprouting and layering of *Acer pensylvanicum* L. in hardwood forests of central New York. J Torrey Bot Soc 124: 246–253.

STEIN, W.I. (1995): Ten-year development of douglas-fir and associated vegetation after different site preparation on Coast Range Clearcuts. PNW-RP-473, USDA Forest Service, Portland. OR.

STONE, W.E. – WOLFE, M.L. (1996): Response of understory vegetation to variable tree mortality following mountain beetle epidemic in lodgepole pine stands in northern Utah. Veg 122: 1–12.
SZABÓ, I. – VARGA, SZ. – BERÉNYI, A. – VIDÓCZI, H. (2007): *Cryphonectria parasitica* in sessile oak in Hungary. Acta Silv Lign Hung Spec Edition: 187–197.
TAPPEINER, J.C. – ZASADA, J. – RYAN, P. – NEWTON, M. (1991): Salmonberry clonal and population structure: the basis for a persistent cover. Ecol 72: 609–618.
THOMAS, F.M. – BÜTTNER, G. (1998): Nutrient relations in healthy and damaged stands of mature oaks on clayey soils: two case studies in northwestern Germany. For Ecol Manag 108: 301–319.
WOODALL, C.W. – GRAMBSCH, P.L. – THOMAS, W. – MOSER, W.K. (2005): Survival analysis for a large-scale forest health issue: Missouri oak decline. Environ Monit Assess 108: 295–307.
ZACZEK, J.J. – GRONINGER, J.W. – VAN SAMBEEK, J.W. (2002): Stand dynamics in an old-growth hardwood forest in Southern Illinois, USA. Nat Areas J 22: 211–219.

DE GRUYTER OPEN DOI: 10.2478/aslh-2014-0002 Acta Silv. Lign. Hung., Vol. 10, Nr. 1 (2014) 23–29

Genetic Studies of Selected „Black-Fruit" Hawthorns: *Crataegus nigra* WALDST. et KIT., *C. pentagyna* WALDST. et KIT. and *C. chlorosarca* MAXIM.

Viktor KERÉNYI-NAGY[ab*] – Tamás DEÁK[c] – Géza KÓSA[d] – Dénes BARTHA[b]

[a] Institute of Horticulture and Technology, Szent István University, Gödöllő, Hungary
[b] Institute of Botany and Nature Protection, University of West-Hungary, Sopron, Hungary
[c] Institute of Viticulture and Oenology, Corvinus University, Budapest, Hungary
[d] Centre for Ecological Research, Institute of Ecology and Botany, National Botanical Garden, Vácrátót, Hungary

Abstract – Genetic relationships of black-fruit hawthorns of the Carpathian basin have been investigated based on intergenic cpDNA sequences; first of all of the endemic *Crataegus nigra* and related species. Considerable infraspecific variation was detected in the East Asian taxon *C. chlorosarca* and some divergence in the Eurasian *C. pentagyna*. Based on the genetic analysis of investigated and reference psbA-trnH sequences, classification of sections *Crataegus* and *Sanguineae* is highly supported. From the studied taxa, *C. pentagyna* and *C. monogyna* was ordered to Sectio *Crataegus*, while *C. nigra* and .*C. chlorosarca* to Sectio *Sanguineae.* Based on our data, *C. nigra* can be considered as maternal parent of the investigated *C.* × *degenii* hybrids.

molecular taxonomy / classification / intergenic cpDNA sequences

Kivonat – Három kiválasztott "fekete termésű" galagonyafaj genetikai vizsgálata: *Crataegus nigra* WALDST. et KIT., *C. pentagyna* WALDST. et KIT. és *C. chlorosarca* MAXIM. Jelen tanulmányban kárpát-medencei "fekete termésű" galagonyák, elsősorban a *Crataegus nigra* és közeli rokonainak genetikai kapcsolatait vizsgáltuk intergénikus cpDNS szekvenciák alapján. Jelentős infraspecifikus variabilitást a kelet-ázsiai *C. chlorosarca* fajnál tapasztaltunk, míg az eurázsiai *C. pentagyna* esetében korlátozott számú nukleotid polimorfizmust azonosítottunk. Az általunk vizsgált és az adatbázis eredetű referencia psbA-trnH szekvenciák alapján a Sect. *Crataegus* és Sect. *Sanguineae* osztályozások támogatást kapnak. A vizsgált taxonok, a *C. pentagyna* és a *C. monogyna* a Sect. *Crataegus*ba, míg a *C. nigra* és a *C. chlorosarca* a Sect. *Sanguineae* kládokra kerültek besorolásra. Vizsgálataink alapján a *C. nigra* a *C.* × *degenii* hibrid anyai szülője.

molekuláris taxonómia / osztályozás / intergénikus cpDNS szakaszok

* Corresponding author: kenavi1@gmail.com; H–2100, GÖDÖLLŐ, Práter K. u. 1.

1 INTRODUCTION

The Hungarian (Danubian) hawthorn (*Crataegus nigra* WALDST. et KIT.) is an endemic species of the Carpathian Basin, occuring in the floodplains of Danube in Hungary and across the Serbian-Croatian border (for recent changes in the area see (BARTHA – KERÉNYI-NAGY, 2010). It is a mesophytic species: grows in the floodplain-forests (*Salici-Populetum nigrae* PARABUĆSKI, *Fraxino pannonicae-Ulmetum* SOÓ, *Leucojo aestivi-Crataegetum nigrae* KEVEY, FERENC et TÓTH). Morphologically, it can be identified easily, the taxon differs strongly from other taxa: it has 7–9–11–13 leaf lobes, the leaves on the upper surface are villose and the lower surface is downy, the stipules are serrate, the fruit is black with 5 seeds. *C. nigra* has 8 forms and 1 hybrid with *C. monogyna* JACQ., this hybrid, *C.* × *degenii* ZSÁK is also endemic in the Carpathian Basin (BARTHA – KERÉNYI-NAGY, 2010). The Degen-hawthorn and its relationship to other native Hungarian hawthorn taxa were not yet studied by genetic methods. This is the first attempt to analyse the proposed origin of *C.* × *degenii* (syn. *C.* × *lambertiana* LANGE) genetically.

The more xerophytic species *C. chlorosarca* MAXIM. in the Far East is vicariant of *C. nigra*. Both species belong to Sectio *Sanguineae* ZABEL ex C. K. SCHNEID. Series *Nigrae* (LOUDON) RUSSANOV. *C. chlorosarca* is morphologically similar to *C. nigra*. It differs however from *C. nigra* with its black-purple fruit and the sepal edges have some teeths (CINOVSKIS, 1971). Genetic relation of *C. nigra* and *C. chlorosarca* has been proved earlier by LO et al (2009). The same study has shown, that East Asian and European taxa show clear divergence based on combined nuclear and chloroplast DNA data with only few exceptions – including *C. nigra*.

Small-flowered black hawthorn (*C. pentagyna* WALDST. et KIT.) has been described from the Carpathian Basin as well, but its distribution area ranges from the southern part of Banat, onto the Balkan Peninsula and to Asia Minor. It differs from *C. nigra* in morphology (3–5 leaf lobes, the leaves are leathery, the upper surface is bright and glabrous, sometimes pubescent too; the lower surface is often lanate-tomentose only in the vein-axils, the stipule is entire, the fruit is black with 5 seeds) (BARTHA – KERÉNYI-NAGY, 2010, *Table 1.*) and belongs to Sectio *Crataegus*. *C. pentagyna* is ordered to the outer basal position of Sectio *Crataegus* (LO et al., 2009). Although *C. pentagyna* and *C. nigra* show different morphological and ecological characteristics, reviewing herbarium specimens reveals that they are confused frequently in the literature.

Based on our earlier morphological studies (BARTHA – KERÉNYI-NAGY, 2010), we would like to answer the following questions with molecular markers: (1) is there any infraspecific divergence in cpDNA sequences of black-fruit hawtorns; (2) is the genetic relatedness of *C. nigra* and *C. chlorosarca*, and the classification of these taxa into the same section supported despite the geographic distance between the distribution areas; (3) are *C. pentagyna* and *C. nigra* different on the genetic level; and (4) whether the parent species of *C.* × *degenii* (*C. nigra* and *C. monogyna*) were identified correctly.

2 MATERIALS AND METHODS

2.1 Plant samples

We collected the samples in Hungary from natural habitats (4 samples of *C. nigra*: Szigetújfalu, 5K, compartment 6AB; 2 samples of *C.* × *degenii*: Szigetújfalu, the road between the compartments 4A–5B; 2 samples of *C. monogyna*: Szigetújfalu, the border of 5K–6AB compartments) or from the live collection of the Institute of Botany of the Hungarian Academy of Sciences, Vácrátót; the origin of the sampled shrubs were Vladivostok (Russia) for *C. chlorosarcha* (4 samples) and Bucarest (Romania) for *C. pentagyna* (6 samples).

It should be noted, that *C. × degenii* and *C. nigra* samples originated physically from the same population, where *C. nigra* was dominant with ~99% frequency.

Table 1. Differential morphological characters between the hawthorn taxa included in the current study

Character	***C. chlorosarca***	***C. nigra***	***C. × degenii***	***C. monogyna***	***C. pentagyna***
Branch	rambling		rigid, straight		
Shoot-hair	permanently downy		soarsely downy and balding	hairless	rare, small hairy
Bracteas	dentated		less dentated	integral	
Leaves shape	triangular	deltoid			
Number of lobes	7–11		5–7–9	3–5	
Fragmentation of leaves	poor		deep		
Upper surface of leaves	hairy		±hairless	hairless	rare hairy
Lower surface of leaves	downy				full of very small and rare hair
Hairs between the veins	even			non	tuft
Basis of leaves	round	straight or wide round	wide round	wedge	wide wedge
Edge of leaves	trough densely dentated		4–6 dentated	integral or 2–3 dentated	4–10 dentated
Sepals	reflexed				erected or V-shaped
Sepal edge	some teeths		integral		
Peduncle	full of hair		±hairless	hairless	rare hairy
Hypanthium	rare hairy				
Fruit-colour	purple-black	black	purple	red	black
Fruit-hair	hairless				±hairless
„Seed" number	5		2–4	1	5
„Seed" position	free				whole or inpart linked with
Habitat	xerotermic	floodplain		xerotermic	

2.2 DNA amplification and sequencing

DNA was extracted from young leaves stored at –20 °C using a modified CTAB method (MSZ EN ISO 21571, 2005) originally introduced by DOYLE and DOYLE (1987). Standard polymerase chain reactions were carried out in 20 µl final volume from ~30 ng template DNA

under following conditions: 2 minutes denaturation at 94 °C was followed by 30 cycles of 30 secs denaturation at 94 °C, 30 secs primer annealing at 56 °C and 1 minute elongation at 72 °C. The reaction was closed by 5 minutes chain elongation at 72 °C.

For amplification of trnL-trnF (5'-AAAATCGTGAGGGTTCAAGTC-3' and 5'-GATTTGAACTGGTGACACGAGG-3') and psbA-trnH (5'-GTTATGCATGAACGTAATGCTC-3' and 5'-CGCGCATGGTGGATTCACAATCC-3') chloroplast intergenic regions, primers used by ALBAROUKI and PETERSON (2007) for hawthorns taxa were applied. Following 1.2% agarose gel-electrophoresis, single band PCR products were isolated using the Wizard PCR Clean-Up System (Promega) according to the manufacturer's instructions. Eluted PCR products were direct sequenced using traditional Sanger sequencing on the ABI 3100 (Applied Biosystems) platform using both forward and reverse primers such accessing two times coverage.

Manually curated sequences have been uploaded to the European Nucleotide Archive (accession numbers HG937792-HG937796for psbA-trnH and HG937797-HG937801 for trnL-trnF).

2.3 Sequence and phylogenetic analysis

Reference sequences of taxa belonging to sections *Sanguineae* and *Crataegus* published by ALBAROUKI and PETERSON (2007) and LO et al. (2009) were fetched from GenBank for *C. nigra* (AJ853470.1), *C. wilsonii* SARG. (EF127141.1), *C. russanovii* CIN. (EU500281.1), *C. sanguinea* PALL. ex BIEB. (EF127143.1), *C. chlorosarca* (EU682698.1), *C. nevadensis* K. I. CHR. (EU500289.1), *C. orientalis* PALL. (EU500290.1), *C. monogyna* JACQ. (AJ853465), *C. laevigata* (POIR.) DC (AJ853468), *C. heldreichii* BOISS. (EU500295.1) and *C. pentagyna* WALDST. et KIT. ex WILLD. (EF127131.1). Multiple alignments of reference and raw sequences were carried out using the ClustalW2 tool (LARKIN et al. 2007). The raw sequences were then manually curated based on the electrophoretorgrams and the alignment. Completely identical sequences were joined under one sample name. Phylogenetic analysis was carried out with 1.000 bootstrap replicates and the neighbor-joining (NJ) method (SAITOU and NEI, 1987).

3 RESULTS

From the two investigated chloroplast intergenic regions, trnL-trnF was less variable with a total alignment length of 453 bases, only two phylogenetically informative character and 8 further nucleotide substitutions or insertions, which were monotypic to one species. The 6 bp indel identified earlier between positions 99–104 (ALBAROUKI and PETERSON, 2007) remained monotypic for *C. azarolus* L. var. *aronia* L. New polymorphic sites were identified at position 62 of the alignment, where a 1 bp deletion was recognized exclusively in the two *C.* × *degenii* specimens; and at position 134, where a G/T single nucleotide polymorphism (SNP) was identified, T being monotypic for *C. pentagyna*.

The psbA-trnH intergenic region, although only 298 bases long, proved to be more polymorphic with 3 phylogenetically informative character, 2 monotypic SNP and a hypervariable region. A new T/A SNP was identified at position 259 of the alignment (alignment positions are based on positions publishd by ALBAROUKI and PETERSON, 2007), where A is monotypic to *C. pentagyna*. Based on the sample set investigated by ALBAROUKI and PETERSON (2007), the authors proposed four indel regions between positions 130 and 190 of the alignment. In our sample set, this region of the alignment proved to be highly variable *(Figure 1)*, which makes clear interpretation challenging.

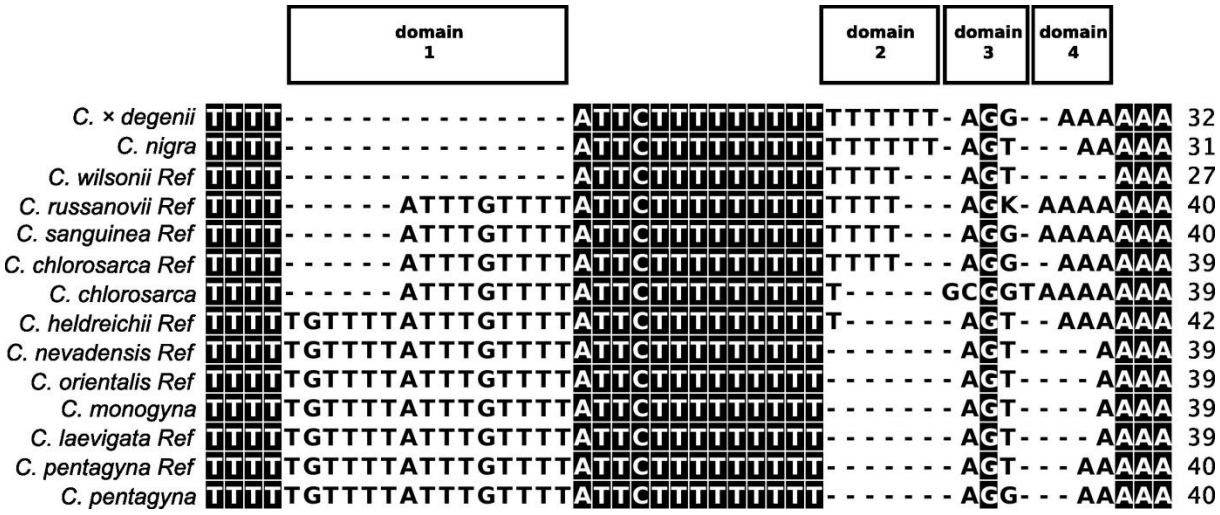

Figure 1. Alignment of the hyper-variable (HV) region of the psbA-trnH chloroplast intergenic region. Shaded background denotes conserved positions of the alignment. Boxes above the sequences identify polymorphic domains 1-4 discussed in the text. The HV region starts with position 134 based on the positions published by ALBAROUKI and PETERSON (2007).

First domain of the hyper-variable (HV) is monotypic in section *Crataegus*, while it is variable in *Sanguineae*, showing infraspecific variability in the case of *C. chlorosarca*. This first domain is missing from *C. nigra*, *C. × degenii* and *C. wilsonii* completely.

Second domain of the HV region is a T mononucleotide repeat, which is less informative and in this case the opportunity of sequencing errors is high. We didn't observe any infraspecific variation in this domain.

The third domain has two main characteristics. There is a GCGGT motif monotypic for all investigated *C. chlorosarca*, but not for the reference *C. chlorosarca* samples nor any other taxa. The second motif is a G/T SNP, which seems to be highly variable (data not shown). *C. russanovii* and *C. dahurica* sequences submitted by LO et al. (2009) having an ambiguous characters at this position, the reference and the investigated Hungarian *C. pentagyna* samples have different states at this position. This is also the one and only of the investigated nucleotide postition, where sequences from *C. nigra* and *C. × degenii* samples are differing.
Domain four of the HV region is built up from an A mononucleotide repeat. Similar to domain two, it is less informative and error-prone. Because of possible ambiguities, domain two and four, further the G/T SNP motif of domain three were excluded from further analysis.

Infraspecific variation wasn't reported earlier for plastid intergenic sequences of hawthorns except for ambiguous bases in the GenBank entries (domain 3 on *Figure 1*), while the present study has shown two cases of such variation. Involved *C. pentagyna* specimens didn't differ in the investigated DNA sequences, but they showed the same T/G polymorphism compared to the reference sequences. The only remarkable infraspecific polymorphism was detected in the case of *C. chlorosarca*. In the HV region the psbA-trnH alignment *C. chlorosarca* specimens from Vladivostok and the reference sequences are differing on two different domains (domain 1 and 3, *Figure 1*).

Neighbor-joining tree of the sequenced and reference accessions show a clear distionction between the two included sections: *Crataegus* and *Sanguineae*. In section *Sanguineae* *C. nigra* and *C. × degenii* are located on the same clade, while the sequenced and reference *C.* chlorosarca samples have been ordered to different clades. The clade of section *Crataegus* has a high bootstrap support, but taxa on this clade are not structured any further.

4 DISCUSSION

Based on the neighbor-joining (NJ) tree of the investigated and reference psbA-trnH sequences *(Figure 2)* classification of sections *Crataegus* and *Sanguineae* is highly supported.

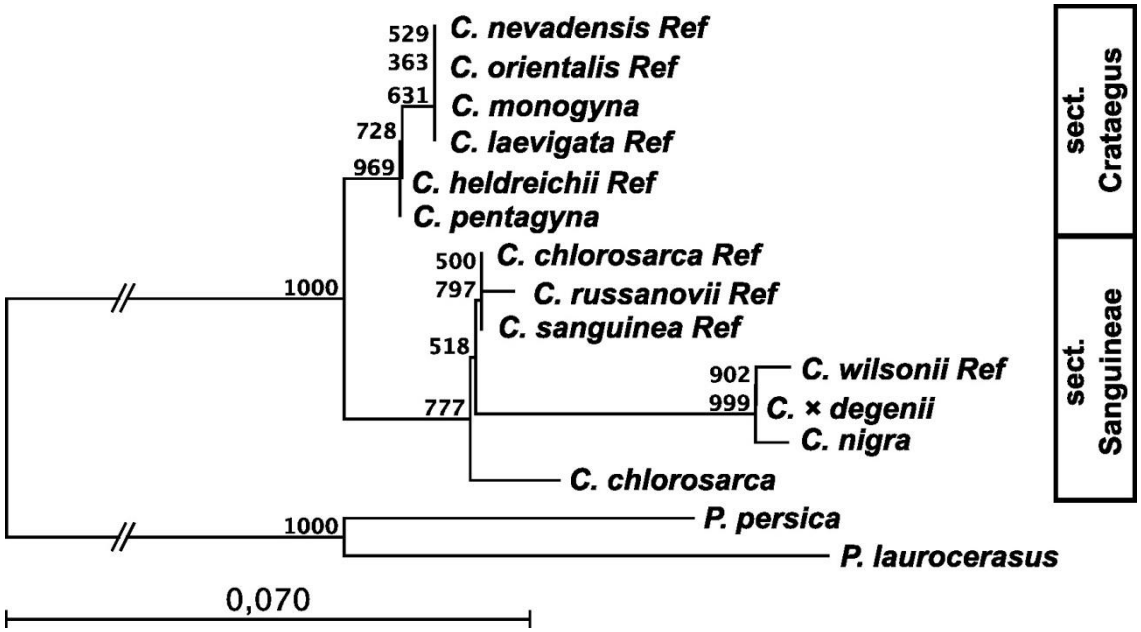

Figure 2. Neighbor joining tree of the psbA-trnH chloroplast intergenic sequences. 'Ref' denotes reference sequences fetched form the GenBank. In the case of C. nigra, C. monogyna and C. pentagyna no differences were found between our results and the reference sequences. Prunus persica and P. laurocerasus were used as outgroup. Numbers indicate bootstrap support from 1000 replicates.

C. pentagyna is correctly ordered to section *Crataegus*, in accordance to the position proposed by LO et al. (2009). The position of *C. pentagyna* is also supported by PHIPPS et al. (2003), who ordered this taxon in an own Series *Pentagynae* (C.K. SCHNEIDER) RUSSANOV. Our results confirmed the genetic differences between *C. pentagyna* and *C. nigra*. The misidentification of *C. pentagyna* in herbarium specimens can be most probably explained by the simple fact, that both hawthorns have black fruits with five seeds.

C. chlorosarca and *C. nigra* were ordered to the clade of Sectio *Sanguineae*. Infraspecific sequence diversity of *C. chlorosarca* can be detected also on the tree, where the investigated and reference specimens are located on different clades. The sample from Vladivostok analysed in this study shows a more distinct position compared to the *C. chlorosarca* specimen investigated by LO et al. (2009). Diversity of *C. chlorosarca* sequences could be possibly related to taxonomic differences or misidentification of the investigated specimens, such the infraspecific variability of *C. chlorosarca* psbA-trnH intergenic sequences need further confirmation. Although *C. nigra* is endemic to the Carpathian basin, it is ordered to section *Sanguineae* with species of mostly Asian origin. This is supported also by the literature (CHRISTENSEN, 1992; PHIPPS et al., 2003; LO et al., 2009). This genetic pattern – namely the similarities of an endemic from the Carpathian basin and taxa from East Asia – isn't unique. Similar phenomenon can be observed between *Syringa josikaea* JACQ. (LENDVAY et al., 2012), which is endemic in the Carpathian basin and the East Asian taxa of the *Syringa* genus. Sectio *Sanguineae* might have had earlier an Eurasian distribution, which later retreated to Asia. *C. nigra* could be considered as a relic of this former distribution.

Based on our data, *C. nigra* could possibly be the maternal parent of the investigated *C.* × *degenii* hybrids. The other parent *C. monogyna* could not be proved, as both hybrid samples were of same hybridization direction.

One of the main goals of this study was to clarify, whether genetic relationships of the East Asian *C. chlorosarca*, the Carpathian Basin endemic *C. nigra* and one hybrid taxon of the latter, *C.* × *degenii* are coherent with the high morphological similarities of these species. On the neighbor-joining tree of the investigated taxa and sequences from GenBank *(Figure 2)* high similarity can be observed between *C. nigra* and its hybrid, *C.* × *degenii* with 100% bootstrap support.

Acknowledgements: The research was supported by the Research Centre of Excellence „17586-4/2013/TUDPOL Szent István University", the project 4.2.1/B-09/1/KONV–2010–0006 „Szellemi, szervezeti és K+F infrastruktúra fejlesztés a Nyugat-magyarországi Egyetemen""KTIA_AIK_12–1–2012–0012" and „EU – Hungary joint project, co-financed by the European Social Fund TÁMOP 4.2.4.A/2-11-1-2012-0001 'National Excellence Program'" and TÁMOP–4.2.1/B-09/1/KONV–2010–0006 „Szellemi, szervezeti és K+F infrastruktúra fejlesztés a Nyugat-magyarországi Egyetemen".

LITERATURE

ALBAROUKI, E. – PETERSON, A. (2007): Molecular and morphological characterization of *Crataegus* L. species (*Rosaceae*) in southern Syria. — Botanical Journal of the Linnean Society 153(3): 255–263.

BARTHA D. – KERÉNYI-NAGY V. (2010): Fekete galagonya – *Crataegus nigra* WALDST. et KIT. — Tilia 15: 54–74.

CHRISTENSEN, K. I. (1992): Revision of *Crataegus* Sect. *Crataegus* and Nothosect. *Crataeguineae* (*Rosaceae-Maloideae*) in the Old World. — Systematic Botany Monographs vol. 35. The American Society of Plant Taxonomists, pp. 1–199.

CINOVSKIS, (1971): Crataegi Baltici – Riga, 385 pp.

DOYLE, J. J. – DOYLE, J. L. (1987): A rapid DNA isolation procedure for small quantities of fesh leaf tissue. — Phytochemistry Bulletin 19(1): 11–15.

LARKIN, M. A. – BLACKSHIELDS, G. – BROWN, N. P. – CHENNA, R. – MCGETTIGAN, P.A. – MCWILLIAM, H. – VALENTIN, F. – WALLACE, I. M. – WILM, A. – LOPEZ, R. – THOMPSON, J. D. – GIBSON, T. J. – HIGGINS, D. G. (2007): Clustal W and Clustal X version 2.0. — Bioinformatics 23 (21): 2947–2948.

LENDVAY B. – PEDRYC A. – KADERIET J. W. – WESTBERG E. – KOHUT E. – HÖHN M. (2012): A Jósika-orgona (*Syringa josikaea* JACQ. fil. ex RCHB.) aktuális és történeti biogeográfiája Kitaibelia 17 (1): 36.

LO, E. Y. Y. – STEFANOVIĆ, S. – CHRISTENSEN, K. I. – DICKINSON, T. A. (2009): Evidence for genetic association between East Asian and western North American *Crataegus* L. (Rosaceae) and rapid divergence of the eastern North American lineages based on multiple DNA sequences. – Molecular Phylogenetics and Evolution 51: 157–168.

MSZ EN ISO 21571:2005: CTAB based DNA extraction method. Hungarian Standard.

PHIPPS, J. B. – O'KENNON, R. J. – LANCE, R. W. (2003): Hawthorns and medlars. Royal Horticultural Society Plant Collector Guide, Cambridge, pp. 1-139.

SAITOU, N. – NEI, M. (1987): The neighbor-joining method: A new method for reconstructing phylogenetic trees. Molecular Biology and Evolution 4(4): 406–425.

DOI: 10.2478/aslh-2014-0003 Acta Silv. Lign. Hung., Vol. 10, Nr. 1 (2014) 31–47

Optimization of the Cutting Process of Wood-Based Agglomerated Materials by Abrasive Water-Jet

Monika KVIETKOVÁ – Štefan BARCÍK – Miroslav GAŠPARÍK*

Department of Wood Processing, Czech University of Life Sciences, Prague, Czech Republic

Abstract – The paper deals with the cutting MDF, OSB, and plywood boards by abrasive water-jet (GMA Garnet Australian, grain size 80, MESH = 0.188 mm), with a kerf width depending on the material properties and technical parameters (material thickness, cutting direction, abrasive flow, and feed speed). The entry of water-jet cutting in the longitudinal direction produces changes in the material due to lateral leads spreading the width of the cut joints by an average of 0.20 mm for MDF boards, 0.3 mm for OSB boards, and 0.17 mm for plywood. On the exit side of the material, the water has the opposite effect. In relation to the thickness of the material, the width of the cut joints increases. The experiment has shown that the optimum value of the feed speed is explicitly 400 mm·min^{-1}, at which the kerf width reaches the lowest dimensions both at entry and exit, and the abrasive flow of 450 g·min^{-1} has been shown as optimum.

feed speed / water-jet / abrasive flow / kerf width / OSB / MDF / plywood

Kivonat – A faalapú agglomerált anyagok folyadéksugaras vágásának optimalizálása. E tanulmány az MDF, OSB és rétegelt lemezek abrazív szemcsés folyadéksugaras vágásának problémájával foglalkozik (GMA Garnet Australian, 80-as szemcseméret, 0,188 mm szitaméret), az anyagtulajdonságoktól és műszaki paraméterektől (anyagvastagság, vágási irány, szemcsekoncentráció és előtolási sebesség) függő vágásrés mérettel. A folyadéksugár longitudinális irányú belépése változásokat okoz az anyagban, mivel ez oldalirányban jobban szétteríti a vágásrés szélességét, MDF esetében átlag 0,20 mm-rel, OSB-nél átlag 0,30 mm-rel, rétegelt lemeznél pedig átlag 0,17 mm-rel. Az anyag kilépési oldalán a víz ezzel ellentétes hatást fejt ki. A vágásrés szélessége az anyagvastagsággal növekszik. A kísérletek megmutatták, hogy kimondottan a 400 mm/min előtolás az optimális, melynél a vágásrés szélessége a legkisebb a bemeneti és a kimeneti oldalon egyaránt. Szemcsekoncentráció tekintetében 450 g/min bizonyult optimálisnak.

előtolási sebesség / folyadéksugár / szemcskoncentráció / vágásrés szélesség / OSB / MDF / rétegelt lemez

1 INTRODUCTION

With the application of the most-used natural resources, water and stone, we can cut almost every material. This makes the method of water-jet cutting (WJC) very efficient. It is a very simple, clean, and reliable technology, and therefore it becomes an alternative to other

* Corresponding author: gathiss@gmail.com; CZ-16521 PRAGUE, Kamýcká 129

methods. But there are also limitations to WJC which should be monitored and improved as a technological process.

Since the first industrial application of cutting materials by abrasive water-jet (AWJ) has happened in a relatively short time, the number of applications has increased considerably and certainly made a significant impact in almost all industries. Use of high-pressure water-jet technology is no longer considered as "additional technology" in classical mechanical tillage. For the efficient, environmentally friendly, and fast processing of different types of (hard-machinable) materials, appropriate technology is needed. The machining of special materials is preferably made by unconventional technologies, which operate on different principles from traditional methods. Non-conventional technologies used for material removal are mainly electro-thermal, electrochemical, chemical, and mechanical. The highest commercial success from technologies based on the mechanical principle comes from a quantum energy/pressure water beam (Barcík et al. 2011a).

We can simply describe water-jet cutting (WJC) technology as a process of reducing material by mechanical impact of a liquid on manufactured material. The technology of applied WJC can be divided into two basic groups: cutting by clean, native water-jet and cutting by abrasive water-jet. In wood-processing practice, cutting by clean, native water-jet is known as chipless cutting and abrasive water-jet cutting as chip producing cutting (Engelmann et al. 2007). The technological process uses a high-pressure and narrow, high-speed stream of water (water pressure around 400 MPa) as a cutting tool (Beer 2007, Maňková 2000). The abrasive water-jet is a wedge tool with an undefined cutting edge (as used in grinding), and the decisive mechanism for removal of machined material is similar to the above-mentioned method. Cutting-wedges are formed with abrasive grains randomly oriented in the beam (Barcík 2007, Matúška 2003). Most equipment for WJC around the world achieves high pressures by using a multiplier. The principle of high pressure generation by the multiplier lies in the combination of two tightly linked pistons (Gerencsér – Bejó 2007, Hashish 1991, Fabian – Hloch 2005).

The focus of this work is optimization of the cutting process, which is carried out by abrasive water–jet, through selected agglomerated materials. This investigation includes the dependence of the kerf width (top kerf width and bottom kerf width) on material properties and also on technical parameters (material thickness, cutting direction, abrasive flow, and feed speed).

2 MATERIALS AND METHODS

2.1 Material preparation

Agglomerated materials used for this experiment were produced by Kronospan Jihlava, Czech Republic. Specific agglomerated materials that have been used for this experiment are: MDF boards, OSB boards, and plywood boards.

Selected agglomerated boards were cut to samples with the following specifications:

- thickness of the test sample:
  - 22 mm / 44 mm / 66 mm — MDF board
  - 16 mm / 32 mm / 48 mm — OSB
  - 18 mm / 36 mm / 54 mm — plywood
- required width of the test sample: b = 180 mm (± 2.5 mm)
- required length of the test sample: l = 500 mm (± 5 mm)
- the moisture content of the test samples: w = 8% (± 2%).

Test samples were cut according to a basic cutting plan for sample preparation (*Figure 1*). Consequently, three cuts were made for each thickness on the samples to eliminate the effect of specific properties of the given sample (*Figure 2*).

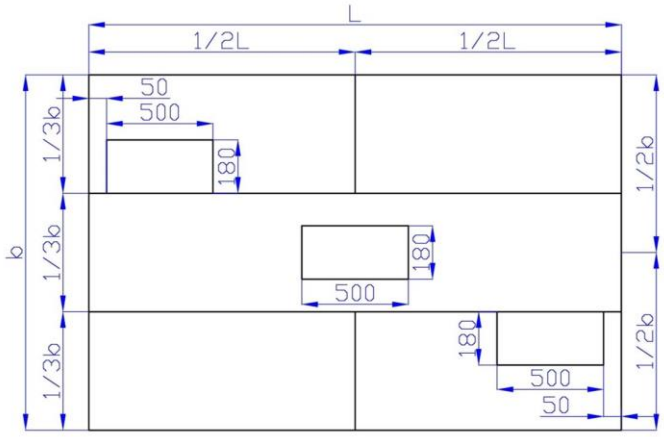

Figure 1. Preparation of test samples

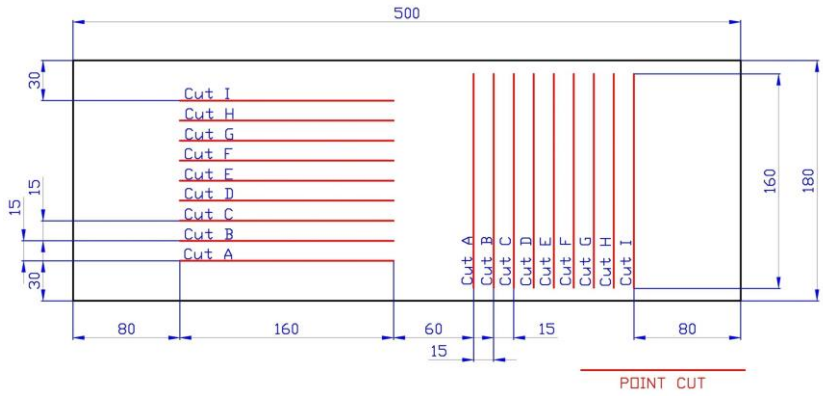

Figure 2. The cutting plan of the samples

2.2 Water-jet equipment

The methods corresponded to experimental tests presented by Barcík et al. (2009, 2011b) and Kvietková (2011). Cutting of samples was done by DEMA Ltd. in Zvolen. The equipment was assembled on the base of components from FLOW (USA) by PTV Ltd. (Prague) (*Figure 3*). It consisted of a high-pressure pump, PTV 37-60 Compact, and a work table with a water-jet head WJ 20 30 D-1Z supplied by PTV.

The technical parameters of the devices were similar to the research of Barcík et al. (2010a). The experiments were performed with the following technical parameters for the equipment:

- cutting liquid pressure: *4000 bar = 400 MPa*
- abrasive: *Australian garnet GMA (grain size 80, MESH = 0.188 mm)*
- diameter of abrasive jet nozzle: *1 mm*
- diameter of water-jet: *0.013 inch = 0.33 mm*
- distance of nozzle above the work piece: *4 mm*
- abrasive mass flow: $m_a = 250\ g \cdot min^{-1}$, $m_a = 350\ g \cdot min^{-1}$, $m_a = 450\ g \cdot min^{-1}$
- feed speed: $v_f = 600\ mm \cdot min^{-1}$, $v_f = 400\ mm \cdot min^{-1}$, $v_f = 200\ mm \cdot min^{-1}$
- water consumption: 3.8 $l \cdot min^{-1}$
- water beam power output: 5*kW*

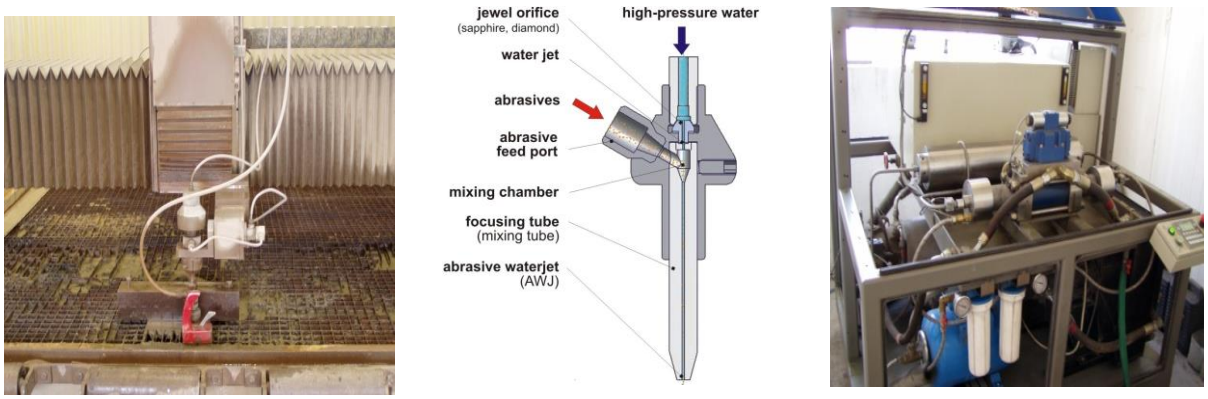

Figure 3. Equipment for cutting by water-jet (left), water-jet nozzle (center) and the high-pressure pump (multiplier) (right)

2.3 Measurement

This experiment was aimed at investigation of the kerf width, specifically top kerf width and bottom kerf width, which are represented in *Figure 4*.

- k_t – kerf width on the entry side (top kerf width): this kerf width, created by the passing of the abrasive water-jet through the material, was measured on the side where the water-jet goes into the material.
- k_b – kerf width on the exit side (bottom kerf width): this kerf width, created by the passing of the abrasive water-jet through the material, was measured on the side where the water-jet comes out of material.

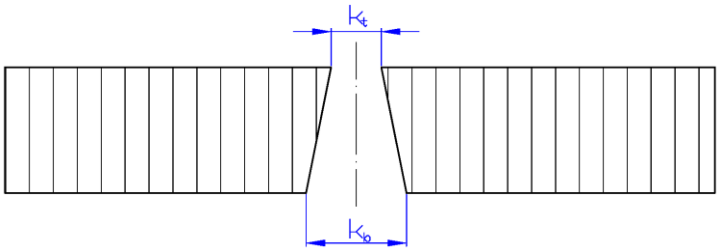

Figure 4. Illustration of the measured kerf widths (k_t – top kerf width, k_b – bottom kerf width)

1. Creation of digital photography

The creation of digital photography, with the kerf width and reference scale, is illustrated in *Figure 5* and *Figure 6*:

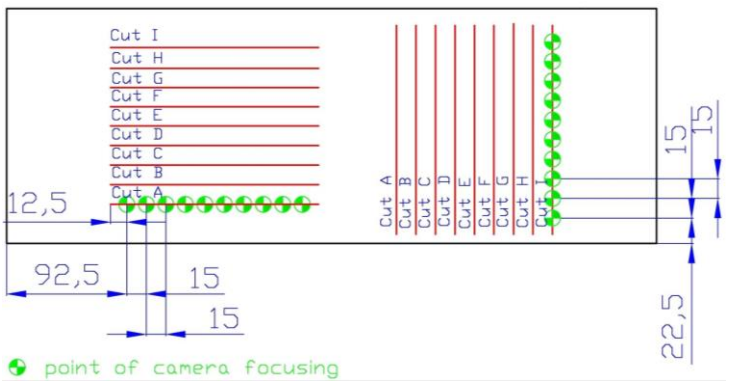

Figure 5. Measuring points of the kerf width

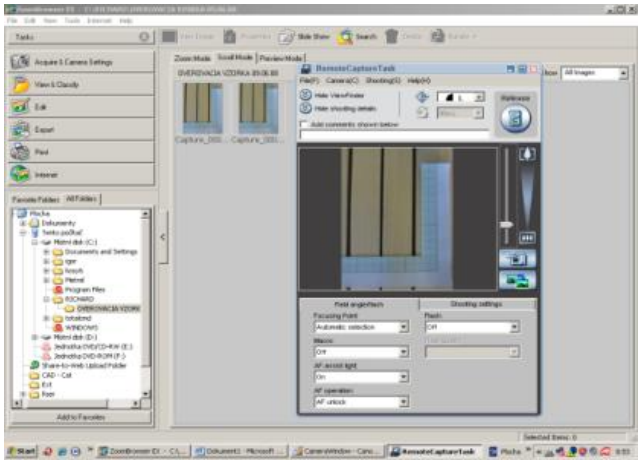

Figure 6. The example of digital picture creation with kerf for verification sample using the Zoom Browser EX 5.0 software

2. Measuring of kerf width

Measuring the kerf width on the exit of the water-jet process from the material becomes harder due to the rippled surface of cutting edge (*Figure 9*). For practical use the maximum size of the kerf is important (from the viewpoint of determining the material allowance for possible further work). The kerf width was measured as the distance of the two most remote parallel tangents placed to the cutting edge, while the evaluated cutting-edge length was always 15 mm.

3. Conversion of relative dimensions

The conversion of relative dimensions was done according to Equation 1:

$$k_b = \frac{k_p * a}{a_p} \tag{1}$$

where k_b is the actual width of the kerf [mm], k_p is the relative width of the kerf (the dimension measured by AutoCAD software from the digital picture), a is the actual dimension of the reference scale unit [mm], and a_p is the relative dimension of the reference scale unit (the dimension measured in AutoCAD software from the digital picture) (*Figure 7*).

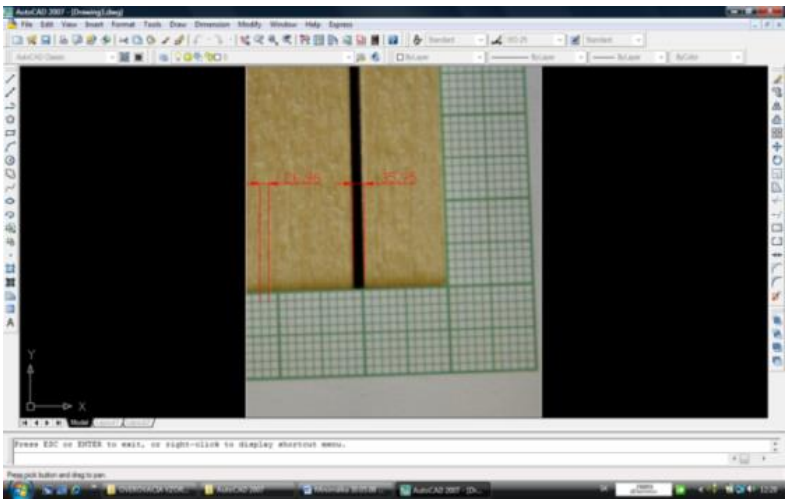

Figure 7. View of the AutoCAD software window during the relative measuring of dimensions

4. Statistical evaluation

From the given procedure we obtained a file of kerf width entry and exit values for all samples. Further, these values were evaluated with STATISTICA 7 software.

The devices and equipment for the measurement and evaluation were the following:

- personal computer *(COMPAQ EVO N 1020v)*,
- digital camera (Canon Power Shot A520) *(Figure 8)*,
- associated processing software for the digital camera (Canon-Zoom Browser EX 5.0) and for the comparative measuring of dimensions (AutoCAD 2007),
- reference scale (Barcík et al. 2010b)

Figure 8. Apparatus for measuring the kerf width

3 RESULTS AND DISCUSSION

3.1 MDF Boards

On the basis of multi-factorial variance analysis, the following sequence of significance of examined factors affecting the kerf width was found. The values are presented in *Table 1* and *Table 2*.

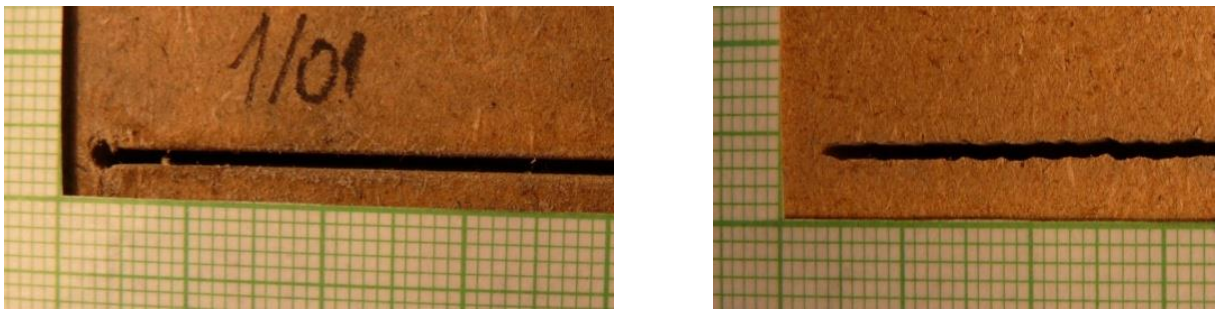

Figure 9. Digital picture of kerf on the MDF verification sample, kerf on the entry side of the material (left) and kerf on the exit side of the material (right)

Significance of entry factors:

1. cutting direction
2. feed speed
3. abrasive flow
4. thickness

Significance of exit factors:

1. thickness
2. feed speed
3. abrasive flow
4. cutting direction

Table 1. Values of multifactor analysis (MANOVA) at entry

Investigated factors	Sum of squares	Degrees of freedom	Scattering	F-test	Level of significance
	734.66	1.00	734.66	35,417.40	0.000
thickness	2.58	2.00	1.29	623.00	0.000
cutting direction	1.58	1.00	1.58	762.70	0.000
feed speed	1.20	2.00	0.60	289.40	0.000
abrasive flow	0.09	2.00	0.04	21.40	0.000
random factors	1.01	486.00	0.00		

Table 2. Values of multifactor analysis (MANOVA) at exit

Investigated factors	Sum of squares	Degrees of freedom	Scattering	F-test	Level of significance
	1,142.04	1.00	1,142.04	10,803.40	0.000
thickness	190.72	2.00	95.36	902.09	0.000
cutting direction	0.27	1.00	0.27	2.54	0.111
feed speed	58.54	2.00	29.27	276.86	0.000
abrasive flow	3.92	2.00	1.96	18.52	0.000
random factors	51.38	486.00	0.11		

Results of the effect of **cutting direction** on the kerf width are presented in *Figure 10*, *Table 3* and *Table 4*.

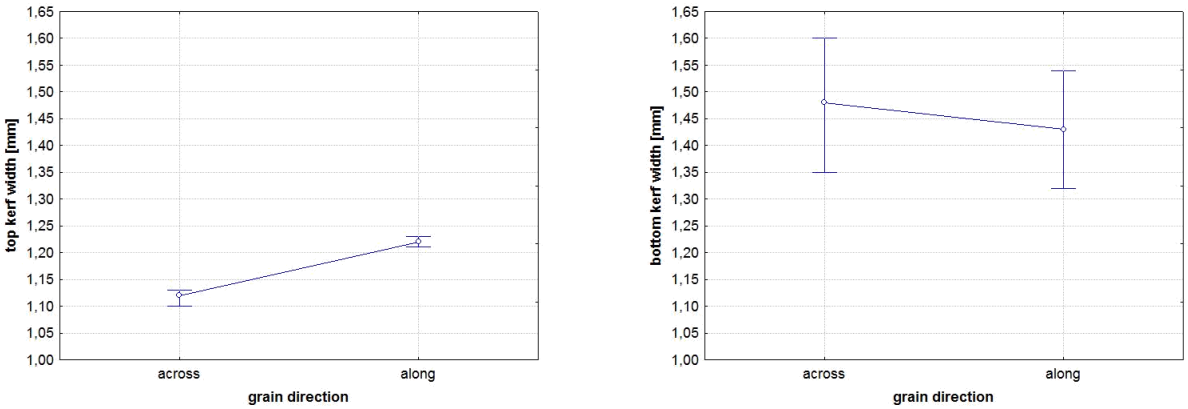

Figure 10. Graph of the kerf width dependence on the cutting direction of the worked material at entry (left) and at exit (right)

Table 3. Values of kerf-width dependence on cutting direction, at entry

Sample number	Cutting direction	Arithmetic mean	Standard deviation	Minimum value	Maximum value	Number of measurements	
				(mm)	(mm)		%
1	across	1.12	0.01	1.10	1.13	270	100
2	along	1.22	0.01	1.21	1.23	270	107.0

Table 4. Values of kerf-width dependence on cutting direction, at exit

Sample number	Cutting direction	Arithmetic mean	Standard deviation	Minimum value	Maximum value	Number of measurements	
				(mm)	(mm)		%
1	across	1.48	0.06	1.35	1.60	270	100
2	along	1.43	0.06	1.32	1.54	270	98.01

During the cutting of samples across the basic technology flow we can see that the values of kerf width at entry are 0.10 mm lower compared with longitudinal cutting. The values of the kerf width at the exit of the water-jet from the work piece reach higher values with cross cutting by 0.05 mm than with longitudinal cutting. At the entry of the water-jet into the material, the kerf width was wider than in longitudinal cutting. These results can be explained by the fact that wood and agglomerated materials in this direction are more resistant to penetration by the water-jet. The time the abrasive particles act on the material is prolonged and due to this fact leads to a side effect of the washing-out of the kerf. This resistance depends not only on the mutual connection of the fibers, but also on the strength of the elements themselves, first of all from libriform fibers, whose strength is influenced by the S_2 layer of the secondary wall. The strength and stability also can vary with the shape and slenderness of the fibers. From the viewpoint of uniformity of kerf width, the dimensions of kerf proved more stable on both sides with the cutting along the grain compared with basic technology flow.

Results of the effect of **material thickness** on the kerf width are presented in *Figure 11*, *Table 5* and *Table 6.*

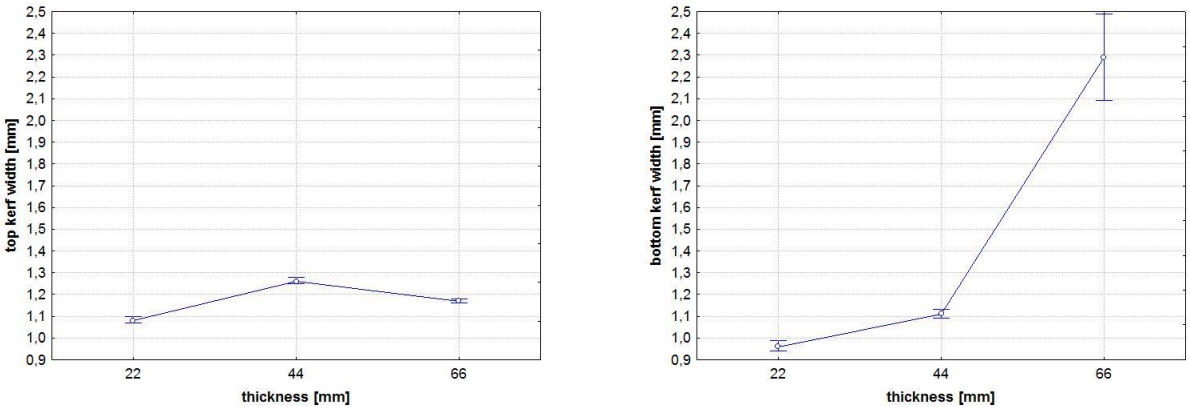

Figure 11. Graph of the kerf-width dependence on thickness of worked material at entry (left) and at exit (right)

Table 5. Values of kerf-width dependence on thickness, at entry

Sample number	Thickness	Arithmetic mean	Standard deviation	Minimum value	Maximum value	Number of measurements	
				(mm)	(mm)		%
1	22	1.08	0.01	1.07	1.10	180	100
2	44	1.26	0.01	1.25	1.28	180	128.28
3	66	1.17	0.01	1.16	1.18	180	117.51

Table 6. Values of kerf-width dependence on thickness, at exit

Sample number	Thickness	Arithmetic mean	Standard deviation	Minimum value	Maximum value	Number of measurements	
				(mm)	(mm)		%
1	22	0.96	0.01	0.94	0.99	180	100
2	44	1.11	0.01	1.09	1.13	180	108.24
3	66	2.29	0.10	2.09	2.49	180	144.33

A 0.18 mm increase in kerf width at entry was reached by the change in thickness of material from 22 mm to 44 mm. A 0.9 mm decrease in kerf width was caused by the change of material thickness from 44 mm to 66 mm.

A change in sample thickness from 22 mm to 44 mm caused a 0.15 mm increase in kerf width at the exit and a change in thickness from 44 mm to 66 mm caused increased kerf width of 1.18 mm. The greater the thickness the higher the amount of abrasive particles gathered in the cut, and these particles apart from the primary effect, severing of material, also cause the side effect of widening of the kerf due to the washing-out of material. The increased values of the kerf width in the test samples of higher thickness were significantly influenced by the lag of the water-jet caused by the gradual loss of its kinetic energy.

From this experiment we can see that the optimum material thickness is 22 mm. This thickness caused the lowest kerf-width values in the entry and also in the exit.

Results of the **feed speed** influence:

At entry, the change of the feed speed from 200 mm·min^{-1} to 400 mm.min^{-1} caused 3 mm lower values in kerf width. The change of feed speed from 400 mm.min^{-1} to 600 mm·min^{-1} caused an increase in kerf width of 5 mm.

At exit, the change in feed speed from 200 mm·min^{-1} to 400 mm·min^{-1} caused an increase of kerf width of 6 mm. The change of feed speed from 400 mm·min^{-1} to 600 mm·min^{-1} caused an increase of 3 mm.

The experiment has shown that the optimum value of the feed speed is explicitly 400 mm·min^{-1}, at which the kerf width reaches the lowest dimensions both at entry and exit.

Results of **abrasive flow** influence on kerf width:

With the change of the added amount of abrasive from 250 g·min^{-1} to 350 g·min^{-1}, the values of the kerf width increased at entry by 2 mm, and then with an increase of the abrasive amount to 450 g·min^{-1} they increased by another 2 mm.

By changing the added amount of abrasive from 250 g·min^{-1} to 350 g·min^{-1}, in the exit of the water-jet process from the worked material, the kerf-width values decreased by 3 mm. With the change of the amount of abrasive from 350 g·min^{-1} to 450 g·min^{-1}, the values decreased by 6 mm.

With an increase of the abrasive mass flow up to 450 g·min^{-1}, the kinetic energy of the particles was consumed by their mutual contact, which created the secondary effect of washing-out of the material at entry and the subsequent narrowing of the kerf width at the exit due to energy loss. However, in comparison with the uniformity of the values at both sides, the value of 450 g·min^{-1} abrasive mass flow has seemed optimum.

3.2 OSB Boards

Cutting of OSB boards was represented by more ripped kerf at entry side in comparison with MDF boards (*Figure 12*). The individual values, for this type of material, are presented in *Table 7* and *Table 8*.

On the basis of multifactorial variance analysis, the following sequence of significance of examined factors affecting the kerf width was found.

Significance of entry factors:

1. cutting direction
2. feed speed
3. abrasive flow
4. thickness

Significance of exit factors:

1. thickness
2. feed speed
3. abrasive flow
4. cutting direction

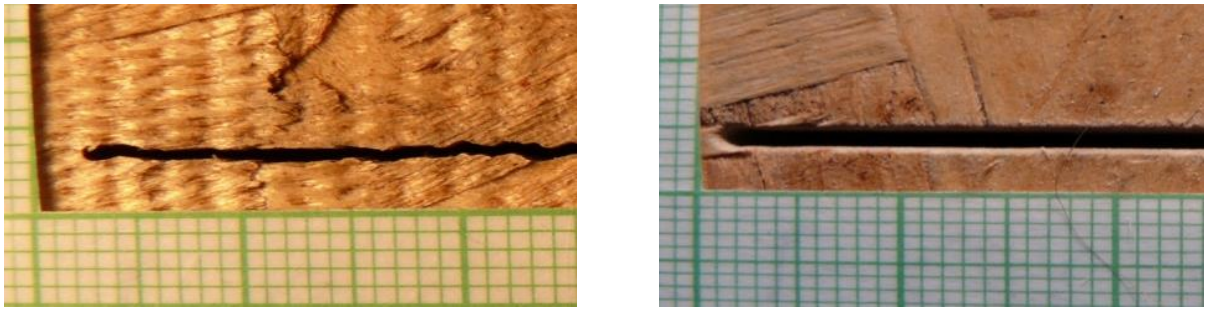

Figure 12. Digital picture of kerf on the OSB verification sample, kerf at the entry of the water-jet into the material (left) and kerf at the exit of the water-jet from the material (right)

Table 7. Values of multifactor analysis (MANOVA) at entry

Investigated factors	Sum of squares	Degrees of freedom	Scattering	F-test	Level of significance
	662.022	1	662.022	296,662.9	0.000
thickness	0.0358	2	0.0179	8.0	0.000
cutting direction	4.1639	1	4.1639	1,865.9	0.000
feed speed	1.4355	2	0.7177	321.6	0.000
abrasive flow	0.2071	2	0.1036	46.4	0.000
random factors	1.0845	486	0.0022		

Table 8. Values of multifactor analysis (MANOVA) at exit

Investigated factors	Sum of squares	Degrees of freedom	Scattering	F-test	Level of significance
	1,040.613	1	1,040.613	25,465.51	0.000
thickness	45.281	2	22.641	554.06	0.000
cutting direction	0.111	1	0.111	2.72	0.100
feed speed	5.681	2	2.841	69.52	0.000
abrasive flow	0.519	2	0.26	6.36	0.002
random factors	19.86	486	0.041		

Results of the effect of cutting direction on the kerf width are presented in *Figure 13*, *Table 9*, and *Table 10*.

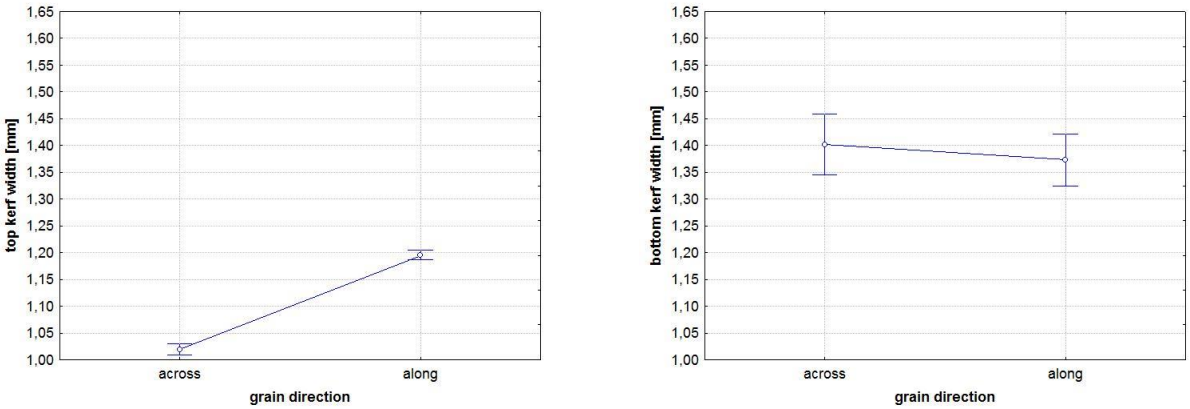

Figure 13. Graph of the kerf-width dependence on cutting direction of worked material, at entry (left) and exit (right)

During the cross cutting of samples according to material flow we can see that the values of kerf width at entry were 0.17 mm lower compared with longitudinal cutting. During the cross cutting of samples according to material flow we can see that values of kerf width at exit are 0.029 mm higher compared with longitudinal cutting.

Table 9. Values of kerf-width dependence on cutting direction, at entry

Sample number	Cutting direction	Arithmetic mean	Standard deviation	Minimum value (mm)	Maximum value (mm)	Number of measurements	%
1	across	1.019	0.006	1.009	1.030	270	100
2	along	1.195	0.004	1.187	1.204	270	117.23

Table 10. Values of kerf-width dependence on cutting direction, at exit

Sample number	Cutting direction	Arithmetic mean	Standard deviation	Minimum value (mm)	Maximum value (mm)	Number of measurements	%
1	across	1.403	0.029	1.346	1.459	270	100
2	along	1.374	0.025	1.325	1.423	270	97.96

Results of the **feed speed** influence:

At the entry of the water-jet, the change of the feed speed from 200 mm·min^{-1} to 400 mm·min^{-1} caused 7.1 mm lower values of kerf width. The change of feed speed to 600 mm·min^{-1} caused lower kerf width by 9.67 mm. At the exit of the water-jet from the material, the change in feed speed from 200 mm·min^{-1} to 400 mm·min^{-1} caused decreased kerf width by 5.21 mm, and the increasing of feed speed to 600 mm·min^{-1} caused an increase of 10.34 mm.

Influence of **abrasive flow** on kerf width:

With the change of the added amount of abrasive from 250 g·min^{-1} to 350 g·min^{-1}, the values of the kerf width decreased at entry by 0.16 mm, and then with an increase of the abrasive amount to 450 g·min^{-1} they increased by 3.71 mm. With the change of the added amount of abrasive from 250 g·min^{-1} to 370 g·min^{-1}, the values of the kerf width decreased at

exit by 3.31 mm, and then with an increase of the abrasive amount to 450 g·min^{-1} they decreased by 5.26 mm.

Results of the influence of **material thickness** on kerf width are presented in *Figure 14*, *Table 11* and *Table 12*.

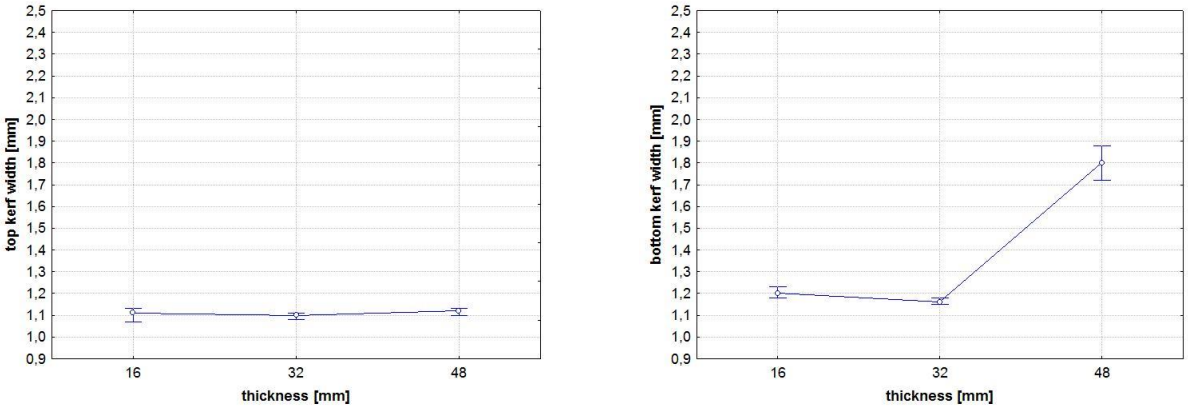

Figure 14. Graph of the kerf-width dependence on thickness of worked material, at entry (left) and exit (right)

The 0.01 mm decrease in kerf width at entry was reached by the change in thickness of material from 16 mm to 32 mm. The 0.02 mm increase in kerf width was caused by the change of material thickness from 32 mm to 48 mm. The 0.04 mm decrease of kerf width at exit was reached by the change in thickness of material from 16 mm to 32 mm. The 0.64 mm increase of kerf width was caused by the change of material thickness from 32 mm to 48 mm.

Table 11. Values of kerf-width dependence on thickness, at entry

Sample number	Thickness	Arithmetic mean	Standard deviation	Minimum value	Maximum value	Number of measurements	
				(mm)	(mm)		%
1	16	1.11	0.01	1.07	1.13	180	100
2	32	1.10	0.01	1.08	1.11	180	98.74
3	48	1.12	0.01	1.10	1.13	180	101.34

Table 12. Values of kerf-width dependence on thickness, at exit

Sample number	Thickness	Arithmetic mean	Standard deviation	Minimum value	Maximum value	Number of measurements	
				(mm)	(mm)		%
1	16	1.20	0.01	1.18	1.23	180	100
2	32	1.16	0.01	1.15	1.18	180	96.74
3	48	1.80	0.04	1.72	1.88	180	149.34

3.3 Plywood

Cutting of plywood was different in relation to kerf width because of wider entry kerf (*Figure 15*). The importance of monitored factors influencing kerf width on plywood is presented in *Table 13* and *Table 14*.

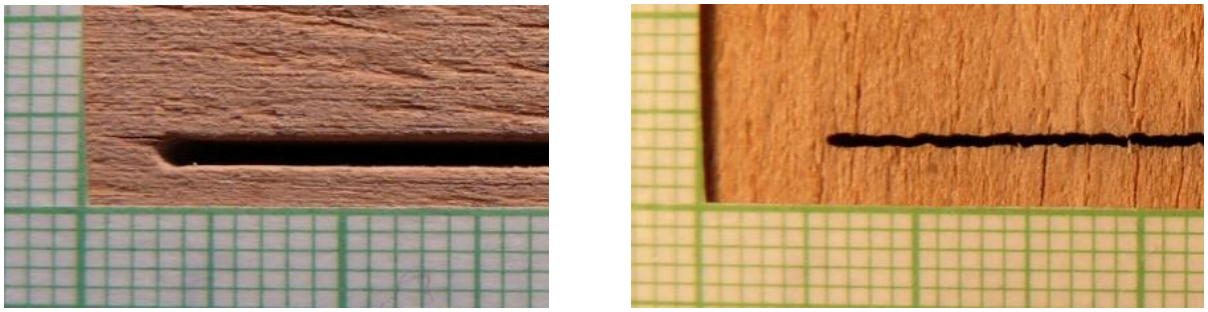

Figure 15. Digital picture of kerf on the plywood verification sample, kerf on the entry of the water-jet into material (left) and kerf on the exit of the water-jet from the material (right)

Table 13. Values of multifactor analysis (MANOVA) at entry

Investigated factors	Sum of squares	Degrees of freedom	Scattering	F-test	Level of significance
	729.335	1	729.3352	24,4285.6	0.000
thickness	0.8664	2	0.4332	145.1	0.000
cutting direction	8.8182	1	8.8182	2,953.6	0.000
feed speed	1.4337	2	0.7169	240.1	0.000
abrasive flow	0.2854	2	0.1427	47.8	0.000
random factors	1.451	486	0.003		

Table 14. Values of multifactor analysis (MANOVA) at exit

Investigated factors	Sum of squares	Degrees of freedom	Scattering	F-test	Level of significance
	768.0995	1	768.0995	5,2711.9	0.000
thickness	15.6655	2	7.8328	537.53	0.000
cutting direction	8.2088	1	8.2088	563.34	0.000
feed speed	1.528	2	0.764	52.43	0.000
abrasive flow	0.0381	2	0.0191	1.31	0.271
random factors	19.86	486	0.041		

Significance of entry factors:

1. cutting direction
2. feed speed
3. thickness
4. abrasive flow

Significance of exit factors:

1. cutting direction
2. thickness
3. feed speed
4. abrasive flow

The effect of cutting direction on kerf width is presented in *Figure 16*, *Table 15* and *Table 16*.

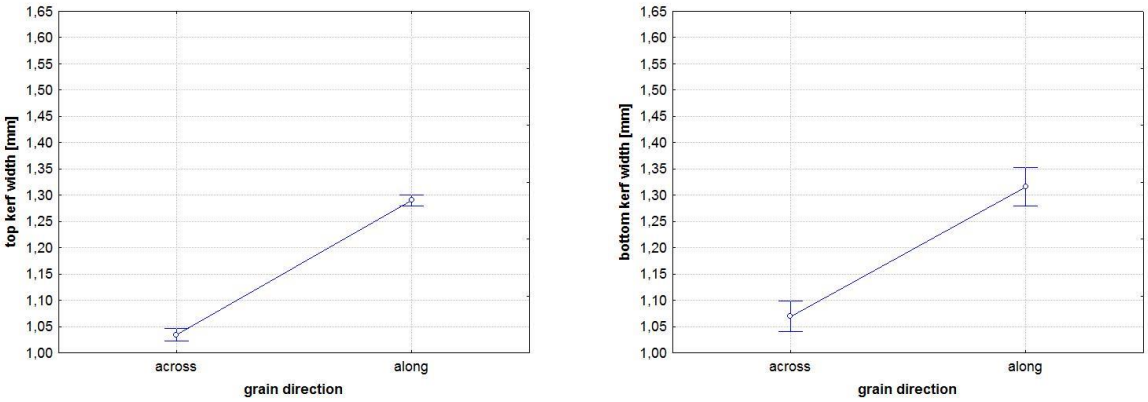

Figure 16. Graph of the kerf-width dependence on cutting direction of the worked material, at entry (left) and exit (right)

Table 15. Values of kerf-width dependence on cutting direction, at entry

Sample number	Cutting direction	Arithmetic mean	Standard deviation	Minimum value	Maximum value	Number of measurements	
				(mm)	(mm)		%
1	across	1.034	0.006	1.022	1.047	270	100
2	along	1.290	0.006	1.279	1.301	270	124.7

Table 16 Values of kerf-width dependence on cutting direction, at exit

Sample number	Cutting direction	Arithmetic mean	Standard deviation	Minimum value	Maximum value	Number of measurements	
				(mm)	(mm)		%
1	across	1.069	0.015	1.040	1.099	270	100
2	along	1.316	0.018	1.280	1.352	270	123.05

The values of kerf width at entry were about 0.256 mm lower compared with longitudinal cutting at cross cutting. Values of kerf width at exit are 0.249 mm lower compared with longitudinal cutting.

Results of the **feed speed** influence:

At the entry of the water-jet, the change of the feed speed from 200 mm·min^{-1} to 400 mm·min^{-1} caused 3.62 mm lower values of kerf width. The change of feed speed to 600 mm·min^{-1} caused lower kerf width by 4.09 mm. At the exit of the water-jet from the material, the change in feed speed from 200 mm·min^{-1} to 400 mm·min^{-1} caused decreased kerf width by 4.2 mm, and the increasing of feed speed to 600 mm·min^{-1} caused its decrease by 1.17 mm.

Results of the influence of thickness on kerf width are presented in *Figure 17*, *Table 17* and *Table 18*.

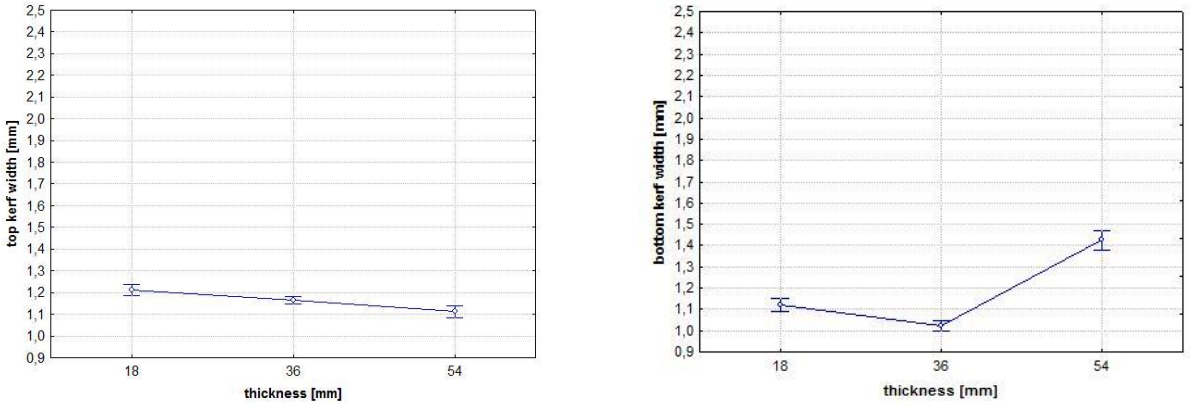

Figure 17. Graph of kerf-width dependence on thickness of worked material, at entry (left) and exit (right)

Table 17. Values of kerf-width dependence on thickness, at entry

Sample number	Thickness	Arithmetic mean	Standard deviation	Minimum value	Maximum value	Number of measurements	
				(mm)	(mm)		%
1	18	1.21	0.1	1.19	1.24	180	100
2	36	1.17	0.1	1.15	1.18	180	97.25
3	54	1.12	0.1	1.09	1.14	180	92.14

Table 18. Values of kerf-width dependence on thickness, at exit

Sample number	Thickness	Arithmetic mean	Standard deviation	Minimum value	Maximum value	Number of measurements	
				(mm)	(mm)		%
1	18	1.12	0.1	1.09	1.15	180	100
2	36	1.03	0.1	1.05	1.00	180	94.59
3	54	1.43	0.1	1.38	1.47	180	132.54

Results of the influence of **thickness**:

A 0.04 mm decrease in kerf width at entry was caused by the change in thickness of material from 18 mm to 36 mm. A 0.05 mm increase in kerf width was caused by the change of material thickness from 36 mm to 54 mm. A 0.09 mm decrease in kerf width at exit was caused by the change in thickness of material from 18 mm to 36 mm. A 0.4 mm increase in kerf width was caused by the change of material thickness to (*Figure 17*).

Influence of **abrasive flow** on kerf width:

With the growth of the added amount of abrasive from 250 g·min^{-1} to 350 g·min^{-1}, the values of kerf width increased at entry by 3.1 mm, and then with the change of the abrasive amount to 450 g·min^{-1}, values increased by 4.9 mm. With the growth of the added amount of abrasive from 250 g·min^{-1} to 350 g·min^{-1}, the values of kerf width increased at exit by 1.73 mm. Growth of the abrasive amount to 450 g·min^{-1} caused increased kerf width by 0.73 mm. See the presented graphical values for the most important factor and for all materials.

Water-jet cutting is an economical way to cut 2D shapes into a wide range of materials with no tooling costs. The unique process of water-jet cutting provides reasonably good edge quality, no burrs, and usually eliminates the need for secondary finishing processes. The

process also generates no heat so the material edge is unaffected and there is no distortion. Water-jet cutting can cut single or multi- layer materials (Rašner et al. 2001).

It is necessary to take an economic view of the whole process of WJC. It should be compared with other cutting techniques from the point of view of costs and benefits. It must be monitored and costs quantified for WJC assembly and the whole material flow, including fixed costs, variable costs (e.g., energy consumption), and also alternative costs related to other (conventional) methods of cutting. Another necessary parameter is time of production (cutting) which affects total capacity and also productivity of an assembly for the material flow. Last but not least, the economic viewpoint must also consider the amount of waste from the water-jet cutting compared with conventional methods of cutting (Rajnoha – Aláč 2003).

4 CONCLUSIONS

The experiments have shown that utilization of the water-jet for cutting agglomerated materials is a suitable method when it is used with the appropriate combination of technical and technological parameters. The most important benefit of this technology is small kerf width compared with other cutting technologies. From the viewpoint of kerf-width equality on both sides of the worked material, we can see more stable dimensions of kerf width with materials cut in the longitudinal direction. From the viewpoint of the technological parameters used, the feed speed of 400 $mm \cdot min^{-1}$ and the abrasive flow of 450 $g \cdot min^{-1}$ have been shown to be optimum. With thicknesses exceeding 44 mm, the method becomes less efficient and it's necessary the improvement of material by additional working.

Acknowledgments: The authors are grateful for the support of CIGA (CULS Grant Agency), project No. 20124311. The authors would like to thank the DEMA Ltd. Zvolen for technical support.

REFERENCES

BARCÍK, Š. (2007): Progresívna metóda obrábania dreva vodným lúčom. [Progressive method of wood manufacturing by water jet]. In: Proceedings of the conference "Woodcut Tools and Woodworking". Zvolen, Slovakia. December 2007. 3–11.

BARCÍK, Š. – KMINIAK, R. – ŠUSTEK, J. (2009): The influence of the parameters of native wood cutting process by abrasive water-jet on the kerf width, In: Proceedings of the 3rd International Scientific Conference "Woodworking Technique". Zalesina, Croatia. 2–6 September 2009. 19–31.

BARCÍK, Š. – KVIETKOVÁ, M. – KMINIAK, R. – REMESELNÍK, J. (2010a): Vplyv hrúbky a smeru rezania na šírku reznej špáry pri rezaní MDF vodným lúčom. [Impact of thickness and cutting direction on the kerf width during the MDF water jet cutting]. In: Proceedings of the conference "Chip and Chipless Woodworking". Terchová, Slovakia. 09-11 September 2010, 33–40.

BARCÍK, Š. – KVIETKOVÁ, M. – KMINIAK, R. – REMESELNÍK, J. (2010b): Vplyv rýchlosti posuvu a hmotnostného toku abrazíva na šírku reznej špáry pri rezaní MDF vodným lúčom. [Effect of feed speed abrasive mass flow landscape kerf when cutting MDF water jet], In: Proceedings of the 1th International video conference "Nábytkárstvo" Zvolen, Slovakia. 26 October 2010, 3–12.

BARCÍK, Š. – KVIETKOVÁ, M. – ALÁČ, P. (2011a): Effect of the chosen parameters on deflection angle between cutting sides during the cutting of agglomerated materials by water jet. Wood Research 56 (4): 577–588.

BARCÍK, Š. – KVIETKOVÁ, M. – KMINIAK, R. – ALÁČ, P. (2011b): Optimization of cutting process of medium density fibreboards by the abrasive water jet. Drvna Industrija 62 (4): 263–268.

BEER, P. (2007): Niekonwencjonalne narzedzia do obróbki drewna. [Unconventional tools for woodworking]. Wydawnictwo Akademii Rolniczej im. Augusta Cieszkowskiego, Poznań. 74 p. (in Polish)

ENGELMANN, B. K. – HERBRICH, H. – KESSLER, B. (2007): *Schneiden mit Laserstrahlung und wasserstrahl.*. Ehningen bei Böblingen: Expert-Verlag, Berlin. 179 p. (in German)

FABIAN, S. – HLOCH, S. (2005): Abrasive water jet process factors influence on stainless steel AISI 304 macrogeometrical cutting duality, In: Scientific Bulletin: Serie C. Volume 19: Mechanics, Tribology, Machine Manufacturing Technology. North University of Baia Mare, Romania, 261–266.

GERENCSÉR, K. – BEJÓ, L. (2007): Investigations into the cutting of solid wood, Wood Research 52 (2): 57-28.

HASHISH, M. (1991): Optimalization factors in abrasive waterjet machining. Journal of Manufacturing Science and Engineering - Transactions of the ASME 113 (1): 29–37.

KRAJNÝ, Z. (1998): Vodný lúč v praxi- WJM. [Water jet in practice]. EPOS, Bratislava. 383 p. (in Slovak)

KVIETKOVÁ, M. (2011): Analýza faktorov vplývajúcich na kvalitu opracovania kompozitných drevných materiálov pri rezaní vodným lúčom. [Analysis of factors which impact the quality of manufacturing wood materials by the abrasive water jet cutting], Ph.D. Thesis, Technical University in Zvolen, Slovakia, p. 157. (in Slovak)

MAŇKOVÁ, I. (2000): Progresívne Technológie. [Progressive Technologies]. Vienala, Košice. 275 p. (in Slovak)

MATÚŠKA, J. (2003): Delenie materiálov vodným lúčom. [Waterjet cutting of materials]. Strojárstvo 7 (11), 35 p. (in Slovak)

RAJNOHA, R. – ALÁČ, P. (2003): Activity based costing—A necessary assumption for the management based on processes, In: Proceedings of the conference "Intercathedra", Komitet Badaň Naukowych: Poznaň. Volume 19. 108–111.

RAŠNER, J. – KOTLÍNOVÁ, M. – DEMOČ, V. – RAJNOHA, R. – ALÁČ, P. (2001): Ekonomika a riadenie logisticko-distribučných systémov podnikov priemyslu spracovania dreva. [Economy and management of logistics and distribution systems of wood industrial enterprises]. Scientific study 1/2001/B, 140 p. (in Slovak)

DE GRUYTER OPEN DOI: 10.2478/aslh-2014-0004 Acta Silv. Lign. Hung., Vol. 10, Nr. 1 (2014) 49–64

Enhancement of the Corporate Environmental Performance

András POLGÁR* – József PÁJER

Institute of Environmental and Earth Sciences, Faculty of Forestry, University of West Hungary, Sopron, Hungary

Abstract – In the course of the implementation of the environmental management system *(EMS)*, during the planning phase, it is of high priority to explore, select and analyse the relevant environmental aspects and impacts. This is the precondition to enhance the real environmental performance *(EP)*. The applied processes are often specific, formal and influenced by the self-interest of a company. The purpose of our work was the uniformly interpretable evaluation of the varied processes, and the creation of an *EMS* enhancement model through which the physical *EP* can be improved. The quantitative empirical research (2010–2011) has been conducted by using questionnaires in 114 domestic and multinational companies applying an *EMS* according to the international standard *ISO 14001*.

In the created database, we have determined the variables which are relevant and adjustable in the process, through a descriptive and multivariable statistical survey. On the basis of the identified performance dimensions, corporate performance indices have been created: the environmental motivation *(MOT)*, environmental performance *(EPI)*, environmental impact evaluation *(EIE)* and environmental management *(EMI)* as well as the aggregative index *(AGG)*. With their help, the evaluation of the surveyed corporate performance can be executed uniformly, in a quantifiable way, without any intervention in the corporate processes. Along the outliers of *EMS* optimization variables, we have identified development points. Their impact was assessed by sensitivity analysis of the indices. The described method offers a model for *EMS* development, based on self-evaluation.

environmental management / impact evaluation / environmental performance indices / development model

Kivonat – A vállalati környezeti teljesítmény fejlesztése. A környezetirányítási rendszer (röviden: *KIR*) mögött rejlő valós környezeti teljesítmény (röviden: *KT*) érdekében a „Tervezési (Plan)” fázisban a környezeti tényezők és –hatások feltárása és elemzése, a releváns környezeti tényezők kiválasztása kiemelt fontosságú a rendszer kiépítése során. A tapasztalatok szerint az alkalmazott eljárások gyakran sajátosak, formálisak, a vállalat egyedi érdekei által meghatározottak. Munkánk során célként tűztük ki a változatos eljárások egységesen értelmezhető értékelését és egy olyan *KIR* fejlesztési modell megalkotását, amely alkalmazásával a fizikai *KT* javítható. A kvantitatív empirikus kutatást (2010–2011) az *ISO 14001* nemzetközi szabvány szerinti *KIR-t* alkalmazó hazai és multinacionális vállalatok között (114 db) végeztük kérdőíves módszerrel.

A létrehozott adatbázisban leíró és többváltozós statisztikai vizsgálatokkal meghatároztuk a releváns és a folyamatban szabályozható, az optimalizálásra ezért potenciálisan alkalmas változókat, a változópárok korrelációit és a témakör főbb teljesítmény dimenzióit jelentő változócsoportokat. Az azonosított teljesítmény dimenziókra alapozottan teljesítmény indexeket (4+1 db) hoztunk létre: környezetvédelmi motivációs *(MOT)*, környezeti teljesítmény *(KTM)*, környezeti hatásértékelési

* Corresponding author: polgar.andras@emk.nyme.hu; H-9400 SOPRON, Bajcsy Zs. u. 4.

(KHÉ) és környezeti menedzsment *(KMR)*, valamint az aggregált index *(AGG)*. Értékeiken keresztül egységesen, relatív, számszerűsíthető módon megadható a vizsgált vállalati teljesítmény adott szintet jellemző értékelése a változatos vállalati folyamatokba történő beavatkozás nélkül. A *KIR* optimalizálási változók szélső értékei mentén az indexek érzékenységvizsgálatával a szignifikáns eltérést okozó változók jelentéstartalma alapján fejlesztési pontokat (36 db) és azok befolyását és területét azonosítottuk. E módszerrel létrehoztuk az önértékelésen alapuló *KIR* fejlesztési modellt.

környezetmenedzsment / hatásértékelés / környezeti teljesítmény index / fejlesztési modell

1 INTRODUCTION

Environmental management system *(EMS)* is part of the management system of an organization with the task to develop and establish, operate and continuously improve the environmental policy of the organization and manage the environmental aspects. The advantage of these systems standardised by international organizations is that they may be certified by specialised certifying systems or authorities (e.g. *ISO 14001*, *EMAS*). Standardized processes providing authoritative (certified) information for competitors and society are being applied worldwide. At the same time it is observable – probably just on the ground of the market competition – that the processes are often specific, formal and influenced by the self-interest of the company.

A number of empirical studies performed in this field have resulted in differing verdicts. Several studies have shown no significant link between measures of environmental performance and profitability (Fogler – Nutt, 1975; Rockness et al., 1986) or between environmental performance and corporate disclosure practices (Freedman – Jaggi, 1982; Wiseman, 1982). But other studies have shown that better pollution performance improved profitability (Bragdon – Marlin, 1972; Spicer, 1978a) and reduced risks (Spicer, 1978b) and that federal compliance liability costs and profitability were negatively related (Holman et al., 1985).

The change in the properties of the environmental elements and systems resulting due to human activity is the *environmental impact*. The *evaluation* of the environmental impact purposes to express the consequence of the change. At the same time, it prepares and establishes measurements and decisions. The evaluation of environmental impacts also provides the basis for the comparison of the different activities according to environmental aspects.

Identification, continuous evaluation and rating of the environmental impacts can be considered as a specific interest for a company. Through the co-operation in environmental protection, it is also of public interest. The environmental management systems (*KÖVET EMS* - Checklist 2007) are playing a key role in managing the domestic corporate environmental impacts (Polgár 2012).

Because of the interrelationships in the complex environmental system, the corporate environmental impacts have to be studied as an integral part of this system. In order to rate the impact on the environment, expert examinations were developed principally in connection to the environmental impact assessments. Beyond that, in the corporate practice, demand emerged for wider systems which measure the necessity of rehabilitation (defining the significant damaging impact). There is a significant need for the indication of positive impacts during performance evaluation (Pájer 2011).

In our survey, we applied the following definition to interpret the concept of the corporate environmental performance *(EP)*: *environmental performance* is the material, energy and information flow which emerges during the normal and abnormal operation state of an organization, impacting the surrounding environmental system in a positive or

negative way, coming from the input or output side (i. e. the physical trend of *EP*), furthermore it is the extent of efficiency of the processes developed in order to manage these flows (i. e. the management trend of *EP*), corrected by the quality properties of the specific impacts regarding the condition and sensitivity of the affected environment.

Due to the rapid spreading of *ISO 14001* more and more companies are applying underlying *EMS* evaluation methods (Savage 2000). During the *EMS environmental impact evaluation process*, the main purpose of the evaluation of the environmental factors is to determine the harmful changes caused in the state of the environment. In the course of the evaluation, the occurrence probability and seriousness of the harmful change is required to be taken into account.

Kerekes – Kindler (1997) draws the attention to the fact that companies possessing the *ISO 14001* certificate need not qualify as environmentally friendly. According to the international standard requirements, improvement of *EP* may be measured and accepted by auditors, based purely on the adequacy regarding regulations (i. e. the management *EP*). The physical, environmental aspects can be overshadowed by the management trend (Seifert 1998).

The *survey, consideration and comprehension of environmental aspects and impacts* of the organization is the element of the 'Plan' phase. It is also the *most essential* element of the whole system implementation. It requires particular consideration, during its examination; engineering and technical accuracy is needed and it is of course the step requiring highest creativity (Nagy – Torma – Vagdalt 2006). This is the basis of the formulation of the environmental policy as well as the set-up for environmental objectives, and for the selection of priorities.

We stated that the *EMS* impact evaluation processes usually generate results during the evaluation (application of ordinal scale) by binary ranging of impacts (significant and non-significant impacts). During our survey, we studied mainly the application and the further developed forms of the *ABC* analysis, from among the matrix techniques of impact assessment methods (Pájer 1998, Rédey – Módi – Tamaska 2002, Nagy – Torma – Vagdalt 2006, Polgár 2011). In order to expand the environmental information achieved by an *EMS* impact evaluation process, we recommend further environmentally aware corporate management instruments, by which the efficiency of the 'Plan' phase can be improved (Polgár 2012).

We found that compared to other environmental performance evaluation methods, the *EMS* impact evaluation process showed the minimum complexity of the application and of the aggregation level (on the basis of the classification of Torma, (2007).

Hofstetter (1998, cited by Frischknecht, 2005), distributed the decision support tools by matrixes between methods being interpretable on micro-, meso- and macro-level, and analysing social, environmental and economic properties. We concluded that in this distribution, the *EMS* environmental impact evaluation is applicable on meso-level (within project level). It can be considered as a method describing the environmental dimension. From the point of view of environmental management system on meso-level, on the basis of the classification modifications recommended by Torma (2007), it provides a technique covering social, environmental, economical dimensions.

We organized the main idea of our survey around the concept of Winter (1997). According to it, the result based on the environmental impacts reflecting in the *EP* will rely on whether the companies and advisers implementing the system, attempt to build up a functioning system, or they are satisfied with an accurately documented (and certifiable) system, which may not function.

The purpose of our survey was the uniformly interpretable evaluation of the varied processes. Furthermore the creation of an *EMS* development model concept aimed at the functional utilization of the results and the improvement of the parameters concerning the physical *EP*. We tried to find the answers to the following questions: Which are the main

efforts of the organizations applying *EMS* to fulfil the international standard requirements? What is the role of the 'Plan' phase in the improvement of the efficiency of *EMS*? Which parameters do play a role in its optimization? Which are the determinant dimensions of environmental performance in the 'Plan' phase? How and at what level can the *EMS* practice of companies be assessed? How can the efficiency of *EMS* be improved in practice?

2 MATERIAL AND METHOD

We assumed that there are factors along which, from the point of view of the physical *EP*, the optimization process of *EMS* is *biased*. This could be, for example, the low level of management of environmental impacts or the overemphasising of management issues.

The cardinal point of the proper operation is to identify and evaluate the relevant pairs of 'environmental factor-environmental impact' in a more accurate way *based on environmental science.* This will be followed by the *integration of this environmental information* in the process of the determination of the environmental objectives. In the *PDCA* cycle (Plan – Do – Check – Act) operating the *EMS*, this process is covered by the 'Plan' phase ("Planning – Execution – Control – Action" or *PDCA* method).

Specifically in the physical *EP* dimension, the description of the *"partial" performance pertinent to the management of the environmental impacts* was defined on the basis of the detection of the variables and *optimization parameters* of the 'Plan' phase and the *EMS* impact evaluation process *(Figure 1.)*.

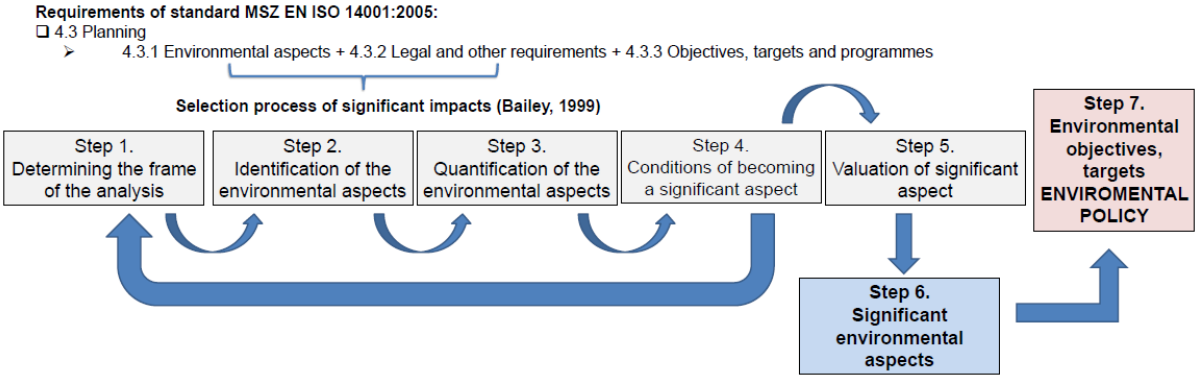

Figure 1. Requirements of the Plan phase and the process of selection of significant impacts in the standard ISO 14001 (Bailey 1999) (own design)

Our quantitative empirical research (2010–2011) has been conducted by using questionnaires in 114 multinational and domestic companies (sampling ratio: 9,89%) applying *EMS* according to the standard *ISO 14001*. The answers were controlled on the basis of the opinion of 10 certification companies (sampling ratio: 62,5%). The sample contained mainly medium-sized companies (55%), but in smaller part, small (13%) and large (18%) as well as micro-enterprises (8%) were represented.

Regarding the industrial classification provided, the following branches were represented mainly equally: metal industry, automobile industry, mining industry, health care, furniture industry, packaging industry, telecommunications, food industry, energy industry, forestry, manufacturing industry, service and trade, machine industry, chemical industry, waste management, waterworks, environmental protection, research and development, agriculture, plastics industry, printing industry, heavy industry, building industry, traffic, transport, glass industry.

In the sample of companies, energy and construction were represented in larger proportion; the organizations of waste management and chemical industry were present in moderate proportion.

Table 1 shows the regional distribution of the examined sample from the company universe, i.e. of the 1153 organizations certified by the international standard *ISO 14001* (*KÖVET EMS* -Checklist 2007).

Table 1. Geographical distribution and proportion of the company universe and of the sample

Region	**Company universe** (number)	**Proportion (universe)** (%)	**Company sample** (number)	**Proportion (sample)** (%)	**Sample ratio** (%)
Foreign countries	3	0,26	9	7,89	300,00
Budapest	315	27,32	27	23,68	8,57
Middle-Hungary	113	9,80	12	10,53	10,62
West-Transdanubia	123	10,67	15	13,16	12,20
Middle-Transdanubia	143	12,40	15	13,16	10,49
South-Transdanubia	135	11,71	7	6,14	5,19
North-Hungary	90	7,81	8	7,02	8,89
North-Alföld	137	11,88	7	6,14	5,11
South-Alföld	94	8,15	6	5,26	6,38
ND	0	0,00	8	7,02	0,00
Total	**1153**	**100,00**	**114**	**100,00**	***9,89***

We analysed the general level and motivations of the environmental management of companies; the characteristics of the methodologies applied in environmental impact evaluation; questions relating *EMS* application and environmental objectives (integrated management, conflicts); the role of *EMS* in influencing the state of environmental elements; the specific environmental arrangements; and the main company efforts in operating of *EMS*.

In case of the main differential factors (customized solutions and purposefulness of *EMS*, application of *EMS* in the future, attitude of the senior management, year of initiation etc.) the ’best practices’ could be filtered out by the processes accommodated to other parameters by strong organizations.

We counted the relevant *optimization parameters* detected in the course of the questionnaire survey for *indicators*. These indices indicated the *manner* of the application of the standard requirements, on the basis of which we *qualified* the efforts. By the *numerical qualification of the specific indices* we *envisaged evaluable developments*.

Besides the descriptive statistics (frequency analysis), we executed multivariable statistical evaluation of the data base of the questionnaire survey (correlation analysis, factor analysis by: varimax rotation and cluster analysis, by hierarchical average linkage clustering and K-means method).

For quantification we constructed performance indices by merging the connectable parameters. We aggregated the information accordant to the meaning of the indices. With the aim of detecting the correspondent variable groups, i. e. the dimensions of performance we applied principal component analysis *(PCA)*.

On the base of the parameters influencing corporate *EP*, we created 4 corporate performance indices: environmental motivation *(MOT)*, environmental performance *(EPI)*, impact evaluation *(EIE)* and management *(EMI)* (applying the method of Pataki – Tóth, 1999).
For the indices we used the quantifiable variables. The structure of the created system and the point values were covered in ’index background tables’ *(Table 3)*. We accomplished

the description of the merged performance of respondents by defining a fifth, aggregative index *(AGG)*.

By the created quantified index values, the post-development, relative evaluation of the corporate performance is uniformly executable, without intervention in the varied corporate processes.

In case of the created indices (answers: *'A'* – unfavourable and *'B'* – favourable group), we examined the performance of respondent organizations by sensitivity survey and histogram analysis depending on the main parameters. In the course of the sensitivity analysis of the indices, we interpreted the variables causing significant differences as development suggestions. The detected effects of parameters and the arrangements made for their improvement give the opportunity to estimate the fields of corporate development for the sake of improvement of *EP* in the course of implementation and operation of *EMS*. Some of the summary of the influences of the identified 36 development opportunities can be found in the'Auxiliary Table' of *Table 4*.

The application of the background and auxiliary tables of indices opens up the opportunity for the expedient development of the performance and efficiency of the *EMS* 'Plan' phase. In order to support this, we elaborated a self-evaluation based *EMS* development model for the determination of most appropriate developments by organizations *(Figure 4)*. With the help of indices, the efforts can be expressed in a quantitative way. The evaluation method identifies the weak and strong points, and determines the appropriate and effective developments, providing a decision support.

3 RESULTS

3.1 The main results of frequency analysis

We detected the efforts of the respondents according to the *EMS* operation. The efforts, examined by the function of the certain phases of *PDCA* cycle and the time, occurred at maximum frequency significantly in the 'Plan' phase (in 68% of the organizations). Increased activity occurred mainly regarding the environmental factors and environmental goals (32%), within the first three years from the implementation of *EMS*. The users were encouraged to significant and permanent efforts by the renewing objective system (18%) and the legal and other requirements (15%).

We have proved the importance of the environmental motivation (attitude) in the environmental impact based optimisation of *EMS*, as one of the determinants of the frame of impact evaluation.

Quantifiable benefits from the application of the *EMS* accrued at more than the half of the organizations (53%). The emergence of benefits had a favourable effect on the motivation of the organizations. It plays an indirect role in the environmental impact based optimisation of *EMS*.

We have concluded that the appropriate customization of *EMS* favourably developed the handling of environmental aspects/impacts.

We evaluated the application frequency of the additional corporate environmental management means playing a role in customization *(Figure 2.)*.

We have stated that techniques requiring profound environmental survey, considerable resources and efforts is still at low level in the *EMS* impact evaluation processes. We have demonstrated that concerning the methods applied in environmental impact assessment, mostly own company methodology (82%) was adopted. In case of the majority (70%) of the organizations the review of factors was required. We have found that certain corporate methods provide environmental information at low level.

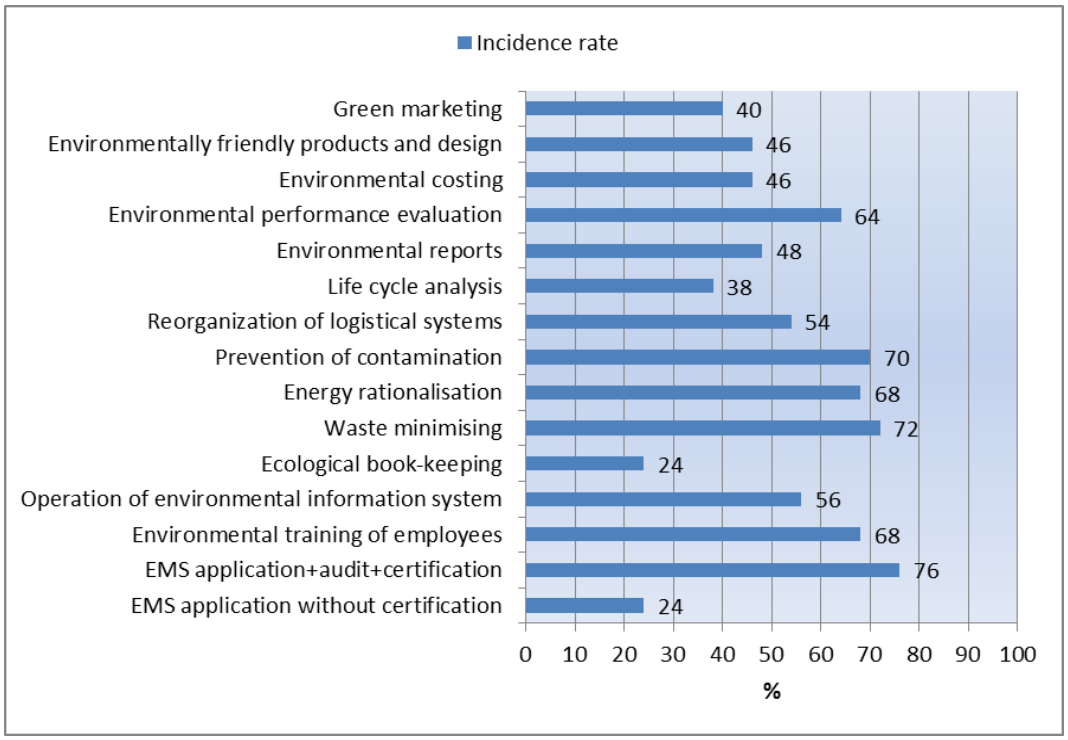

Figure 2. Application frequency of environmental management means in organizations (%)

Among the conditions of becoming significant factor, we identified the data, derived from the technological knowledge, as strong environmental information with regard to the detection and evaluation of the impact factors in the company practice. By this also the important criterions of legal and environmental science become strong aspects in the decision process. We mainly had available data related to the environmental impacts of technology, which we had found well covered in the corporate material and energy balances.

Realization effectiveness of objectives, compared to the envisaged ones, has brought slightly better results in the long-term (87%) than after the first *EMS* certification (79%).

We examined the progress of the facilitating/aggravating factors of the operation of *EMS* in the first three years, presented in *Figure 3*.

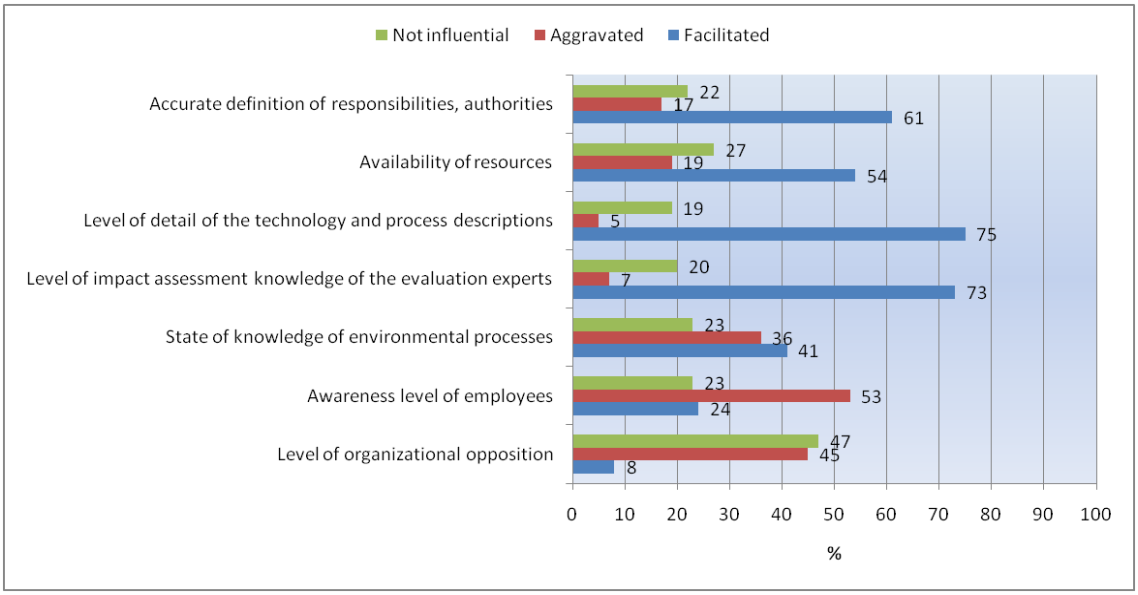

Figure 3. Influencing factors of the operation of EMS in the first three years

Regarding the role of *EMS* in influencing the condition of environmental components, a definitely strong positive influence (average value: 4,10; range: 1,00–5,00) can be noticed among those companies applying *EMS*.

3.2 Factor and cluster analysis

The reduced database of questionnaire survey was subjected to principal component analysis. The result of factor analysis indicated that the *EP* of the industrial companies performing in the survey and the effectiveness of *EMSs* can be explained and separated characteristically along six dimensions:

- factors of proactivity, verification of environmental impacts, adequate objectives and *EMS* procedure proved to be common principal components, while
- factors of exterior motivation (business partners) and interior audit occurred as specific indices.

As an auxiliary step of the survey, we executed the rotation recommended for validation. The Varimax rotation confirmed the above interpretation of the factor matrix.

By simplifying the dimensions of performance we have created a manageable structure eligible for further examinations. The dimensions are as follows:

- motivation for environmental protection
- environmental performance
- environmental impact evaluation
- environmental management.

On the basis of the results of the factor analysis, we have grouped the companies with cluster analysis. Firstly, we run a hierarchical cluster analysis, measuring the distance by average linkage clustering. The analysis has demonstrated 2 separated cluster structures. Following that, we carried out the K-means cluster analysis, where again 2 clusters appeared:

- 41 elements in the first cluster (‘Formalists’)
- the second cluster contained 73 companies (‘Environmental performance oriented’)

The result confirmed the opinion of Winter (1997), according to which the companies belong to distinct groups, the *formal* and the *EP-oriented* group. Thus, the optimisation of the application of *EMS* has the potential for the development of physical *EP* and a beneficial influence on the environment.

3.3 Summary of developments

3.3.1 Construction of performance indices

We have demonstrated that the improvement of physical *EP* can be executed through the development of the ‘Plan’ phase and through evaluation of the *EMS*. Our research has detected the factors and the characteristics of best practice which influences the result of the ’Plan’ phase process directly and the whole *EMS* indirectly.

We have demonstrated that the relevant *EMS* optimisation variables affect the level of the ’Plan’ phase and the *EMS* impact evaluation process. According to the meaning of the variables we executed their grouping (partial performance dimensions).

In order to characterise variable groups as dimensions, we constructed the following indices: environmental motivation *(MOT)*, environmental performance *(EPI)*, environmental impact evaluation *(EIE)* and environmental management *(EMI)*. We have summarised the performance indices and the values of the company sample in *Table 2*.

Table 2. Data of constructed EMS performance indices

EMS performance index	Abbrevi-ation	Number of variables	Index value (1,00–5,00)	Deviation
1. Environmental motivation index	MOT	15	3,14	0,74
2. Environmental performance index	EPI	6	3,49	0,66
3. Environmental impact evaluation index	EIE	16	3,09	0,61
4. Environmental management index	EMI	26	3,05	0,50
5. Aggregative index	AGG	–	3,20	0,20

The structure of each index is found in a background table *(Table 3),* which provides detailed, quantifiable information about the partial performance peculiar to the corporation.

Table 3. Example. Construction of the environmental motivation index (MOT)

Motivation topic	Variable	Evaluation
Motivation of environmental actions	External motivations ***Strict regulatory system*** ***Expectations of banks and insurers*** ***Requirements of business partners*** Expectations of competitors Market and customer demands ***Strong influence of local population*** *Civil organizations* Internal motivations ***Expectations of the owners*** Nature of product/service Expectations of the employees	yes = 5 points no = 1 point
Motivation implied by the quantifiable benefits	Quantifiable benefit	yes = 5 points no = 1 point
Motivation for the future application of *EMS*	***Future application of* EMS**	essential = 5 points neutral = 3 points unnecessary = 1 point
Environmental awareness of the senior management in the determination of environmental objectives	Determination of the environmental objectives ***Environmental awareness of the senior management*** ***Environmental strategy of the organization***	yes = 5 points no = 1 point
Motivation for the environmental purpose orders (in the last 3 years)	Order for environmental purpose	yes = 5 points no = 1 point

Variables in italics: parameter identified by correlation analysis; **variable marked in bold:** parameter with large principal component weight; non-marked variable: variable built in with process-oriented approach.
The index represents the following environmental motivations: extent of the environmental external-internal motivation, occurrence of the quantifiable benefits, approach for the future application of the *EMS*, environmental awareness of the senior management, environmental strategy of the organization and the orders for environmental purpose.

In order to weigh the variables, we could have used either the relevant variables of the correlation analysis on the basis of the equivalency ratios (classification factors) or the direct application of factor weights. The calculation of independent variables with smaller weight would not have been accurate, because by this we would have ignored the individual importance of the information content of the variables. We dispensed with these techniques the opinion of Miakisz (1999).

We chose the average of the variables as the appropriate method to calculate the values of the indices, in which we calculated the variables with equal weight.

We created the aggregative index *(AGG)* by averaging the values of the *EMS* indices, in order to express the result of the survey in one single number without dimension. The different sensitivity of the indices influences the *AGG* value. This effect is largely originating from the higher sensitivity of the *EPI* index. The more robust sensitivity of the *EMI* index results from the fact that the included variables are almost the twice of the variables of the other indices. *MOT* and *EIE* indices have normal sensitivity. The value of the aggregative index *(AGG)* was 3,20, i. e. average (range: 1,00–5,00; deviation: 0,20).

We developed an evaluation method to apply the indices, by which we have the possibility to rate the performance per dimension and the aggregate partial performance of the participants. Furthermore, the method enables intra-corporate self-assessment under certain conditions, additionally inter-corporate comparison concerning the survey period. We achieved this without modification of the processes identified in the organizations.

Performance indices were established per organization. In order to quantify environmental information we used the evaluation of each variable as a base (range of values: 1–5). By quantifying the information we gave the organizations the opportunity for self-evaluation. The results were usable for status review concerning each index and their variables. In the variable groups (in partial performance dimensions) we calculated the typical performance characterized by the index averages. This provided information about the efficiency of the 'Plan' phase development in the given period.

3.3.2 EMS development model based on self-evaluation

In the course of the sensitivity analysis of the indices, we interpreted the variables causing significant differences as development suggestions. We identified the potential result of the improvements from index averages. Targeted developments can be assigned to certain performance dimensions. To support the assignment process, we elaborated detailed auxiliary tables *(Table 4).* In case of the certain indices, we ranked the significance of the impact of *EMS* variable from 1 to 4. Finally we interpreted the differences observed in the aggregative index, as the complete, partial, specific or neutral speciality of the impact related to index dimensions. The ranking of the *EMS* variables was based on the differences of the average values experienced in the aggregative index.

To put our research achievements into practice, we evolved the self-evaluation based *EMS* development model *(Figure 4).*

Table 4. Example. Auxiliary table: Identified impact of EMS variables upon the indices

EMS variable	**Impact of EMS variable**					**Ranking: difference experienced in aggregative index (B-A)**
	MOT	**EPI**	**EIE**	**EMI**	**AGG**	
Application of environmental performance evaluation system	2	(1)	3	4	complete	0,7
Articulation of environmental objectives to the local significant aspects	2	3	(1)	4	complete	0,47
Importance of the future application of *EMS*	(1)	3	4	2	complete	0,46
Targetedness of *EMS*	2	(1)	3	4	complete	0,45
Extension of the data in the material and energy balance of the organization to the factors on which the organization has an expectable influence	1	3	4	(2)	complete	0,44
Environmental awareness of senior management in setting environmental objectives	(1)	3	4	2	complete	0,43
Application of impact register	4	(1)	3	2	complete	0,41
Customization of *EMS*	3	2	4	(1)	complete	0,4
Preventive approach in the documented environmental processes of the organization regarding the material/ energy consumption and emissions	2	3	4	(1)	complete	0,35
Careful treatment in the documented environmental processes of the organization regarding the material/ energy consumption and emissions	2	3	0	(1)	complete	0,51
Adequacy for legal requirement in the selection of significant environmental factors	2	0	(1)	0	partial	0,44
Environmental strategy of the organization in setting the environmental objectives	(1)	3	2	0	partial	0,43
Expectation of the owners	(1)	0	0	0	specific	0,43
Certification of the suppliers	0	(1)	0	0	specific	0,37
Recycling in the documented environmental processes of the organization regarding the material/ energy consumption and emissions	1	0	0	(2)	partial	0,34
Application of LCA	3	(1)	2	0	partial	0,34

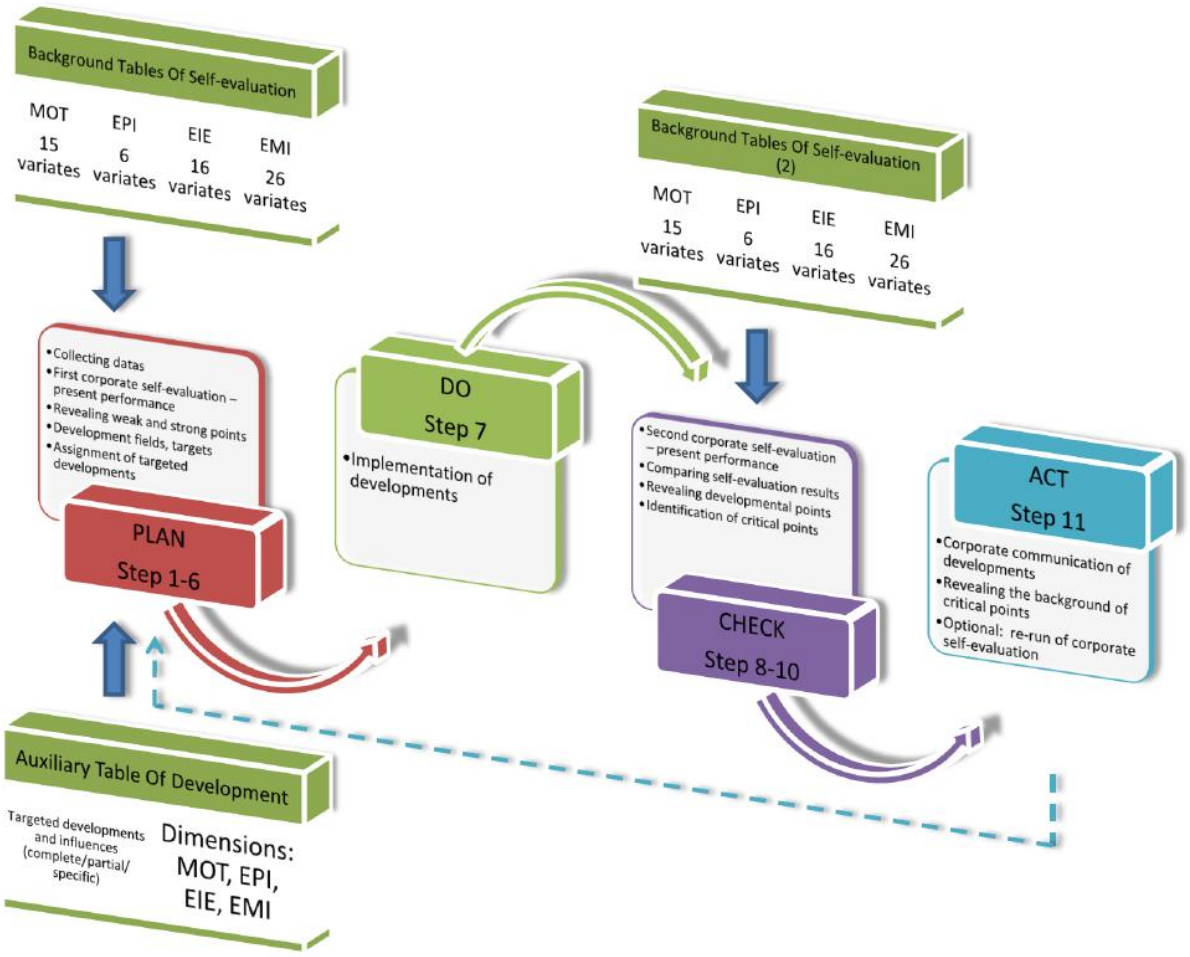

Figure 4. Model flowchart: the EMS development model based on self-evaluation for the 'Plan' phase of EMS according to the principle PDCA

Through the model, we created a system of correlations and formulated technical recommendations for defining and programming the targeted development tasks. This is a decision support tool *(Step 1-11)* for the continuous improvement of *EMS*, in the surveyed partial performance dimension according to the principle *PDCA*.

From Step 1 to Step 11:

I. 'Plan' phase of the model:

Step 1, START:

- *Function:* Study of the *EMS* performance indices (4+1 pcs) and their variables applied in the model in regard of the values definable by the organization. Collection of data.
- *Result:* Criterion: All of the *EMS* variables are evaluable concerning the organization: MOT (15 variables), EPI (6 variables), EIE (16 variables), EMI (26 variables), AGG.
  Preparation of evaluation: background tables of the indices and their variables, development auxiliary tables. Collected environmental data of company.

Step 2:

- *Function: First corporate self-evaluation* by the indices meaning the performance dimensions and their valuable variables. Status review. Completion background tables.
- *Result:* First completed self-evaluation. Quantifiable values by variables and indices, as well as in case of aggregated index. Completed background tables. Registration of the certain environmental performance of *EMS*. (1,00–5,00).

Step 3:

- *Function:* Examination of the results of self-evaluation by variables and indices.
- *Result:* Detection of weak and strong points. Interpretation of the first self-evaluation of organization.

Step 4:

- *Function:* Analysing the manageability of the weak points.
- *Result:* Establishment of order of priority for the development of weak points.

Step 5:

- *Function:* Determination of development fields on the level of evaluated variables and indices (by priorities), application of background tables.
- *Result:* Development objectives set out concerning the certain variables and indices (by priorities).

Step 6:

- *Function:* Assignment of the relevant *EMS* variables relating to the selected development objective(s), forecast of their expected impact by using the auxiliary tables 1 and 2.
- *Result:* Development program: *EMS* variables assigned to the targeted development(s). Identified targeted development field(s) and expected impact(s).

II. 'Do' phase of the model:

Step 7:

- *Function:* Realising the development objective(s) according to the meaning of the *EMS* variable and in view of the expected impact.
- *Result:* Execution of development(s).

III. 'Check' phase of the model:

Step 8:

- *Function: Second corporate self-evaluation* by the indices meaning the performance dimensions and their valuable variables for the assessment of achievement(s). Completion background tables.
- *Result:* Second corporate self-evaluation. Quantifiable values by variables and indices, as well as in case of aggregated index. Completed background tables. Registration of the environmental performance of *EMS*. (1,00–5,00).

Step 9:

- *Function:* Comparison of the achievements of the targeted and realized development field(s). Controlling of the field and extent of development by variables and indices.
- *Result:* Interpretation of the second self-evaluation of organization. Comparison with the results of the first self-evaluation by variables and indices.

Step 10:

- *Function:* Detection and identification of development point(s). Determination of critical point(s).
- *Result:* Detected development and critical point(s).

IV. 'Act' phase of the model:

Step 11, STOP:

- *Function:* Inter-corporate communication of the realised development(s). Detection of the background of critical points. *Optional:* Re-run of the corporate self-evaluation after the carry out of the priorities based on the first self-evaluation.
- *Result:* Feedback to the 'Plan' phase *(Step 1.)*.

4 CONCLUSIONS

The *EMS* impact evaluation process is one of the uppermost means of environmentally aware corporate management at the disposal of the organizations for developing their *EP*.

In certain cases, corporate methods are below the minimal requirements of the *ISO 14001* international standard. They only provide environmental information at low level. The development of this situation and improvement of environmentally aware corporate management are key points in the course of improvement of physical *EP* of the *EMS*.

In the course of our methodical research, we have achieved a potential indirect development of the physical *EP*. The identified, potential development efforts affected the planning parameters pertinent to the treatment of the environmental aspects and impacts. We ensured the uniform evaluation of different organizations. It does not require the modification of the varied corporate processes, and provides the opportunity for comparison. The developed model is a development and decision support tool. Through applying the model, the organizations will be able to improve the efficiency of the 'Plan' phase and their environmental management system.

Acknowledgement: We express our sincere thanks to ass. prof. Dr. Botond Héjj CSc., Dr. László Tamaska, director, Dr. Olivér Bogdán, director and János Nagy, head auditor, who all assisted us with useful advice. Without the cooperation of the companies and certification authorities this work could not have been achieved.

REFERENCES

BAILEY, A. (1999): Környezeti auditálás [Environmental audit]. In: BAILEY, A. – BEZEGH A. – FRIGYER A. – BÁNDI GY. – GALLI M. – KEREKES S. – TÓTH G. (1999): Környezeti vezető és auditor képzés. [Training of Environmental Managers and Auditors] Magyar Szabványügyi Testület (MSZT), Budapest : 79–88. (in Hungarian)

BRAGDON, J. H., MARLIN, J. A. T. (1972): Is pollution profitable? Risk Management, 19(4): 9–18.

FOGLER, H. R., & NUTT, F. (1975): A note on social responsibility and stock valuation. Academy of Management Journal, 18: 155–160.

FREEDMAN, M., – JAGGI, B. (1982): The SEC's pollution disclosure requirements – Are they meaningful? California Management Review, 24(2): 60–67.

FRISCHKNECHT (2005): Methoden der Umweltbewertung technischer Systeme, Teil 1: Ökobilanzen (Life cycle assessment, LCA), ETH Zürich, Studiengang Umweltnaturwissenschaften, Sommersemester, Zürich

HERCZEG, M. (2005): Környezetmenedzsment. [Environmental Management] Budapesti Műszaki és Gazdaságtudományi Egyetem Környezetgazdaságtan Tanszék. Budapest (in Hungarian)

HOFSTETTER, P. (1998): Perspectives in Life Cycle Impact Assessment. A Structured Approach to Combine Models of the Technosphere, Ecosphere and Valuesphere. Kluwers Academic Publishers

HOLMAN, W. R., NEW, J. R., & SINGER, D. (1985): The impact of corporate social responsiveness on shareholder wealth. In L. Preston (Ed.), Research in corporate social performance and policy, vol. 7: 137–152. Greenwich, CT: JAI Press.

ISO 14001: Environmental management systems. Specification with guidance for use (ISO 14001:2004), Hungarian Standards Institution, Budapest, 2005

ISO 14031: Environmental management. Environmental performance evaluation. Guidelines (ISO 14031:1999). Hungarian Standards Institution, Budapest, 2001.

KEKEKES, S. – KINDLER, J. (eds.) (1997): Vállalati környezetmenedzsment. [Corporate Environmental Management] Budapesti Közgazdaságtudományi Egyetem, Budapest. (in Hungarian)

KÓSI, K. – VALKÓ, L. (1999): Környezetgazdaságtan és –menedzsment. [Environmental Economy and –Management] Eötvös József Főiskola Műszaki Fakultás, Baja (in Hungarian)

KÖVET Egyesület a Fenntartható Gazdálkodásért, KIR – lista [KÖVET Association for Sustainable Economies, EMS Check-list]. 2007
(On-line: http://www.kovet.hu/ISO14001/Linkek/KIRnyilvantartas.htm) (in Hungarian)

KUN-SZABÓ, T. (1999): A Környezetvédelem minőségmenedzsmentje. [The Quality Management of Environmental Care.] Műszaki Könyvkiadó, Magyar Minőség Társaság, Budapest (in Hungarian)

MIAKISZ, J. (1999): Measuring and Benchmarking Environmental Performance in the Electric Utility Sector: The Experience of Niagara Mohawk. In: BENNETT, M. – JAMES, P. (eds.): Sustainable Measures, Greenleaf Publishing, Sheffield, p. 221–245.

NAGY, G. – TORMA, A. – VAGDALT, L. (2006): A környezeti teljesítmény javítása és értékelése [The Development and Evaluation of Environmental Performance]. Universitas-Győr Nonprofit Kft., Győr, (in Hungarian)

PÁJER, J. (2011): A környezeti terhelés minősítése. [The Qualification of the Environmental Loads.] In: LAKATOS F., SZABÓ Z. (eds.): Nyugat-magyarországi Egyetem Erdőmérnöki Kar Kari Tudományos Konferencia Kiadvány. [Proceedings of the Scientific Conference of the University of West Hungary Faculty of Forestry] NyME Kiadó, Sopron, p. 14. (in Hungarian)

PATAKI, GY. – TÓTH, G. (1999): Vállalati környezettudatosság, GEMS-HU jelentés [Corporates' Environmental Awareness, Global Environmental Management Survey in Hungary (GEMS-HU) Report], KÖVET , Környezettudatos Vállalatirányítási Egyesület, Budapest (in Hungarian)

POLGÁR, A. (2011): Környezetirányítási rendszerek hatáselemzésének vizsgálata. Analysis of Impact Assesment of Environmental Management Systems.] In: A Nyugat-magyarországi Egyetem Savaria Egyetemi Központ Tudományos Közleményei XVIII. Természettudományok 13. Supplementum – VI. Euroregionális Természettudományi Konferencia Konferencia Kiadványa. NymE Kiadó. NymE-SEK-TTK: 163–168., Szombathely. ISSN 0864-7127, HU ISSN 2061-8336 (in Hungarian)

POLGÁR, A. (2012): Környezeti hatásértékelés a környezetirányítási rendszerekben. [Environmental Impact Evaluation in the Environmental Management Systems]. Doctoral (PhD) Dissertation. Sopron, 380 p. (Online: http://ilex.efe.hu/PhD/emk/polgarandras/disszertacio.pdf) (in Hungarian)

RÉDEY, Á. – MÓDI, M. – TAMASKA, L. (2002): Környezetállapot-értékelés. [Environmental State Evaluation] Veszprémi Egyetemi Kiadó. Veszprém, p. 8., 50. (in Hungarian)

RÉDEY, Á. (2008): Környezetmenedzsment rendszerek. A felsőoktatás szerkezeti és tartalmi fejlesztése. [Environmental Management Systems. Structural and Material Development of the Higher Education] HEFOP 3.3.1-P.-2004-0900152/1.0. Veszprém, p. 24., 27., pp: 81–82. (in Hungarian)

ROCKNESS, J., SCHLACHTER, P., & ROCKNESS, H. O. (1986): Hazardous waste disposal, corporate disclosure, and financial performance in the chemical industry. In M. Neimark (Ed.), Advances in public interest accounting, vol. 1: 167–191. Greenwich, CT: JAI Press.

SAVAGE, E. (2000): MSV and public disclosure of performance goals are key agenda issues, Chemical Market Reporter, May 22, 2000, Vol. 257, Iss. 21, New York, p. 25.

SEIFERT, E. K. (1998): Kennzahlen zur Umweltleistungsbewertung – Der internationale ISO 14031-Standard im Kontext einer zukunftsfähigen Umweltberichterstattung. In: SEIDEL, E. – CLAUSEN, J. – SEIFERT, E. K.: Umweltkennzahlen, Verlag Vahlen, München, p. 71–120.

SPICER, B. H. (1978a): Investors corporate social performance and information disclosure: An empirical study. Accounting Review, 53: 94–111.

SPICER, B. H. (1978b): Market risk, accounting data, and companies' pollution control records. Journal of Business, Finance, and Accounting, 5: 67–83.

TORMA, A. (2007): A környezeti teljesítményértékelés aggregáló módszerei és az anyagáram-elemzés kapcsolatrendszere – Egy integrált vállalati modell megalapozása. Doktori értekezés [The Relationship Between the Aggregation Methods of Environmental Performance Evaluation and Material Flow Analysis. Establishment of an Integrated Corporate Method.] Doctoral (PhD) Dissertation. BMGE-GTK, Budapest. (in Hungarian)
(On-line: http://www.omikk.bme.hu/collections/phd/Gazdasag_es_Tarsadalomtudomanyi_Kar/2008/Torma_Andras/ertekezes.pdf)

WINTER, G. (1997): Zölden és nyereségesen. [Green and Profitable.] Műszaki Könyvkiadó Budapest, (in Hungarian)

WISEMAN, J. (1982): An evaluation of environmental disclosures made in corporate annual reports. Accounting, Organizations, and Society, 7: 53–63.

Introduction to Papers on Catchment Processes in Regional Hydrology: from Experiment to Modelling in Carpathian Drainage Basins

Regional understanding and modelling of hydrological processes in catchments is becoming increasingly essential for addressing questions in science as well as in practical water resource management questions. Evaluation of process representation in hydrological catchment models compared with results from modelling and catchment experiments has become therefore more important in recent years especially in the context of climate change.

Data availability and assimilation based on latest developments in remote sensing, experiments on hillslopes, and tracer studies in catchments gave hydrologists the opportunity to compare different models of the same type (e.g. distributed) or different types of models (e.g. distributed vs. lumped, process based vs. conceptual) on a regional basis. The new data also supports the study and generalisation of hydrological regimes. All these activities support better process representation in both deterministic and stochastic models in diverse hydrological environments.

In the series of similar symposia, the *International Symposium on Catchment processes in regional hydrology: from experiment to modelling in Carpathian drainage basins (Hydrocarpath 2013)* was organised by the Department of Water Management, at the Institute of Geomatics and Civil Engineering, Faculty of Forestry, at the University of West Hungary in Sopron, in cooperation with the Department of Land and Water Resources Management, Faculty of Civil Engineering, at the Slovak University of Technology in Bratislava. This conference welcomed contributions on hydrology which focus on the following issues: Presentation of results from catchments experiments leading to better process understanding and representations; Regionalisation and generalisation of hydrological regimes on various temporal and spatial scales using increased process knowledge; Comparison of similar model types as well as different model types (conceptual, process based, distributed, lumped); Soil, vegetation and atmospheric interactions especially focusing on forests. The texts of the presentations were published in a reviewed proceeding.

In cooperation with the editorial board, some authors were invited to submit their manuscripts to *Acta Silvatica* & *Lignaria Hungarica.* The papers were selected and reviewed by international experts in hydrological science mainly from the scientific committee of the conference, based on scientific excellence and relevance of the problem that was investigated. It is the expectation of the organisers that these papers will contribute to the better knowledge of the hydrology and catchment processes.

Zoltán Gribovszki
guest editor

DE GRUYTER OPEN DOI: 10.2478/aslh-2014-0005 Acta Silv. Lign. Hung., Vol. 10, Nr. 1 (2014) 67–75

Diurnal Method for Evapotranspiration Estimation from Soil Moisture Profile

Zoltán GRIBOVSZKI*

Institute of Geomatics and Civil Engineering, University of West Hungary, Sopron, Hungary

Abstract – Water use of plants is manifested in diurnal signal of soil moisture changes, and also in water table fluctuations in shallow water table environments. The signal can be especially strong in case of groundwater dependent forest vegetation with high water demand, where the water uptake is partly happening across the capillary zone. A new technique for water uptake estimation was elaborated on the basis of high frequency soil moisture profile data taking into account diurnally changing replenishment rates. The method is of great benefit to provide sufficient accuracy without soil specific calibration. The method was tested on the soil moisture dataset of a riparian alder forest in Hidegvíz Valley experimental catchment. Using this new method significantly higher and more realistic water uptake can be calculated compared to the traditional soil moisture method. The method is taking into account soil moisture replenishment from groundwater, which can provide a high portion (up to 90%) of evapotranspiration in dry periods. For the above mentioned reason the new technique is recommended to be used for evapotranspiration estimation in groundwater discharge areas, where the traditional methods and simple one-dimensional hydrological models are generally inaccurate.

diurnal signal / water uptake / replenishment rate / discharge areas

Kivonat – A talajnedvesség profil napi ingadozásán alapuló párolgásbecslő módszer. A növényi vízfelvétel hatása sekély talajvízű területeken megjelenhet a talajnedvesség és a talajvízszint napi ciklusú ingadozásában is. Ez az ingadozás különösen erős lehet a nagy vízigénnyel jellemezhető, talajvízfüggő erdőtársulások esetében, ahol a vízfelvétel részben a kapilláris zónán keresztül történik. A talajnedvesség nagy frekvenciás mérésén alapuló új vízfelvétel becslésére alkalmas technika került kifejlesztésére, amely napon belül változó talajvízutánpótlás figyelembevételével dolgozik. A módszer nagy előnye, hogy talajspecifikus kalibrálás nélkül is megfelelő pontosságot szolgáltat. Az új eljárás az Alpok keleti lábainál fekvő Hidegvíz-völgy kísérleti vízgyűjtőjében található vízfolyásmenti égeres talajnedvesség profil adatain került tesztelésre. Az új módszerrel lényegen nagyobb és az adott körülményeknek pontosabban megfelelő vízfelvétel számítható, mint a tradicionális talajnedvesség mérésen alapuló módszerekkel. Az új eljárás a talajvízből táplálkozó talajvízutánpótlódással számol, ami igen jelentős részét (akár 90%) is képezheti a száraz periódusokban az evapotranszspirációnak. Az előbbi okból kifejezetten javasolt az eljárás a párolgás becslésére, a sekély talajvíztükörrel rendelkező talajvíz feláramlási zónákban, ahol a szokványos módszerek és az egyszerű egy-dimenziós hidrológiai modellek általában pontatlanul működnek.

napi ingadozás / vízfelvétel / utánpótlódás / feláramlási területek

* Corresponding author: zgribo@emk.nyme.hu; H-9400 SOPRON, Bajcsy-Zs. u. 4.

1 INTRODUCTION

In Hungary the evapotranspiration (*ET*) is about 90% of the precipitation therefore it is a very important part of the water balance (it must be noted that globally "only" 62% of the rainfall is evapotranspired from the continents (Dingman 2002)). In spite of its significance, ET is treated generally as a lumped residual flux from a water budget of a watershed, or estimated from an energy budget using dataset of a local meteorological station. Nowadays researchers start to use remotely sensed data and hydrologic models to determine evapotranspiration in spatially distributed manner. Despite the developments in above mentioned methods, their application in shallow water table environments with mosaic land cover characteristic remains very limited (Nachabe et al. 2005).

In shallow water table environments transpiration of plant communities induce diurnal signal of soil moisture and water table (Gribovszki et al. 2010). These fluctuations are especially strong in arid and semi arid climate and can be detected mainly in groundwater discharge areas. Some researchers attempted to estimate *ET* rate of shallow groundwater areas with their own developed techniques (Bauer et al. 2004, Engel et al. 2005, Gribovszki et al. 2008, Loheide 2008, Nachabe et al. 2005, Schilling 2007, White 1932) using the observed groundwater or soil moisture fluctuations.

ET-induced diurnal signal is characterized by an early morning maximum and an afternoon minimum in the soil moisture (*Figure 1*) and also in groundwater level. In case of ET induced diurnal signal, a relationship can be detected between the daily courses of these values and that of the relative humidity, the latter mainly a function of surface irradiation at a diurnal time-scale. The direct driving force however is not radiation and relative humidity, but rather evapotranspiration (in forested areas the latter dominated by transpiration) regulated by the former variables as the plants use soil moisture or directly groundwater via their root systems.

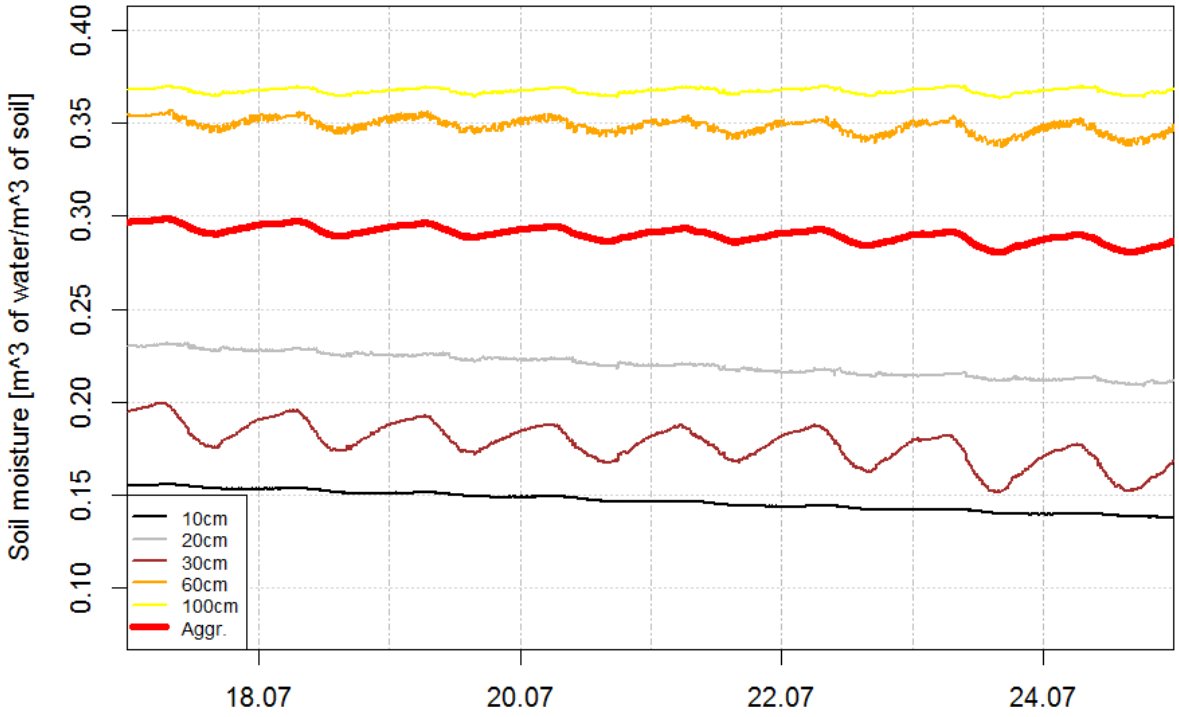

Figure 1. Diurnal signal in soil moisture profile (Aggr. means total soil moisture for profile)

As first attempt White (1932) proposed a method that uses observations of shallow water table diurnal signal to calculate the groundwater uptake by plants. This method was widely used later for estimation of ET. The limitation of the former and of all groundwater signal based methods lies in the difficulty of specific yield estimation. Nachabe et al. (2005) adapted White's (1932) original method for high frequent soil moisture profile data to eliminate the application of the specific yield. With that method a grassland and a neighbouring forest evapotranspiration were successfully estimated. Nachabe's (2005) constant upwelling recharge rate of soil moisture profile was used throughout the day for his calculation. In this paper a new technique is demonstrated by which evapotranspiration values can be calculated from aggregated soil moisture taking into account diurnally changing replenishment rate.

2 MATERIAL AND METHODS

The dataset used for testing the new method originated from a valley position (*Figure 2*) of the Hidegvíz Valley experimental catchment in Hungary, located at the eastern foothills of the Alps close to Austro-Hungarian border in the neighbourhood of city Sopron.

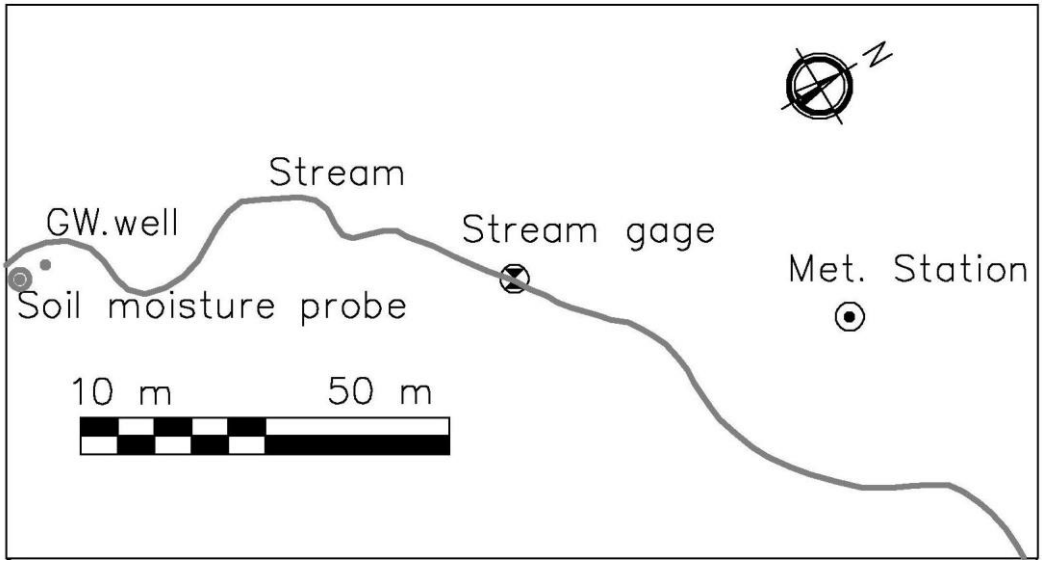

Figure 2. Location of the study site close to the outlet point of the experimental catchment at the eastern foothills of the Alps

The geological basis of the catchment is fluvial sediments deposited in five distinct layers (hundreds of meters thick) in the tertiary (Miocene) period on crystalline bedrock. On the surface only the two upper layers of the latter appear. Over the slopes and hilltops the strongly unclassified (coarse gravel and fine loam as well) formation is found in a 10–50 m-thick layer. In the valley bottoms, a finer-grained layer appears, which is a good aquifer, giving rise to perennial streams (Kisházi–Ivancsics 1985).

The soil type of the sampling point is loamy sand determined by grading test of the sampled soil profile.

The vegetation in the valleys is a typical phreatophyte intrazonal ecosystem dominated by alder (Alnus glutinosa (L.) Gaertn.). The mean height of the middle-aged riparian forest stand (where the sensors are located close to the outlet point of the experimental catchment) is about 15 m with a mean trunk diameter (at a height of 1.3 m) of 13 cm. Leaf area index (*LAI*) of this forest stand was approximately 7.

The area has a sub-alpine climate, with daily mean temperatures of 17 °C in the summer, 0 °C in the winter, and with an annual precipitation of 750 mm. In that region late spring and early summer are the wettest and fall is the driest seasons (Danszky 1963; Marosi–Somogyi 1990). Detailed characterisation of the research area can be found in Gribovszki et al. 2006.

2.1 Soil moisture data collection

A profile probe carrying six soil moisture sensor was installed in a riparian alder forest for soil moisture monitoring (*Figure 2*). Access tube was installed for probe and soil moisture sensors were distributed at 10, 20, 30, 40, 60 and 100 cm bellow the ground surface. Sensors work on capacitance principle and provide volumetric water content ranging from oven dryness to saturation with accuracy: ± 0.06 m^3/m^3. The default calibration equation provided by DeltaT company for profile probes were used in this study (http://www.delta-t.co.uk/). Soil moisture data were collected at each depth every 10 minutes.

The dataset of soil moisture sensors were used for estimation of total soil moisture of the soil column (1m soil profile) using the following equation:

$$\theta_T = \int_0^{1.0} \theta \cdot dz \tag{1}$$

where θ_T is total soil moisture (m), z is depth (m) below the ground surface, and θ is the water content (m^3 water in m^3 soil). Because there is no water content measurement at the ground surface (z = 0 depth), a uniform water content is assumed in the top 15 cm. Numerically the total soil moisture was calculated using the former approximation (1):

$$\theta_T = \sum_{i=2}^{6} \left(\frac{z_{i+1} + z_i}{2} - \frac{z_i + z_{i-1}}{2} \right) \cdot \theta_i + \left(\frac{z_2 + z_1}{2} - 0 \right) \cdot \theta_1 \tag{2}$$

where z_i is depth (m) of the i-th sensor from the ground surface, and θ_i is the water content at the i-th sensor (m^3 water in m^3 soil). The total soil moisture data for a selected period can be seen on *Figure 1.* with red thick line (*Aggr.*).

A screened (screened to the bottom (1.6 m), starting 25 cm below the surface) groundwater well was also installed close to the profile probe. Water table (h) in the well was recorded by a pressure transducer at a 10-min sampling interval and with an accuracy of 1 mm (www.dataqua.hu). The well was dug with a 70-mm drill. The PVC well casing has a diameter of 50 mm.

Using groundwater well dataset it can be stated that depth to the groundwater in the riparian zone varied between 0.8 to 1.1 m during typical drought periods. Consequently, the root system of the trees is in direct contact with the saturated zone, or at least the capillary fringe throughout the year. Following Shah et al. (2007), the decoupling of the groundwater dynamics from the vadose zone in the soil of our experimental site was found to start at a depth of 0.8–0.9 m, therefore almost all year long the total *ET* is very close to groundwater *ET*.

2.2 Theoretical basis of the new method

The diurnal method for ET_{gw} (evapotranspiration from groundwater) estimation using groundwater level data developed by Gribovszki et al. (2008) can be applied also for soil moisture data after some modifications.

The basic expression is the water balance equation for soil moisture profile (3):

$$\frac{dS}{dt} = \frac{d\theta_T}{dt} = Q_i - Q_o - ET = Q_{net} - ET \tag{3}$$

where S is stored volume of water in the soil moisture profile in a unit area (m^3/m^2), which is the same as θ_T (total soil moisture) in this case (m), Q_i is the incoming and Q_o the outgoing water flux ($m^3/s/m^2$) to and from the soil column, $Q_{net} = Q_i - Q_o$ is the net flux/supply ($m^3/s/m^2$) or replenishment rate and ET is evapotranspiration ($m^3/s/m^2$).

The transpirational need of the vegetation is generally met by the soil moisture. In drought periods the soil moisture profile of the shallow water table areas used by evapotranspiration is typically replenished via groundwater flow or by so-called induced recharge. Around the timing of the soil moisture extrema, supply and demand are in an equilibrium, while along the rising limb of the soil moisture signal the ET rate exceeds the rate of replenishment (Q_{net}), and vice versa on the falling limb (Gribovszki et al. 2008, Troxell, 1936)

For estimation of Q_{net} water balance equation (3) for late night hours when ET is almost zero was used:

$$\frac{dS}{dt} = \frac{d\theta_T}{dt} = Q_{net} \tag{4}$$

In order to obtain the net supply rate (Q_{net}) a so called empirical submethod (after Gribovszki et al. 2008) is employed.

The maximum of Q_{net} for each day was calculated by selecting the largest positive time rate of change value in the total soil moisture ($Q_{net\_max} = max(d\theta_T/dt)$), while the minimum was obtained by calculating the mean of the smallest time-rate of change in θ_T taken in the predawn/dawn hours ($Q_{net\_min} = mean(d\theta_{Tpredawn}/dt)$). The averaging is necessary in order to minimize the relatively large role of measurement error when the changes are small. The resulting values of the Q_{net} extrema ("Characteristic points" in *Figure 3*) then were assigned to those temporal locations where the soil moisture extrema took place. It was followed by a spline (or when the data are very noisy a linear) interpolation of the Q_{net} values to derive intermediate values between the specified extrema (after Gribovszki et al. (2008), *Figure 3.*). For calculation of time-rate of change in soil moisture (soil moisture difference) 30 minutes time step was used.

Finally, when Q_{net} values have been obtained the ET rates of new method (ET_{new}) can be obtained by rearranging the former water balance equation as

$$ET_{new} = Q_{net} - \frac{d\theta_T}{dt} \tag{5}$$

30-min water uptake data were aggregated along the day to get daily ET_{new}.

Traditional ET calculation (ET_{trad}) from soil moisture data without replenishment is the following:

$$ET_{trad} = \theta_{Tj} - \theta_{Tj-1} \tag{6}$$

where: θ_{Tj} is a total soil moisture of an j-th day, θ_{Tj-1} is a total soil moisture of an (j–*1*)-th day. This method is used for comparison with ET_{new}. It has to be noted that soil moisture difference in equation (6) is calculated for daily and not for 30 minutes time step compared to equations (3), (4) and (5).

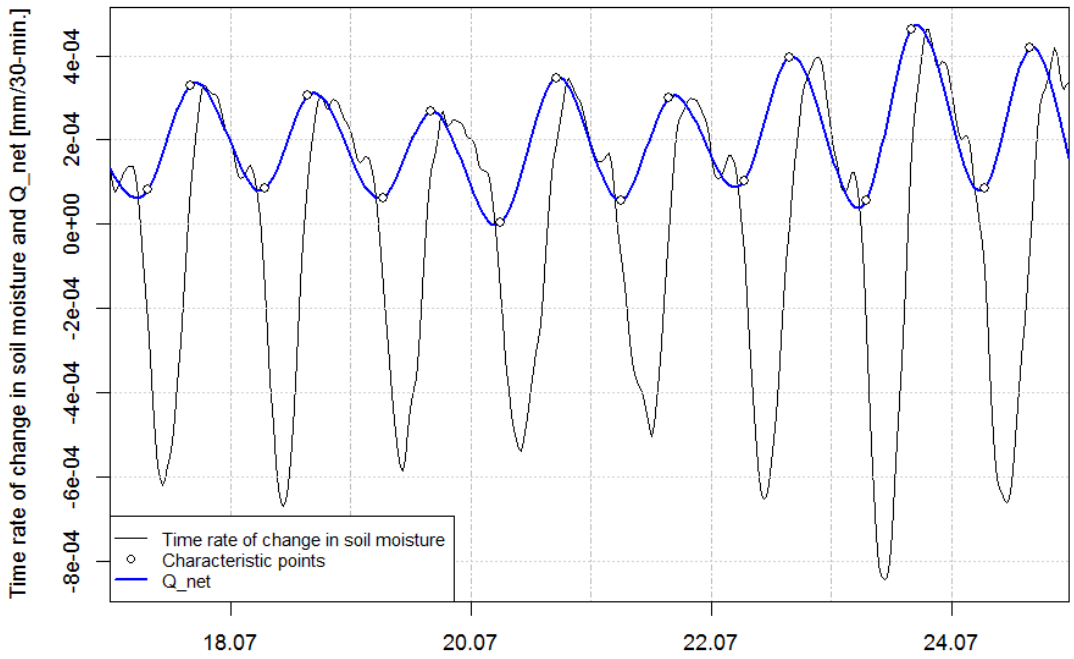

Figure 3. Graphical representation of the estimation method. See details in text.

3 RESULTS AND DISCUSSION

Figure 4 shows us daily ET_{new} values from June to September of 2013 for only dry days (daily rainfall is less than 5 mm). Mean average values for dry days of 2013 summer is 8.8 mm, a little lower in June and a bigger in July and August *(Table 1).* Daily water uptake seems to be great amount, but taking account that this is a groundwater discharge area in a valley bottom location (where positive groundwater flux toward to the unsaturated soil profile acts to support the high *ET*) and all around dry and warm environment can be found (therefore oasis effect can enhance *ET*) the data is acceptable.

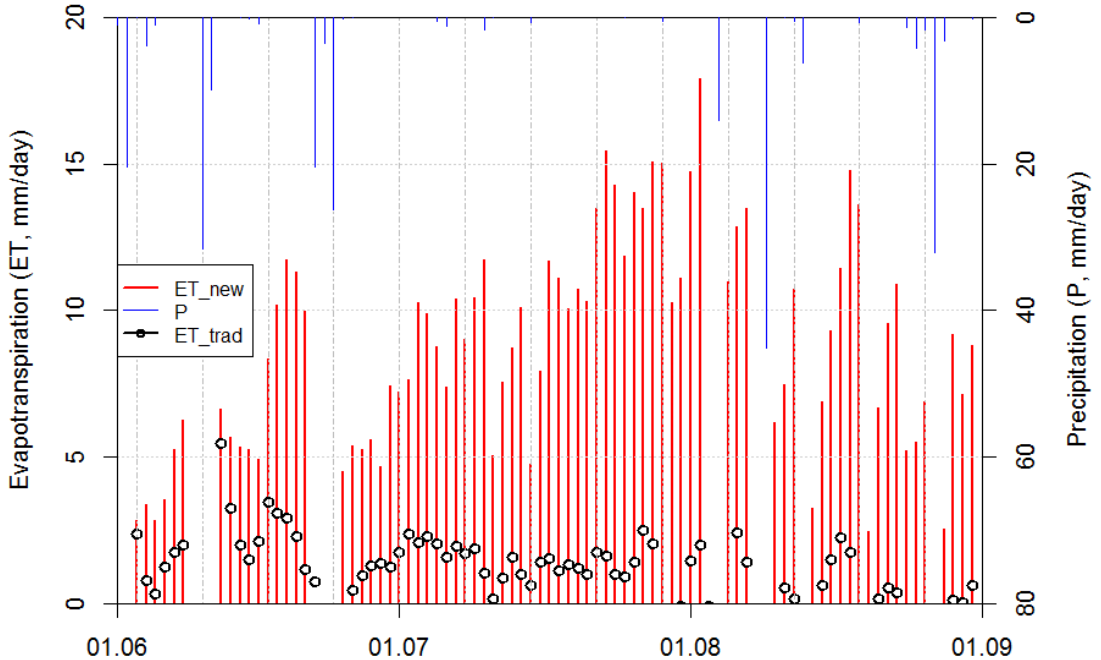

Figure 4. Daily ET values calculated by new (ET_{new}) and traditional (ET_{trad}) methods for dry days from June to August in 2013

If we compare *ET* values determined by traditional method (ET_{trad}) with estimates obtained by the new technique (*Figure 4*) a significant difference can be found. Mean average values of ET_{trad} for dry days of 2013 summer is only 1.50 mm, and a decreasing trend can be seen from data along summer (*Figure 4* and *Table 1*). The diminishing of ET_{trad} values are caused by the almost continuous drying out processes of the soil profile parallel with the increasing importance of replenishment rate in real *ET*. The ratio of ET_{trad} and ET_{new} is about 20% and also generally decreased from June to August. This significant deviation between two methods is probably caused by the continuous water uptake from groundwater across the capillary zone which is not considered in traditional method.

Soil moisture replenishment from groundwater provided nearly 80% of the total *ET* represented by ET_{new} (*Figure 5* and *Table 1*). For the visualization of seasonal trend of ET_{new} and replenishment rate (Q_{net}) a scatter-plot smoother (loess, Cleveland et al. 1992) was also applied on *Figure 5*. The data and the trends show us the importance of the net inflow rate, which was tendentiously increased along the summer (from 60% of June to 88% of August, *Figure 5*). The values of the replenishment ratio can explain the difference between the traditional and new method (roughly 4/5 of *ET* is not detected when calculating *ET* by traditional method).

The higher positive correlation coefficient between ET_{new}–Q_{net} (0.92) compared to ET_{new}–ET_{trad} (0.12) also confirmed the significance of the replenishment rates in *ET* of the groundwater discharge areas and the inaccurate values of the traditional calculation.

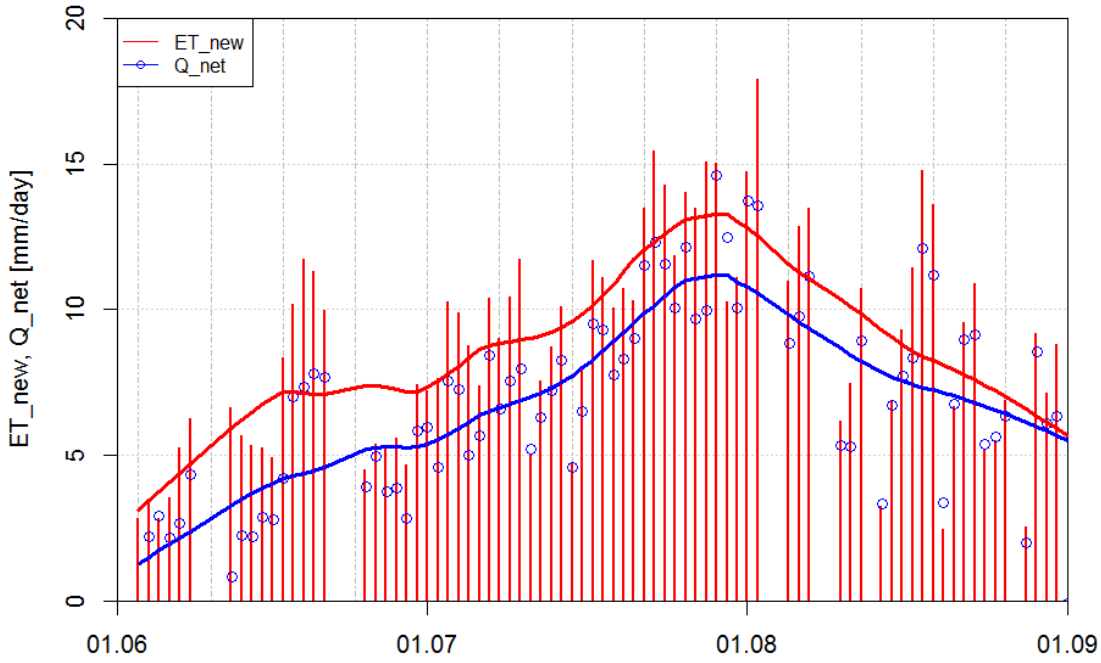

Figure 5. Daily ET_{new} values and replenishment rates (Q_{net}) for dry days with loess (local regression) smoothers for trend visualization from June to September

The magnitude of the soil moisture replenishment rate from below clearly illustrates the dependence of hygrophyte forests on groundwater. These groundwater discharge areas in Hungary can be found not only on the narrow bands of the valley locations in the mountainous and hilly regions (as our test area) but also on the broad lowland areas in Hungarian plains. Therefore for exact water uptake determination of high water demand forests located in groundwater discharge areas these kinds of methods are indispensable.

It can be also stated that hydrological models and methods, which ignore this above mentioned replenishment rate will estimate *ET* with big bias in groundwater discharge areas, and the magnitude of the bias can be 5–10 fold.

Table 1. Calculated monthly mean ET values and Replenishment rates (Q_{net}) for dry days of summer 2013

	June	July	August	June to August
ET_{new} (mm/day)	6.19 (2.61)	10.48 (2.78)	9.14 (4.04)	8.84 (3.61)
ET_{trad} (mm/day)	1.89 (1.19)	1.48 (0.56)	0.99 (0.82)	1.50 (0.93)
ET_{trad} / ET_{new}	0.33 (0.20)	0.15 (0.06)	0.08 (0.06)	0.19 (0.16)
Q_{net} (mm/day)	3.80 (2.22)	8.48 (2.56)	7.78 (3.07)	6.94 (3.28)
Q_{net} / ET_{new}	0.60 (0.27)	0.81 (0.12)	0.88 (0.14)	0.78 (0.21)

Standard deviations in brackets after each mean values

4 CONCLUSIONS

A new technique was elaborated using the diurnal signal of an aggregated soil moisture dataset. This method was successfully tested on the riparian soil moisture profile dataset in the summer of 2013. The water uptake values seem to be acceptable if oasis effect (Morton 1983) is taken into account in a well watered valley situation in a period when hot and dry environment can add significant amount of heat enhancing ET. Compared to traditional ET determination from soil moisture data, this new method gives much higher water uptake taking into account continuous soil moisture replenishment from shallow groundwater. The advantage of the new technique over the traditionally used method is that only a soil moisture profile dataset (down to the groundwater) is needed for calculation of both ET and replenishment rate and there is no need for specific soil calibration. However, future users of the new technique are cautioned, that the absolute value of ET is not available for the analysed period, thus nothing can be said about the real accuracy of the method. On the other hand the results obtained are promising and have potential benefits. As the climate changes, warmer and drier summer is forecasted. This hot and dry environment will significantly enhance the ET of the well watered areas, therefore this method can be a very useful technique for the more precise detection of impact of climate change on groundwater discharge areas.

Acknowledgements: The research of Zoltán Gribovszki was supported by the European Union and the State of Hungary, co-financed by the European Social Fund in the framework of TÁMOP 4.2.4. A/2-11-1-2012-0001 'National Excellence Program'.

REFERENCES

BAUER, P. – THABENG, G. – STAUFFER, F. – KINZELBACH, W. (2004): Estimation of the evapotranspiration rate from diurnal groundwater level fluctuations in the Okavango Delta, Botswana. Journal of Hydrology 288 (3–4): 344–355.

DANSZKY, I. (Ed.) (1963): Magyarország Erdőgazdasági Tájainak Erdőfelújítási, Erdőtelepítési Irányelvei és Eljárásai, I. Nyugat-Dunántúl Erdőgazdasági Tájcsoport [Regeneration and Afforestation Guidelines of Hungarian Forest Regions, I. Western-Transdanubian Forest Region]. Országos Erdészeti Főigazgatóság, Budapest pp. 557 (in Hungarian).

DINGMAN, S. L. (2002): Physical Hydrology, Prentice Hall, Upper Sadle River, New Jersey.

CLEVELAND, W.S. – GROSSE, E. – SHYU, W.M. (1992): Local regression models. In: CHAMBERS, J. – HASTIE, T. (Eds.), Statistical Models in S. CRC, pp. 309–376 (Chapter 8).

ENGEL, V. – JOBBÁGY, E.G. – STIEGLITZ, M. – WILLIAMS, M. – JACKSON, R.B. (2005): The hydrological consequences of Eucalyptus afforestation in the Argentine Pampas. Water Resources Research 41. W10409. http://dx.doi.org/10.1029/2004WR003761.

GRIBOVSZKI, Z. – KALICZ, P. –KUCSARA, M. (2006): Streamflow characteristics of two forested catchments in Sopron Hills. Acta Silvatica et Lignaria Hungarica 2: 81–92. URL http://aslh.nyme.hu/

GRIBOVSZKI, Z. – KALICZ, P. – SZILÁGYI, J. – KUCSARA, M. (2008): Riparian zone evapotranspiration estimation from diurnal groundwater level fluctuations. Journal of Hydrology 349: 6–17 http://dx.doi.org/10.1016/j.jhydrol.2007.10.049

GRIBOVSZKI, Z. – SZILAGYI, J. – KALICZ, P. **(**2010): Diurnal fluctuations in shallow groundwater levels and in streamflow rates and their interpretation – A review, Journal of Hydrology 385, 371–383, http://dx.doi.org/10.1016/j.jhydrol.2010.02.001.

KISHÁZI, P. – IVANCSICS, J. (1985): Sopron Környéki Üledékek Összefoglaló Földtani Értékelése [Geological Assessment of Sediments in the Neighbourhood of Sopron]. Manuscript, Sopron, 48 pp. (in Hungarian).

LOHEIDE, II. S. P. (2008): A method for estimating subdaily evapotranspiration of shallow groundwater using diurnal water table fluctuations. Ecohydrology, 1: 59–66, doi: 10.1002/eco.7.

MAROSI, S. – SOMOGYI, S. (eds.) (1990): Magyarország Kistájainak Katasztere I. [Cadastre of Small Regions in Hungary I.]. MTA Földrajztudományi Kutató Intézet, Budapest, 479 pp. (in Hungarian).

MORTON, F. I. (1983): Operational estimates of areal evapotranspiration and their significance to the science and practice of hydrology. Journal of Hydrology 66, 1–76.

NACHABE, M. – SHAH, N. – ROSS, M. – WOMACKA, J. (2005): Evapotranspiration of two vegetation covers in a shallow water table environment. Soil Science Society of America Journal 69, 492–499.

SCHILLING, K.E. (2007): Water table fluctuations under three riparian land covers, Iowa (USA). Hydrological Processes 21, 2415–2424. doi:10.1002/hyp6393.

SHAH, N., – NACHABE, M., – ROSS, M. (2007): Extinction depth and evapotranspiration from ground water under selected land covers. Ground Water 45 (3), 329–338. doi:10.1111/j.1745-6584.2007.00302.x.

TROXELL, H. C. (1936): The diurnal fluctuation in the groundwater and flow of the Santa Ana River and its meaning, Trans.Amer. Geophys.Union 17: 496-504.

WHITE, W.N. (1932): Method of Estimating Groundwater Supplies Based on Discharge by Plants and Evaporation from Soil – Results of Investigation in Escalant Valley. Tech. Rep., Utah – US Geological Survey. Water Supply Paper 659-A.

www.dataqua.hu

www.delta-t.co.uk

DE GRUYTER OPEN DOI: 10.2478/aslh-2014-0006 Acta Silv. Lign. Hung., Vol. 10, Nr. 1 (2014) 77–90

Applicability of Different Hydrological Model Concepts on Small Catchments: Case Study of Bükkös Creek, Hungary

Péter TORMA* – Borbála SZÉLES – Géza HAJNAL

Department of Hydraulic and Water Resources Engineering,
Budapest University of Technology and Economics, Budapest, Hungary

Abstract – This study aims to test and compare the applicability and performance of two different hydrological model concepts on a small Hungarian watershed. The lumped model of HEC-HMS and the semi-distributed TOPMODEL have been implemented to predict streamflow of Bükkös Creek. Models were calibrated against the highest flood event recorded in the basin in May, 2010. Validation was done in an extended interval when smaller floods were observed. Acceptable results can be achieved with the semi-distributed approach. Model comparison is made by means of sensitivity analysis of model parameters. For TOPMODEL the effect of spatial resolution of the digital terrain model, while for HMS the complexity of the model setup was further explored. The results were quantified with model performance indices.

rainfall-runoff modelling / small watershed / TOPMODEL / HEC-HMS / model intercomparison

Kivonat – Különböző hidrológiai modellkoncepciók alkalmazhatósága magyarországi kisvízgyűjtőkön: esettanulmány a Bükkös-patak példáján. A tanulmány célja, hogy két különböző hidrológiai modell koncepció alkalmazhatóságát teszteljük és vessük össze magyarországi kisvízgyűjtők esetén. A koncentrált paraméterű HEC-HMS modellt és a térben félig osztott TOPMODEL-t alkalmaztuk a Bükkös-patak vízgyűjtőjének kifolyási szelvényében kialakuló árhullámok számítására. A modelleket az eddig mért legnagyobb, 2010. májusi árhullámra kalibráltuk. A validációt egy rövid, kiterjesztett időszakra végeztük, amikor kisebb árhullámok alakultak ki. A térben félig osztott megközelítéssel elfogadható eredményeket kaptunk. A modellek összehasonlítását érzékenységvizsgálat segítségével végeztük. A paramétereken túl, a TOPMODEL esetében a digitális terepmodell felbontásának, míg a HMS esetében a modell összetettségének hatását vizsgáltuk. Az eredmények értékelése a közismert, illeszkedés jóságát leíró paraméterekkel történt.

csapadék-lefolyás modellezés / kisvízgyűjtő / TOPMODEL / HEC-HMS / modell összehasonlítás

INTRODUCTION

An appropriate introspection into hydrological processes of small and medium sized mountainous catchments (up to 1000 m a.s.l.) of Hungary has become necessary due to a recent increase in flash flood events (Hegedüs et al 2013). It is especially challenging to predict floods (stage levels and discharge volumes) in data-poor catchments. In such environments adaptation of hydrological models can only be useful if they are robust for

* Corresponding author: torma@vit.bme.hu; H-1111 BUDAPEST, Műegyetem rkp. 3-9.

streamflow estimation (Gumindoga et al 2011). Due to the huge number of available hydrological models it is difficult to select the most effective one. Different model classifications exist (e.g. deterministic or stochastic etc.), but the most basic one concerns spatial structure. Lumped models handle the basin as one unit while fully distributed models solve equations on a finite number of discrete cells that cover the basin. In the latter case parameter values may vary in each computational point. Semi-distributed models do not calculate hydrological processes by cells but take into account the spatial variation of some characteristics of the watershed by dividing it into smaller homogeneous units (Beven 2001).
Depending on their structural concept, rainfall-runoff (RR) models usually require at least half a dozen model parameters to be optimized. Robustness is difficult to ensure when a large number of parameters have to be defined. The optimization procedure requires as long a rainfall-runoff record as possible. With different parameter combinations, similar runoff values can be achieved meaning that a number of local minima exist in the parameter space with different interpretations of the modelled mechanisms (Duan et al 1992, Iorgulescu – Jordan 1994). Selection from these parameter combinations can be obtained with various hydrological and geographical analyses.

In Hungary little effort has been put into testing the applicability of different model concepts. Only a few studies report of successful applications of lumped RR models in small Hungarian watersheds (Hegedüs et al 2013, Koch – Bene 2013). This study aims to simulate streamflow during a large flood event in the small watershed of Bükkös Creek using two different RR models. The watershed of Bükkös Creek is data-poor, only a water level gauge has been in operation in it, which is typical in Hungary. The main goal is to test the applicability of two different model concepts and to estimate their robustness and sensitivity. A lumped (HEC-HMS) and a semi-distributed (TOPMODEL) models are implemented.

First, a one-dimensional hydrodynamic model of the main creek was set up to derive a reliable rating curve at the outlet cross-section of the watershed to transform stage records into runoff time series for the calibration and validation of the hydrological models. The already applied lumped model of HEC-HMS (Széles et al. 2012) fitted with a digital elevation model was successfully recalibrated and validated against corrected runoff data. The semi-distributed TOPMODEL has also been implemented, achieving better results throughout calibration and validation. Sensitivity study made the results even more reliable. The effect of digital terrain model resolution and the complexity of the hydrological model regarding the number of free parameters with different physical content were analysed. The results were quantified with well-known model performance tests.

1 STUDY AREA

The catchment is found south of the Danube's Bend in Hungary. The creek flows into the Danube at Szentendre, it is the largest permanent watercourse of the city (*Figure 1*).

The total area of the catchment is 39.2 km^2. The creek is 16 km long, having a constructed bed in the urban area protected by flood levees. It originates in the southern slopes of Dobogókő, nearly 600 m above m.s.l., where from through various waterfalls traversing a level difference of 500 m, arrives to downtown of Szentendre (*Figure 2*).

The aquifer is made up of andesite and andesite-tufa with a strongly watertight nature (due to the secondary porosity its hydraulic conductivity coefficient is about 10^{-7}-10^{-8} m/s). Runoff fluctuates within a large range: enhanced discharge in spring when snow melts and in summer when flash floods dominate. The creek cannot form ponds along its course because the evolving hollows are quickly filled up with alluvium (Dövényi 2010).

As it is shown in *Figure 1* a water level gauge is operated at the border of the settlement. Water level is recorded in every 15 minutes since 2005 which is occasionally complemented with discharge measurement by the Water Directorate at low and medium waters. Hourly precipitation data were obtained from the Hungarian Meteorological Service. The rainfall gauge is operated about 10 km south from the watershed.

The basin is covered by forest above the gauge, the area of open fields is negligible. The topography of the catchment is displayed in *Figure 2*. Hydrological modelling tools require a structured grid, therefore from the manually digitalized contour levels a TIN model was created which was then interpolated onto structured grids. Digital terrain models were generated with four different horizontal resolutions: 25, 50, 100, 200 m.

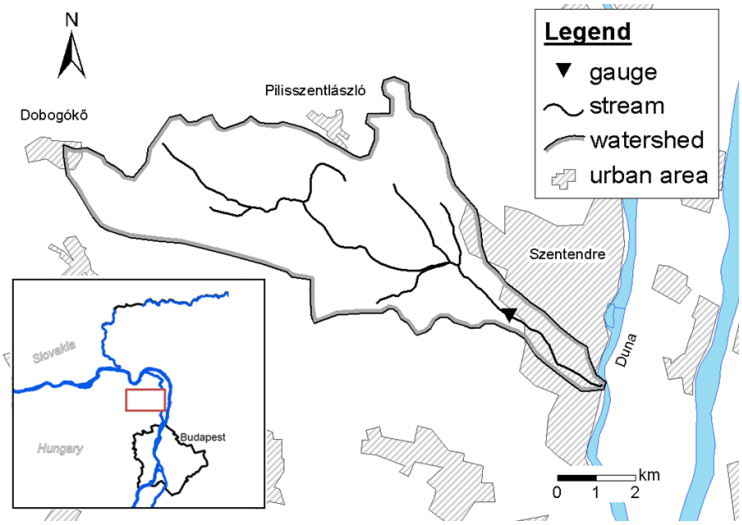

Figure 1. Location of the watershed of Bükkös Creek

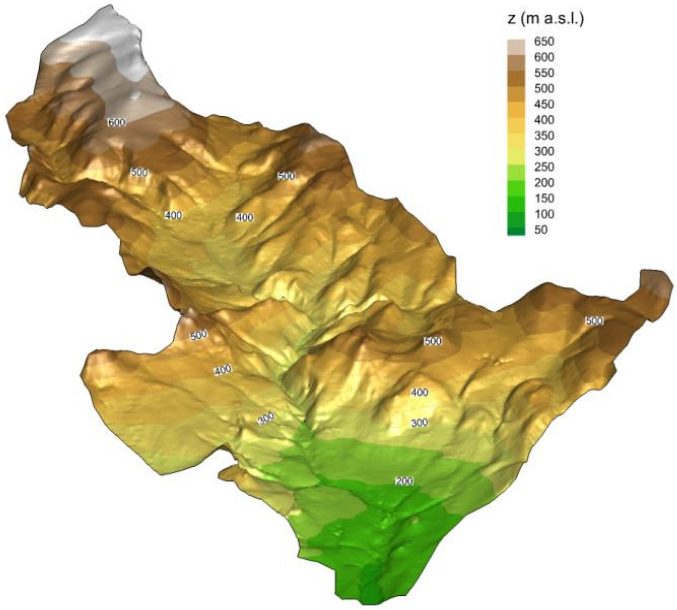

Figure 2. Digital elevation model of the Bükkös watershed derived from triangulation of contours

2 MODELS AND METHODS

2.1 1D hydrodynamic creek model

The one-dimensional (1D) hydrodynamic model of the main channel was based on the geodesic survey of the stream. The average density of cross-sections is about 20 m in the urban area and 100 m above the gauge in the rural area. Manning's roughness coefficient was neither horizontally nor vertically varied throughout calibration, channel and banks could have the same value along the stream because calculated water surface levels are affected mostly by the large slope of the water surface instead of friction caused by the channel's roughness. Sensitivity analysis performed with measured data verified this assumption.

The previously calculated rating curve, based on a simple curve fitting method (Széles et al 2012), was inaccurate due to extrapolation in the range of high waters. The 1D hydrodynamic model of the main channel generates reliable discharge time series from the water level measurements which also fit the measured low discharge data of the Central Danube Valley Environmental and Water Management Directorate. *Figure 3* displays the rating curves obtained by curve fitting and modelling. From the observed water levels discharge data of the flood event in May 2010 were recalculated with the new rating curve (*Figure 4*). This flood has been the greatest one measured since 2005, the calibration period of model analysis. The peak flow according to the rating curve derived from the 1D model is almost twice as large as the earlier extrapolated value.

Routing time of the watercourse was also calculated with the river model which meant to be an estimation of hydrologic response time of the watershed for severe thunderstorms.

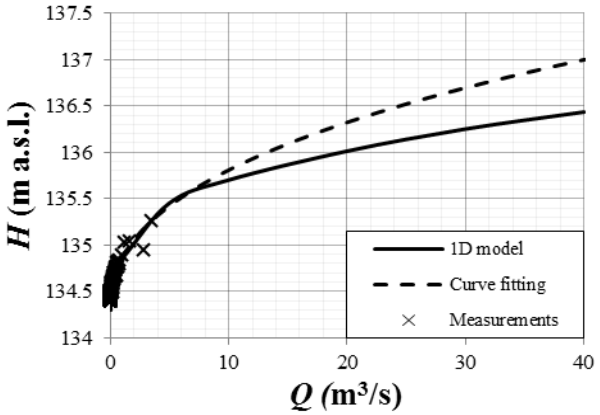

Figure 3. Rating curves calculated by 1D stream model and simple curve fitting

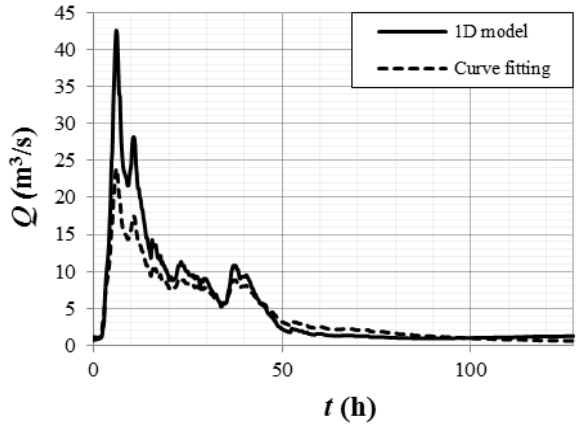

Figure 4. Discharge time series of the flood event in May 2010 derived by the rating curve of the 1D model as well as by simple curve fitting

2.2 Lumped model

HEC-HMS is designed to simulate the precipitation-runoff processes of dendritic watershed systems. The main components of the program are: basin and meteorological models, as well as input data and control specifications.

The basin model represents the physical watershed by adding and connecting hydrological elements. Three of them were used by us: watershed, reach and junction (USACE 2010). *Figure 5* shows the basin model of Bükkös Creek with three subbasins created by HEC-GeoHMS.

The meteorological model calculates the frozen or liquid precipitation and evapotranspiration. We dealt with only liquid precipitation. We assumed a homogeneous spatial distribution of rain in the meteorological model, because only one precipitation station was available. Hourly measured precipitation data and discharge data with a temporal resolution of 15 minutes constituted the input data pairs.

Models with three and five subbasins were calibrated and validated. Altogether ten free parameters were optimized: a specified amount of water remaining on the leaves of trees (*Canopy*), the sum of infiltration and precipitation left on the surface (*Loss*), surface runoff calculation (*Transform*), subsurface processes (*Baseflow*) and parameters of runoff time in channels (*Routing*). The total runoff time of the main creek was calculated by the 1D model and divided between branches in proportion of the length of each reach elements during the calibration of lag routing. The time between the centroid of precipitation mass and the peak flow of the resulting hydrograph was divided between each watershed in proportion of watersheds' area during the calibration of the *Transform* method.

Figure 5. Basin model of Bükkös watershed with three (left) and with five (right) sub-basins in the lumped model

2.3 Semi-distributed model

The geomorphology of the catchment plays an important role in runoff generation, especially in hilly terrains. Various approaches focus on different topographic characteristics. The geomorphologic unit hydrograph theory and the geomorphologic nonlinear-cascade (Szilágyi – Parlange 1999) concepts identify physical parameters from the drainage network, while in the concept of TOPMODEL by Beven and Kirkby (1979), topographic derivatives are the responsible hydrological drivers.

The concept of TOPMODEL (Beven – Kirkby 1979, Beven et al. 1984) was implemented in the watershed to model rainfall-runoff processes. Topography is represented in the model through the so-called topographic index, defined as $\ln(a/\tan \beta)$, where a is the total upslope contributing area, and $\tan(\beta)$ is the local downslope angle. The topographic index is used to estimate water table depths in any point of the catchment. Its distribution for the basin of Bükkös Creek is shown in *Figure 6*.The concept is based upon three main assumptions

(Beven 2001): (i) saturated zone is in equilibrium state due to the draining of the upslope contributing area, (ii) hydraulic gradient of the saturated zone is assumed to be equal with the topographic slope, (iii) the transmissivity with depth of the saturated zone is an exponential function of storage deficit. The semi-distributed feature arises from the assumption that areas with the same index value behave in the same hydrological manner. Originally TOPMODEL was developed for humid watersheds with thin soil but it has been used successfully in highly different circumstances, for instances in the Mediterranean (Candela et al 2005) or at the tropics (Plesca et al 2012). Topographic index can be derived from digital terrain models. GRASS, the free and open source GIS software was used to calculate index distribution in the catchment and as the run environment of TOPMODEL (GRASS 2012).

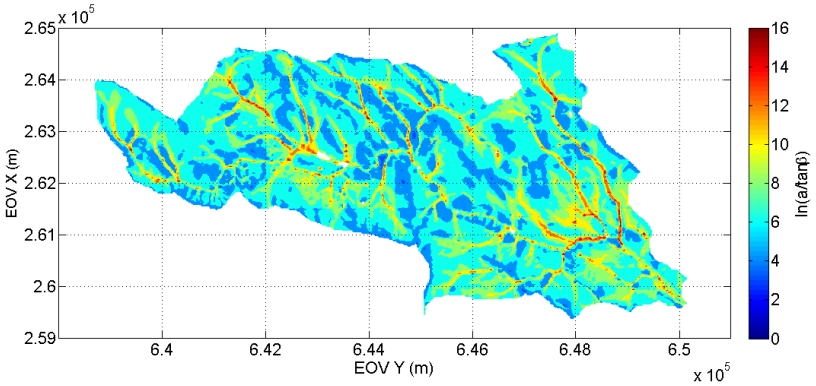

Figure 6. Topographic index distribution in the watershed with 25 m DEM resolution

2.4 Goodness of fit criteria

Quantifying goodness of fit between simulated and measured data during calibration, validation and sensitivity studies is important. Four statistical indices were used which are described in details in e.g. Das et al.(2008):

1) *Nash-Sutcliffe coefficient (R_m^2)*:

$$R_m{}^2 = 1 - \frac{\sum_{i=1}^{N}(Q_s(t_i) - Q_0(t_i))^2}{\sum_{i=1}^{N}(Q_0(t_i) - Q_{0,a})^2}$$

where $Q_o(t_i)$is the observed, $Q_s(t_i)$ is the simulated discharge at time step t_i, $Q_{o,a}$ is mean observed discharge and N is the number of time steps.

2) *Relative bias*:

$$Rel_{bias} = \frac{\sum_{i=1}^{N} Q_s(t_i) - Q_0(t_i)}{\sum_{i=1}^{N} Q_0(t_i)}$$

3) Peak error:

$$Peak\ error = \frac{Q_{s,max} - Q_{0,max}}{Q_{0,max}}$$

where $Q_{s,max}$ is the simulated and $Q_{o,max}$ is the observed peak discharge.

4) *RMSE (Rout mean squared error)*:

$$RMSE = \sqrt{\frac{\sum_{i=1}^{N} Q_s(t_i) - Q_0(t_i)}{N}}$$

3 RESULTS

3.1 Rainfall-runoff simulations

The same flood event was simulated with the two RR models providing comparability. The highest water levels ever recorded occurred during the flood event in May 2010 and caused significant damage in the town of Szentendre. Both models were calibrated against the observed discharge time series determined by the rating curve derived from the 1D model. To validate the models the calibration period was extended from April to June, when smaller flood-waves were observed.

Figure 7 illustrates observed runoff time series at the outlet with the simulation result of HEC-HMS lumped model for May 2010. The measured and simulated flood waves are in moderately good agreement. The magnitude and the phase of the peak are captured well, but the modelled wave is long-drawn, therefore the simulated runoff volume is remarkably overestimated (*Figure* 13). The model was validated on the extended interval for which a similar statement can be made (*Figure 8*). Calibration and validation accuracy was quantified with goodness of fit indices in *Table 2*.

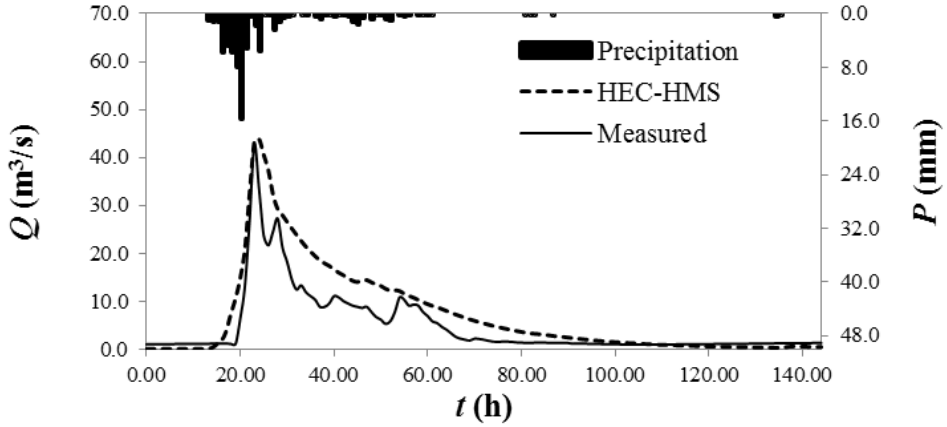

Figure 7.Observed and simulated runoff with HEC-HMS using three sub-basins for the calibration period

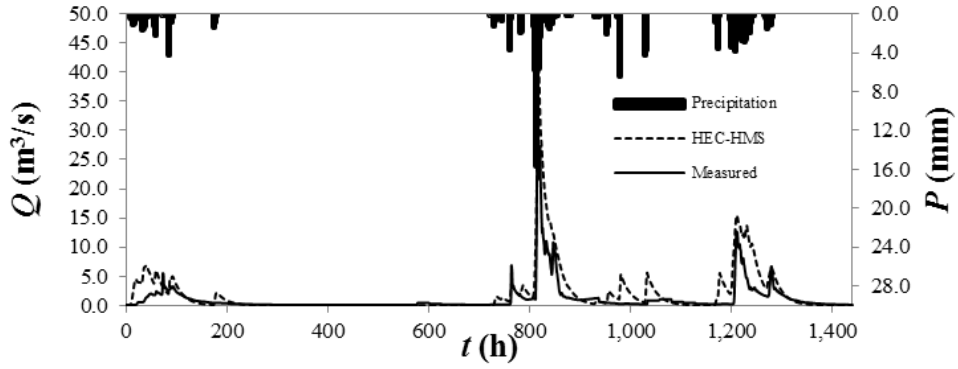

Figure 8.Observed and simulated runoff with HEC-HMS using three sub-basins from April to June 2010.

The results of the runoff simulation for TOPMODEL is shown in *Figure 9*. The calibration and validation periods correspond to the time intervals used before. The free model parameters are displayed in *Table 1*, although many of these were explicitly determined. *Figure 10* shows the result of the validation (from April 2010 to June 2010).

Table 1 – Model parameters of TOPMODEL

Parameter	Dimension	Physical meaning
Q_0	(m/h)	Initial subsurface flow per unit area
$T_e = T_0$	(m^2/h)	Transmissivity of saturated soil
m	(m)	Transmissivity decline rate
Sr_0	(m)	Initial root zone storage deficit
Sr_{max}	(m)	Maximum available root zone storage deficit
t_d	(h)	Unsaturated zone time delay per unit storage deficit
v_{ch}	(m/h)	Main channel routing velocity
v_r	(m/h)	Internal sub-catchment routing velocity
nch	(-)	Number of sub-basins
d	(m)	Distance from outlet
Ad_r	(-)	Cumulative area ratio of sub-catchment

Table 2 demonstrates that prominently good results were achieved with TOPMODEL. Nash-Sutcliffe coefficient is close to 0.9 also for the validation period. Peak error for the calibration is of the order of two decimal places. Furthermore, the second peak is also appearing on the times series, although it is overestimated and occurs earlier. The simulated cumulative runoff volume is also approximated more accurately than in case of the lumped model.

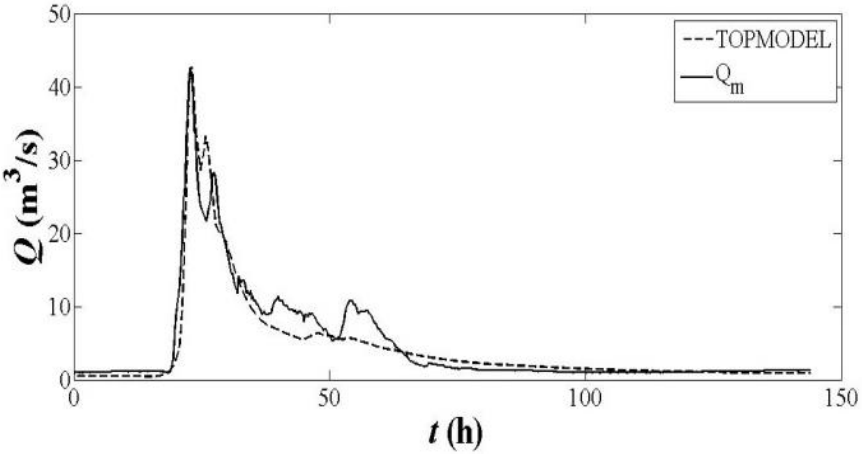

Figure 9. Observed (Q_m) and simulated runoff with TOPMODEL for the calibration period

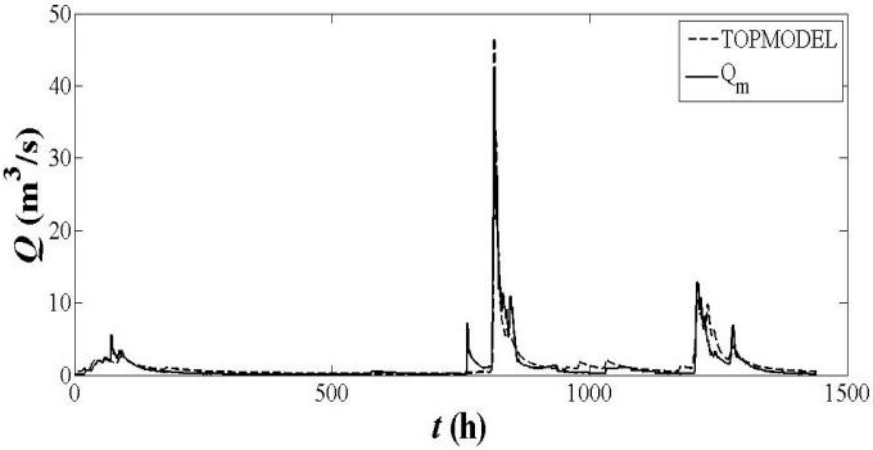

Figure 10. Observed (Q_m) and simulated runoff with TOPMODEL from April to June 2010

Table 2. Goodness of fit indices, calibration and validation of TOPMODEL and HEC-HMS

Model	Type of simulation	Rel.Bias	R_m^2	Peak error	RMSE
HEC-HMS (3 subbasins)	Calibration	0.51	0.60	0.05	4.35
	Validation	0.75	0.38	0.06	2.22
HEC-HMS (5 subbasins)	Calibration	0.51	0.54	0.03	4.64
	Validation	0.75	0.36	0.05	2.26
TOPMODEL	Calibration	–0.0821	0.9077	0.0016	2.0841
	Validation	0.1653	0.8797	0.0978	0.9790

3.2 Sensitivity analysis

One of the main goals of this study is to explore robustness of model concepts. To this end, sensitivity analysis was performed. As it clearly seen from *Table 2* and from the runoff time series, TOPMODEL performs considerably better. In the international literature many researchers work with HEC-HMS and even the previously mentioned Hungarian studies applied this lumped model (Széles et al 2012, Hegedüs et al 2013, Koch – Bene 2013), thus the sensitivity analysis focuses on TOPMODEL.

With HMS the modeller has to adjust the level of model's complexity during model building. In practice the number of sub-basins and consequently the number of side streams have to be decided. The amount of model parameters increases rapidly with sub-basins. In order to check the sensitivity of HMS for complexity, simulations were performed by delineating three and five sub-catchments. Remarkable differences in the results did not occur as it can be seen by the indices of *Table 2*. It was not possible to model the second peak of the main flood event of May by the more sophisticated structure.

In case of TOPMODEL, a more detailed investigation was performed. Sensitivity of the model parameters was analysed: the values were perturbed with ±10% (changing only one at a time) and the effects were measured through goodness of fit indices. The list of model parameters and their physical interpretation is specified in *Table 1*. According to *Table 3*, the most sensitive parameter was *m* which controls the rate of decline of transmissivity with increasing storage deficit, followed by T_e representing the transmissivity of the soil in saturated state.

Table 3 Results of the sensitivity analysis

Parameters	Rel. Bias	R_m^2	Peak error	RMSE
Calibration	–0.0821	0.9077	0.0016	2.0841
m–10 %	–0.0658	0.8653	0.3535	2.5169
m+10 %	–0.0994	0.8759	–0.2538	2.4162
ln$\mathbf{T_e}$-10 %	–0.0818	0.9146	0.0251	2.0043
ln$\mathbf{T_e}$+10 %	–0.0824	0.9006	–0.00075	2.1629
Sr_0-10 %	–0.0786	0.9083	0.0204	2.0768
Sr_0+10 %	–0.0857	0.9067	–0.0133	2.0955
Sr_{max}-10 %	–0.0821	0.9077	0.0016	2.0841
Sr_{max}+10 %	–0.0821	0.9077	0.0016	2.0841
t_d–10 %	–0.0820	0.9131	0.0230	2.0216
t_d+10 %	–0.0822	0.9006	–0.0114	2.1627

Further sensitivity analyses were performed with the two most sensitive parameters (m and T_e) in order to find those parameter pairs when the value of the NS coefficient has a local maximum (*Figure 11*). The results show that the calibrated parameters are not the optimal data pair in this aspect, however they are close to it and the aimed agreement is reached. Furthermore this method could be used to optimize model parameters.

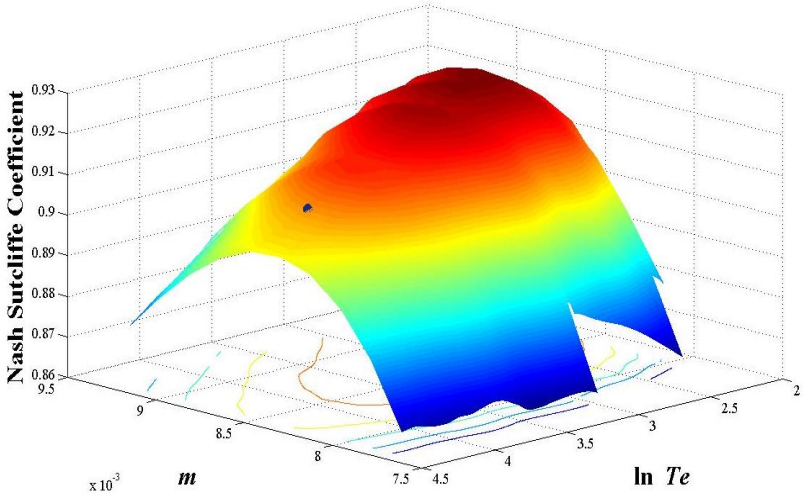

Figure 11. Sensitivity analysis of the two most sensitive parameters of TOPMODEL, a circle shows the applied parameter combination at calibration

As it was described in section 2.3, runoff generation in TOPMODEL is principally controlled by topography, hence the accuracy of the DEM has primary importance. Many researchers analysed grid size dependency of this concept (e.g. Lin et al 2010). Brasington and Richards (1998) showed that cell-size-independent results can be reached with about 100 m resolution. When using a finer DEM resolution, accuracy can be maintained by recalibration of the model. Effects of spatial resolution on model performance were analysed applying different grid size: 25 m, 50 m, 100 m and 200 m. Spatial resolution has direct influence on the topographic index (γ). *Figure 12* shows the distribution of the topographic index under different spatial resolutions. Our aim was to find a mesh independent solution which has almost been achieved. The distribution of γ does not differ significantly using 25 m or 50 m resolution.

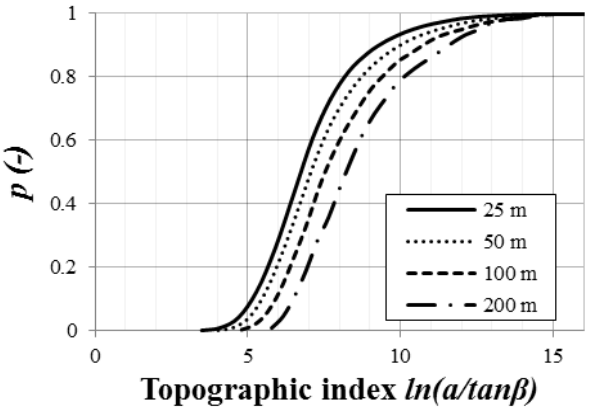

Figure 12.Topographic index distributions under different spatial resolution

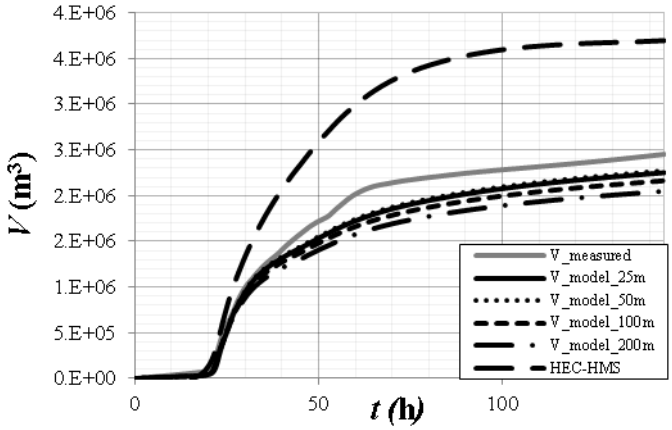

Figure 13.Cumulative discharge volumes in May 2010, under different DEM resolution (25, 50, 100, 200 m)

Recognizable differences can be discovered in the cumulative discharge volumes using digital terrain models with different spatial resolutions (*Figure 13*). Volumes with 25 m x 25 m and 50 m x 50 m grid sizes were almost the same, however differences were evident with a coarser resolution (100 m and 200 m). Changing spatial resolution of DTM influenced primarily the magnitude of the discharge peak value, the flood itself was not shifted in time.

3.3 Model comparison

One of the main purposes of this study is to compare the lumped and semi-distributed approaches as to their accuracy and applicability.

Probably the most important item in the comparison is model performance. It is clearly shown that TOPMODEL simulated the chosen flood wave with more accuracy. Not only its shape and the peak flow were well estimated, but the runoff volumes were also acceptable, which is not the case for HMS.

TOPMODEL uses only one hydrological approach, whereas HMS offers a broad range of hydrologic and hydraulic methods to describe watershed processes properly. This can be even disadvantageous if a robust tool is looked for since it is already challenging to select among the different approaches possessing parameters with different physical meaning.

The number of calibrated parameters was ten with HEC-HMS. By the lumped model the number of free parameters is increasing while the calibration process is getting more complicated by dividing the catchment into several sub-basins. In case of TOPMODEL, seven parameters have to be optimized, however we have found that the model was sensitive to only a few of them. This is partly due to the fact that some hydrological parameters are derived from the topography. For this reason this approach requires an accurate digital elevation model, but nowadays they are typically available. It can be stated that the semi-distributed model could be more easily calibrated.

Considering the availability of TOPMODEL and HEC-HMS, both can be legally and freely used. While for TOPMODEL model generation and simulations can be performed with the open-source GRASS-GIS software, the basin model preparation for HEC-HMS can only be realized with GeoHMS which is also free but works only as an extension of ArcGIS.

Input data format, data processing and run of TOPMODEL is similar to open source codes, results are not graphically displayed in GRASS, therefore separate scripts were coded for visualisation purposes. On the contrary HEC-HMS is more user-friendly with its graphical environment and detailed users' guides.

The complex HMS model can work with spatially inhomogeneous precipitation data. However the applied version of TOPMODEL was not able to use gridded precipitation data, however, this disadvantage can be easily eliminated throughout the open source nature of the tool.

Another advantage of the semi-distributed TOPMODEL concept is that saturated zones can be calculated from the outputs of the model and topographic index raster. *Figure 14* illustrates the simulated saturated zones at the moment of peak. These calculations were not validated with measured data. The results of model calculations can be correct in those areas where one of the preliminary simplifying assumptions of TOPMODEL is true: the downslope topographic gradient is assumed to be a good approximation of the downslope hydraulic gradient. This theory is certainly incorrect on a terrain with a major depression or deeper valley where changes in the surface of groundwater occur. After the saturation map is validated, it can be used e.g., to delineate borders of riparian zones. Verification can be made by extensive groundwater surface level registering. Such measurements in Hungary take place in the Hidegvíz Valley Forest Experimental Watershed (Gribovszki et al 2011), which is also a small, hilly catchment, where TOPMODEL may work properly.

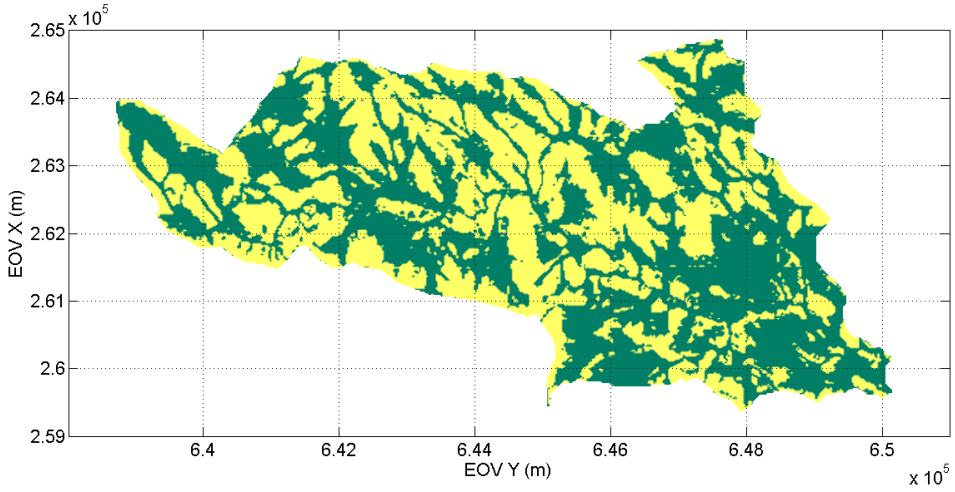

Figure 14. Snapshot of calculated saturated zones (dark green) at t=23 h, with 25 m spatial resolution

4 CONCLUSIONS

However numerous empirical formulas exist to describe rainfall-runoff processes, extreme circumstances of weather conditions and the lack of gauges in numerous Hungarian watersheds present an urgent need for a proper and reliable hydrologic modelling of the small and medium sized catchments in order to predict floods and discharge volumes.

Two rainfall-runoff models with different stuctures and complexity were tested in our case study for the watershed of Bükkös Creek: the lumped model of HEC-HMS and the semi-distributed TOPMODEL. Better results were achieved with the latter concept. The principal reason is the fact that the basic assumptions of the TOPMODEL concept were realized in the catchment, owing to a hilly terrain with a thin soil layer and underlain by andesite as an aquifer. Detailed sensitivity analysis of parameters was performed as well as the effect of DTM's resolution was explored.

The main purpose of this study is a comparison of modelling approaches, aided by the watershed of Bükkös Creek, to narrow the list of hydrological models which can be used to predict streamflows of small Hungarian catchments. The models were investigated with respect to performance and robustness. The main conclusions are the followings:

The lumped HEC-HMS model performance is not satisfactory. It is challenging to apply it in poorly instrumented catchments due to its many optional modules and parameters.

In contrast, runoff simulations made by the semi-distributed TOPMODEL are in good agreement with observations. The model possesses less sensitive parameters and seems to be more robust. It can be explained by the fact that the model builds on topography as the main driver of hydrological processes. The semi-distributed approach (not only TOPMODEL) is more promising than the lumped description as a streamflow prediction tool in small watersheds. Nevertheless, care must always be taken if model assumptions are met in the given watershed. Further investigations are required in various basins of the country to verify a more extensive applicability of TOPMODEL or other geomorphologic semi-distributed approaches.

Methods adopted in this study for the catchment of Bükkös Creek could also be applied in better instrumented watersheds, allowing for drawing similar conclusions and generalizations that could be extended to other ungauged watersheds.

REFERENCES

BEVEN, K. J. (2001): Rainfall-Runoff Modelling, The Primer, John Wiley and Sons, LTD, Chichester.

BEVEN, K. J. – KIRKBY, M. J.(1979): A physically based, variable contributing area model of basin hydrology, Hydrological Sciences, 24: 43–69.

BEVEN, K. J. – KIRKBY, M. J. –SCHOEFFIELD, N. – TAGG, A.(1984): Testing a physically-based flood forecasting model (TOPMODEL) for three UK catchments, Journal of Hydrology 69: 119–143.

BRASINGTON, J. – RICHARDS, K. (1998): Interactions between model predictions, parameters and DTM scales for TOPMODEL, Computers and Geosciences, 24: 299–314.

CANDELA, A. – NOTO, L. V. – ARONICA, G. (2005): Influence of surface roughness in hydrological response of semiarid catchments, Journal of Hydrology, 313: 119–131.

DAS, T. – BÁRDOSSY, A. – ZEHE, E. (2008): Comparsion of conceptual model performance using different representations of spatial variability, Journal of Hydrology 356:106–118.

DÖVÉNYI, Z. (editor) (2010): Inventory of microregions in Hungary, Geographical Research Institute of the Hungarian Academy of Science, Budapest (in Hungarian).

DUAN, Q. – SOROOSHIAN, S. – GUPTA, V. (1992): Effective and efficient global optimization for conceptual rainfall-runoff models, Water Resources Research, 28 (4): 1015–1031.

GRASS DEVELOPMENT TEAM (2012): Geographic Resources Analysis Support System (GRASS) Software. Open Source Geospatial Foundation Project. http://grass.osgeo.org

GRIBOVSZKI, Z. – KALICZ, P. – SZILÁGYI, J. (2011): Numerical validation of diurnal streamflow-pattern-based evapotranspiration estimation method, Acta Silvatica et Lignaria Hungarica, 7: 63–74.

GUMINDOGA, W. – RWASOKA, D. T. – MURWIRA, A. (2011): Simulation of streamflow using TOPMODEL in the Upper Save River catchment of Zimbabwe, Physics and Chemistry of the Earth, 36, pp. 806–813.

HEGEDÜS, P. – CZIGÁNY, SZ. – BALATONYI, L. – PIRKHOFFER, E. (2013): Analysis of soil boundary conditions of flash floods in a small basin in SW Hungary, Central European Journal of Geosciences, 5: 97–111.

IORGULESCU, I. – JORDAN, J. P. (1994): Validation of TOPMODEL on a small Swiss catchment, Journal of Hyrology, 159: 255–273.

KOCH, R. – BENE, K. (2013): Continuous hydrologic modelling with HMS in the Aggtelek Karst Region, Hydrology, 1 (1): 1–7.

LIN, K. – ZHANG. Q. – CHEN, X. (2010): An evaluation of impacts of DEM resolution and parameter correlation on TOPMODEL modeling uncertainty, Journal of Hydrology, 394: 370–383.

PLESCA, I. – TIMBE, E. – EXBRAYAT, J. F. – WINDHORST, D. – KRAFT, P. – CRESPO, P. – VACHÉ, K. B. – FREDE, H. G. – BREUER, L. (2012): Model intercomparison to explore catchment functioning: results from a remote tropical rainforest, Ecological Modelling, 239: 3–13.

SZÉLES, B. – TORMA, P. – HAJNAL, G. (2012): Simulating the rainfall-runoff processes on the basin of Bükkös Creek, In: Proceedings of the conference on Catchment processes in regional hydrology: from experiment to modelling in Carpathian drainage basins, 28-30. October 2012, Sopron, Hungary, Paper 25.

SZILAGYI, J. – PARLANGE, M. B. (1999): A geomorphology based semi-distributed watershed model, Advances in Water Resources, 23: 177–187.

US ARMY CORPS OF ENGINEERS (2010): Hydrologic Modeling System HEC-HMS, User's Manual, Version 3.5, Hydrologic Engineering Center, Davis, CA, USA.

DOI: 10.2478/aslh-2014-0007 Acta Silv. Lign. Hung., Vol. 10, Nr. 1 (2014) 91–101

Forest Litter Interception Model for a Sessile Oak Forest

Katalin Anita ZAGYVAINÉ KISS* – Péter KALICZ –
Péter CSÁFORDI – Zoltán GRIBOVSZKI

Institute of Geomatics and Civil Engineering, University of West Hungary, Sopron, Hungary

Abstract – Models that describe hydrological processes in forests may help to estimate the consequences of forestry interventions or of climate change. The authors employed a hydrologic model for estimation of forest litter interception of a middle-aged sessile oak (*Quercus petraea*) stand. Antecedent water content and the storage capacity of the forest litter were the main parameters of the model. The antecedent water content of the litter was estimated by the daily precipitation and temperature data, collected in Hidegvíz Valley research catchment in a three year measurement period (2006–2008). The measurements were done by an instrument of own development, where the undisturbed forest litter samples were enclosed in frames and measured in daily time steps.

interception model / forest litter / forest hydrology

Kivonat – Avarintercepció modellezése egy kocsánytalan tölgyesben. Az erdőben lezajló hidrológiai folyamatokat leíró modellek segítenek megbecsülni az erdészeti beavatkozások, és a klímaváltozás következményeit. Jelen munka egy hidrológiai modellel foglalkozik, ami egy középkorú kocsánytalan tölgy (*Quercus petraea*) állomány avarintercepcióját becsüli. Az avar megelőző víztartalma és tározási kapacitása a modell fő paraméterei. Az avar megelőző víztartalmát a napi csapadék és hőmérséklet adatokból becsültük, melyek a Hidegvíz-völgyi kísérleti vízgyűjtőből származnak a három éves mérési periódus időtartamára (2006–2008). Az adatgyűjtést saját fejlesztésű eszközzel végeztük úgy, hogy a bolygatatlan avarminták tömegét zárt keretekben napi gyakorisággal mértük.

intercepciós modell / avar / erdészeti hidrológia

1 INTRODUCTION

Forest litter interception is an important element of the water balance of the forest and can be an important parameter of the rainfall runoff models in a forested area. Forest litter interception has been dealt with since the middle of the last century but it has been the focus of research only in recent decades.

Ijjász (1936) examined the role of forest litter in the water balance of a forest in Hungary. He focused on the volumetric water content proportion of the three litter sub-layers (litter, fermentation and humus layers). Helvey (1964) investigated the forest litter interception in a southern Appalachian hardwood stand. Monthly values of litter interception and water content

* Corresponding author: zagyvaine@emk.nyme.hu; H–9400 Sopron, Bajcsy-Zsilinszky utca 4.

of litter after rainfall were measured. According to Helvey (1964), litter interception depends mainly on the annual quantity of forest litter.

Führer (1994) calculated litter interception values for the growing and dormant seasons using data of small lysimeters, for determination of water retention of tree stands in Hungary. In their forest litter interception research, Putuhena and Cordery (1996) did not made a distinction between parts of the living and dead plants. All of the organic materials were involved in the study which was a maximum 50 cm above the soil surface. Wang and Weng (2002) analysed the role of litter, the water retaining capacity of litter and the influencing factors (amount of litter, decomposition stage, tree species, amount of rainfall, and topography) were evaluated related to soil protection and erosion. Sitkey (2006) dealt with the full interception loss in connection with water balance investigations in forest climate zones (from forest beech climate to forest-steppe zones) in Hungary. Gerrits et al. (2006) continuously measured litter interception as a parameter of runoff models using a new technique of measurement in a beech (Fagus *sylvatica*) stand. Bulcock and Jewitt (2012) gave canopy and litter interception values as components of a forest hydrologic cycle in three different tree species in Africa: flooded gum (*Eucalyptus grandis*), spreading leaved pine (*Pinus patula*) and Australian acacia (*Acacia mearnsii*). For forest litter interception, there are different results (usually 2–12%) in proportion to the gross precipitation due to the different climate (rainfall and evaporation conditions), measurement methodology, litter weight and tree species.

2 DEFINITION OF INTERCEPTION

A part of the gross precipitation (*P*) falls through the canopy (*T*) and reaches the forest litter. After saturation of the leaf storage capacity, another part of the precipitation, drips down from the canopy (*D*), adsorbs on leaves and partly evaporates during and after the rain event (*E*) or flows down the trunk (stemflow: *SF*) (Horton 1919; Delfs 1955). That can be symbolized by with the next equation:

$$P = T + D + SF + S + E \tag{1}$$

The interception loss (I) is that part of precipitation which does not reach the soil (Leonard 1967):

$$I = S + E \tag{2}$$

Interception in a forest has two main parts: canopy and litter interception. Forest litter interception is the difference between the stand and effective precipitation:

$$E_S = P_{atot} - P_{eff} \tag{3}$$

where $P_{atot} = T+D+SF$, P_{eff} is the effective precipitation which can infiltrate into the soil (Lee 1980).

The canopy and also the litter interception processes can be described by the saturation function, because leaves cannot store more moisture after reaching their storage capacity. Drying of the canopy is faster due to the less saturated and more turbulent environment of the leaves than the litter, where the air is much closer to saturation and the stratified leaves keep the moisture longer. There is an additional difference between the two processes that the canopy leaves characteristically are wetted only on the surface, but the leaves of the litter store the water inside of them due to their composited structure.

However, due to the similarity of the two processes, canopy interception models can be a good starting point for employing litter interception functions. As an example, the Merriam (1960) formula for canopy interception can be a good basis for a litter interception model:

$$E_{su} = S \cdot \left(1 - e^{-c \cdot P}\right) + K \cdot P \tag{4}$$

where E_{su} is the canopy interception (mm), S is the storage capacity (mm), c is a constant (without dimension), P is the gross precipitation (mm) and K is the rate of the evaporation under the precipitation and the gross precipitation. The first component of the equation is the wetting up of canopy and the second component is the evaporation.

There is an essential difference between the forest litter and canopy interception. The quantity of the water storage of the leaves (the amount of adsorbed water, not on the surface of the leaves) can be disregarded in the canopy interception. In the forest litter interception, litter stores water not only on its surface but precipitation also can infiltrate into the body of the litter layer. Forest litter rarely dries out entirely during the rainless period between two precipitation events. Therefore the stored volume of water in the litter layer is never zero. This means that the actual storage capacity never reaches the total storage capacity. Thus, if the water content is high, the current storage capacity is low. This relation is described by the equation which is developed in this paper *(Eq. 5)*:

$$E_S = (S - w_{(i-1)}) \cdot \left(1 - e^{-\left(\frac{Th}{(S - w_{i-1})}\right)}\right) \tag{5}$$

where $w_{(i-1)}$ is the antecedent water content (mm).

Therefore Eq. 5 is the Merriam equation completed with the antecedent water content, which reduces the maximum storage capacity to the current storage capacity. The second evaporation term from the original equation is neglected, because the evaporation can be disregarded under the canopy near the soil surface during the rainfall event in those closely saturated conditions of air.

3 MATERIAL AND METHODS

A new instrument has been developed for measurement of forest litter interception. This method supports the data collection, eliminating the subjectivity of the observer compared to traditional methods (Helvey 1964) Thus consecutive data can be compared with each other. Ten frames (50 cm wide and 50 cm long, 0.25 m2 in area) were settled in the forest stand following the contour lines and slopes (5–5 pieces). The frames are covered with fly screen on each side (and also on the top) so the movement of any insect, snail, etc. does not disturb the measurement. Quasi-undisturbed litter was placed into these frames from the same area as the frames. Before starting the measurements, the frames were uncovered for 1 or 2 weeks in the field to allow precipitation to settle the litter leaves.

We applied an UWE HS-7500 digital hanging scale with 5 g accuracy (www.uwe.com) for weighing the forest litter.

Measurements provided data each day, from May to November/December in every study year (05/05/2006-14/12/2006, 10/05/2007-14/12/2007, and 28/05/2008-29/08/2008).

At the end of each study year, the dry weight can be determined in each frame. Dry weight values support the calculation of the litter water content at each time. After the measurement period (according to the dates above, usually one growing season), the frames

were emptied. The next measurement period was started with new litter samples. A measuring period is represented by *Figure 1*.

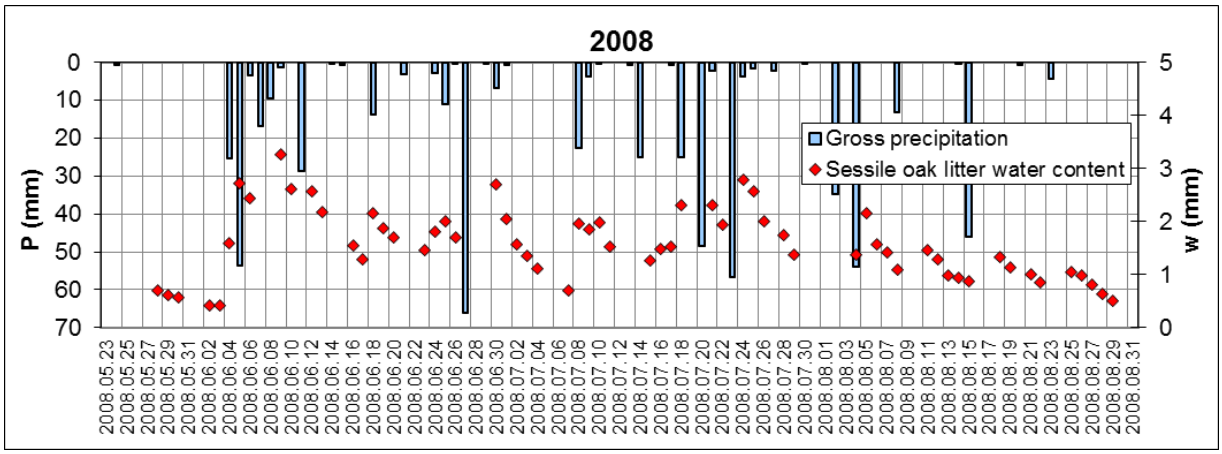

Figure 1. Gross precipitation and water content of the forest litter in the sessile oak stand during the year 2008

4 THE STUDY SITE

The study site (Hidegvíz Valley, *Figure 2.*) is located in Sopron Hills at the eastern border of the Alps. (Lat: 47-35-08 - 47-39-06, Lon: 16-25-31 - 16-28-15 above WGS 84 datum.)

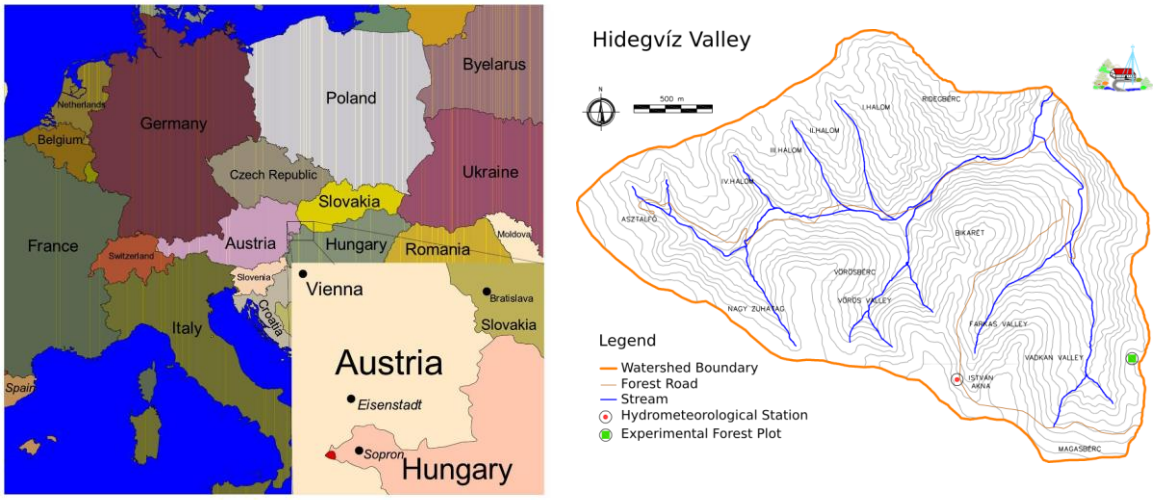

Figure 2. The study site in Hidegvíz Valley

The area enjoys a sub-alpine climate, with daily mean temperatures of 19 °C in July, and -2 °C in January, and with an annual precipitation of 750 mm. Late spring and early summer are the wettest and fall is the driest season (Marosi and Somogyi, 1990; Dövényi, 2010).

The slope of the sessile oak stand is 3–6%, located on the west side at an altitude of 500 m above sea level. The soil is classified as Cutanic Luvisol (Epidystric). The stand forming tree species is sessile oak (*Quercus Petraea*). The average height of the middle-aged stand (40 years old at the start of these measurements) was 14–15 m, canopy closure was 87%, and the average diameter at breast height of the stand was 14–16 cm. The undergrowth of sessile oak stand was sparse.

Gross precipitation values were registered by an automatic rain gauge located about 1 km from the oak interception garden (N: 47°39'21, 16", E: 16°27'16, 28", m ASL: 515 m, WGS84). Temperatures were measured by an automatic thermometer located next to the automatic rain gauge.

5 CALCULATION OF THROUGHFALL

Since no continuous throughfall records are available, throughfall data (*Th=T+D* from *Eq. 1*) applied for the interception analyses have been determined with iteration using the gross precipitation data with the following equation:

$$P = S' \cdot \left(1 - e^{-\frac{Th}{S'}}\right) + K' \cdot Th \tag{6}$$

In the *Eq. 6 P* is the gross precipitation; *S'* is the parameter depending on the water storage capacity of forest canopy; *K'* is the multiplicator factor which describes the slope of the line approximating the relation between gross precipitation and throughfall data above the limit of storage capacity. In our case *K'*=1 and *Th* is the throughfall (*Figure 3*). According to the literature (Kucsara, 1996), rainfall with low intensity and rainfall depth can be almost entirely stored on the surface of leaves, while almost the total amount (i.e. the amount reduced by the evaporation) of precipitation falls through the canopy at heavy rainfalls when the storage capacity is exceeded. *Eq. 6* represents this process.

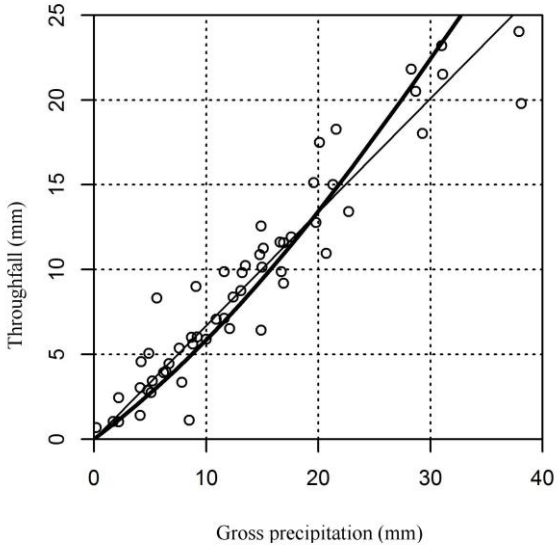

Figure 3. Connection of throughfall with gross precipitation

The iteration has been performed with the script using the R free software (R Core Team 2012). Throughfall data calculated with this method served as basis for the further analyses.

6 CALCULATION OF THE FOREST LITTER INTERCEPTION CONSIDERING THE WATER STORAGE

Litter weight in the frames changes year by year; thus maximum storage capacity changes as well. To apply the selected data from the 3 years in one combined estimation, data from the given year have been divided by the average weight of forest litter in the same year and

multiplied by the 3-year average litter weight. Results of the estimation (*Eq. 7*) related to the normalised data are shown in *Table 1*. Statistical analysis utilized nonlinear regression by the least-squares method performed with R software.

$$E_S = (1.799 - w_{(i-1)}) \cdot \left(1 - e^{-\left(\frac{Th}{(1.799 - w_{(i-1)})} \right)} \right) \tag{7}$$

Due to the spatial heterogeneity of the throughfall, there can be greater differences in the moisture changes of the 10 frames. The previous estimation was made using the average values based on the measurement of 10 frames. One extreme value can greatly offset the average values, thus distorting the estimation. Therefore, the approximation has also been made with weights. A reciprocal of the standard deviation for the ten data at the same time has been applied as a weight at that time. Results of this estimation (*Eq. 8*) are summarized in *Table 1*.

$$E_S = (1.702 - w_{(i-1)}) \cdot \left(1 - e^{-\left(\frac{Th}{(1.702 - w_{(i-1)})} \right)} \right) \tag{8}$$

Table 1. Results of the forest litter interception calculation based on the three-year dataset

	S	p-values	Standard residual error
Sessile oak	1.799	< 2e–16	0.4199
Sessile oak, weighted	1.702	< 2e–16	1.599

No significant deviation (< 0.1 mm) has been obtained between the storage capacities estimated with the two formulas (*Eq. 7–8*). *Figure 4* demonstrates the results of the weighted estimation.

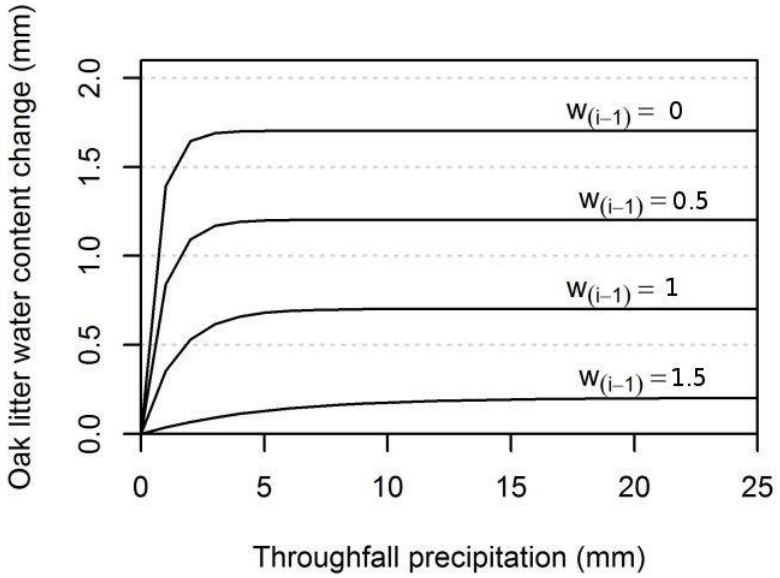

Figure 4. Water content change of the forest litter in a sessile oak stand with different antecedent water content (weighted estimation)

7 CALCULATION OF THE ANTECEDENT WATER CONTENT OF THE FOREST LITTER

The antecedent water content of the forest litter is an important question in terms of the litter interception. If the forest litter is not entirely dry, the maximum value of the storage capacity will be lower. Antecedent precipitation (API) has been calculated by the estimation of the effective storage.

According to the literature (Kontur et al. 2001), one method of the API calculation is based on a weighting process using linearly decreasing weights.

Water content of the forest litter decreases faster at the beginning of the desiccation process, and decreases more slowly to the end of the process. As the forest litter desiccation is non-linear, application of linear weights in the API calculation is incorrect. The speed of desiccation of the forest litter depends on the ambient temperature as well. In conclusion, a reliable equation to determine the API uses weights which regard the real desiccation and which are corrected with the temperature. We adapted the soil moisture relation of Jakeman and Hornberger (1993) for calculation of the antecedent water content of the forest litter:

$$w_i = c \cdot \left[P_1 + \left(1 - \frac{1}{\tau}\right) \cdot P_2 + \left(1 - \frac{1}{\tau}\right)^2 \cdot P_3 + \left(1 - \frac{1}{\tau}\right)^3 \cdot P_4 + \ldots \right], \quad (9)$$

where c is the normalising parameter, P_1, P_2, … is the rainfall depth which has fallen 1, 2… days before the rainfall event inducing the water content recharge of the forest litter. The current τ detention time has been computed using the *Eq. 10*:

$$\tau_i = \tau_0 \cdot \exp\left[g \cdot (T_0 - T_i)\right], \text{ where } \tau \geq 1, \quad (10)$$

where g is the factor of temperature-change (it shows how the τ changes as a function of the temperature), τ_0 is the reference detention time, T_0 is the reference-temperature, T_i is the temperature at the current time.

Parameters from the equations above have been calculated on the basis of our field observations. As the first step, we selected the desiccation periods according to the measurements, which lasted at least 5 days. Variables describing the speed of recession (desiccation process) have been determined using the equation of the exponential fitting based on the data of the observed periods:

$$w_i = w_0 \cdot e^{-\alpha \cdot t}, \quad (11)$$

where w_i is the water content related to the current day (mm)
w_0 is the initial water content (mm)
α speed of recession ($^1/_{\text{day}}$)
t is the elapsed days (day).

The τ detention times can be obtained as the reciprocals of the α rates of the decrease of water content. Average temperature values have also been computed for the desiccation periods.

Taking 0 °C for the reference temperature, parameters of the *Eq. 10* were estimated by applying a linear regression model with a logarithmic transformation. Results of the estimation are the followings in the sessile oak (*Figure 5*, *Table 2*):

Table 2. τ_0 and g values for the observed desiccation periods, the determination coefficient (R^2) and p-value of the estimation

	τ_0	g	R^2	p-value
Sessile oak	21.926	0.088	0.80	$7.047\ e^{-06}$

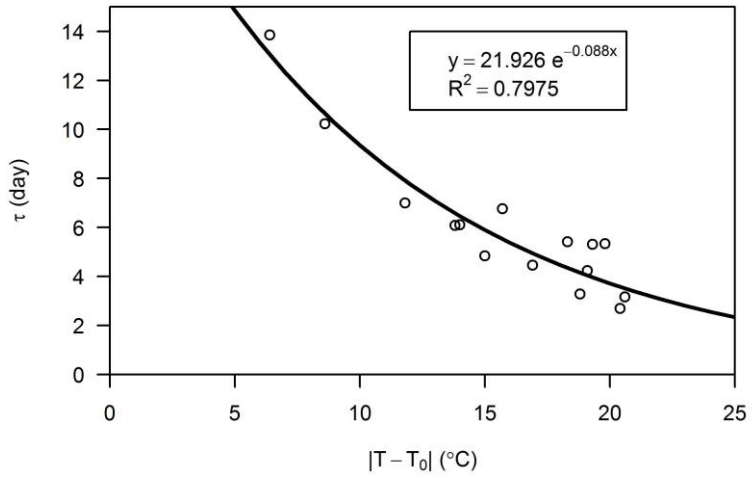

Figure 5. The τ detention time against the difference between the temperature of the desiccation period and the reference-temperature of sessile oak

Estimated parameters are the basis for calculating the antecedent water content (w_i). The determination coefficients were examined between the water content of the forest litter and the API (Jakeman-Hornberger 1993). The strength of the relation is moderate in the years 2007 and 2008, while a weak relation was obtained in 2006. In general, according to the Jakeman-Hornberger (1993) model, the API_{30} shows the strongest correlation with the water content of the forest litter, and the second strongest correlation was with the API_{20}. *Figure 6* demonstrates the strength of relations between the API according to the Jakeman-Hornberger (1993) model and the water content of the sessile oak litter in the year 2008. The strength of the relation increases from 0.56 to 0.69 neglecting only two outliers (*Figure 6*). After appropriate reordering, the equations of fitted lines provide the *c* parameters (*Eq. 9*) related to the given time periods in the given years. Considering the values of the *c* parameters, similar values were recorded in the years 2007 and 2008, while c parameters are the half of the values from 2007 and 2008 in the year 2006. The reason of this phenomenon is not yet known.

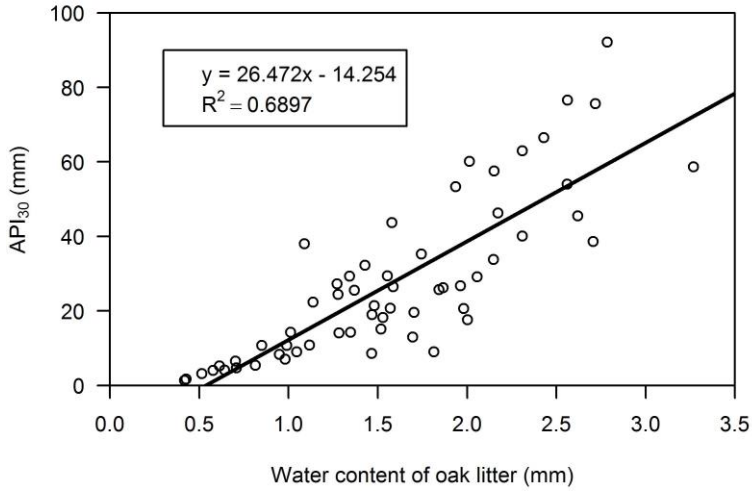

Figure 6. Relation between the API_{30} (according to the Jakeman-Hornberger (1993) model) and the water content of the sessile oak litter in 2008 after neglecting outliers.

8 APPLICATION OF THE MODEL

The model developed for estimating the forest litter interception can be used under changing environmental (different climate and litter mass, etc.) conditions. Reliable adaptation of the model depends on having information about the litter mass of the forest stand which can be determined from the maximum storage capacity of the litter in the given stand. The throughfall from the gross precipitation can be estimated on the basis of the leaf area index. The antecedent moisture content of the litter can be calculated with the Jakeman – Hornberger model (1993) using the daily temperature and precipitation data, and as a result, litter interception can be estimated. However, for the universal model application, a multi-year data set is required. Using different input climate data, the impact of the climate change can be forecast, e.g. the effect of different temperatures (change in speed of recession) or precipitation amount and distribution (changes in the length of the drying period). If the litter production is changing due to climate change (Black 2009), further modifications of the model should be made regarding the storage capacity. The impact of forestry interventions can be also estimated with this model, such as the hydrological aspects of litter interception related to clear cuts or gaps.

The effect of climate change was estimated by the model. It was found that the rate of litter interception is decreased (*Table 3*) due to the change of the distribution of precipitation. Rainfall less than 2 mm does not reach the forest litter (Kucsara 1996). Under the impact of climate change, precipitation becomes more extreme. In our estimations, the sequentially 2–4 rainfall events were merged, and the maximum rainfall decrease (30 mm over 10 years in the summer half-year) predicted by Gaál (2007) was validated with a linear equation. Iterating the new predicted data series, a throughfall dataset was calculated which serves as a basis for further estimations (*Th* for 2016–2018). An assumed increase in temperature and changes in litter mass (Kotroczó et al. 2012) were not taken into account. *Table 3* shows the calculated data for the growing season.

Table 3. Forest litter interception estimation for three years by the model we developed (growing season

Year	E_s (mm)	E_s (%)	Year	E_s (mm)	E_s (%)
2006	23.70	4.74	2016	12.87	2.74
2007	43.29	7.32	2017	25.13	4.48
2008	42.63	6.01	2018	25.12	3.70

The impact of climate change on litter interception is a complex process. Due to a lower rate of small rainfall events (less than 2 mm) more precipitation can reach the litter. An extreme rainfall event does not increase the water content of the litter after the saturation of the storage capacity. Heavy rains show a proportionately lower impact on the litter. Forest litter interception was reduced about 2–3% in the proportion of gross precipitation over 10 years according to this hypothesis (*Table 3*). Taking into account the effect of higher temperature, this reduction would be smaller, because the litter can dry out between two rainfall events. Therefore, the current storage capacity would be larger.

9 DISCUSSION

According to our model estimation, the litter interception was 5–7% of the gross precipitation. Other authors also published data about litter interception of gross precipitation or annual value (*Table 4*). Litter interception data of the net precipitation (throughfall) was 8–12% in mixed oak stands (Pathak et al. 1985), and 34% for November 2004 in beech forests (Gerrits et al. 2006).

Table 4. Forest litter interception values according some authors

	Study site	Tree species	Litter interception (%) of gross precipitation
Pathak et al. (1985)	India (Kumaun Himalaya)	*mixed oak forest*	8–12
Führer (1994)	Central Europe	*(Quercus petraea)*	8 (summer) 16 (winter)
Bulcock és Jewitt (2012)	South Africa	*(Pinus patula)*	12.1
		(Eucalyptus grandis)	8.5
		(Acacia mearnsii)	6.6

The comparison of our data is uncertain because of different climatic conditions and tree species (mainly due to the weight of litter) and different methods of measurement.

10 SUMMARY

A simple formula was developed to describe the water retention properties of litter using daily gross precipitation and forest litter mass measurement data series. This equation takes into account the moisture content of the forest litter before rainfall events, thus considering the current storage capacity. To determine the antecedent moisture content, the Jakeman – Hornberger (1993) model has been adapted which refers to the soil moisture. It has been found that the antecedent precipitation index, which applies exponential weights (taking temperature into account), are suitable to estimate the antecedent moisture content of the litter. The model we developed provide an opportunity to estimate litter interception under changing climatic conditions and thus the effects of climate change can be detected.

Acknowledgements: The research was supported by TÁMOP-4.2.2.A-11/1/KONV-2012-0013. The research of Zoltán Gribovszki was supported by the European Union and the State of Hungary, co-financed by the European Social Fund in the framework of TÁMOP 4.2.4. A/2-11-1-2012-0001 'National Excellence Program'.

REFERENCES

BULCOCK, H.H. – JEWITT, G.P.W. (2012): Field data collection and analysis of canopy and litter interception in commercial forest plantations in the KwaZulu-Natal Midlands, South Africa, *Hydrology and Earth System Sciences*, 16: 3717–3728.

DÖVÉNYI, Z. (ED.) (2010): Magyarország kistájainak katasztere [Cadastre of Small Regions in Hungary]. MTA Földrajztudományi Kutatóintézet, Budapest, 876 p. (in Hungarian).

DELFS, J. (1955): Die Niederschlagszurückhaltung im Walde. [Retention of the precipitation in the forest] In.: Mitteilungen des Arbeitkreises "Wald und Wasser". Nr. 2. Koblenz. (in German)

FEKETE Z. (1949): A koronaátmérő és a mellmagassági átmérő kölcsönös viszonya. [Mutual relationship of the crown diameter and the diameter at breast height.] *Erdészeti lapok*, 85 (10): 234–237. (in Hungarian)

FÜHRER E. (1994): Csapadékmérések bükkös, kocsánytalan tölgyes és lucfenyves ökoszisztémában. [Precipitation measurements in beech, sessile oak and spruce forest ecosystem] *Erdészeti Kutatások*, 84: 11–35. (in Hungarian)

GAÁL M. (2007): A kukoricatermelés klimatikus feltételeinek várható változása a B2 szcenárió alapján. [Expected changes of climatic conditions of maize production under the B2 scenario] In. Csete L. (ed.): „Klíma-21" Füzetek. 51: 48–56. (in Hungarian)

GERRITS, A.M.J. – SAVENIJE, H.H.G. – HOFFMANN, L., PFISTER, L. (2006): Measuring forest floor interception in a beech forest in Luxembourg. *Hydrology and Earth System Sciences Discussions*, 3: 2323–2341.

HELVEY, J.D. (1964): Rainfall interception by hardwood forest litter in the southern Appalachians. U.S. Forest Service Research Paper, SE 8: 1–8.

HORTON, R.E. (1919): Rainfall interception. *Monthly Weather Review*., 47: 603–623.

IJJÁSZ E. (1936): A nyersalomtakaró szerepe az erdők vízháztartásában. [The role of the non-fermented forest litter in the water balance of forests] *Hidrológiai Közlöny*, 16: 72–101. (in Hungarian)

JAKEMAN, A.J., HORNBERGER, G.M. (1993): How much complexity is warranted in a rainfall-runoff model?. Water Resources Research 29 (8): 2637–2649.

KONTUR I. – KORIS K. – WINTER J. (2001): Hidrológiai számítások. [Hydrological calculation] Linograf Kft. Gödöllő. (in Hungarian)

KOTROCZÓ, Zs. –VERES, Zs. –FEKETE, I. –PAPP, M. –TÓTH, J.A. (2012): Effects of Climate Change on Litter Production in a Quercetum petraeae-cerris. *Acta Silvatica et Lignaria Hungarica* 8: 31–38.

KUCSARA M. (1996): Csapadék és lefolyás erdészeti kisvízgyűjtőn. [Precipitation and runoff in forested catchment] Doktori értekezés, Sopron. (in Hungarian)

LEE, R. (1980): Forest Hydrology. Columbia University Press, New York.

LEONARD, R.E. (1967): Mathematical Theory of Interception. In.: W. E. Sopper and H. W Lull (ed.), International Symposium on Forest Hydrology. Pergamon Press, Oxford.

MAROSI, S. – SOMOGYI, S. (Eds.) (1990): Magyarország Kistájainak Katasztere I. [Cadastre of Small Regions in Hungary I.]. MTA Földrajztudományi Kutató Intézet, Budapest. 479 p. (in Hungarian).

MERRIAM, R.A. (1960): A note on the interception loss equation. Journal of Geophysical Research, 65 (11): 3850–3851.

PATHAK, P.C. – PANDEY, A.N. – SINGH, J.S. (1985): Apportion of rainfall in central Himalayan forests (India). Journal of Hydrology, 76: 319–332.

PUTUHENA, W.M. – CORDERY, I. (1996): Estimation of interception capacity of the forest floor, Journal of Hydrology, 180: 283–299.

R CORE TEAM (2012): R: A language and environment for statistical computing. R Foundation for Statistical Computing, Vienna, Austria. ISBN 3-900051-07-0, URL http://www.R-project.org/.

SITKEY, J. (2006): Water cycle investigations in Hungarian forest ecosystems. Forestry Studies in China, 8 (4): 82–86.

YOUMIN, W. – JUNHUA W. (2002): The Water and Soil Conservative Function of Litter on Forestland, 12th ISCO Conference. Beijing, China. Online: http://www.tucson.ars.ag.gov/isco/isco12/VolumeII/TheWaterandSoilConservativeFunction.pdf (Access date: 25.10.2013)

http://www.uwe.com.tw/en/home.php (Access date: 25.10.2013)

DOI: 10.2478/aslh-2014-0008 Acta Silv. Lign. Hung., Vol. 10, Nr. 1 (2014) 103–114

Comparison of Groundwater Uptake and Salt Dynamics of an Oak Forest and of a Pasture on the Hungarian Great Plain

Zoltán GRIBOVSZKI[a*] – Péter KALICZ[a] –
Kitti BALOG[b] – András SZABÓ[b] – Tibor TÓTH[b]

[a] Institute of Geomatics and Civil Engineering, University of West Hungary, Sopron, Hungary
[b] Institute for Soil Sciences and Agricultural Chemistry, Centre for Agricultural Research, Hungarian Academy of Sciences Budapest

Abstract – The forest area in Hungary has increased during the last century from 1.1 to 2.0 million ha. The European Union supports further afforestation so roughly 15 –18 000 hectares might be planted each year, mostly on the Hungarian Great Plain. Water uptake of forests from groundwater can be significant in shallow groundwater areas of the Hungarian Great Plain especially in drought periods. Therefore forests can induce water table depression and subsurface salt accumulation above saline water table in areas with a negative water balance.

The impact of forests was examined by a systematic study on the Hungarian Great Plain. An oak forest and a pasture groundwater uptake and salt accumulation effect were compared at the stand scale. Under the forest the water table levels were roughly 0.5 m lower than under the pasture, and the groundwater uptake of the oak plot was more than twice as great. Larger forest groundwater use is not followed by a higher salt uptake. Therefore slight salt accumulation was measured both in the soil and also in the groundwater. Higher groundwater uptake may cause more significant salt accumulation under pronounced drought conditions of a warmer climate.

evapotranspiration / shallow groundwater / diurnal fluctuation / salt accumulation / forest

Kivonat – Egy alföldi kocsányos tölgyes és egy szomszédos gyepterület talajvízfelvételének és sódinamikájának összehasonlítása. Magyarország erdősültsége a 20. század folyamán 1.1 millió haról 2.0 millió hektárra nőtt. Az Európai Unió támogatja az erdősítést, így évente megközelítőleg 15–18 000 hektár nagyrészt mezőgazdasági területet erdősítenek be az Alföldön. A felszínközeli talajvízszinttel rendelkező területeken, így a Nagyalföld jelentős részén is, az erdők talajvízfelvétele, főként a száraz periódusokban, igen nagymértékű lehet. Előbbiek miatt az erdők a talajvízszint süllyedését és egyes helyeken esetlegesen só akkumulációt idézhetnek elő a talajvízben és a talajvízszint fölötti talajrétegekben az erősen negatív vízmérlegű területeken.

Egy nagyalföldi mintavételi pontokat tartalmazó szisztematikus vizsgálat keretében kezdtük el keresni a fenti kérdésekre a választ. Jelen cikkben egy kocsányos tölgyes és egy szomszédos legelő talajvíz-felhasználását és só-felhalmozódásra gyakorolt hatását hasonlítjuk össze. A vizsgálatok szerint az erdő durván fél méterrel csökkenti a talajvízszintet és több, mint kétszeres a talajvízből történő vízfelvétele, mint a gyepvegetációnak. Az erdő nagyobb talajvíz-felhasználása viszont nincs arányban a sófelvételével, így mind a talajban, mind a talajvízben kismértékű só-akkumuláció tapasztalható. A

* Corresponding author: zgribo@emk.nyme.hu; H-9400 SOPRON, Bajcsy-Zs. u. 4.

klímaváltozás kapcsán a hosszabb száraz periódusokban előálló nagyobb párolgási kényszer (és nagyobb talajvízfelvétel) a mértnél sokkal jelentősebb sófelhalmozódást okozhat.

evapotranszspiráció / sekély talajvíz / napi ingadozás / só akkumuláció / erdők

1 INTRODUCTION

Significant afforestration is planned in Hungary (700 000 ha), and this plan is also supported by the EU (Andrasevits et al., 2005). The areas available for afforestration are generally less profitable for field crop production. Based on the analysis of the soil types of the formerly forested areas, Führer and Járó (2005) stated that the Hungarian Great Plain can be the most important region for afforestration. However the hydrological and climatic role of the forest is most critical in the Hungarian Great Plain. From a hydrological viewpoint, two basic situations are encountered:

- When the water table is deeper than the root zone (these are very critical sites for afforestration), and
- when groundwater can be a source of transpiration. In the later situation groundwater uptake of a forest is the most frequent theme of this research.

In the shallow water table areas, forest vegetation can change the water and salt balance of the soil (Nosetto et al., 2007) and these effects are manifested in the lowering of the water table (Major, 2002) and increase of salt concentration in certain soil and subsoil layers (Jobbágy and Jackson, 2004; Nosetto et al., 2007; Nosetto et al., 2008). In a shallow groundwater environment, the impact of a forest on groundwater and salt dynamics are reviewed by Szabó et al. (2012) specially focusing on the processes going on in the Hungarian Great Plain *(Figure 1).*

Forest evapotranspiration (sum of transpiration and interception) is generally higher than the evapotranspiration of neighbouring grasslands, because of the increased LAI (leaf area index) and root depth of the woody vegetation (Calder, 1998; Nosetto et al., 2005). These properties of a forest are especially true in the Great Plain with a subhumid climate, where the precipitation is less than the water demand of woody vegetation, so trees can survive arid periods if they can use groundwater resources as well (Ijjász, 1939; Magyar, 1961).

Móricz et al. (2012) compared the water balance of different land uses in Nyírség (Northeast part of the Hungarian Great Plain), and found that a common oak forest has approximately 30% more evapotranspiration (758 mm a^{-1}) than a neighbouring fallow land (623 mm a^{-1}). The difference is more significant (3 fold) in groundwater use of different vegetation types (oak: 243 mm a^{-1}, fallow: 85 mm a^{-1}). The groundwater consumption was close to 60% of the total transpiration in the oak forest and approximately 30% on the fallow plot. Groundwater consumption was approximately 40% less in the wetter vegetation period of 2008 than in the drier growing season of 2007, despite the fact that the groundwater level was deeper during the drier summer. Thus, during the drier period both vegetation covers relied considerably on the available groundwater resources.

Magyar (1961) analyzed the root growth of seedlings in a saline environment and found that in a moderately saline soil environment, roots of seedlings can reach 3.5 m down to the water table in three years, but roots of elms can be detected 5.15 m deep two years after planting.

Under a forest, the water table can be detected deeper than under grassland if the trees are able to reach it. The difference of the water table level is larger in the growing season (Ijjász, 1939). Jobbágy and Jackson (2004) stated that the groundwater level can be 75 cm deeper under a forest. On the basis of their measurements in shallow groundwater areas of Kiskunság, the researchers Szodfridt and Faragó (1968) found that forest vegetation generally

lowers a water table 50–60 cm compared to herbaceous vegetation. But they also stated that on the sites where groundwater levels (in April) are found deeper than 2.5 m, only sparse herbaceous vegetation can survive under natural conditions. Major (2002) observed that under a coniferous forest compartment in Kiskunság, the water table can be 0.8–1.1 m deeper than under the neighbouring non-forested areas.

Szilágyi et al. (2012) analysed the evapotranspiration (determined by linear transformation of the MODIS daytime land surface temperature) in the Danube-Tisza Sand Plateau of the Hungarian Great Plain. According to land cover, the largest ET (about 505 mm a^{-1}) was found over deciduous forests where the regional annual precipitation was 550 mm. On some locations ET is estimated to be larger than precipitation. These groundwater discharge areas in many locations overlap with forest cover. Often the dense and deep root system of forests can tap the shallow groundwater level (if it exists), thus leading to a high ET rate, frequently exceeding the rate of precipitation which the area receives. In the groundwater discharge areas, the average annual ET for the forests is 620 mm a^{-1}, which is about 70–80 mm more than the mean annual precipitation rate of the region. This negative water balance can be maintained if forests create a local depression in the water table so as to induce groundwater flow directed toward them (*Figure 1*).

Detailed investigation of the afforestation in the Hungarian Great Plain is being carried out through the systematic study of all affecting factors, like climatic water balance, water table depth and salinity, tree species, subsoil layering and stand age (in the frame of the OTKA NN 79835 project). The aim of this paper is to describe the complex interrelation of these factors in such a way that the effect of planned new afforestations could be predicted.

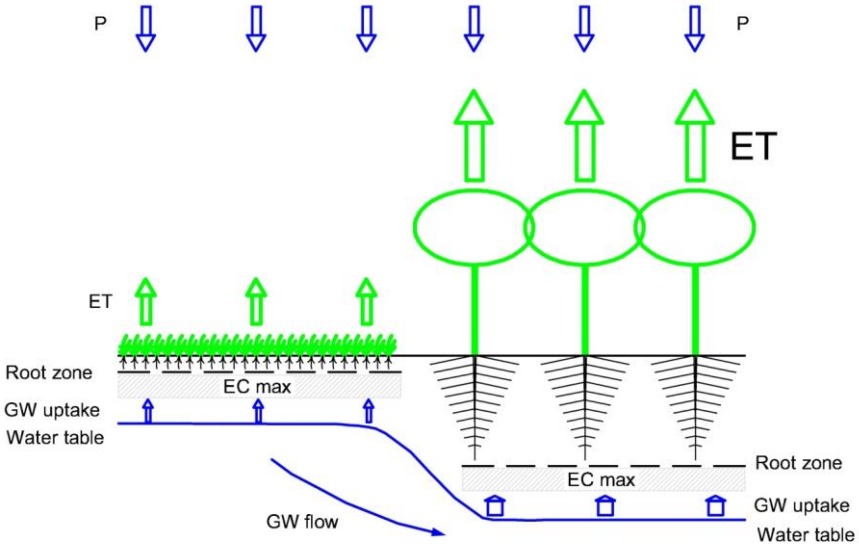

Figure 1. Impact of forest vegetation on water and salt balance of a shallow groundwater site (hypothetical model). ET evapotranspiration, P precipitation, EC (electrical conductivity), GW groundwater.

2 MATERIALS AND METHODS

2.1 Site description

Altogether 108 plots of forested and nearby non-forested land were sampled in the above mentioned project. At the stand scale, 18 representative forested and accompanied non-forested stands (from the 108) are monitored intensively. In this paper the dataset of two

neighbouring plots (a common oak forest [60 years old, 22 m high closed forest] and a grass stand [without shrubs]) were compared next to Jászfelsőszentgyörgy (47 29' N, 19 46' E) in the very dry summer of 2012 (*Figure 2*). These vegetation types are very typical in the Hungarian Great Plain.

On historical land use maps, no forest cover could be found in the area between 1780 and 1914. Afforestation started after 1914 on the oak plot, but the pasture site was never forested. The area has a flat topography. The geological basis of the research area is fluvial sediments, mostly sand and silt.

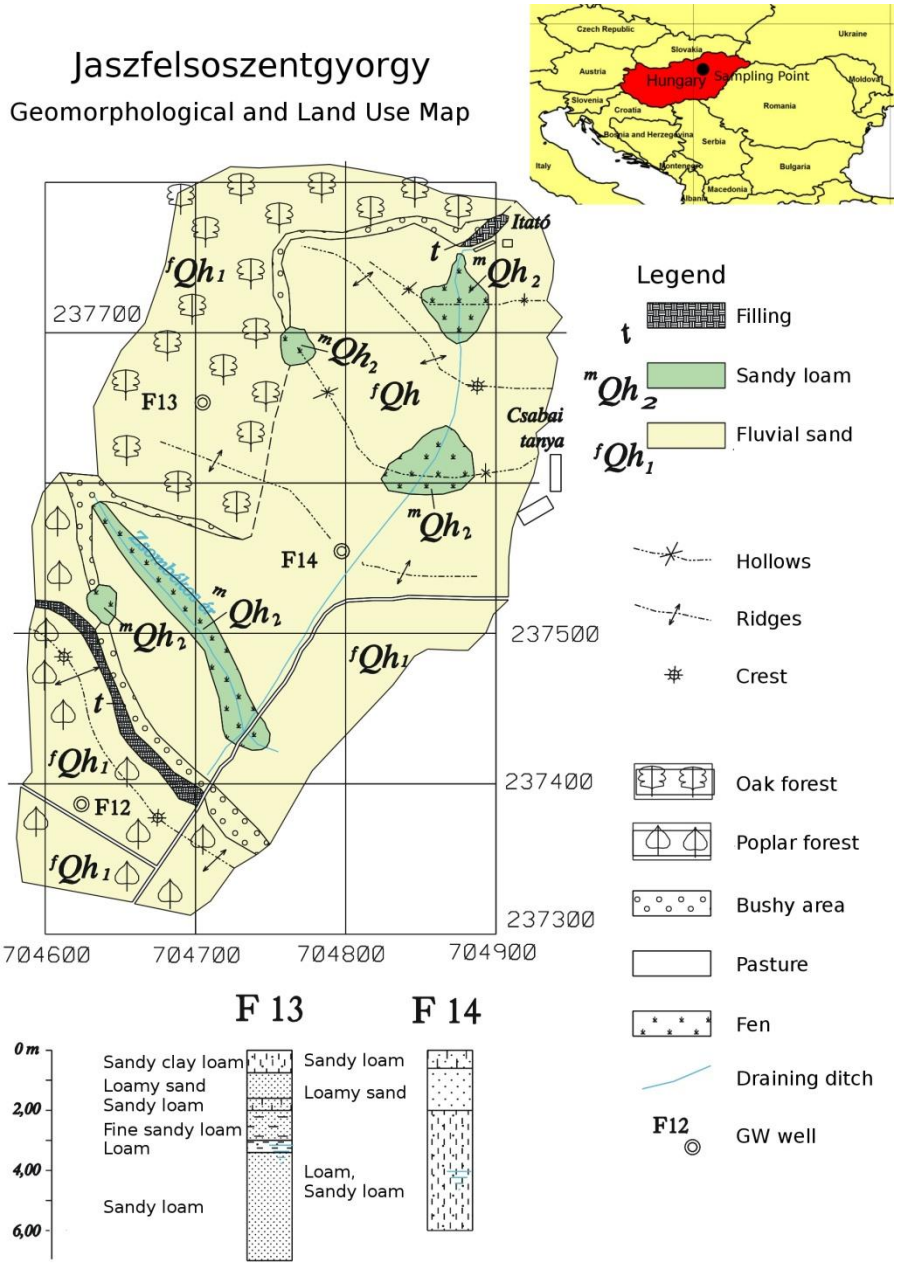

Figure 2. Geomorphological map with land use and location of monitoring plots with GW wells. Oak plot well is indicated by F13 and pasture plot well by F14.

2.2 Data collection

GW wells are installed in the common oak forest (F13) and in the grass covered pasture (F14) 7 and 6 m deep in the neighbourhood of Jászfelsőszentgyörgy (located in northern part of

Great Plain). The geological layers of the plots can be seen in *Figure 2*. GW wells were instrumented with vented pressure transducers (www. dataqua.hu) and a meteorological station was placed in the neighbourhood on a pasture in the first days of July, 2012. Pressure transducers take readings at 15 minute intervals (for calculation of ET from groundwater) and the meteorological station collects standard meteorological parameters (temperature, relative humidity, net radiation, wind speed and precipitation) every 5 minutes (for calculation of reference ET). Only the first month of dataset is adequate for further analysis because of an error in the data collectors.

Water table levels from the surface and precipitation can be seen in *Figure 4* as a representation of the collected dataset.

At both sites a mineral soil was sampled at depths of 10, 30, 50, 70, 90 cm (20 cm intervals) and at 50 cm intervals down to the depth of the GW wells. Electrical Conductivity was determined in a 1:2.5 soil-water extract (for calculation of salt content). Soil texture was specified according to particle size distribution determined by the pipette method. Groundwater was also sampled for electrical conductivity, measured by a conductivity meter.

2.3 Evapotranspiration calculation method

In shallow groundwater areas, vegetation can take up water both from unsaturated or saturated zones. If groundwater was used by vegetation, a diurnal signal can be detected in the water table hydrograph (White 1932, Gribovszki et al. 2010). The amplitude of the signal depends on the soil texture and magnitude of groundwater uptake (*Figure 5*). The riparian-zone groundwater ET estimation technique of Gribovszki et al. (2008), based on the diurnal fluctuations of the groundwater levels (by further developing of the original White (1932) method), were used.

The ET-estimation method employs the water balance equations (written for the saturated zone)

$$\frac{\partial S}{\partial t} = S_y(t,h)\frac{\partial WT}{\partial t} = Q_i - Q_o - ET_{gw} = Q_{net} - ET_{gw} \qquad (1)$$

where dS / dt [L^3T^{-1}] is the time-rate of change in groundwater storage (S), h [L] the average groundwater level (above reference), S_y the specific yield, Q_i, the incoming discharge [L^3T^{-1}] to the unit land area, and Q_o, the outgoing discharge from the unit land area [L^3T^{-1}].

The net supply/replenishment rate is the difference of the incoming and outgoing discharges to and from, $Q_{net} = Q_i - Q_o$, [L^3T^{-1}]. ET_{gw}, is evapotranspiration (directly or indirectly) from the groundwater.

In order to obtain the net supply rate (Q_{net}), an empirical method (using characteristic points) was employed (*Figure 3*):

- The maximum of Q_{net} for each day was calculated by selecting the largest positive time-rate of change value in the groundwater level readings, such as $Q_{net} = S_y \Delta h/\Delta t$.
- The minimum of Q_{net} was obtained by calculating the mean of the smallest time-rate of change in h taken in the predawn/dawn hours. The averaging is necessary in order to minimize the relatively large measurement error when the changes are small.
- The resulting values of the Q_{net} extrema then were assigned to those temporal locations where the groundwater level extrema took place.
- It was followed by a spline interpolation of the Q_{net} values to derive intermediate values between the specified extrema (Gribovszki et al. 2008).

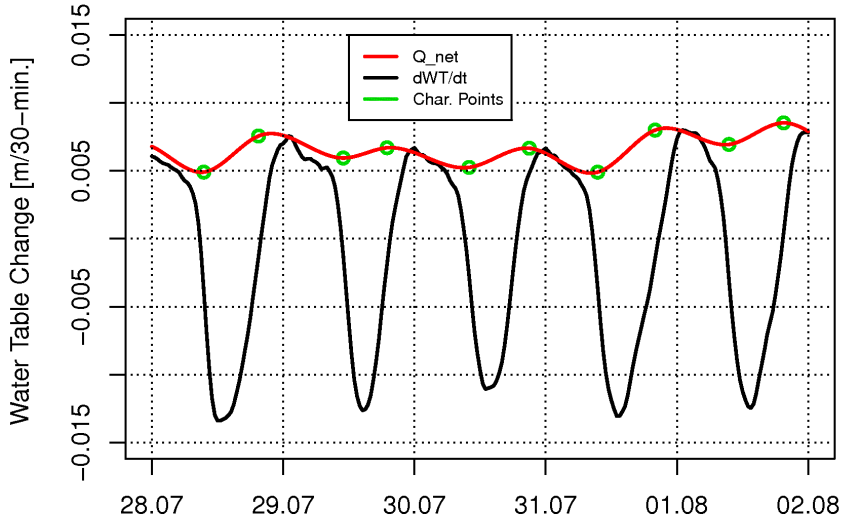

Figure 3. Graphic representation of the empirical method, Q_{net} is replenishment rate, dWT/dt is the time rate of change of water table, Char. Points is the characteristic points of replenishment rate

Finally, after calculating the Q_{net} values, the ET_{gw} rates can be obtained by rearranging the former water balance equation as

$$ET_{gw} = S_y\left(Q_{net} - \frac{dh}{dt}\right) \quad (2)$$

S_y values (as readily available specific yield) were estimated on the basis of the texture class of soil layers in the depth interval of diurnal fluctuations according to Loheide et al. (2005). The soil texture class (similar for both stands) was loam and sandy loam in the depth of the water table. Therefore S_y is between 0.045–0.055 roughly 0.05.

ET values Penman-Monteith ET (*PM_ET*) rates (for a grass reference surface) were calculated from the meteorological dataset as a comparative reference (Allen et al., 1998).

3 RESULTS AND DISCUSSION

3.1 Water table levels and fluctuation

Water table depression in the forest next to an adjacent pasture together with a significant difference in the amplitude of diurnal fluctuations suggested an increased groundwater use of the forest (*Figure 4*).

Differences in water table levels from the surface were 0.44 m on average during July 2012 (*Figure 4)*. In contrast when groundwater levels are expressed in absolute values (a.s.l) the difference became 0.9 m (because of the lower elevation of the oak stand). Both of the differences mean a depression in water table under the forest. The magnitude of the depression was similar to the water table drop determined by Nosetto et al. (2007) on a planted oak forest and adjacent grassland in the Hortobágy region (0.26–0.60 m) and those determined by Móricz et al. (2012) by comparing a common oak stand and a neighboring fallow plot in Nyírség (in a dry period of the growing season 0.5–0.6 m).

The sinking of the water table was similar during the sampled period (0.37 m/month for oak and 0.35 m/month for pasture). It should be noted that the period analyzed was after a dry

spring. Therefore the water table was almost in its lowest position. (Therefore we are close to the very end of the general groundwater recession curve, where further decay is very slow).

Rainfall interrupted the fluctuations at both places (e.g. July 11) but this is probably not the effect of a surplus recharge to the groundwater (because the water table was relatively deep) nor a cessation of groundwater use of vegetation (*Figure 4*).

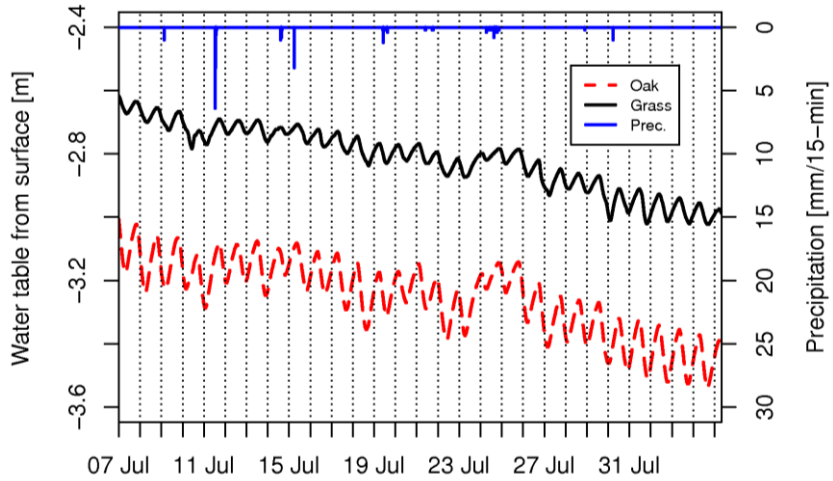

Figure 4. Water table from the surface under the oak (forest) and grass (pasture) sites (07. 07. 2012. – 05/ 08/ 2012.)

The amplitude of groundwater fluctuation for a forest is more than twice as large (16/2 cm) than for a pasture (7.2/2 cm) (*Figure 5)*. The appearance of a diurnal signal under a pasture shows us the groundwater uptake of grass vegetation. The magnitude of the fluctuation has a strong connection to groundwater use (Soylu et al. 2012) so it shows us the more significant groundwater use of a forest (because the soil textures of the two plots are similar: sandy-loam, loam). The magnitude of the fluctuation was higher than calculated by Nosetto et al. (2007) (5.5 cm on average for oak forest), but similar to that determined by Móricz et al. (2012) (14 cm for an oak forest and 2 cm for the fallow plot in dry periods) for similar soil types.

The time of the maximum and minimum groundwater levels were the same for both land covers (9h for max. and 20h for min.) validating that the inducing effect is the same (*Figure 5*).

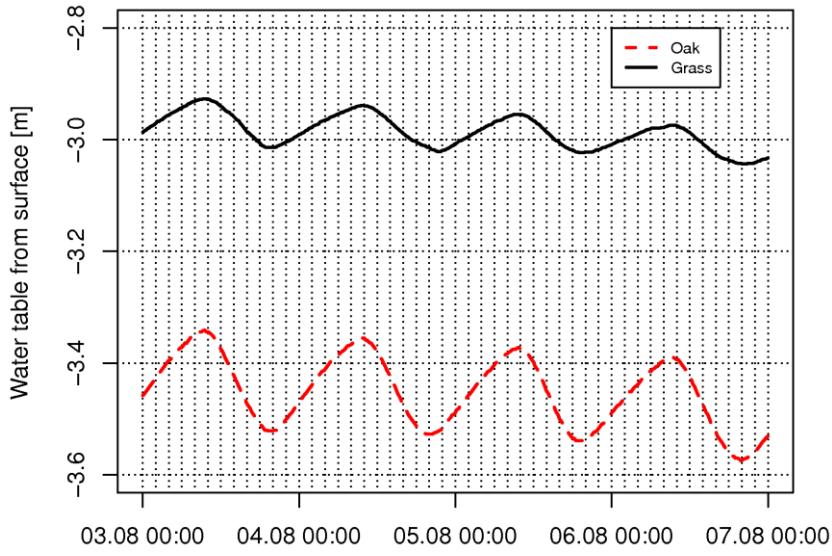

Figure 5. Diurnal fluctuations in water table levels comparing an oak (forest) and a grass (pasture) site

3.2 ET_{gw} values for an oak and a pasture site

Using the empirical ET estimation technique of Gribovszki et al. (2008), the groundwater uptake of different vegetation types, were calculated in a very dry period of summer 2012.

Figure 6 shows *ET* rates with 30-min frequency and in *Figure 7 ET* rates with daily frequency are shown.

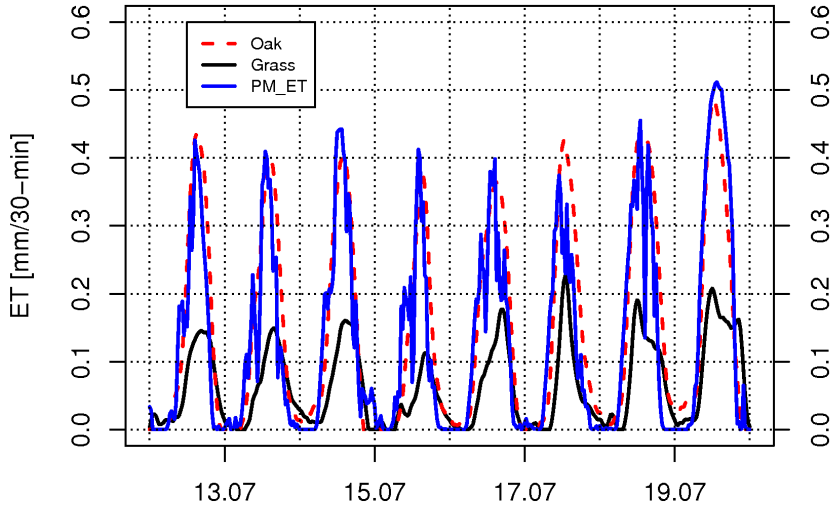

Figure 6. Calculated ET rates with 30-min frequency

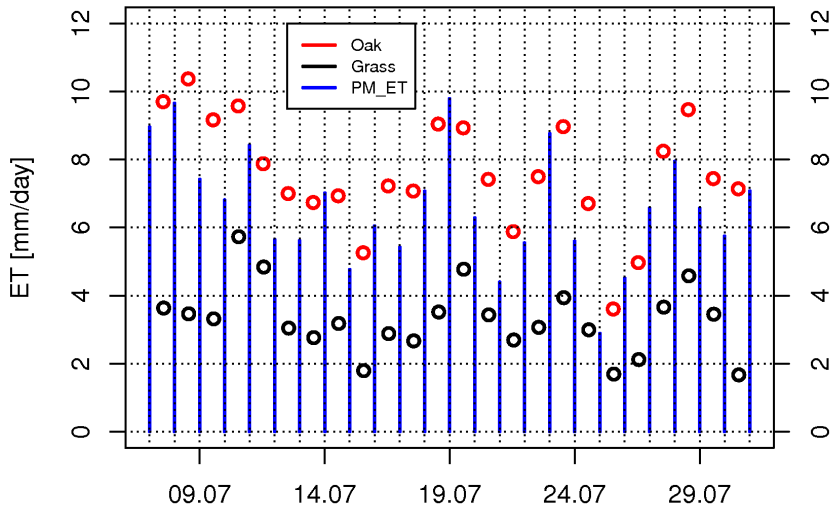

Figure 7. ET rates aggregated to a daily scale

ET rates have the following characteristics:
Groundwater uptake of an oak stand (mean: 7.5 mm/day) is a bit higher than *PM_ET*, (mean: 6.6 mm/day). Pasture (grass) ET_{gw} (mean: 3.5 mm/day) is less than half of the oak.

A rate higher than the potential rate values for oak can be found because the potential ET value was calculated for a grass reference surface. If calculation of potential ET had been conducted for rougher surface conditions and for higher LAI of the forest, the ET values would have been higher because of the greater atmospheric and canopy conductance of the forest canopy.

The daily groundwater uptake seems to be great, but the data seem to be acceptable taking into account that the period of analyses was very hot and till July of 2012 soil profile

had already lost almost all of the moisture stored in preceding periods and all around there is a dry and warm environment. (Therefore the oasis effect can enhance *ET*).

As a comparison, ET values of Nosetto et al. (2007) in Hortobágy determined a 1.9 mm/day (up to 3.2 mm/day) groundwater ET for an oak forest on the basis of diurnal fluctuation of the water table. In that study the groundwater levels were significantly lower (on average 5 m) and the measurement period was in autumn. Therefore the higher values are possible in our case. In contrast using a diurnal method Butler et al. (2007) obtained groundwater ET rates of 2.9–9.3 mm/day for mixed vegetation types based on continuous groundwater level readings at groundwater depths between 0.3 and 3.4 m from the surface. Therefore calculated groundwater ET rates were close to total ET as in our case.

It must be noted that determination of readily available S_y is a weak point in all diurnal signal based ET estimation methods. Therefore the above determined ET values are not absolutely accurate, but the ratio of ET for different land covers is more accurate.

The correlation values between *PM_ET* and estimated groundwater ET rates are the following (*Table 1*).

Table 1. Correlation coefficients (r) between reference PM_ET and estimated ET_{gw} values

Stand	30-min scale	Daily scale
Oak-PM	0.938***	0.853***
Pasture-PM	0.816***	0.743***

Oak-PM means correlation between ETgw of Oak site and reference ET (PM_ET)
Pasture-PM means correlation between ETgw of Pasture site and reference ET (PM_ET)
*** Signif. code, p-value is less than 0.001

The stronger correlations (also for 30-min and daily scales) between *Oak_ET* and *PM_ET* showed that during the analyzed period these parameters are very similar. It means that *Oak_ET* reached the magnitude of potential ET and the water used for *ET* was mostly consumed from groundwater according to the meteorological constraint because there is no usable soil moisture in the soil column in this very dry period. The better correlation of pasture at a 30-min scale means that the diurnal shape of the two curves is similar, but the lower correlation for the daily scale shows a lower correspondence of *Pasture_ET* to meteorological factors. (Probably the root system of grass is not as adequate for as much groundwater uptake as that of the forest).

3.3 Salt Dynamics

Specific electric conductivity, which is strongly correlated with salt content, was measured to evaluate salt accumulation (*Figure 8*). The greatest difference in soil salt content between two land use types was detected in the upper part of the soil and at a depth of 350 cm. The specific conductivity values were 127 and 70 μS/cm higher in the soil of an oak forest at that depth. As a comparison, conductivity values measured by Nosetto (2007) in a similar oak and grassland comparison in Hortobágy) were generally 2–5 times higher than in this study. The vertical profile distribution was different in Hortobágy (Nosetto 2007) showing significantly higher conductivity values for grass in upper soil layers, which cannot be detected in Jászfelsőszentgyörgy. The higher conductivities of lower soil layers (above the groundwater) for oak forests showed a similar tendency at Jászfelsőszentgyörgy and Hortobágy.

The salt content of the groundwater was also slightly greater under the oak plot. (The conductivities of groundwater are: oak-1023, pasture-960 μS/cm). The differences do not mean any problem for forest vegetation productivity and vitality, but salt accumulation

induced by climate change can be a long term effect of afforestration in these kinds of soils and hydrological combinations. Nosetto et al. (2007) also detected a higher conductivity of groundwater under an oak forest than under grassland in Hortobágy, but the absolute magnitudes were significantly higher at 4900 µS/cm and 2000 µS/cm under an oak forest and grassland.

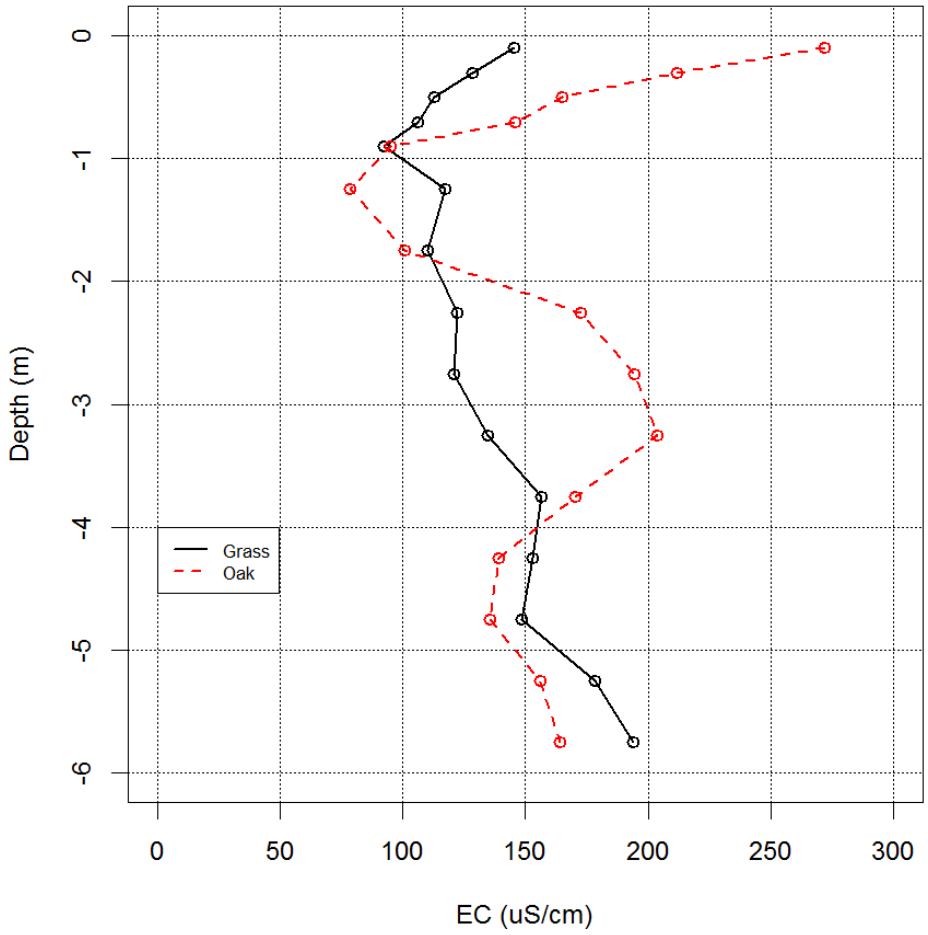

Figure 8. Electrical conductivity (EC) profile under the pasture and oak forest

4 CONCLUSIONS

Hydrological characteristics of earlier land uses during the last century (grassland and arable land) in the Great Plain are significantly different from those of the forest. A larger biomass needs a higher amount of transpiration which can be taken up from the groundwater by the deeper root system of the forest if precipitation is insufficient. Increased groundwater uptake results in a depression of the water table under forest covered sites in areas with a shallow groundwater table.

The larger amount of forest groundwater use is not parallel with salt uptake. Therefore salts can accumulate in both the soil and groundwater. The measured differences in salt content are small compared to similar research results for clayey soils (Nosetto et al. 2007). However in the long run, and taking into account longer dry periods induced in the future by climate change, this process can result in the decline of biological production of a forest.

Table 1 summarizes the results of these processes comparing an oak forest and neighboring pasture on the basis of the dataset of this study.

Table 1. Summary of impacts of an oak forest on water and salt dynamics (EC=electric conductivity; GW=groundwater)

Parameter	Oak	Pasture	Process
EC GW (μS/cm)	1023	960	Salt cc. of GW increases
EC soil 0–20 cm (μS/cm)	272	145	Salt accumulation in upper soil layer
EC soil 300–350 cm (μS/cm)	204	134.9	Salt accumulation in lower soil layer
GW level (asl [mBf])	101.5	102.4	Water table depression (0.9 m)
Water table depth (m from suface)	3.26	2.82	Water table difference from surface (0.44 m)
Diurnal signal amplitude (cm)	16	7.2	Stronger diurnal signal of oak (ratio 2.2)
ET from GW (mm/day)	7.6	3.3	Greater GW uptake of oak (ratio 2.3)

Acknowledgements: The research of Zoltán Gribovszki was supported by the European Union and the State of Hungary, co-financed by the European Social Fund in the framework of TÁMOP 4.2.4. A/2-11-1-2012-0001 'National Excellence Program'. The relating research group was also supported by a fund from OTKA (NN 79835) and TAMOP-4.2.2.A-11/1/KONV-2012-0013 project.

REFERENCES

ALLEN, R.G. – PEREIRA, L.S. – RAES, D. – SMITH, M. (1998): Crop evapotranspiration – Guidelines for computing crop water requirements. Vol. 56 of FAO Irrigation and Drainage. FAO, Rome, URL http://www.fao.org/docrep/X0490E/x0490e06.htm.

ANDRASEVITS, Z. – BUZÁS, GY. – SCHIBERNA, E. (2005): Current afforestation practice and expected trends on family farms in West Hungary. Journal of Central European Agriculture, (5): 297–302.

BUTLER, J.J. – KLUITENBERG, G.J. – WHITTEMORE, D.O. – LOHEIDE II, S.P. – JIN, W. – BILLINGER, M.A. – ZHAN, X. (2007): A field investigation of phreatophyte-induced fluctuations in the water table. Water Resour. Res. 43: W02404. doi: 10.1029/2005WR004627.

CALDER, I. R. (1998): Water use by forests, limits and controls. Tree Physiol, 18: 625–631.

FÜHRER, E. – JÁRÓ, Z. (2005): Az erdővagyon bővítése a mezőgazdaságilag gazdaságosan nem hasznosított földterületek beerdősítésével [Forest cover enlargement by afforestration of economically non rentable agricultural lands] (in Hungarian) In: Molnár S. (Szerk.): Erdő-fa hasznosítás Magyarországon. NyME FMK. Sopron. 130–136.

GRIBOVSZKI, Z. – KALICZ, P. – SZILÁGYI, J. – KUCSARA, M. (2008): Riparian zone evapotranspiration estimation from diurnal groundwater level fluctuations. Journal of Hydrology 349: 6–17, http://dx.doi.org/10.1016/j.jhydrol.2007.10.049

GRIBOVSZKI, Z. – SZILÁGYI, J. – KALICZ, P. (2010): Diurnal fluctuations in shallow groundwater levels and in streamflow rates and their interpretation - a review. Journal of Hydrology 385: 371–383, http://dx.doi.org/10.1016/j.jhydrol.2010.02.001

IJJÁSZ, E. (1939): A fatenyészet és az altalajvíz, különös tekintettel a nagyalföldi viszonyokra [Forest and groundwater connections in Hungarian Great Plain] (in Hungarian) Erdészeti Kísérletek, 42: 1–107.

JOBBÁGY, E. G. – JACKSON, R. B. (2004): Groundwater use and salinization with grassland afforestation. Global Change Biol., 10: 1299–1312.

LOHEIDE II, S.P. – BUTLER, J.J. – GORELICK, S.M. (2005): Use of diurnal water table fluctuations to estimate groundwater consumption by phreatophytes: A saturated–unsaturated flow assessment. Water Resour. Res. 41: W07030. doi: 10.1029/2005WR003942.

MAGYAR, P. (1961): Alföldfásítás II. [Afforestration in Hungarian Great Plain II.] (in Hungarian) Akadémiai Kiadó. Budapest.

MAJOR, P. (2002): Síkvidéki erdők hatása a vízháztartásra [Effect of lowland forest on water balance] (in Hungarian) Hidrológiai Közlöny, 82: 319–324.

MÓRICZ, N. – MÁTYÁS, C. – BERKI, I. – RASZTOVITS, E. – VEKERDY, Z. – GRIBOVSZKI, Z. (2012): Comparative water balance study of forest and fallow plots. iForest 5: 188–196 [online 2012-08-02] URL: http://www.sisef.it/iforest/contents?id=ifor0624-005

NOSETTO, M. D. – ESTEBAN, E. G. – PARULEO, J. M. (2005): Land use change and water losses. The case of grassland afforestation across a soil textural gradient in central Argentina. Global Change Biol. 11: 1101–1117.

NOSETTO, M D. –JOBBÁGY, E. G. – TÓTH, T – DI BELLA, C. M. (2007): The effects of tree establishment on water and salt dynamics in naturally salt-affected grasslands. Oecologia (152): 695–705.

NOSETTO M.D. – JOBBÁGY M. G. – TÓTH T. – JACKSON R. B. (2008): Regional patterns and controls of ecosystem salinization with grassland afforestation along a rainfall gradient. Global Biogeochemical Cycles 22: GB2015, doi: 10.1029/2007GB003000

SOYLU, M. E. – LENTERS, J. D. – ISTANBULLUOGLU, E. – LOHEIDE II, S. P. (2012): On evapotranspiration and shallow groundwater fluctuations: A Fourier-based improvement to the White method, Water Resour. Res. 48: W06506, doi: 10.1029/2011WR010964.

SZABÓ, A. – KISS, K. – GRIBOVSZKI, Z. – TÓTH, T. (2012): Erdők hatása a talaj és altalaj sóforgalmára, valamint a talajvíz szintjére [Effect of forests on the salt accumulation of soils and subsoils and on the watertable level.] (in Hungarian) Agrokémia és Talajtan. 61: 195–209.

SZILÁGYI, J. – KOVÁCS, Á. – JÓZSA, J. (2012): Remote sensing based groundwater recharge estimates in the Danube-Tisza Sand Plateau region of Hungary. J. Hydrol. Hydromech. 60: 64–72, doi: 10.2478/v10098-012-0006-3

SZODFRIDT, I. – FARAGÓ, S. (1968): Talajvíz és vegetáció kapcsolata a Duna–Tisza köze homokterületén [Vegetation and groundwater connections in Kinkunság sand areas] (in Hungarian) Bot. Közlem. 55: 69–75.

WHITE, W.N. (1932): Method of estimating groundwater supplies based on discharge by plants and evaporation from soil – results of investigation in Escalante Valley, Utah - US Geological Survey. Water Supply Paper 659-A: 1–105.

ACTA SILVATICA ET LIGNARIA HUNGARICA

Vol. 10, Nr. 2

Contents

ACTA SILVATICA ET LIGNARIA HUNGARICA

Vol. 10, Nr. 2

Tartalomjegyzék

DOI: 10.2478/aslh-2014-0009 Acta Silv. Lign. Hung., Vol. 10, Nr. 2 (2014) 117–131

Hydrological Impacts of Various Land Cover Types in the Context of Climate Change for Zala County

Péter CSÁKI* – Péter KALICZ – Gábor Béla BROLLY – Gergely CSÓKA – Kornél CZIMBER – Zoltán GRIBOVSZKI

Institute of Geomatics and Civil Engineering, University of West Hungary, Sopron, Hungary

Abstract – The water balance of Zala County was analyzed using remote-sensing based actual evapotranspiration (ET_A) and runoff (R) in the context of land cover types. The highest mean ET_A rates were determined for water bodies (658 mm/year) and wetlands (622 mm/year). Forests have higher values than agricultural areas, and the lowest rates belong to artificial surfaces. Mean annual runoff is the largest on artificial surfaces (89 mm/year). For climate change impact analysis a Budyko-model was used in spatially distributed mode. The parameter of the Budyko model (α) was calculated for pixels without surplus water. For the extra water affected pixels a linear model with β parameter (actual evapotranspiration / pan evapotranspiration) was used. These parameters (α and β) can be used for evaluating future ET_A and R in spatially distributed mode. According to the predictions, the mean annual evapotranspiration may increase about 27 mm while the runoff may decrease to one third of the present amount by end of the century.

evapotranspiration / runoff / land cover / Budyko-model / climate change

Kivonat – Különböző felszínborítások vízforgalomra gyakorolt hatása a klímaváltozással összefüggésben Zala megye példáján. Zala megye területi vízmérlegének elemzése távérzékelési adatokon alapuló aktuális evapotranszspiráció (ET_A) és lefolyás (R) alapján, a felszínborítás függvényében történt. A legmagasabb átlagos párolgásértékek a vizek (658 mm/év) és a vizenyős területek (622 mm/év) esetében jelentkeztek. Az erdők magasabb párolgással jellemezhetők, mint a mezőgazdasági területek, a legalacsonyabb értékek a mesterséges felszínekhez tartoznak. Az éves átlagos lefolyás a legnagyobb a mesterséges felszíneken (89 mm/év). A klímaváltozás hatásának vizsgálata egy térben osztott Budyko féle modell használatával történt. A Budyko modell kalibrációs paramétere (α) a többletvízhatástól független pixelekre került kiszámításra. A többletvízhatású pixelek esetében egy lineáris β paraméterű modellt (aktuális párolgás / kádpárolgás) vezettünk be. A két paraméter (α és β) segítségével becsülhető a jövőbeli ET_A és R, térben osztott módon. Az előrejelzés alapján az éves átlagos aktuális párolgás 27 mm-el növekedhet, míg a lefolyás a harmadára csökkenhet a század végére.

evapotranszspiráció / lefolyás / felszínborítás / Budyko-modell / klímaváltozás

* Corresponding author: csakipeti.nyme@gmail.com; H-9400 SOPRON, Bajcsy-Zs. u. 4.

1 INTRODUCTION

More precipitation evaporates than runs off and stored on the land surface (Hewlett 1982). Generally, in Hungary about 90% of precipitation evaporates and only 10% goes to streams, soil and groundwater storage. Due to the high latent heat of vaporization value of water evapotranspiration (ET) is a very effective indicator for mass and energy () transfer between the land- or vegetation surface and the ambient atmosphere (Szilágyi – Józsa 2009).

Obtaining spatially distributed ET estimates is crucial in most water balance calculations for identifying mass and energy fluxes across the area of interest (Szilágyi – Kovács 2011). Monthly actual evapotranspiration (ET_A) has been mapped for Hungary by Kovács (2011) over the 2000-2008 period. On an annual scale – using ET_A and precipitation data – the spatially distributed runoff can be calculated using the long-term water-balance equation:

$$R = P - ET_A \tag{1}$$

where P is the precipitation, ET_A is the evapotranspiration and R is the runoff (each members in mm/period). The spatially distributed ET_A and R maps are suitable to analyze the data in the context of land cover types (CLC 2006).

2 MATERIAL AND METHODS

2.1 Description of the ET mapping technique

Morton et al. (1985) presented an algorithm (called the WREVAP model) – based on Bouchet's (1963) complementary relationship – for estimating regionally representative ET_A rates for periods longer than 5 days. Szilágyi – Józsa (2009), Szilágyi et al. (2011) devised a method of disaggregating the regional ET_A values into spatially variable ET_A rates. It is based on the assumption that at a large enough scale (for example 1 km) where surface heterogeneities of a terrain become largely smoothened out, surface temperatures are proportional to the ET_A rates, since evaporation is an endothermic process, providing an effective cooling (due to the high latent heat of vaporization) of the evaporating surface.

The spatial disaggregation of the regionally representative ET_A rates is based on a linear transformation of the 8-day composite MODIS (Moderate Resolution Imaging Spectroradiometer) daytime surface temperature (T_s) values into ET_A rates (Szilágyi – Józsa 2009). The transformation requires specifying two anchor points in the T_s – ET plane (*Figure 1*). The first is defined by the spatially averaged daytime surface temperature (T_s) and the corresponding regionally representative ET_A rate (from WREVAP, using spatially averaged values of the required climate variables). The second anchor point comes from a spatial average of the coldest pixel values for well watered cells within the region (T_{WS} – wet surface temperature) and the corresponding wet environment evaporation rate (ET_W), out of consideration that the coldest pixels are the wettest (Szilágyi – Kovács 2010). The two points define the linear transformation of the T_S pixel values into ET_A rates for the examined period (for example a month).

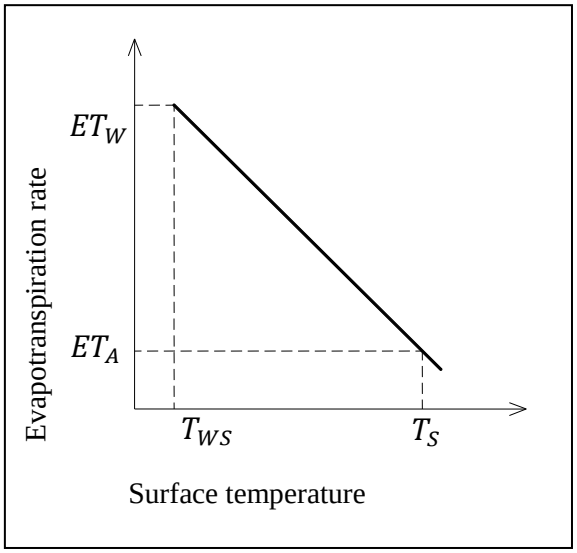

Figure 1. Schematic representation of the linear transformation of the MODIS daytime surface temperature values into ET rates (after Szilágyi et al. 2011)

The 8-day composited MODIS daytime T_s data for Hungary over the 2000–2008 period was collected and the T_s maps were averaged for each month to yield one surface temperature map per month by Kovács (2011). Further necessary data for calculation (mean annual precipitation, mean monthly air temperature, specific humidity as well as sunshine duration values) were provided by the Hungarian Meteorological Service. The monthly ET_A maps were prepared from March till November each year, because in the winter-time with possible patchy snow cover on the ground the quasi-constant surface net energy assumption of the T_s versus ET_A transformations break down (due to the snow cover's vastly different albedo from that of the land) (Szilágyi – Józsa 2009). ET in Hungary is small from December through February, the sum total is about 20 mm (Kovács 2011). We made calculations for total water years (from November 1 to October 31), so a 20 mm correction was added for all pixels of each mean annual ET maps (1999 November was prepared as the average of the other Novembers). The mean annual ET maps were averaged for the period of 1999-2008.

2.2 The Budyko type model

The Budyko curve (Budyko 1974) is often used to estimate the actual evaporation as a function of the aridity index. In any location, depending on the dryness of the climate, either the available water or the available energy is the limiting factor (Gerrits et al. 2009).
The Budyko curve is based on two balance equations, the water balance and the energy balance:

$$\Delta S = P - ET_A - R \tag{2}$$

$$Q_{nT} = L \cdot ET_A + H + G \tag{3}$$

where ΔS is the water storage change over time (m/year), P the precipitation (m/year), ET_A the actual evaporation (m/year), R the runoff (m/year), Q_{nT} the net radiation (J/m^2/year), L the latent heat of vaporization (J/m^3), H the sensible heat flux (J/m^2/year), and G the ground heat flux (J/m^2/year).

On an annual time scale we can assume (Arora 2002) that the water storage change is negligible (ΔS = 0) and that the net ground heat flux approaches zero (G = 0), thus:

$$P = ET_A + R \tag{4}$$

$$Q_{nT} = L \cdot ET_A + H \tag{5}$$

By dividing *Eq. 5* by *Eq. 4* we obtain:

$$\frac{Q_{nT}}{P} = \frac{L \cdot ET_A}{P} + \frac{H}{P} \tag{6}$$

Arora (2002) interprets potential evaporation as (different from the above ET_P):

$$ET_0 = \frac{Q_{nT}}{L} \tag{7}$$

Displacement of *Eq. 6* by *Eq. 7*:

$$\frac{ET_0}{P} = \frac{ET_A}{P} + \frac{(H/L)}{P} \tag{8}$$

If we define the Bowen ratio as $B_r = H/L \cdot ET_A$ (Gerrits et al. 2009), we obtain:

$$\frac{ET_0}{P} = \frac{ET_A}{P} + \frac{B_r \cdot ET_A}{P} = \phi = \frac{ET_A}{P}(1 + B_r) \tag{9}$$

with ϕ the aridity index.

Since the Bowen ratio can also be expressed as a function of the aridity index ($B_r = f(\phi)$) (Arora 2002), *Eq. 9* can be rewritten as:

$$\frac{ET_A}{P} = \frac{\phi}{1+f(\phi)} = f(\phi) \tag{10}$$

So, the evapotranspiration ratio $\left(\frac{ET_A}{P}\right)$ is a function of aridity index.

A lot of studies have been done on finding this relation. The best-kown classical studies were done by Schreiber, Ol'dekop, Turc, Pike, Budyko and Porporato et al. (Gerrits et al. 2009). Their equations are summarized in *Table 1*.

Table 1. Equations for the relation of the evapotranspiration ratio $\left(\frac{ET_A}{P}\right)$ and the aridity index (ϕ) (after Gerrits et al. 2009)

Equation	Reference
$\frac{ET_A}{P} = 1 - \exp(-\phi)$	Schreiber (1904)
$\frac{ET_A}{P} = \phi \tanh(1/\phi)$	Ol'dekop (1911)
$\frac{ET_A}{P} = \frac{1}{\sqrt{0.9+(1/\phi)^2}}$	Turc (1954)
$\frac{ET_A}{P} = \frac{1}{\sqrt{1+(1/\phi)^2}}$	Pike (1964)
$\frac{ET_A}{P} = [\,\phi \tanh(1/\phi)(1 - \exp(-\phi))]^{0.5}$	Budyko (1974)
$\frac{ET_A}{P} = 1 - \frac{\phi \cdot \gamma^{\frac{\gamma}{\phi}-1} \exp(-\gamma)}{\Gamma\left(\frac{\gamma}{\phi}\right) - \Gamma\left(\frac{\gamma}{\phi}, \gamma\right)}$	Porporato et al. (2004)

From the above models we are using the Schreiber equation (Schreiber 1904), because of its simplicity. The actual evapotraspiration estimated by Schreiber's method (hereinafter the evapotranspiration, the precipitation and the runoff are understood in mm/year instead of m/year):

$$ET_A = P(1 - \exp(-\phi)) = P\left(1 - \exp\left(-\frac{ET_0}{P}\right)\right) \tag{11}$$

The determination of runoff by Schreiber (Fraedrich 2009):

$$R = P - ET_A = P \exp\left(-\frac{ET_0}{P}\right) \tag{12}$$

After rearrangement we get the following equation for potential evapotranspiration:

$$ET_0 = -P\left(\ln\left(\frac{R}{P}\right)\right) \tag{13}$$

ET_0 can also be expressed as a function of pan-evaporation (ET_{pan}), according to the general relation for Hungary (Nováky 2002):

$$ET_0 = f(ET_{pan}) = -\alpha ET_{pan} = -\alpha\left(36400\frac{T}{P} + 104\right) \tag{14}$$

where α is a calibration parameter, which aggregates all of the factors affecting ET (dominantly the surface cover) (Keve – Nováky 2010), and T is the mean annual temperature (°C).

Knowing the above equations, α can be calculated:

$$\alpha = -\frac{ET_0}{ET_{pan}} \tag{15}$$

According to Nováky, the spatially distributed version of the Budyko model is applicable to analyze the climatic impacts (Nováky 1985, 2002). The spatially-distributed determination of α parameter was the following: ET_0 (*Eq. 13*) and ET_{pan} (the part in parentheses of *Eq. 14*) values of Zala county were calculated for the 1999-2008 period (in the same resolution as the ET_A maps), and they were substituted for *Eq. 15*.

When the ET_A value was higher than the P value of the pixel, so R became negative, the α parameter could not be determined, because the natural logarithm of a negative number is undefined (*Eq. 13*). For these pixels another calibration parameter (β) was calculated according to the next formula (McMahon et al. 2012):

$$\beta = \frac{ET_A}{ET_{pan}} \tag{16}$$

α and β parameters must be calculated in spatially distributed mode (maps). The parameter maps (α and β) are suitable to analyze this data in the context of land cover types. They can be used for evaluating future ET and R in spatially-distributed mode, for that only temperature and precipitation predictions are required.

The calculations were done with the help of DigiTerra Map software, the temperature and precipitation data were available in the "Agroclimate 2 (VKSZ_12-1-2013-00-34)" project.

3 STUDY SITE DESCRIPTION

Zala County is situated in the south-western part of Hungary (*Figure 2*). It is one of the smallest counties of Hungary. It covers 3784 km^2. The population was 282 179 people in 2011 (less than the 3% of the total population of Hungary). The mean population density is 75 people per km^2 (KSH 2011).

The county has a varying landscape of hills and valleys. The settlement density is one of the highest in Hungary, although the average size of the settlements is less than the half of the national average. It has no distinctive isolation from adjacent territories. It is a transition through a series of grades. The highest point of the county is 445 m (Köves-tető) in the Keszthelyi Mountains on the eastern edge of the county.

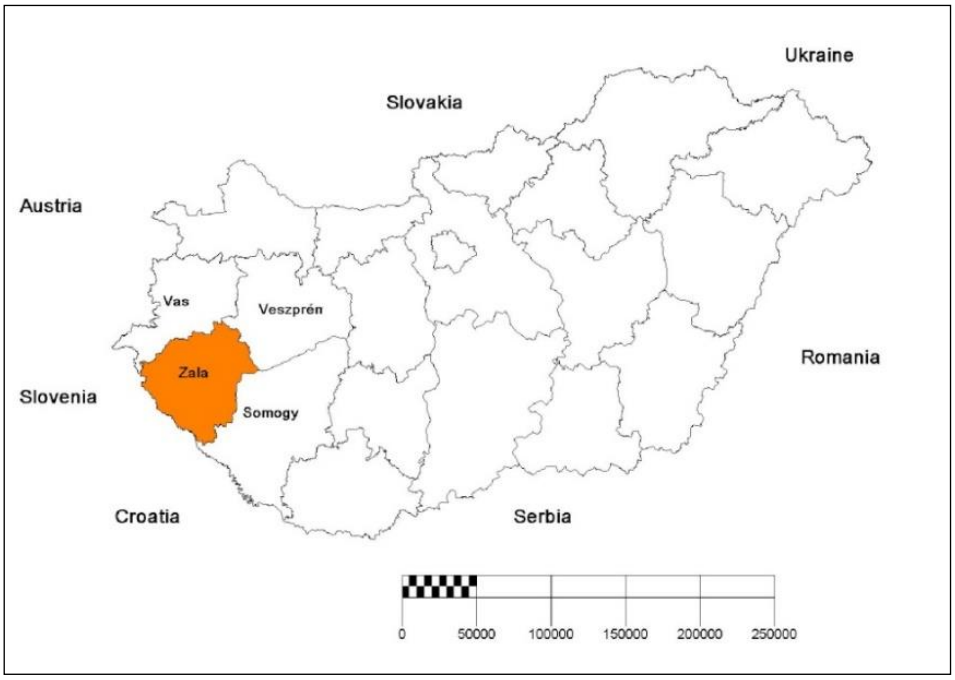

Figure 2. Location of Zala County within Hungary

The climate is moderated by atlantic effects, so the mean annual temperature was about 11.6 °C between 1999 and 2008. Winters are relatively mild and summers tend to be cooler than the norm for the Carpathian Basin. It is one of the wettest parts of the country. The average annual rainfall during this period was about 700 mm in the west, and 600 mm in the east.

Agriculture is the dominant land use (54%) in the County, with a significant presence of forest and semi natural areas, which cover more than 37% of the total area (*Figure 3 and Table 2*).

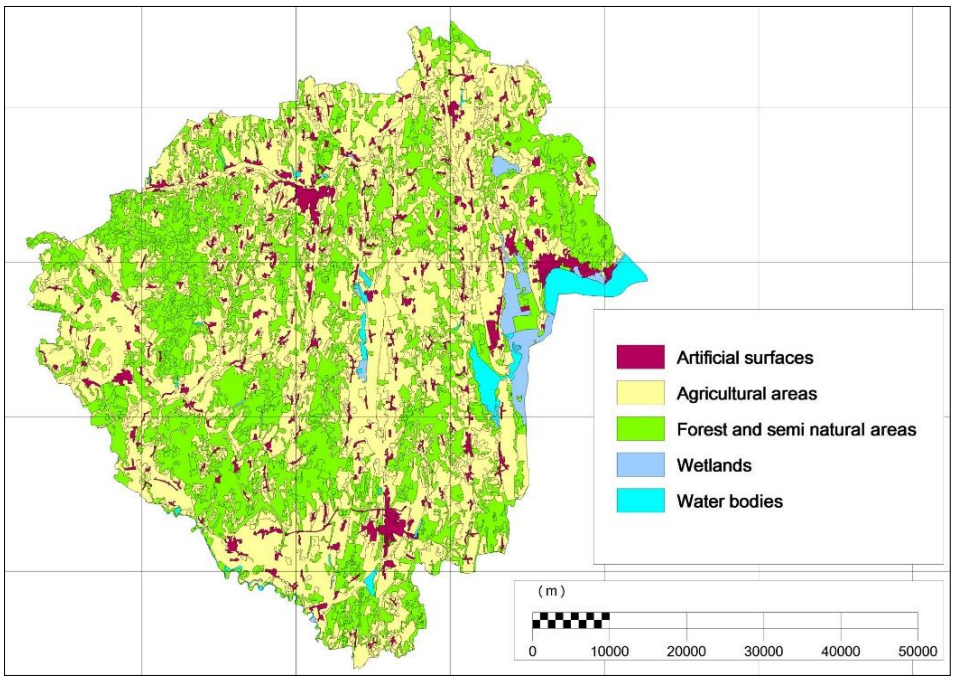

Figure 3. Land cover of Zala County (CLC 2006)

Table 2. Land cover distribution of Zala County

Land cover type	Area (km^2)	Percentage (%)
Artificial surfaces	195.90	5.18
Agricultural areas	2040.71	53.94
Forest and semi natural areas	1406.01	37.16
Wetlands	62.97	1.66
Water bodies	77.94	2.06
Total	3783.54	100.00

4 RESULTS

The averaged (1999-2008 period) mean actual evapotranspiration and runoff for Zala County were analyzed in the context of land cover types. Moreover, the Budyko type α and the β parameters were calculated, mapped and analyzed too.

4.1 Evaluation of evapotranspiration

The mean annual actual evapotranspiration over Zala County (1999-2008) is displayed in *Figure 4*. The average ET_A of the County was 577 mm/year, which is 88% of the mean annual precipitation (655.7 mm/year). The brown pixels show lower rates on the map. The bigger cities are distinctly visible as brown patches. Higher ET_A values (blue pixels) belong to water bodies and wetlands,.

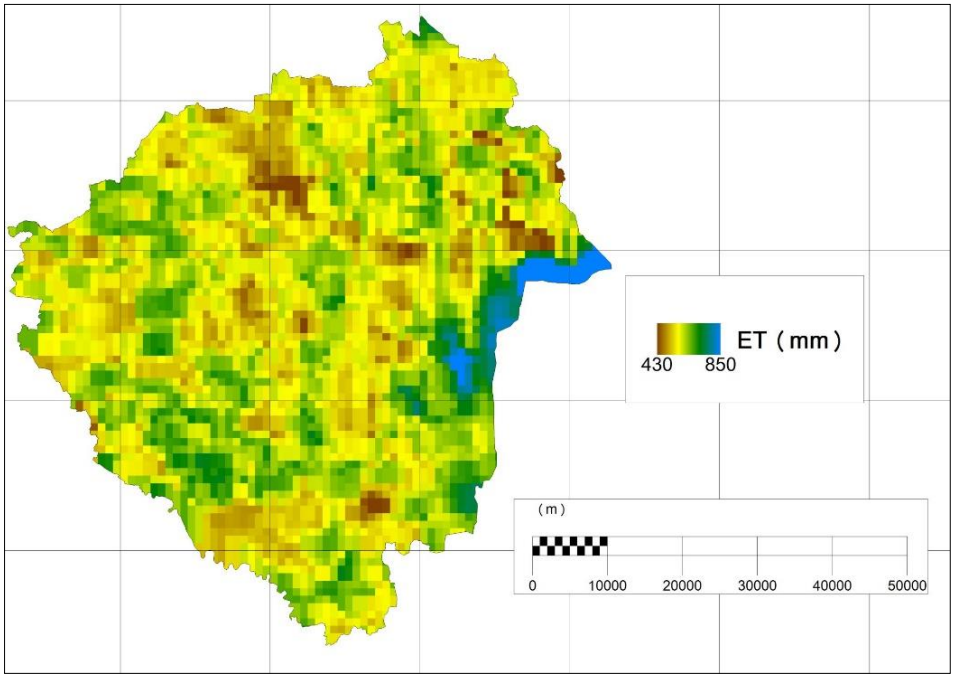

Figure 4. Mean annual ET_A rates over Zala County (1999-2008)

Table 3 contains the ET_A values belonging to the each Corine Land Cover (CLC 2006) type. The evapotranspiration, the runoff, the Budyko α and the β parameter maps have a 1·1 km resolution. They were examined with a vector land cover map, so more land cover types might belong to one pixel. The value of these 'mixed pixels' were counted in more land cover types, so it distorts the differences between the categories.

The highest mean annual ET_A rates were determined for water bodies (658 mm/year) and wetlands (622 mm/year). Forest and semi natural areas have higher values than agricultural areas and the lowest rates belong to artificial surfaces. Standard deviation is the highest in case of water bodies (97 mm).

Table 3. Mean annual ET_A rates of different land cover types over Zala County (1999-2008)

Land cover type	Mean annual ET (mm)				
	Min	Max	Average	P%*	Std. dev
Artificial surfaces	450	703	562	86	38
Agricultural areas	434	721	569	87	35
Forest and semi natural areas	434	828	582	89	37
Wetlands	461	729	622	95	53
Water bodies	486	846	658	100	97

* In the percentage of the mean annual precipitation

Figure 5 shows the mean annual ET_A over forest and semi natural areas. In the north-eastern part of Zala County the ET_A values of forest are generally lower than the south-western part and the neighborhood of wetlands.

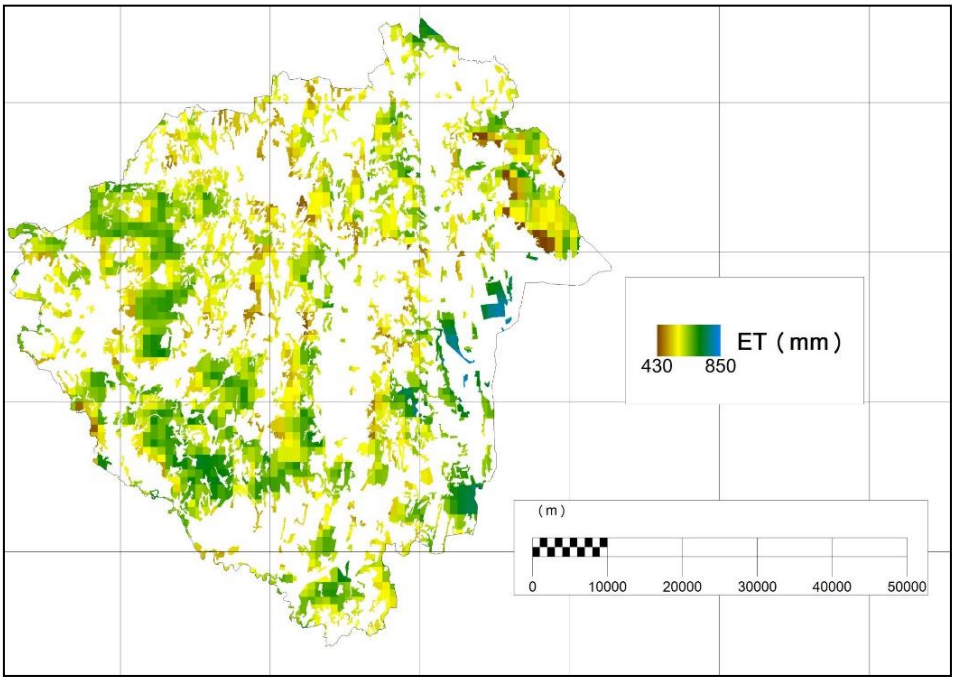

Figure 5. Mean annual ET_A rates over forest and semi natural areas in Zala County (1999-2008)

4.2 Evaluation of runoff

The mean annual runoff (R, 1999–2008) was calculated from the water-balance equation, as the difference of annual precipitation and mean annual actual evapotranspiration ($R = P - ET_A$). The 10×10 km spatial resolution precipitation map was downscaled for 1×1 km using the bicubic convolution interpolation technique, and after it was validated by field measurements. (The data from field measurements were not used for preparation of the original map.)

Figure 6 shows the mean annual runoff over Zala County and *Table 4* contains the rates of the different types of land cover. The average runoff was 78 mm/year, which is 12% of the mean annual precipitation (655.7 mm/year). The runoff is the highest on artificial surfaces, and it decreases in the other categories. It is especially low for wetlands, and negative for water bodies, where the ET_A is generally higher than the precipitation. Moreover, the standard deviation is the highest over water bodies (119 mm).

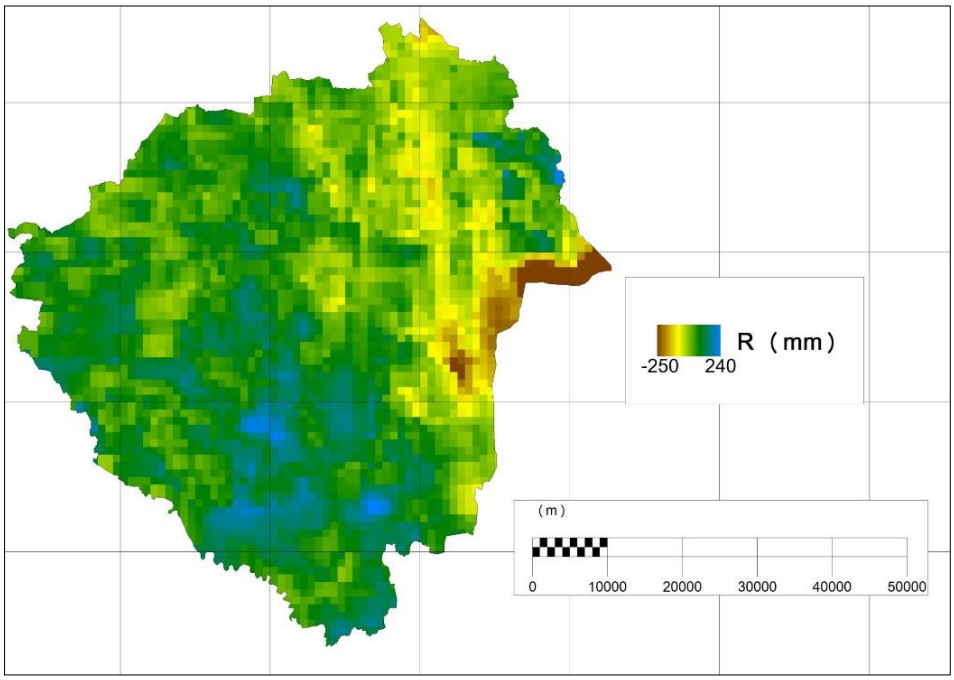

Figure 6. Mean annual R rates over Zala County (1999-2008)

Table 4.Mean annual runoff rates of different land cover types over Zala County (1999-2008)

Land cover type	Mean annual R (mm)				
	Min	Max	Average	P%*	Std. dev
Artificial surfaces	–86	231	89	14	48
Agricultural areas	–88	231	87	13	45
Forest and semi natural areas	–181	214	77	12	46
Wetlands	–98	140	2	0	58
Water bodies	–250	211	–19	–3	119

* In the percentage of the mean annual precipitation

4.3 Evaluation of α and β parameters

The calculated Budyko type α parameter can be seen in *Figure 7*, and the values belonging to the each land cover type are in *Table 5*.

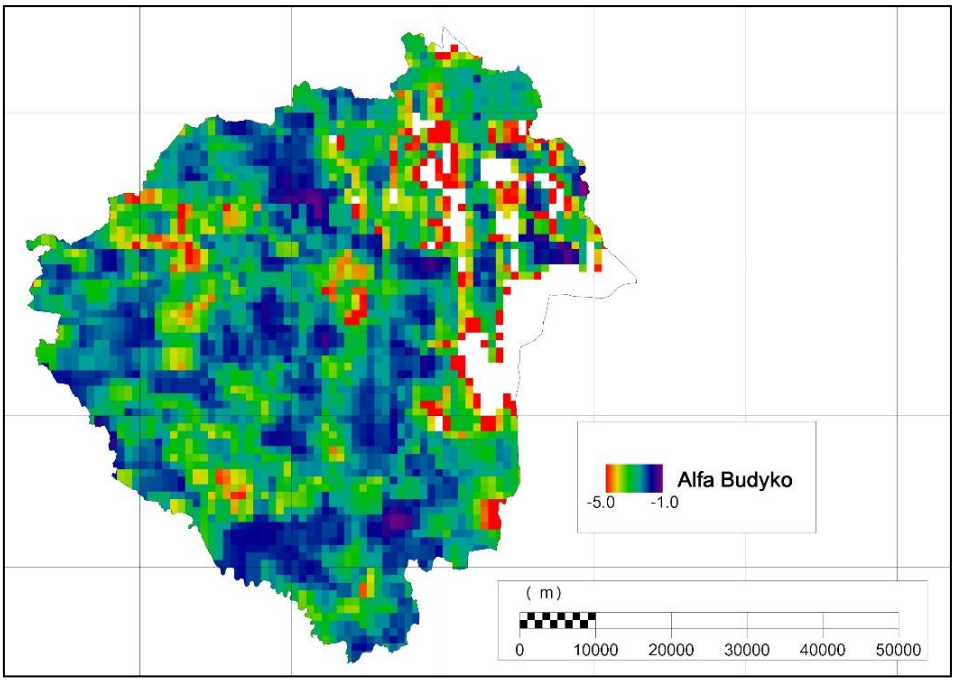

Figure 7. The calculated Budyko type α parameter rates in Zala County

Table 5. The calculated Budyko type α parameters (absolute values) of different land cover types over Zala County

Land cover type	α parameter			
	Min	Max	Average	Std. dev.
Artificial surfaces	1.03	4.59	1.80	0.42
Agricultural areas	0.96	7.48	1.86	0.46
Forest and semi natural areas	0.96	7.48	1.98	0.51
Wetlands	1.08	5.88	2.42	1.05
Water bodies	1.15	6.30	2.16	0.87

Compared to the α values determined by Keve – Nováky (2010), the comparable categories according to land cover types show similar tendencies (*Table 6*), but the differences between the categories are smaller. High absolute α values are calculated for forest, lower for agricultural areas and much lower for artificial surfaces. The α parameters are not comparable for wetlands and water bodies. The deviation from the values estimated by Keve and Nováky arises from two sources. The first reason is the different climatic conditions because they modelled a plain catchment basin, second is that the values of their parameters were not based on calculations but on estimations considering the land cover.

Table 6. α values determined by Keve – Nováky (2010)

Description	α
Artificial surface, with channel	2.3
More channels in the area	2.4
Big channel in the area	2.5
Agricultural area, with channel	2.7
Agricultural area, without channel	2.8
Area far from channel, forest	2.9

We calculated the β parameter (which gives the relationship between ET_{pan} and ET_A) for those pixels, where ET_A value was higher than P value, because the Budyko type model for this type of pixels is not valid. Typically this is the case for wetlands and water bodies. The β parameter map is displayed in *Figure 8*, and the rates of the different land cover types can be seen in *Table 7*. From agricultural areas to water bodies, β shows increasing values. (For artificial surfaces it is inadequate, because the pixel number of the category was very small.) The highest maximum values were detected over water bodies (1.08) as well as forest and semi natural areas (1.07), exceeding the calculated pan-evaporation (U-pan) rates by 7–8%.

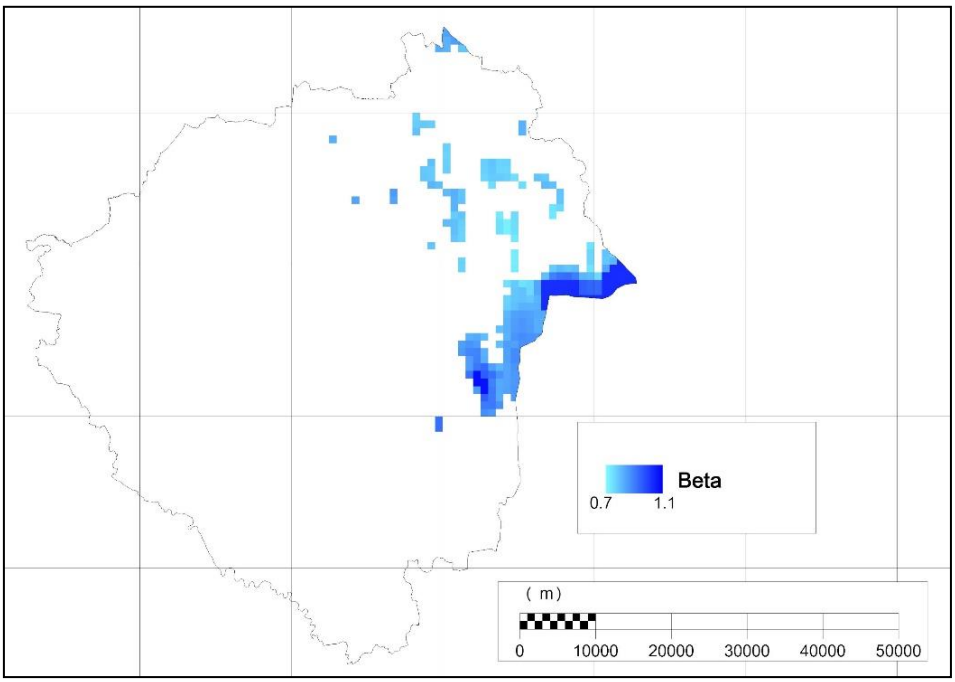

Figure 8. β parameter pixels and rates in Zala County

Table 7. The calculated β parameter rates of different land cover types over Zala County

Land cover type	β parameter			
	Min	Max	Average	Std. dev.
Artificial surfaces	0.71	0.91	0.80	0.05
Agricultural areas	0.71	0.93	0.79	0.05
Forest and semi natural areas	0.71	1.08	0.80	0.06
Wetlands	0.72	0.98	0.82	0.05
Water bodies	0.76	1.08	0.92	0.10

5 EVAPOTRANSPIRATION AND RUNOFF PREDICTIONS

Temperature and precipitation data were required for estimating future ET_A and runoff of Zala County, besides the prepared Budyko-α and β parameter maps. They were obtained for three periods (2011–2040, 2041–2070, 2071–2100) by averaging of 12 Regional Climate Models data (RCM, *Table 8*, Csóka 2013). The original grid size of the RCM maps was 25×25 km. They were disaggregated to 1×1 km spatial resolution by the bicubic convolution interpolation technique.

Table 8. Main parameters of the Regional Climate Models (Csóka 2013)

Nr.	Institute	Model	Scenario	Resolution
1.	C4I	RCA3	A1B	25 km
2.	MPI-M	REMO	A1B	25 km
3.	ETHZ	CLM	A1B	25 km
4.	KNMI	RACMO2	A1B	25 km
5.	DMI	HIRHAM5	A1B	25 km
6.	DMI	HIRHAM5	A1B	25 km
7.	SMHI	RCA	A1B	25 km
8.	SMHI	RCA	A1B	25 km
9.	SMHI	RCA	A1B	25 km
10.	HC	HadRM3Q0	A1B	25 km
11.	HC	HadRM3Q3	A1B	25 km
12.	HC	HadRM3Q16	A1B	25 km

The *11, 14, 15* and *16 Equations* were used for calculating spatially distributed future ET_A. The runoff data were obtained as the difference of precipitation and ET_A. These calculations were done for Zala County, not on a catchment scale.

Figure 9 shows the estimated mean annual ET_A values belong to the period 1999–2008 and the three predicted periods (2011–2040, 2041–2070, 2071–2100) in the context of climatic index (100·T/P, Nováky 1985). According to the predictions a mean annual temperature increase of about 3 degrees (from 11.6 °C to 14.6 °C) and a 25 mm decrease in precipitation can be expected by the end of the century. The mean annual evapotranspiration may increase by about 27 mm, from 577 mm to 604 mm (from 88 to 96 percent of the precipitation).

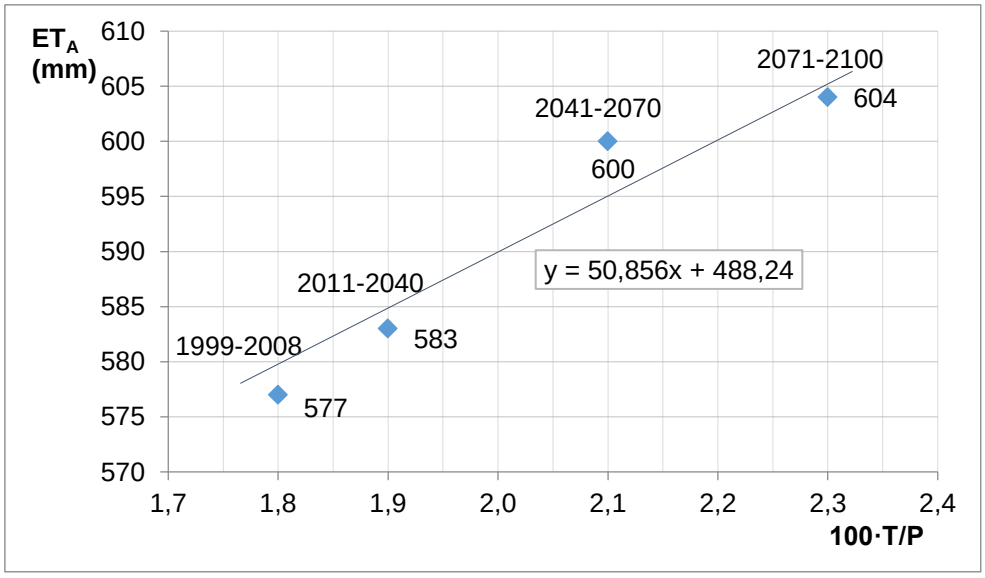

Figure 9. The trend of the mean annual evapotranspiration in the context of the climatic index (100·T/P)

Table 9 contains the estimated mean annual ET_A values belonging to each land cover type. The largest increase (90–100 mm) can be expected in wetlands and water bodies. The

ET_A increments are similar for artificial surfaces, agricultural areas, forest and semi-natural areas.

Table 9. The annual actual evapotranspiration of different land cover types, and annual precipitation, mean annual temperature and climatic index for the 1999–2008 period and for three future periods

Period	Mean annual ET_A (mm)					P (mm)	T (°C)	100·T/P
	AS*	ACA	FSN	WL	WB			
1999–2008	562	569	582	622	658	655.7	11.6	1.8
2011–2040	567	574	586	646	684	642.6	12.3	1.9
2041–2070	583	590	602	677	718	648.7	13.5	2.1
2071–2100	585	592	604	714	759	630.4	14.6	2.3
Slope#	45.730	43.524	44.213	167.610	182.730	–	–	–

* AS: artificial surfaces, ACA: agricultural areas, FSN: forest and semi natural areas, WL: wetlands, WB: water bodies.

#Slope of the trend line.

Figure 10 shows the mean annual runoff values belonging to the 1999-2008 period and the three predicted periods in the context of climatic index. The mean annual runoff may significantly decrease (from 78 mm/year to 27 mm/year, from 12 to 4 percent of the precipitation) by the end of the 21st century.

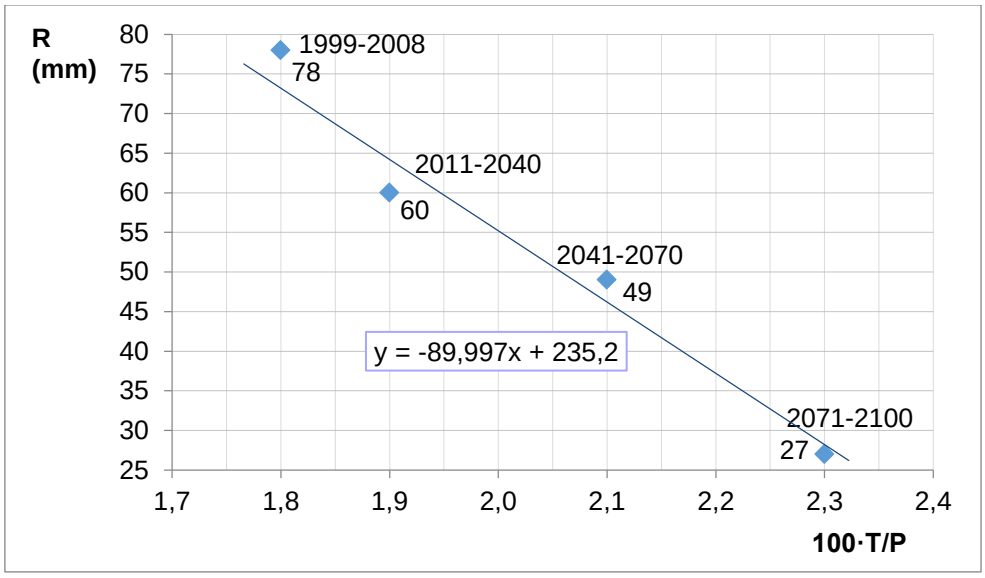

Figure 10. The trend of the mean annual runoff in the context of the climatic index (100·T/P)

The estimated mean annual runoff values belonging to the each land cover type are shown in *Table 10.* Obviously the increasing evapotranspiration prevails in case of the wetlands and water bodies: –144 mm and –115 mm negative water balance can be detected for future. If we compare artificial surfaces, agricultural areas as well as forest and semi natural areas, for the latter the lowest annual runoff is calculated.

Table 10. The annual runoff of different land cover types, and annual precipitation, mean annual temperature and climatic index for the period of 1999–2008 and for three future periods

Period	Mean annual R (mm)					P (mm)	T (°C)	100·T/P
	AS*	ACA	FSN	WL	WB			
1999–2008	89	87	77	2	–19	655.7	11.6	1.8
2011–2040	71	69	59	–36	–58	642.6	12.3	1.9
2041–2070	61	59	50	–61	–86	648.7	13.5	2.1
2071–2100	40	39	29	–115	–144	630.4	14.6	2.3
Slope[#]	–84.625	–83.215	–83.281	–205.770	–220.090	–	–	–

* AS: artificial surfaces, ACA: agricultural areas, FSN: forest and semi natural areas, WL: wetlands, WB: water bodies.

[#] Slope of the trend line.

6 CONCLUSIONS

The spatially-distributed ET_A and runoff maps are suitable to analyze the data in the context of land cover types. The average ET_A of Zala County from 1999-2008 was 577 mm/year, or 88% of the mean annual precipitation (655.7 mm/year). The highest mean annual ET_A rates were determined for water bodies (658 mm/year) and wetlands (622 mm/year). Forest and semi natural areas have higher values than agricultural areas. The lowest rates belong to artificial surfaces. The mean annual runoff is the largest on artificial surfaces (89 mm/year), and it decreases on the other land cover types.

We used the Budyko type model (α parameter) and a linear model with β parameter for evaluating the effects of climate change on evapotranspiration. The β parameter was used for the extra water affected pixels. These calculations were not done on a watershed, but in the future the α and β parameters can be validated on a catchment scale using historical precipitation and streamflow measurements. By using the two parameter maps and future data of climate models (mean annual temperature and precipitation) evapotranspiration and runoff predictions have been made until the end of the 21st century. According to the predictions, the mean annual evapotranspiration may increase about 27 mm while the runoff may decrease to the one third of the present amount by the end of the century.

Acknowledgements: This research has been supported by "Agroclimate 2 (VKSZ_12-1-2013-00-34)" project. The research of Zoltán Gribovszki was supported by the European Union and the Government of Hungary, co-financed by the European Social Fund in the framework of TAMOP 4.2.4. A/2-11-1-2012-0001 'National Excellence Program'.

REFERENCES

ARORA, V. K. (2002): The use of the aridity index to assess climate change effect on annual runoff. J. Hydrol., 265, 164–177.

BOUCHET, R. J. (1963): Evapotranspiration reelle, evapotranspiration potentielle, et production agricole. [Actual evapotranspiration, potential evapotranspiration, and agricultural production.] Ann. Agron., 14, 543–824. (in French)

BUDYKO, M. I. (1974): Climate and Life. Academic, Orlando, Fla.

CLC (2006): Corine Land Cover. European Environment Agency, European Topic Centre for Spatial information and Analysis, Copenhagen, Denmark. Online: http://sia.eionet.europa.eu/CLC2006

CSÓKA, G. (2013): A klímaváltozás vízgazdálkodási hatásainak vizsgálata éghajlat-lefolyási modellekkel. [Analysis of climate change effects on water management using climate-runoff models.] MSc thesis, University of West Hungary, Sopron. (in Hungarian)

FRAEDRICH, K. (2010): A Parsimonious Stochastic Water Reservoir: Schreiber's 1904 Equation. J. Hydrometeor., 11, 575–578.

GERRITS, A. M. J. – SAVENIJE, H. H. G. – VELING, E. J. M. – PFISTER, L. (2009): Analytical derivation of the Budyko curve based on rainfall characteristics and a simple evaporation model. Water Resources Research 45:4.

HEWLETT, J. D. (1982): Principles of forest hydrology. The University of Georgia Press, Athens

KEVE, G. – NOVÁKY, B. (2010): Klímaváltozás hatásának vizsgálata a Bácsbokodi-Kígyós csatorna vízgyűjtőjén Budyko modell alkalmazásával. [Effects of climate change in the catchment of Bácsbodoki-Kígyós channel by using Budyko-model.] XXVIII. National Conference of Hungarian Hydrological Society, Sopron, 7–9th July, 2010. (in Hungarian)

KOVÁCS, Á. (2011): Tó- és területi párolgás becslésének pontosítása és magyarországi alkalmazásai. [Specifying lake and areal evapotranspiration rates in Hungary.] PhD thesis, Budapest University of Technology and Economics, Budapest. (in Hungarian)

KSH (2011): Regional data – Zala County. Hungarian Central Statistical Office, Budapest, Hungary. Online: http://www.ksh.hu/nepszamlalas/tables_regional_20

MCMAHON, T. A. – PEEL, M. C. – LOWE, L. – SRIKANTHAN, R. – AND MCVICAR, T. R. (2012): Estimating actual, potential, reference crop and pan evaporation using standard meteorological data: a pragmatic synthesis. Hydrol. Earth Syst. Sci. Discuss., 9, 11829-11910, doi:10.5194/hessd-9-11829-2012

MORTON, F.I. – RICARD, F. – FOGARASI, S. (1985): Operational estimates of areal evapotranspiration and lake evaporation – Program WREVAP. National Hydrological Research Institute Paper #24, Ottawa, Ontario, Canada

NOVÁKY, B. (1985): A lefolyás éghajlati adottságai a Zagyva-Tarna vízrendszerben. [The runoff climatic facilities in the Zagyva-Tarna water system.] Vízügyi Közlemények, 1.: 78–93. (in Hungarian)

NOVÁKY, B. (2002): Mapping of mean annual actual evaporation on the example of Zagyva catchment area. Időjárás (Quarterly Journal of the Hungarian Meteorological Service), 3–4, 227–238.

SCHREIBER, P. (1904): Über die Beziehungen zwischen dem Niederschlag und der Wasserführung der Flüsse in Mitteleuropa. Z. Meteorol., 21(10), 441–452.

SZILÁGYI, J. – JÓZSA, J. (2009): Estimating spatially distributed monthly evapotranspiration rates by linear transformations of MODIS daytime land surface temperature data. Hydrol. Earth System Sci. 13(5), 629–637.

SZILÁGYI, J. – KOVÁCS, Á. (2010): Complementary-relationship-based evapotranspiration mapping (CREMAP) technique for Hungary. Periodica Polytechnica - Civil Engineering, 54(2), 95-100.

SZILÁGYI, J. – KOVÁCS, Á. (2011): A calibration-free evapotranspiration mapping technique for spatially-distributed regional-scale hydrologic modeling. J. Hydrol. Hydromech., 59, 2011, 2, 118–130.

SZILÁGYI, J. – KOVÁCS, Á. – JÓZSA, J. (2011): A calibration-free evapotranspiration mapping (CREMAP) technique. In: L. Labedzki (ed.): Evapotranspiration, InTech, Rijeka, Croatia

DE GRUYTER OPEN DOI: 10.2478/aslh-2014-0010 Acta Silv. Lign. Hung., Vol. 10, Nr. 2 (2014) 133–144

Detecting Trends in the Annual Maximum Discharges in the Vah River Basin, Slovakia

Katarína JENEIOVÁ[a*] – Silvia KOHNOVÁ[a] – Miroslav SABO[b]

[a] Department of Land and Water Resources Management, Faculty of Civil Engineering, Slovak University of Technology, Bratislava, Slovakia
[b] Department of Mathematics and Descriptive Geometry, Faculty of Civil Engineering, Slovak University of Technology, Bratislava, Slovakia

Abstract – A number of floods have been observed in the Slovak Republic in recent years, thereby raising awareness of and concern about flood risks. The paper focuses on the trend detection in the annual maximum discharge series in the Vah River basin located in Slovak Republic. Analysis was performed on data obtained from 59 gauging stations with minimum lengths of the observations from 40 years to 109 years. Homogeneity of the time series was tested by Alexandersson test for single shift at 5% level of significance. The Mann-Kendall trend test and its correction for autocorrelated data by Hamed and Rao (1998) were used to analyse the significance of detected changes in discharges. The series were analysed at different lengths of 40, 50, 60 years and whole observation period. Statistically significant rising and decreasing trends in the annual maximum discharge series were found in different regions of the Vah River catchments.

maximum annual discharges / homogeneity / Mann-Kendall trend test

Kivonat – Az évi maximális vízhozamok trend elemzése a Vág (Vah) vízgyűjtőjében, Szlovákiában. Az árhullámok száma igen jelentős napjainkban a Szlovák Köztársaságban, ezért egyre nagyobb az igény az árvízi kockázat elemzésekre. Jelen tanulmány az évi maximális vízhozamok tendenciájának elemzésére koncentrál a Szlovák Köztársaságban található Vág vízgyűjtőjében. Az elemzés alapját 59 vízmérce állomás idősoros adatai adták, amely idősorok hossza 40-től 109 évig változott. Az idősorok homogenitása Alexandersson tesztel lett értékelve 5%-os megbízhatósági szinten. A vízhozamban bekövetkező változások szignifikanciájának elemzésére Mann-Kendall tesztet, illetve annak Hamed és Rao (1998) által továbbfejlesztett, autokorrelált adatokra értelmezett változatát használtuk. Az idősorokat egységes hosszakban, 40, 50, 60 év, és a teljes észlelési időszakra vonatkozóan is értékeltük. Az eredmények alapján statisztikailag szignifikáns emelkedő és csökkenő trendek is kimutathatók voltak a maximális évi vízhozamokban a Vág vízgyűjtőjének különböző régióiban.

évi maximális vízhozam / homogenitás / Mann-Kandall trend teszt

* Corresponding author: katarina.jeneiova@stuba.sk, Radlinského 11, 813 68 BRATISLAVA, Slovakia

1 INTRODUCTION

A number of floods have been observed around Europe in recent decades, which have raised awareness of and concerns about flood risks. The observation and detection of changes in long-term hydrological time series is important for scientific and practical reasons, especially when designing water management structures.

There is a need to understand hydrological processes on small and also large temporal and spatial scales, land-atmosphere interactions, land use and climate change impacts (Szolgay, 2011). Further Blöschl et al. (2007) discuss the scales of climate variability and land cover change impact on flooding. In the note they debate, that climate change impact is likely to occur at large scales and to be consistent in both small and large catchments and regions, while land cover change is usually a local phenomenon, which effects are decreasing at larger spatial scale. Therefore the major driving forces behind hydrological phenomenons can vary depending on the factor and spatial scale

Many studies dealing with analyses of trends concerning floods have been published; many of them have found decreasing or increasing trends in their magnitudes and occurrences, and many have also found no changes (Strupczewski et al. 2001, Xiong – Guo 2004, Delgado et al. 2010, Armstrong et al. 2012, Rougé et al. 2013). The Mann-Kendall test (Kendall 1975, Kliment et al. 2011, Armstrong, 2012) is widely used in engineering hydrology to detect trends. When the data do not follow the normal distribution or are autocorrelated, authors have suggested the use of test corrections (Douglas et al. 2000, Burn – Hag Elnur 2001, Zhang et al. 2001, Yue et al. 2002, Lang 2012, Seoane – Lopez 2007, Danneberg 2012).

Strupczewski et al. (2001) investigated trends in 70-year-long observations of the annual maximum flows of Polish rivers. A decreasing tendency in the mean and standard deviations of annual peak flows was found with the use of the maximum likelihood method for estimating parameters and the Akaike Information Criterion for identification of an optimum model. Xiong and Guo (2004) tested maximum annual discharge series, including the mean annual maximum of the Yangtze River during a 120-year-long time period. No significant trend at the 5% significance level was found by the use of the Mann-Kendall test and Spearman's rho at the tested station. Delgado et al. (2010) examined over 70-year-long annual maximum discharge series from 4 gauging stations in the Mekong river in Southeast Asia with use of Mann Kendal test, ordinary least squares with resampling and non-stationary generalised extreme value functions. The results of the study pointed out increasing likelihood of extreme floods during the last half of century. They also concluded that the absence of detected positive trends was a result of methodological misconception due to simplistic models.

Armstrong et al. (2012) analysed peak over threshold data with a recorded average period of 71 years. An increasing trend was found with the use of the Mann-Kendall trend test in 22 stations out of the 23 investigated, and a hydroclimatic shift towards a rising number of flood occurrences was found. Rougé et al. (2013) studied trend and step-change detection methods in hydrological time series (rainfall, river flows) and applied a combined Mann-Kendall and Pettitt test (1979) on 1217 data sets in the United States during the years 1910–2009.

In Slovakia, a long-term annual time series was investigated by Pekarova et al. (2008). In a IHP UNESCO report (Pekarova et al., 2008), daily discharges of the Danube River from 1976-2005 were analysed, and a rising tendency was detected, but no change was found in the annual and monthly time series. The Mann-Kendall trend test was used in Tegelhoffova (2012) to detect trends in the average annual and monthly discharges in Slovak rivers. However, no thoughtful trend analysis of annual maximum discharges in Slovak catchments has been provided.

This paper focuses on a time series analysis and significance assessment of trends detected in annual maximum discharge series in the Vah River catchment in the Slovak Republic and the lessons learned concerning the occurrence of extreme discharges in the Vah River catchments. The paper is organised as follows: methodology, input data description, results and discussion, and conclusions.

2 METHODS

In engineering hydrology, time series analysis usually operates under the assumption of homogeneity, stationarity and independence of time series. Homogeneity in the time series can be tested by Alexandersson test (Alexandersson – Moberg 1997), which is able to detect abrupt changes in analysed data set. We used Alexandersson test (Standard normal homogeneity test, SNHT) for single shift programmed in AnClim software (Stepanek 2007).

The significance of monotonic linear trend present in the time series is possible to assess by Theil (1950) and Sen (1968) slope defined as:

$$\beta = \text{Median}\left(\frac{x_j - x_l}{j - l}\right) \forall\, l < j, \tag{1}$$

where β is the estimate of slope of the trend and x_j is value of observation from j= 1...l. Positive value of β reveals increasing trend, negative value is sign of decreasing trend.

Changes in a trend can be detected by a rank-based, non-parametric Mann-Kendall trend test for monotonic trends (WMO 2000).

The test statistic S equals to (Yue et al. 2012):

$$S = \sum_{k=1}^{n-1} \sum_{j=k+1}^{n} sign(x_j - x_k), \tag{2}$$

where x_j are the values of the data; n is the length of the time series and

$$\begin{aligned} \text{Sign}(x_j - x_k) &= 1, \text{ if } x_j - x_k > 0 \\ &= 0, \text{ if } x_j - x_k = 0 \\ &= -1, \text{ if } x_j - x_k < 0. \end{aligned} \tag{3}$$

In case the time series has $n \geq 8$, the statistic S has and almost normal distribution, and its variance is computed as:

$$VAR(S) = \frac{1}{18}\left[n(n-1)(2n+5) - \sum_{p=1}^{g} t_p(t_p - 1)(2t_p + 5)\right], \tag{4}$$

where g is the number of tied groups, and t_p is the amount of data with the same value in the group p=1...g.

The normalised test statistic Z:

$$Z = \begin{cases} \frac{S-1}{\sqrt{Var(S)}} & \text{for } S > 0 \\ 0 & \text{for } S = 0 \\ \frac{S+1}{\sqrt{Var(S)}} & \text{for } S < 0 \end{cases} \tag{5}$$

If the normalised test statistic Z is equal to zero, the data are normally distributed, and the positive values of Z mean a rising trend and negative a decreasing trend (Yue et al. 2012).

The p-value is computed as:

$$p = 0{,}5 - \Phi(|Z|)\ kde\ \Phi(|Z|) = \frac{1}{\sqrt{2\pi}} \int_0^{|Z|} e^{\frac{t^2}{2}} dt. \quad (6)$$

If the data are not independent a correction of the MK trend test should be used. Autocorrelation can influence the results of the analysis (Lang 2012, Yue et al. 2002). Hamed and Rao (HR) (1998) correction addresses the issue of autocorrelation in the time series. The modified MK equation for any variance is:

$$\mathrm{V}^*(\mathrm{S}) = \mathrm{VAR}(\mathrm{S}) \frac{\mathrm{n}}{\mathrm{n}^*}, \quad (7)$$

where VAR(S) is a variance from the original MK test (4); n is the length of the time series; n^* is the effective number of observations and $\frac{n}{n^*}$ is the correction factor in the case of autocorrelation in the sample.

The modified MK statistic:

$$Z^* = \begin{cases} \frac{S-1}{\sqrt{V^*(S)}} \text{ pre S } > 0 \\ 0 \qquad \text{pre S } = 0. \\ \frac{S+1}{\sqrt{V^*(S)}} \text{ pre S } < 0 \end{cases} \quad (8)$$

The correction factor can be calculated as:

$$\frac{n}{n^*} = 1 + \frac{2}{n(n-1)(n-2)} \sum_{j=1}^{n-1} (n-k)(n-k-1)(n-k-2) r_k^R, \quad (9)$$

where r_k^R is the autocorrelation function of the ranks of the observations. It can also be calculated by the equation by Salas et al. (1980):

$$r_k = \frac{\frac{1}{n-k} \sum_{t=1}^{n-k} (X_t - E(X_t))(X_{t+k} - E(X_t))}{\frac{1}{n} \sum_{t=1}^{n} (X_t - E(X_t))^2}, \quad (10)$$

where

$$E(X_t) = \frac{1}{n} \sum_{t=1}^{n} X_t, \quad (11)$$

where r_k is the correction factor for the data X_t; $E(X_t)$ is the average of the input data.

Hamed and Rao (1998) also suggest using only statistically significant values of r_k, because other values have a negative influence on the values of variance S.

The null hypothesis of the MK and HR tests states that there is no perceptible trend in the sample data. If the resulting p-value is lower than level of significance, then we can reject the null hypothesis (Diermanse et al. 2010).

The Sen's slope and trend analysis tests were programmed and performed in the R free software programming language using the fume and Kendall packages (McLeod 2011, Santahter Meteorology Group 2012, R Core Team 2013).

3 INPUT DATA

Annual maximum discharges from 59 gauging stations in the Vah River basin (*Figure 1*) were obtained from the Slovak Hydrometeorological Institute in Bratislava, Slovakia. The annual maximum discharge series for the trend analysis chosen are based on the length of the observations, which is more than 40 years, with a maximum length of 109 years. Annual maximum discharges represent the observed peak maximum values during hydrological year. Mean record length of data set was 53.9 years, median 48 years and mode 41 years. *Table 1* summarised the selected gauging stations with starting year of observation in the Vah River basin.

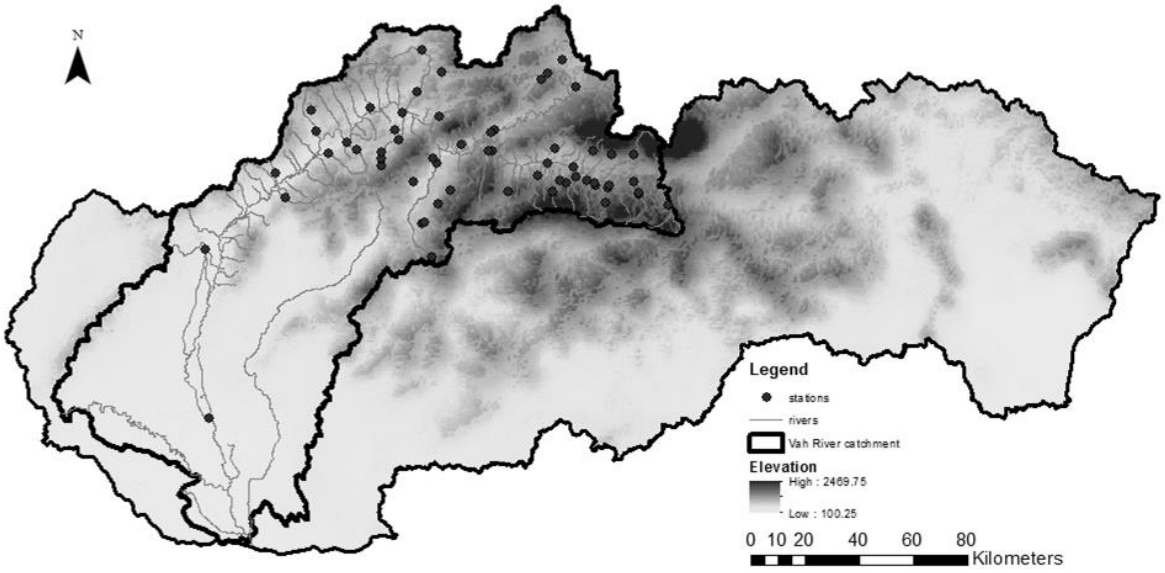

Figure 1. Location of the gauging stations in the Vah River basin, Slovak Republic.

4 RESULTS AND DISCUSSION

The homogeneity was tested on all 59 stations by the SNHT method for a single shift using AnClim software (Stepanek. 2007); 18 stations were found not to be homogeneous at a 5% level of significance (*Figure 2*). *Table 2* gives an insight when the critical values of SNHT were exceeded. It is possible to re-evaluate homogeneity after shortening the time series in 7 cases (5330, 5340, 5350, 5740, 5810, 5880 and 6150). After removing the extreme floods, all of the shortened time series were found to be homogenous at a 5% level of significance. Calculations were further performed with all 59 stations, and the final results were evaluated with an emphasis on the homogeneous stations.

Table 1. List of selected gauging stations in the Vah River basin

Station number	Name of the station	Catchment	Starting year of observations	Station number	Name of the station	Catchment	Starting year of observations
5300	Liptovská Teplička	Čierny Váh	1967	5890	Turany	Čiernik	1970
5310	Čierny Váh	Ipoltica	1961	5930	Turček	Turiec	1967
5311	Čierny Váh	Čierny Váh	1921	5970	Turčianske Teplice	Teplica	1963
5330	Východná	Biely Váh	1923	5980	Háj	Somolan	1969
5336	Malužiná	Boca	1970	6030	Brčna	Sloviansky P.	1969
5340	Kráľova Lehota	Boca	1931	6070	Blatnica	Gaderský P.	1969
5350	Kráľova Lehota	Hybica	1965	6110	Necpaly	Necpalsky P.	1970
5370	Liptovský Hrádok	Váh	1951	6130	Martin	Turiec	1937
5400	Podbanské	Belá	1928	6140	Martin	Pivovarský P.	1969
5460	Račková Dolina	Račkový P.	1963	6150	Stráža	Varínka	1957
5480	Liptovský Hrádok	Belá	1965	6190	Zborov N/Bystricou	Bystrica	1949
5520	Liptovský Ján	Štiavnica	1963	6200	Kysucké Nové Mesto	Kysuca	1931
5530	Žiarska Dolina	Smrečianka	1963	6230	Rajecká Lesná	Lesňanka	1968
5540	Iľanovo	Iľanovianka	1969	6240	Šuja	Rajčianka	1968
5550	Liptovský Mikuláš	Váh	1932	6260	Rajec	Čierňanka	1968
5590	Demänová	Demänovka	1969	6290	Rajecke Teplice	Kunedradsky P.	1969
5650	Prosiek	Prosiečanka	1969	6300	Poluvsie	Rajčianka	1930
5660	Horáreň Hluché	Paludźanka	1970	6330	Lietava, Majer	Lietavka	1969
5680	Liptovský Sv. Kríž	Paludźanka	1969	6340	Závodie	Rajčianka	1967
5720	Liptovské Vlachy	Kľačianka	1962	6360	Bytča	Petrovička	1961
5730	Partizánska Ľupča	Ľupčianka	1961	6370	Prečín	Domanižanka	1969
5740	Podsuchá	Revúca	1929	6380	Považská Bystrica	Domanižanka	1961
5780	Hubová	Váh	1921	6390	Vydrná	Petrinovec	1961
5790	Ľubochňa	Ľubochnianka	1959	6400	Dohňany	Biela Voda	1961
5800	Lokca	Biela Orava	1951	6420	Visolaje	Pružinka	1961
5810	Oravská Jasenica	Veselianka	1951	6450	Horné Srnie	Vlára	1961
5820	Zubrohlava	Polhoranka	1951	6460	Trenčianske Teplice	Teplička	1962
5840	Trstená	Oravica	1961	6470	Čachtice	Jablonka	1961
5870	Párnica	Zázrivka	1963	6480	Šaľa	Váh	1901
5880	Dierová	Orava	1931				

Table 2. Non- homogeneous stations at a 95% level of significance according to the SNHT test (To is the highest computed value of SNHT test statistics for the station; homogeneous stations after the removal of the extreme floods are marked in bold)

Station	Start year of observation	Statistic To	Critical values (Khaliq and Ouarda, 2007)	Critical value exceeded (Years)
5330	**1923**	**14.272**	**9.047**	**1940–1957**
5340	**1931**	**9.303**	**8.951**	**1931**
5350	**1965**	**9.015**	**8.331**	**1965**
5520	1963	8.711	8.382	1985–87
5650	1969	16.409	8.214	2009
5720	1962	17.566	8.382	1972–1984
5740	**1929**	**15.753**	**8.976**	**1938–1963**
5780	1921	19.802	9.067	1958–1995
5810	**1951**	**9.079**	**8.647**	**1960**
5840	1961	21.673	8.432	1999–2008
5870	1963	10.691	8.382	1993–1995
5880	**1931**	**16.197**	**8.951**	**1940–1967**
5890	1970	10.887	8.151	1979–1984
5970	1963	10.479	8.382	2009
6150	**1957**	**11.616**	**8.524**	**1958, 1960**
6360	1961	21.434	8.432	1995–2007
6390	1961	10.089	8.432	1973
6470	1961	15.362	8.432	2000–2005

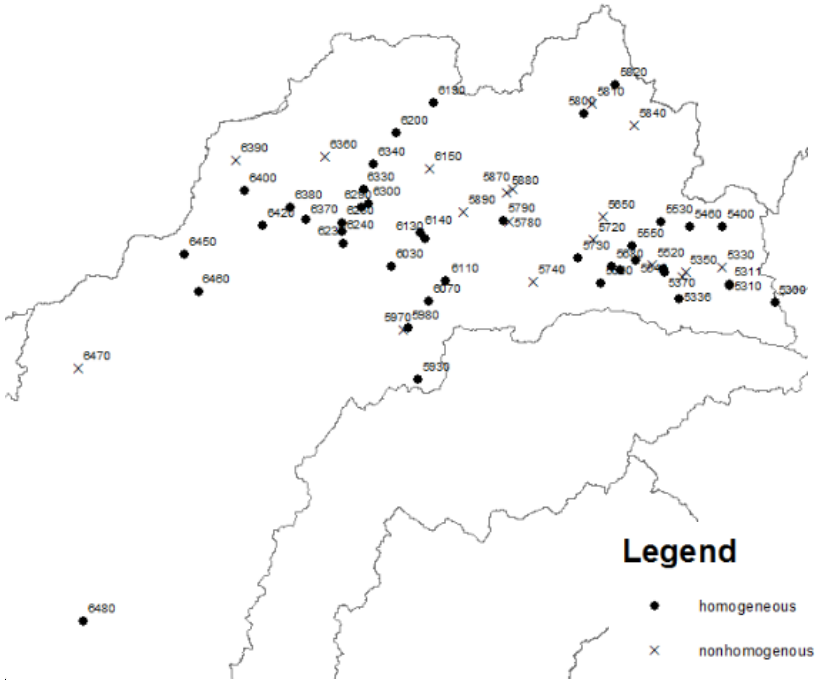

Figure 2. Map with locations and station number of homogeneous and nonhomogeneous stations at a 95% level of significance in the Vah River basin

For each of the 59 stations, the positive or negative direction of the trend was calculated by Sen's slope. The trend detected was positive in 27 cases and negative in 32 cases.

The MK and HR tests were applied to the discharge series in the Vah River catchment to assess the significance of the trend for different observation lengths: 40 years from 1970 to 2010; 50 years from 1960 to 2010; 60 years from 1950 to 2010; and the whole period of time observed at all the stations (40 years was the shortest and 109 years was the longest period). In the case of the autocorrelation in the time series, the test results of the MK and HR tests differ; therefore, there is a need to use the corrected HR test. The results were evaluated at the significance levels of 5, 10 and 20% (*Table 3*).

Table 3. Number of catchments at the levels of significance of 5, 10 and 20% by the MK and HR tests at different lengths of the observations

	Number of gauging stations	59		20		14		59	
	Time period (years)	40		50		60		40–109	
	Trend test	MK	HR	MK	HR	MK	HR	MK	HR
Significance level (number of stations)	5%	8	12	3	3	3	2	16	15
	10%	17	16	4	3	3	3	22	19
	20%	24	23	5	5	4	4	25	24

The null hypothesis (no trend in the time series) could not be rejected at the 20% significance level in 24 cases for the MK and 23 cases for the HR tests in the 40-year-long time period, in 5 cases for both the MK and HR in the 50-year-long time period, in 4 cases for both the MK and HR in the 60-year-long time period; and in 25 cases for the MK and in 24 cases for the HR for the whole time series. At the 10% level of significance, a trend was observed in 17 cases for the MK test and 16 for the HR test in the 40 year-long-period, 4 cases for the MK and 3 cases for the HR in the 50-year-long period, 3 cases for both the MK and HR during the 60-year-long-period; and in 22 cases for the MK and in 19 cases for the HR for the whole available time series. A trend at the 5% significance level was found in 8 cases for the MK and in 12 cases for the HR tests in the 40-year-long time period, in 3 cases for both the MK and HR in the 50-year-long time period, in 3 cases for the MK and in 2 cases for the HR in the 60-year-long time period, and in 16 cases for the MK and in 15 cases for the HR for the whole available time series.

Due to the autocorrelation present in the time series, the results for the MK trend test and HR test differ; therefore, the HR results were chosen for further analysis. The results of the HR trend test are presented in Figure 3, which describes the spatial distribution of rising or decreasing trends detected with significance at the 5%, 10% and 20% levels. The results of the 40 years of observations and the whole observed time period suggest the centralisation of a significant rising trend in the upper parts of the catchment and a decreasing trend in the lower parts of the upper Vah River basin. For the length of 50 years, the number of stations decreased to 20, and a significant trend was found in 5 stations, with a centralised rising trend present in the upper parts of the Vah River catchment. Sixty years of observations were available for 14 stations with a statistically significant trend in 4 stations with no clear spatial pattern.

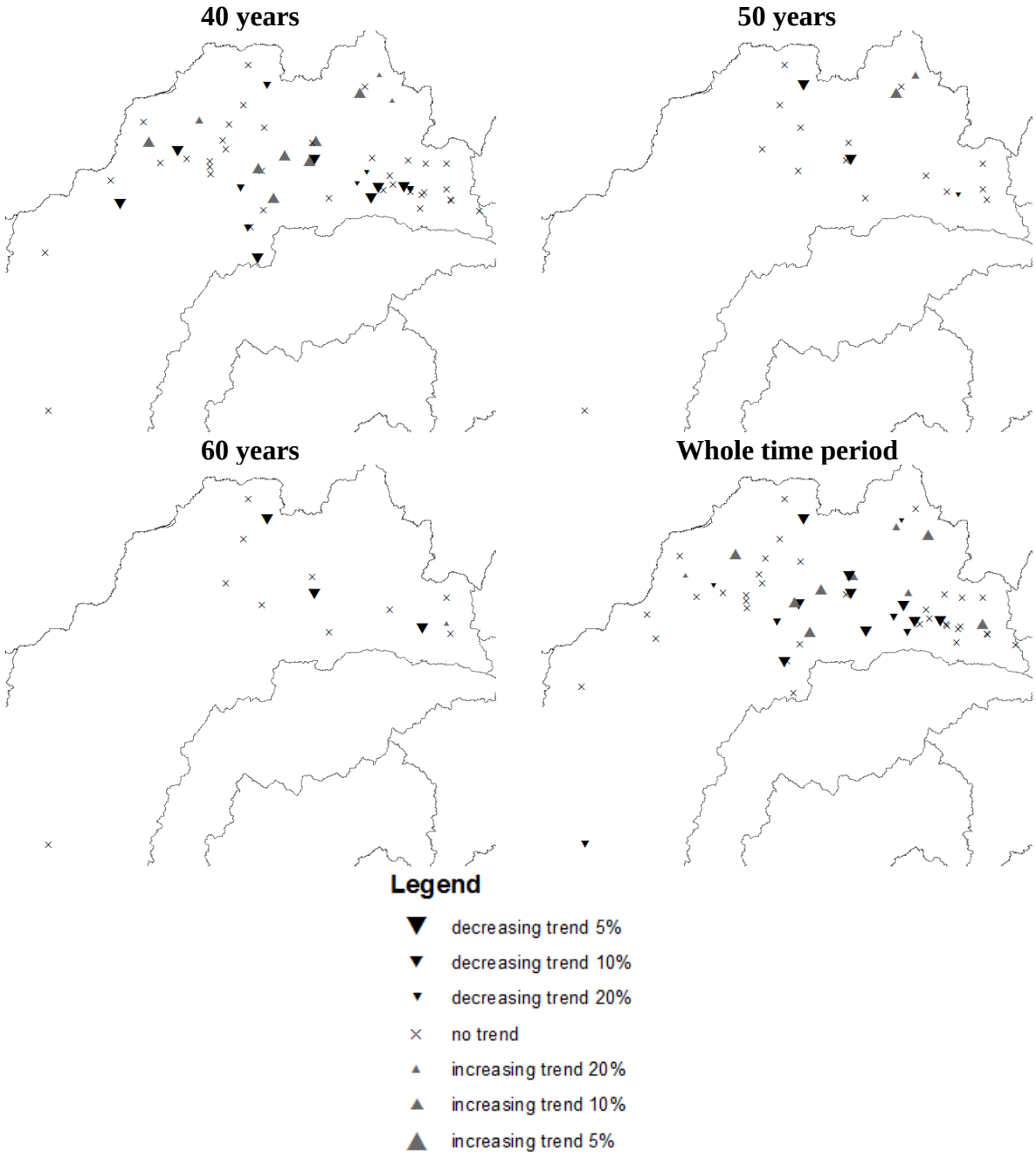

Figure 3. The results of the testing at the 5-, 10- and 20-% significance level

Subsequently, we took a closer look at 13 stations with observation periods longer than 60 years (*Table 3*). In the last column of *Table 4*, it can be seen that in stations with lengths of observations longer than 60 years, a statistically significant decreasing trend was found (Podsuchá, Hubová, Dierová, Martin, Zborov nad Bystricou and Šaľa); three of those time series (Podsuchá, Hubová and Dierová) were found to be non homogeneous by the SNHT test. A statistically significant rising trend was found at the Východná station, no trend was detected at the rest of the stations.

Table 4. Results of the significance analysis for catchments with 60 or more years of observations (the p-value is displayed in %); bold – statistically significant values for a rising trend, bold-italic – statistically significant values for a decreasing trend

Station	Name	Homogeneity	Years of observation	Sen's slope	P-value (%)			
					40y	50y	60y	whole
5311	Čierny Váh	Yes	89	increasing	69.42	70.87	39.38	52.15
5330	Východná	No	87	increasing	93.73	38.04	**15.23**	**0**
5340	Kráľova Lehota	No	79	decreasing	24.73	***19.16***	***2.67***	30.09
5400	Podbanské	Yes	82	decreasing	81.35	94.17	65.41	66.24
5550	Liptovský Mikuláš	Yes	62	decreasing	26.09	58.9	65.57	36.57
5740	Podsuchá	No	81	decreasing	46.53	40.28	49.36	***0.77***
5780	Hubová	No	89	decreasing	***0.53***	***0.3***	***0.03***	***0***
5880	Dierová	No	79	decreasing	87.5	66.92	25.79	***0***
6130	Martin	Yes	73	decreasing	86.62	53.7	62.02	*3.53*
6190	Zborov nad Bystricou	Yes	61	decreasing	***6.74***	***0.17***	***7.42***	***7.15***
6200	Kysucké Nové Mesto	Yes	79	decreasing	94.26	27.58	85.26	47.61
6300	Poluvšie	Yes	80	increasing	62.11	25.89	96.24	98.39
6480	Šaľa	Yes	109	decreasing	62.91	32.97	27.07	***6.48***

5 CONCLUSIONS

The paper was focused on an analysis of changes in annual maximum discharges in the Vah River basin by the use of trend significance analysis methods. The quality of the data set was tested by the Alexandersson SNHT test. The MK and HR trend tests were applied to different observation lengths – 40, 50, 60 and more than 60-year-long time series obtained from 59 gauging stations in the Vah River catchment.

A more detailed analysis of 13 stations with the longest periods of observations revealed that with a prolonged length of observation, the possibility of detecting a statistically significant trend increases. The short length of the time series (in some cases, 40 years) may have influenced the possibility of detecting a significant trend in the Vah River catchment, in that any prolongation of a time series observed can significantly influence the detection of a significant trend at the 5% significance level (Diermanse et al. 2010). When we also took into consideration the homogeneity analysis results of the SNHT method, a statistically significant decreasing trend was present at the Dierová, Martin, Zborov nad Bystricou and Šala stations.

Finally, we can conclude that a significant rising trend was detected in the upper part of the catchment, mainly in the east Tatra Mountain region and a decreasing trend in the lower part of the upper Vah River basin. These results can help when mapping flood risk areas and developing river basin management plans in the Vah River basin.

Acknowledgement: This work was supported by the Slovak Research and Development Agency under Contract Nos. 0015-10. The support is gratefully acknowledged.

REFERENCES

ALEXANDERSSON, H. – MOBERG, A. (1997): Homogenization of Swedish temperature data. Part I: Homogeneity test for linear trends. Int. J. Climatol. (17): 25–34.

ARMSTRONG, W.H. – COLLINS, M.J. – SNYDER, N.P. (2012): Increased Frequency of Low-Magnitude Floods in New England, Journal of The American Water Resources Association. 48 (2): 306–320.

BLÖSCHL, G. – ARDOIN-BARDIN, S. – BONELL, M. – DORNINGER, M. – GOODRICH, D. – GUTKNECHT, D. – MATAMOROS, D. – MERZ, B. – SHAND, P. – SZOLGAY, J. (2007): At what scales do climate variability and land cover change impact on flooding and low flows? (Note). 21 (9): 1241–1247.

BURN, D.H. – HAG ELNUR, M.A. (2002): Detection of Hydrologic Trends and Variability, Journal of Hydrology (255): 107–122.

DANNEBERG, J. (2012): Changes in Runoff Time Series in Thuringia, Germany, Mann-Kendall Trend Test and Extreme Value Analysis, Adv. Geosci. (31): 49–56.

DELGADO, J. M. – APEL, H. – MERZ, B. (2010): Flood trends and variability in the Mekong river, Hydrol. Earth Syst. Sci. (14): 407–418.

DIERMANSE, F.L.M. – KWADIJK, J.C.J. – BECKERS, J.V.L. – CREBAS, J.I. (2010): Statistical Trend Analysis of Annual Maximum Discharges of the Rhine And Meuse Rivers. BHS Third International Symposium, Managing Consequences of a Changing Global Environment, Newcastle 2010, UK

DOUGLAS, E.M. – VOGEL, R.M. – KROLL, C.N. (2000): Trends in Floods and Low Flows in the United States: Inpact of Spatial Correlation, Journal of Hydrology. 240 (1–2): 90–105.

HAMED, K.H. – RAO, A.R. (1998): A Modifed Mann-Kendall Trend Test for Autocorrelated Data, Journal of Hydrology. (204): 182–196.

KENDALL, M.G. (1975) Rank Correlation Methods. London: Griffin.

KHALIQ, M. N. – OUARDA, T. B. M. J. (2007): Short Communication: On the critical values of the standard normal homogeneity test (SNHT), Int. J. Climatol. 27: 681–687

KLIMENT, Z. – MATOUŠKOVÁ, M. – LEDVINKA, O. – KRÁLOVEC, V. (2011): Hodnocení Trend Trendů v Hydro-Klimatických Řadách Například Vybraných Horských Povodí (Evaluating of trends in hydroclimate time series, for example mountain streams). Středová, H., Rožnovský, J., Litschmann, T. (Eds): Mikroklima a Mezoklima Krajinných Struktur a Antropogenních Prostředí (Microclimate and mezoclimate of landscapes and antropogene landscapes). Skalní Mlýn, 2. – 4.2. 2011.

LANG, M. (2012): Statistical Methods for Detection of Changes Within Hydrological Series. Floodfreq Action, Subgroup WG4-3 "Trend Analysis of Hydrological Extremes", Vienna, Austria 5.Sept. 2012.

MCLEOD, A.I. (2011): Kendall: Kendall rank correlation and Mann-Kendall trend test. R package version 2.2. http://CRAN.R-project.org/package=Kendall.

PEKÁROVÁ, P. – MIKLÁNEK, P. – ONDERKA, M. – HALMOVÁ, D. – BAČOVÁ MITKOVÁ, V. – MÉSZÁROŠ, I.– ŠKODA, P (2008): Flood Regime of Rivers in the Danube River Basin A case study of the Danube at Bratislava, National report for the IHP UNESCO, Regional cooperation of Danube Countries

PETTITT, A.N. (1979): A Non-Parametric Approach to the Change-Point Detection, Appl.Stat. (28): 126–135.

R CORE TEAM (2013): R a Language and Environment for Statistical Computing. R Foundation for Statistical Computing, Vienna, Austria. URL http://www.R-project.org/.

ROUGE, C. – GE, Y. – CAI, X. (2013): Detecting Gradual and Abrupt Changes in Hydrological Records, Advances in Water Resources (53): 33–44.

SALAS, J.D – DELLEUR, J.W. – YEVJEVICH, V. – LANE, W.L. (1980): Applied Modeling of Hydrologic Time Series, Water Resources Publications, Littleton, CO, USA.

SANTANDER METEOROLOGY GROUP (2012): fume: FUME package. R package version 1.0. http://CRAN.R-project.org/package=fume

SEN, P.K. (1968): Estimates of the regression coefficient based on Kendall's tau. J. Am. Statist.Assoc. (63): 1379–1389.

SEOANE, R. – LOPEZ, P. (2007): Assessing the Effects of Climate Change on the Hydrological Regime of the Limay River Basin, Geojournal (70): 251–256.

SZOLGAY, J. (2011): Soil-water-plant-atmosphere interactions on various scales. Contributions to Geophysics and Geodesy 41 (Spec. Issue): 37–56.

STEPANEK, P. (2007): AnClim - software for time series analysis (for Windows). Dept. of Geography, Fac. of Natural Sciences, Masaryk University, Brno. 1.47 MB.

STRUPCZEWSKI, W.G. – SINGH, V.P. – MITOSEK H.T (2001): Non-stationary approach to at-site flood frequency modelling. III. Flood analysis of Polish rivers, Journal of Hydrology 248 (1–4): 152–167.

TEGELHOFFOVÁ, M. (2012): Hodnotenie zmien hydrologického režimu priemerných ročných a mesačných prietokov Slovenských tokov (Evaluation of the changes in hydrologic regime of average annual and monthly discharges in Slovakia), Phd. thesis, Svf STU in Bratislava.

THEIL, H. (1950): A rank-invariant method of linear and polynomial regression analysis, I, II, III. Nederl. Akad. Wetensch. Proc. (53) 386–392, 512–525, 1397–1412.

WMO (2000): Detecting Trend and Other Changes in Hydrological Data. WCDMP-45, WMO/TD 1013.

XIONG, L. – GUO, S. (2004): Trend Test and Change–Point Detection for the Annual Discharge Series of the Yangtze River at the Yichang Hydrological Station, Hydrological Sciences Journal. 49 (1): 99 –114.

YUE, S. – KUNDZEWICZ, Z.W. – WANG, L. (2012): Detection of Changes. Changes in Flood Risk in Europe, Chap. 2, 11–26, IAHS Special Publication 10.

YUE, S. – PILON, P. – PHINNEY, B. – CAVADIAS, G. (2002): The Influence of Autocorrelation on the Ability to Detect Trend in Hydrological Series, Hydrological Processes. 16 (9): 1807– 1829.

ZHANG, X. – HARVEY, K.D. – HOGG, W.D. – YUZYK, T.R. (2001): Trends in Canadian Streamflow, Water Resources Research. 37(4): 987–998.

DE GRUYTER OPEN DOI: 10.2478/aslh-2014-0011 Acta Silv. Lign. Hung., Vol. 10, Nr. 2 (2014) 145–159

Changes in Snow Storage in the Upper Hron River Basin (Slovakia)

Katarína KOTRÍKOVÁ[a*] – Kamila HLAVČOVÁ[a] – Róbert FENCÍK[b]

[a] Department of Land and Water Resources Management, Faculty of Civil Engineering, Slovak University of Technology, Bratislava, Slovakia
[b] Department of Mapping and Land Consolidation, Faculty of Civil Engineering, Slovak University of Technology, Bratislava, Slovakia

Abstract - An evaluation of changes in the snow cover in mountainous basins in Slovakia and a validation of MODIS satellite images are provided in this paper. An analysis of the changes in snow cover was given by evaluating changes in the snow depth, the duration of the snow cover, and the simulated snow water equivalent in a daily time step using a conceptual hydrological rainfall-runoff model with lumped parameters. These values were compared with the available measured data at climate stations. The changes in the snow cover and the simulated snow water equivalent were estimated by trend analysis; its significance was tested using the Mann-Kendall test. Also, the satellite images were compared with the available measured data. The results sow a decrease in snow depth and in snow water equivalent from 1961–2010 in all months of the winter season, and significant decreasing trends were indicated in the months of December, January and February.

snow depth / snow water equivalent / trend analysis / MODIS satellite images

Kivonat – A tározott hókészlet változásai a Garam (Hron) felső vízgyűjtőjében, Szlovákiában. A tanulmány Szlovákia hegyvidéki vízgyűjtőiben a hóborítottság változását értékeli, és bemutatja a MODIS műhold képek értékelését is ehhez kapcsolódóan. A hóborítottság változásának analízise magában foglalta a hótakaró vastagságának, a hóborítottság időtartamának és a szimulált hó-víz egyenértéknek a napi időlépcsőben történő értékelését, amelyhez a szerzők egy koncentrált paraméterű csapadék-lefolyás modellt használtak fel. Az modellezés során kapott értékeket a meteorológiai állomásokon rendelkezésre álló terepi mérési adatokkal hasonlították össze. A hóborítottság és a szimulált hó-víz egyenérték változását trend analízis segítségével becsülték, a megbízhatóság értékelésére Mann-Kendall tesztet használtak. A távérzékelési alapú adatokat a terepi mérési adatokkal is összehasonlították. Az eredmények alapján valószínűsíthető a hótakaró vastagságának és a hó-víz egyenértéknek általában a csökkenése a vizsgált 1961–2010-es időszakban minden egyes téli (téli félév) hónapra vonatkozóan, avval a kiegészítéssel, hogy a csökkenési tendencia szignifikáns a december, január és február hónapok esetében.

hótakaró vastagság / hó-víz egyenérték / trand elemzés / MODIS képek

[*] Corresponding author: katarina.kotrikova@stuba.sk; Radlinského 11, 813 68 BRATISLAVA, Slovakia

1 INTRODUCTION

Snow cover is a very important part of a hydrological balance. The most important value of snow is the snow water equivalent (SWE). The snow water equivalent is the value of the amount of water in snow. Knowledge of the temporal and spatial variability of SWE is significant for the correct assessment and prediction of runoff from snow melting processes.

Snow data is rarely available in Slovakia from the second half of the 19th century, but it is regularly available from the second half of the 20th century from standard rain gauge stations. The measured data include the height of the snow cover, the date of the first and last days with snow cover, the duration of the snow cover, the snow water equivalent, etc.

Several authors investigated the spatial and temporal changes in the snow depths, and the density of the snow cover, the spatial and temporal changes in snow water equivalent, the impact of vegetation during the snow melt, and the impact of vegetation and catchment characteristic on hydrological balance (Hood – Hayashi 2010, Kuchment et al. 2010, Artan et al. 2013), and also several authors in Slovakia (Holko 2000, Holko et al. 2011, Pekárová et al. 2009, Gaál et al. 2012). Another authors in Slovakia have used rainfall-runoff models for modelling extreme runoff from snow melt in river basins (Holko 2000). They used models such as the UEB EHZ model (Holko et al. 2005), the WaSiM-ETH model, or the HBV model with semi-distributed parameters (Parajka 2001, Pekárová – Miklánek 2006, Halmová et al. 2006, Lapin et al. 2007, Danko et al. 2010).

Snow is a main element of stream flow in alpine basins, and quantifying snow depth and its distribution is important for hydrological modelling. In this paper we analysed the changes in snow storage during recent decades in alpine basin, the upper Hron River basin. The analysis was performing by assessing changes in snow duration and changes in the simulated snow water equivalent by hydrological modelling using the rainfall-runoff model Hron. The significance of the changes was evaluated by a trend analysis.

In the individual chapters of this paper we describe the input data, the concept and parameters of the rainfall-runoff model Hron, the methodology for assessing the duration of the snow cover measured in selected climate stations, a simulation of the snow water, the results of the assessment of any changes in the snow duration and simulated SWE for the period 1961–2010, and the identification of any trends in snow duration and the SWE for the months from November to April.

In 3.3. chapter we describe another source of snow data, i.e., the satellite images of the Moderate Resolution Imaging Spectroradiometer (MODIS) snow product. These data were evaluated and validated by measured data from 2000–2010 in five climate stations. The overall degree of agreement and the misclassifications were evaluated and filtered for increasing the accuracy of the satellite images.

2 INPUT DATA

The river basin analysed in this paper is the upper Hron River basin with its outlet at Banská Bystrica. The Hron River is the second longest river in Slovakia; its length is 298 km. It has a snow-rain runoff regime; the highest mean monthly flows occur in April and the lowest mean monthly flows in January and February. The catchment belongs to a cold and wet climate region; the highest measured mean daily air temperature is 29°C; the mean annual air temperature is between 4 and 5°C; the highest average monthly air temperature is between 14 and 16°C; and the lowest average monthly air temperature is between –4 and –6°C (Pekárová – Szolgay 2005).

The data representing the snow cover included measurement of the daily data of the snow depths and the weekly data of the snow water equivalent at 5 climate stations on the Hron river basin from the period 1961–2010. The input data for modelling the basin's snow water equivalent by the rainfall-runoff model were daily rainfall data from 23 rain gauge stations, the mean daily values of the air temperature from 6 climate stations, and the mean daily discharges in the profile of Banská Bystrica for the period 1961–2010. The basin's daily rainfall was processed by the interpolation method of inverse distance weighting; the basin's average air temperature values were calculated by linear regression between the stations' mean daily air temperatures and the altitudes of the climate stations. The daily evapotranspiration values were calculated by the Blaney-Criddle method (Parajka et al. 2003). The calculations were based on the basin's average daily air temperature and the sunshine index of the river basin.

Satellite images of the Moderate Resolution Imaging Spectroradiometer (MODIS) snow product were available from the official website of the National Snow and Ice Data Centre (http://nsidc.org/) in a daily time step from 2000–2010. These data were obtained from the MODIS sensor on the Aqua and Terra satellites of NASA's Earth Observing System (EOS). The spatial resolution of the data was 500 m.

The list of climate stations with the available measured data of the snow depths and snow water equivalent is in *Table 1*, and their location is in *Figure 1*.

Table 1. List of climate stations with the available measured data of the snow depth and snow water equivalent

Station	Chopok	Lom nad Rimavicou	Telgárt	Brezno	Banská Bystrica
Altitude [m asl]	2008	1018	901	487	427

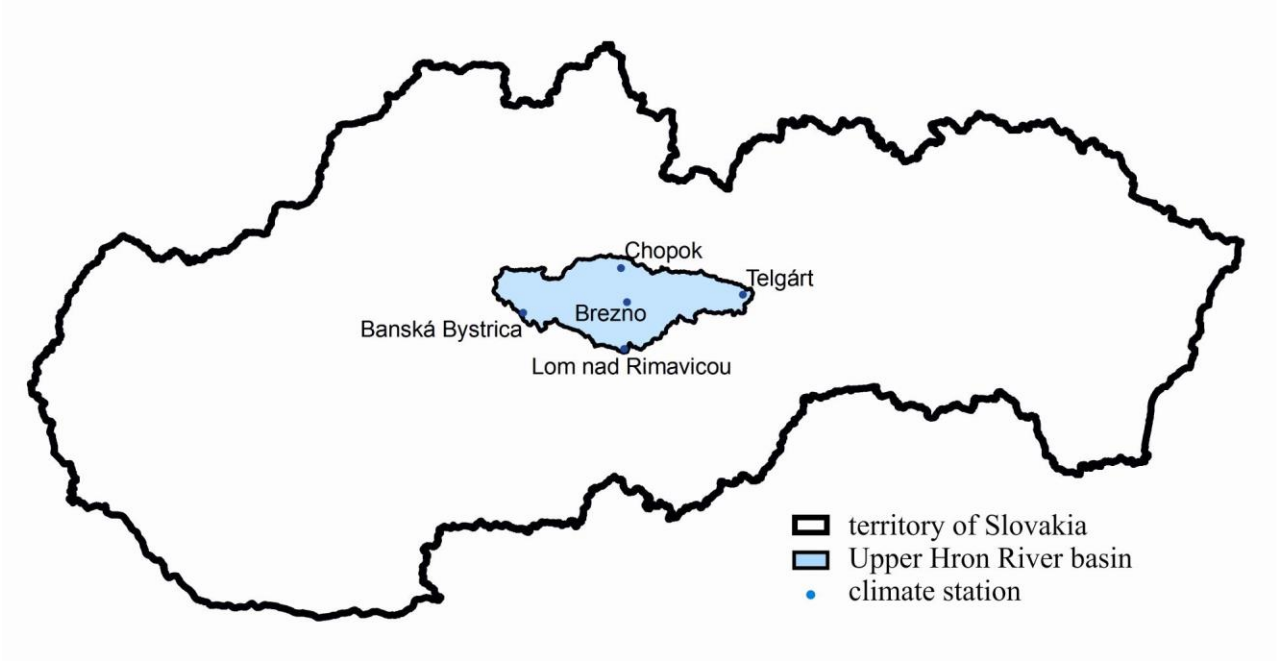

Figure 1. Location of climate stations with the available measured data of the snow depth and snow water equivalent

3 METHODOLOGY

3.1 Changes in duration of snow

The changes in snow cover from 1961–2010 were estimated by an analysis of the measured snow depth and its duration in the individual years and climate stations. In every year we totaled the number of days with a measurable snow depth. The data with values lower than 0.5 cm of snow depth we considered to be statistically irrelevant; therefore, only days with values higher than 0.5 cm of snow depth were taken into account.

The significance of the trend at the 95% level of significance was tested using the Mann-Kendall test. The Mann-Kendall test, which is one of the many methods used to detect trends, is the most widely used test. It is a non-parametric test which has the ability to deal with non-normalities, e.g., missing values. Its disadvantages include results that are not as strong as parametric tests.

3.2 Changes in snow water equivalent

The snow water equivalent was simulated by a rainfall-runoff model with lumped parameters. Its changes were assessed by a trend analysis, and the significance of the trends was tested using the Mann-Kendall test.

3.2.1 The rainfall-runoff model Hron

The model Hron is a rainfall-runoff model developed at the Department of Land and Water Resources Management of the Faculty of Civil Engineering of Slovak University of Technology in Bratislava (Kubeš 2007, Kubeš – Hlavčová 2002). The structure of this model is derived from the concept of the HBV model (Bergström 1976, 1992). This is a conceptual model with lumped parameters, which divides a river basin into 2 linear or nonlinear reservoirs according to the scheme in *Figure 2.*

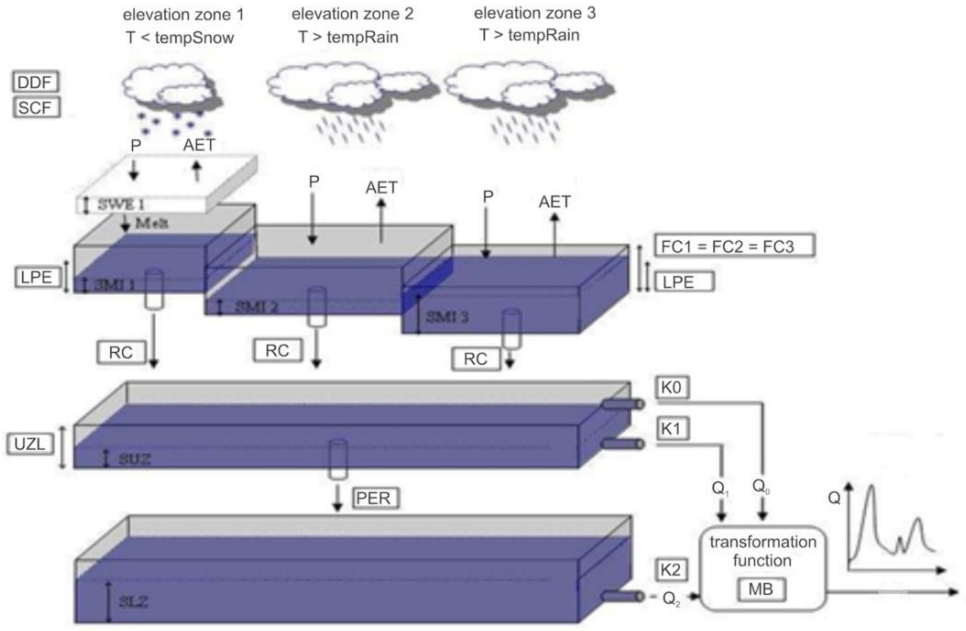

Figure 2. Scheme of the rainfall-runoff model Hron (Valent et al. 2011)

The model works in an hourly or daily time step and has three sub-models. The first sub-model is a snow sub-model for the simulation of snow accumulation and melting. The second, a soil sub-model, simulates the amount of water in soil and the actual evapotranspiration. The third, a runoff sub-model, simulates the transformation of the runoff in a river basin, respectively, the transformation of the flow in a river bed.

The manual or automatic calibration of model parameters is based on genetic algorithms or harmonic searching as well as on several objective functions for assessments of the reliability of the model's calibration. The actual version of the model Hron is programmatically processed in Matlab (Valent et al. 2011).

The calibrated model parameters are:

FC – field capacity [mm],
RC – recharge coefficient [–],
UZL – upper zone limit [mm],
tempRain – threshold temperature, above which all precipitation is liquid [°C],
tempMelt – threshold temperature, determining the snow melting process [°C],
tempSnow – threshold temperature, under which all the precipitation is solid [°C].
DDF – degree-day factor [mm/°C/day],
PER – percolation [mm],
LPE – limit of potential evapotranspiration [–],
K0 – parameter influencing the surface (Q_0) flow [–],
K1 – parameter influencing the subsurface (Q_1) flow [–],
K2 – parameter influencing the base (Q_2) flow [–],
SCF – snow correction factor,
MB – parameter determining the amount of days into which the total runoff is divided using a triangular weighted function.

The simulated basin states in every time unit are characterized by the state variables of the model: the values of the soil moisture *SM* [mm], the water level in the upper basin *SUZ* [mm], the water level in the lower basin *SLZ* [mm], and the snow water equivalent *SWE* [mm].

3.2.2 Calibration of model parameters

The aim of modelling the hydrological processes by the rainfall-runoff model Hron was to obtain the simulated daily values of the snow water equivalent. The reliability of the calibration of the model parameters using genetic algorithms was assessed by 1) compliance of the simulated and measured mean daily discharges in the basin outlet by the Nash-Sutcliffe coefficient; 2) validation with other samples of data by the differential split-sample test; and 3) comparison of the simulated and measured values of SWE.

In the process of calibrating the model parameters, the whole period of 1961–2010 was divided into five shorter periods, i.e., decades (starting in June 1961), for increasing the reliability of the simulated SWE in each decade. The parameters of the model were calibrated individually for each decade, and other decades were used for the validation of the model's parameters.

It was assumed that the SWE values obtained by the simulation with the parameters calibrated for the decades are more reliable than the values obtained by the simulation with the parameters calibrated for the whole 50 years. Therefore, the representative series of the snow water equivalent (the most reliable) was created by a combination of the simulated SWE from the decades with the calibrated parameters of each decade. The other series were created by a simulation of the period 1961–2010 with the parameters calibrated step by step from the first, second, third, fourth, and fifth decades.

The next step was the validation of the simulated SWE with the measured data. We compared the simulated daily values from the representative SWE series, which represents the basin's average data, with the measured basin's SWE averages. The basin's SWE averages were calculated from the measured SWE values at the climate stations by linear regression with the altitudes of the climate stations.

Finally, the changes in the simulated snow water equivalents in the basin were assessed by the trend analysis, and the significance of the trends was tested using the Mann-Kendall test.

3.3 Validation of the MODIS satellite data

The accuracy of the MODIS data was compared with the data measured from the area studied (Hall – Rigss 2007, Mauer et al. 2003). Two types of errors were evaluated in this validation. The sum of the misclassification of snow as land was divided by the total number of cloud-free days in percentages – the underestimation error; and the sum of the misclassification of land as snow was divided by the total number of cloud-free days in percentages – the overestimation error. The sum of correctly classified days (snow, snow and no snow, no snow) divided by the total number of cloud-free days in percentages represents the overall degree of agreement (Parajka – Blöschl 2006, 2008a, b, Parajka et al. 2012).

Subsequently, the temporal filtering of the MODIS images was used to increase the accuracy of the images. The pixels classified as clouds were replaced by the values of the same cells of the previous day to decrease these pixels. So, a pixel classified as a cloud was replaced by a pixel value if the pixel of the previous day was snow or land. Various time steps were used for the temporal filtering. Next, the MODIS data were compared with the measured data. The overall degree of agreement, underestimation and overestimation were calculated for all the decades at each station in all the months of the winter season.

4 RESULTS

4.1 Duration of snow cover

A graphic illustration of the changes in snow duration for the period 1961–2010 at 5 climate stations on the Hron River basin is shown in *Figures 3–7*. The graphs demonstrate the decreasing trend in the duration of the snow cover at 4 stations and the increasing trend at the Banská Bystrica climate station. The significance of the increasing and decreasing trends at the 95% level of significance was tested using the Mann-Kendall test.

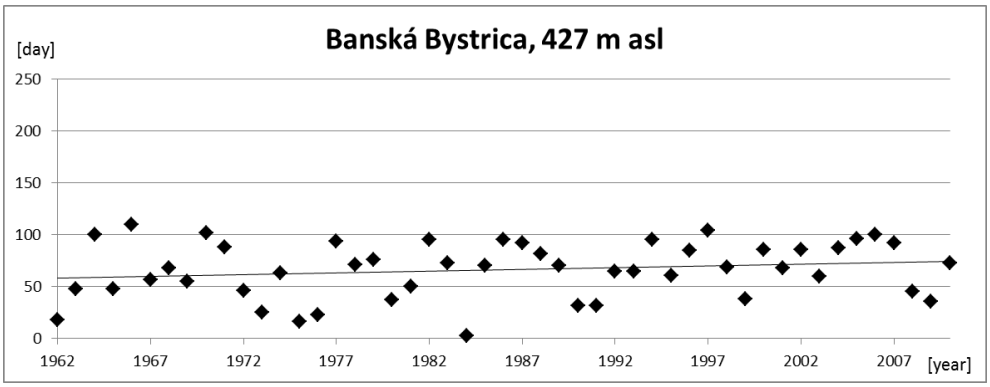

Figure 3. The duration of the snow cover at the Banská Bystrica climate station

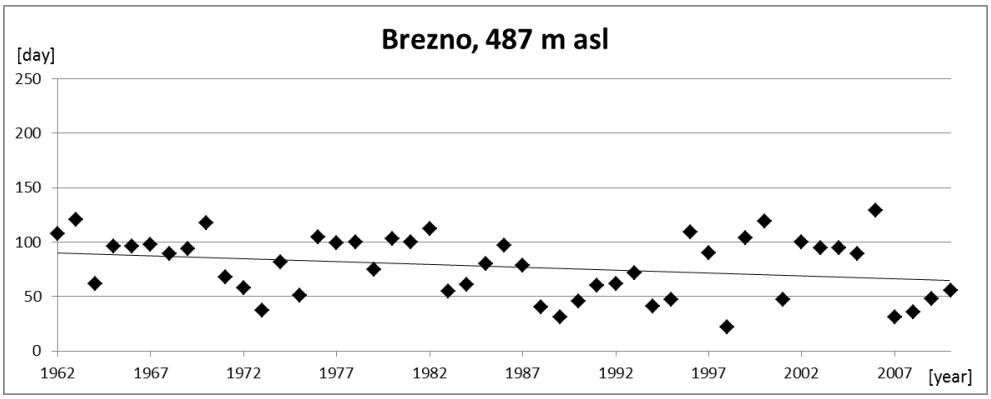

Figure 4. The duration of the snow cover at the Brezno climate station

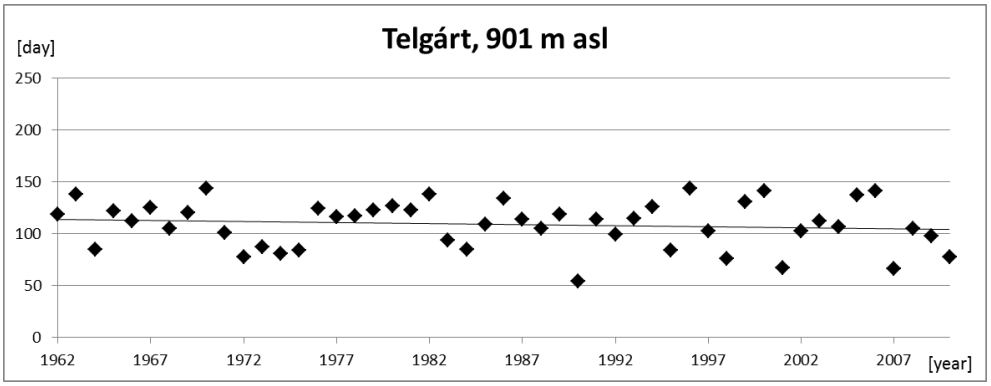

Figure 5. The duration of the snow cover at the Telgárt climate station

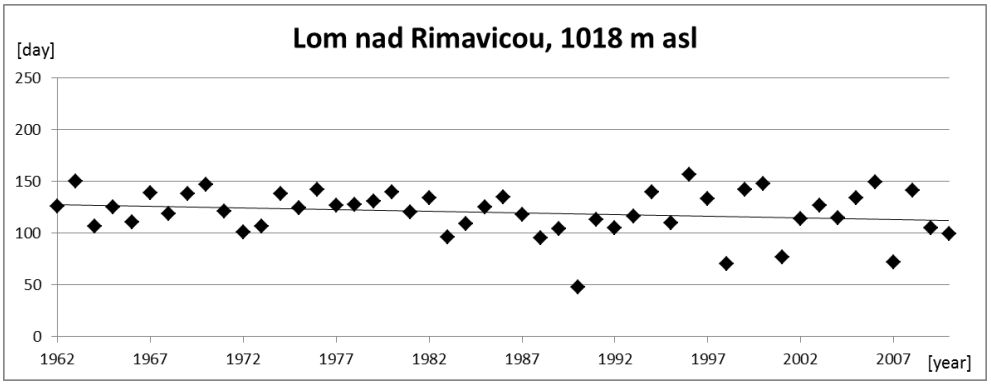

Figure 6. The duration of the snow cover at the Lom nad Rimavicou climate station

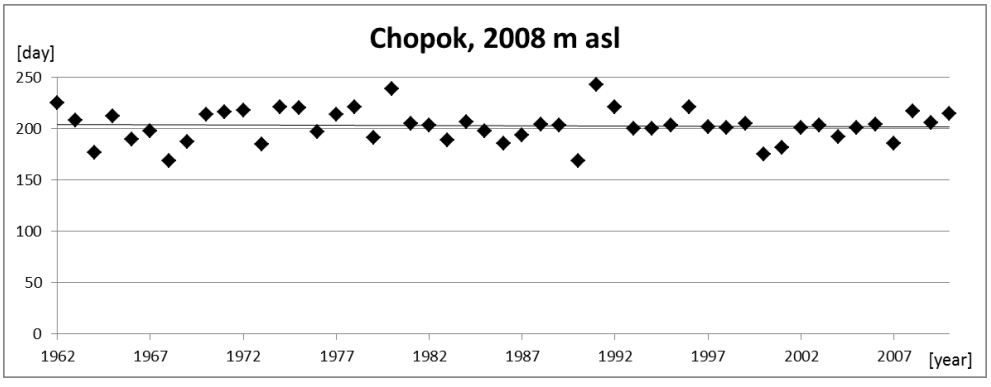

Figure 7. The duration of the snow cover at the Chopok climate station

We can see a decreasing trend in the duration of the days with snow cover, but no significantly trend were detected using the Mann-Kendall test.

4.2 Simulation of snow water equivalent

4.2.1 Calibration and validation of model parameters

It was mentioned that the parameters of the model were calibrated individually for each decade, and other decades were used for the validation of the model's parameters. The values achieved of the Nash-Sutcliffe coefficient are listed in *Table 2*.

Table 2. Values of the Nash-Sutcliffe coefficient for the calibration and validation periods (grey – calibration, white – validation)

↑ Validation ↓	1961–1971	1971–1981	1981–1991	1991–2000	2000–2010
1961–1971	0.7987	0.689	0.7301	0.7187	0.7162
1971–1981	0.7124	0.8041	0.7466	0.7379	0.7608
1981–1991	0.7175	0.7499	0.7341	0.7423	0.6546
1991–2000	0.7386	0.784	0.804	0.7911	0.6505
2000–2010	0.6701	0.7031	0.6889	0.6506	0.7595

A comparison of the simulated mean monthly SWE for the months of the winter season and the period 1961–2010 is shown in *Table 3* (Juričeková et al. 2013).

Table 3. Mean monthly basin averages of SWE for the period 1961 –2010

	Nov [mm]	Dec [mm]	Jan [mm]	Feb [mm]	March [mm]	April [mm]
Representative series of SWE	3.79	25.46	56.53	79.67	71.41	16.18
SWE simulated with parameters from period 1961–1971	3.67	24.58	54.46	75.82	67.14	14.34
SWE simulated with parameters from period 1971–1981	4.02	23.57	49.51	70.00	61.18	11.81
SWE simulated with parameters from period 1981–1991	3.94	26.36	58.52	82.97	75.82	18.63
SWE simulated with parameters from period 1991–2000	3.58	23.36	51.58	72.63	65.63	15.50
SWE simulated with parameters from period 2000–2010	4.06	24.09	52.04	69.98	59.58	10.14

The next step was the validation of the simulated SWE with the measured data. From the comparison of the simulated daily values from the representative SWE series with the measured basin's SWE averages, we can see a satisfactory compliance between the simulated and measured daily SWE values. Some differences could be caused by a problematic determination of the basin's average value of the measured SWE, which was caused by the missing data in some climate stations. As illustration, a comparison of the measured and simulated basin's SWE for the period's 1981–1990 *(Figure 8)* and 1991–2000 *(Figure 9)* are presented here.

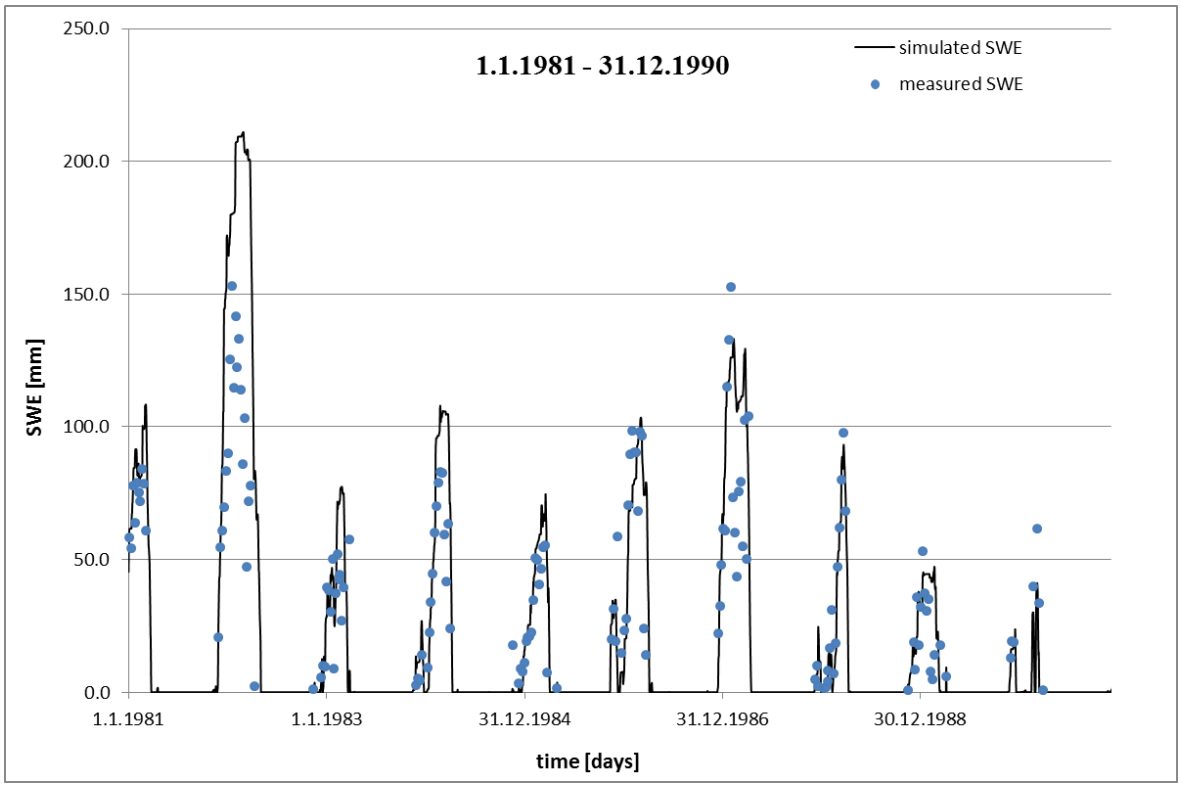

Figure 8. Comparison of the measured and simulated basin's SWE for the period 1981–1990

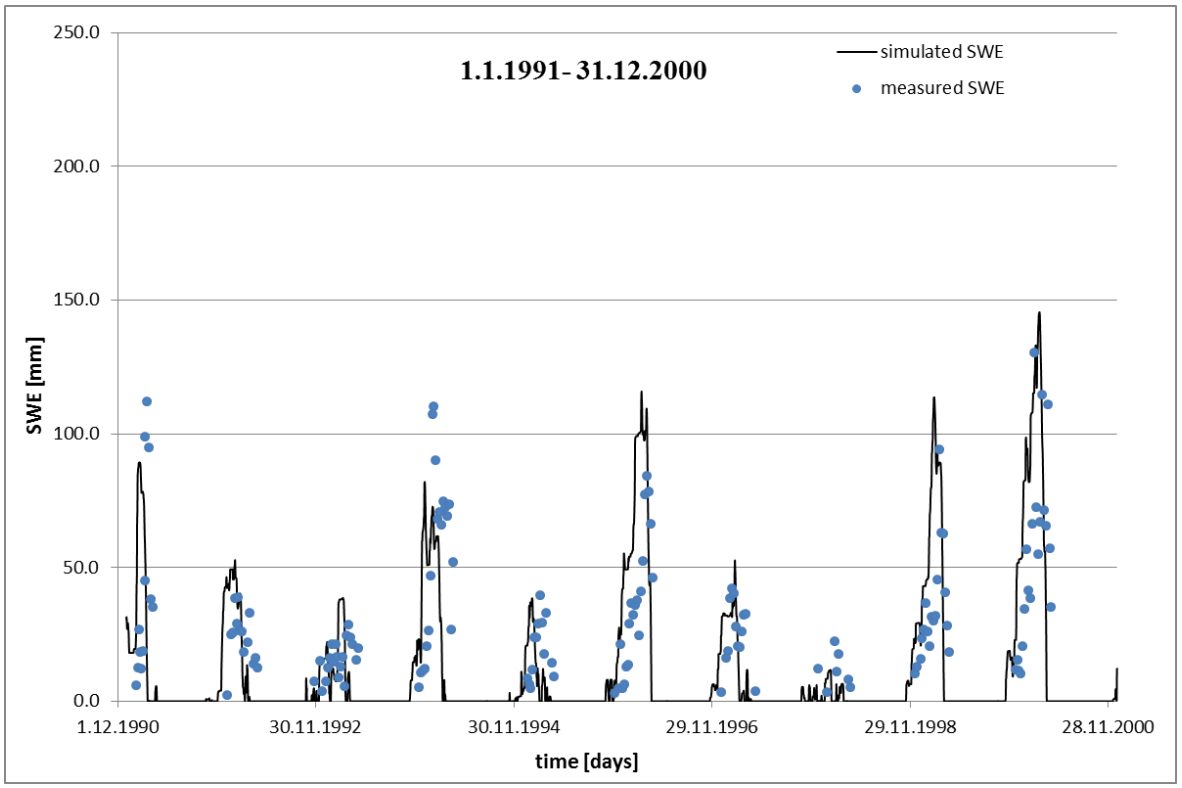

Figure 9. Comparison of the measured and simulated basin's SWE for the period 1991–2000

The changes in the simulated snow water equivalents in the basin were assessed by the trend analysis, and the significance of the trends was tested using the Mann-Kendall test *(Table 4)*. From the table we can see a statistically confirmed significant trend at the 95% level of significance in some months. From the results it is possible to indicate a decrease in the snow water equivalent on the upper Hron River basin in the period of 1961–2010 in all the months of the winter season, and significantly decreasing trends were indicated in the months of December, January and February.

Table 4. Significance of decreasing trends of the simulated basin's SWE in the individual months

Month	Significant trend (level of 95% significance)
November	No
December	Yes
January	Yes
February	Yes
March	No
April	No

4.3 MODIS satellite images

In this part of the study the validation of the MODIS data by comparing it with the measured data from the study area was provided. Next, the temporal filtering of the MODIS images was applied to increase the accuracy of the images. Finally, the MODIS data were compared with the measured data.

4.3.1 Validation of the MODIS satellite images

The monthly values of the overall degree of agreement of the MODIS satellite images are shown in *Table 5*, and the yearly values of the accuracy index of the overall agreement and misclassification of the original MODIS data are shown in *Table 6*.

Table 5. The monthly values of the overall degree of agreement of the original MODIS satellite images

	Banská Bystrica (%)	Brezno (%)	Telgárt (%)	Lom nad Rimavicou (%)	Chopok (%)
November	95.455	90.909	86.49	92.929	41.250
December	94.681	87.273	93.00	81.746	65.546
January	92.593	89.655	97.98	92.000	93.976
February	90.000	86.598	80.52	89.109	95.946
March	85.185	79.661	63.73	86.842	94.318
April	99.432	99.375	77.12	90.977	23.009

Table 6. Yearly values of the accuracy index of the overall degree of agreement and misclassification of the original MODIS data

	Banská Bystrica (%)	Brezno (%)	Telgárt (%)	Lom nad Rimavicou (%)	Chopok (%)
Overall degree of agreement	91.802	88.822	79.836	89.732	76.812
Underestimation	0.119	0.577	1.00	2.589	1.072
Overestimation	2.380	3.926	7.31	3.070	28.637

Subsequently, the temporal filtering of the MODIS images was used to increase the accuracy of the images. Next, the MODIS data were compared with the measured data. The overall degree of agreement, underestimation and overestimation were estimated for all the decades in each station in all the months of the winter season *(Tables 7–12).*

Table 7. The monthly values of the overall degree of agreement of the satellite images after temporal filtering (time step: 1 day)

	Banská Bystrica (%)	Brezno (%)	Telgárt (%)	Lom nad Rimavicou (%)	Chopok (%)
November	94.44	92.64	85.47	93.17	40.91
December	93.06	86.14	92.36	80.66	66.07
January	93.85	90.14	96.03	90.57	93.23
February	89.68	88.11	81.67	87.42	96.30
March	86.54	78.61	68.39	88.02	95.35
April	98.74	99.10	75.71	89.58	21.56

Table 8. Yearly values of the accuracy index of the overall degree of agreement and misclassification of the sensor after temporal filtering (time step: 1 day)

	Banská Bystrica (%)	Brezno (%)	Telgárt (%)	Lom nad Rimavicou (%)	Chopok (%)
Overall degree of agreement	92.20	88.99	80.45	88.90	76.61
Underestimation	0.13	0.57	1.27	2.65	1.24
Overestimation	2.71	4.21	7.44	3.49	28.96

Table 9. The monthly values of the overall degree of the agreement of satellite images after temporal filtering (time step: 2 days)

	Banská Bystrica (%)	Brezno (%)	Telgárt (%)	Lom nad Rimavicou (%)	Chopok (%)
November	93.12	93.20	83.18	90.73	40.00
December	90.06	83.90	90.55	81.48	66.67
January	88.62	87.29	95.74	88.78	92.73
February	89.24	88.07	83.44	88.20	96.38
March	86.91	79.05	69.39	87.08	95.65
April	98.53	98.43	76.96	88.39	21.89

Table 10. Yearly values of the accuracy index of the overall degree of agreement and misclassification of the sensor after temporal filtering (time step: 2 days)

	Banská Bystrica (%)	Brezno (%)	Telgárt (%)	Lom nad Rimavicou (%)	Chopok (%)
Overall degree of agreement	90.83	88.21	81.38	88.11	76.66
Underestimation	0.14	0.52	1.42	2.77	1.31
Overestimation	3.53	4.79	7.68	3.91	29.12

Table 11. The monthly values of the overall degree of the agreement of satellite images after temporal filtering (time step: 3 days)

	Banská Bystrica (%)	Brezno (%)	Telgárt (%)	Lom nad Rimavicou (%)	Chopok (%)
November	91.56	93.70	81.40	89.83	39.20
December	88.57	82.55	88.28	81.97	67.53
January	86.15	86.12	96.31	89.19	91.62
February	88.59	87.06	85.55	89.05	96.27
March	86.88	78.75	69.60	87.29	95.72
April	98.63	98.19	76.23	88.26	21.93

Table 12. Yearly values of the accuracy index of the overall degree of agreement and misclassification of the sensor after temporal filtering (time step: 3 days)

	Banská Bystrica (%)	Brezno (%)	Telgárt (%)	Lom nad Rimavicou (%)	Chopok (%)
Overall degree of agreement	90.06	87.53	81.92	88.45	76.39
Underestimation	0.16	0.51	1.54	2.90	1.49
Overestimation	4.10	5.24	7.99	3.90	29.22

The mean value of the overall degree of the agreement of the original satellite images is 85.4%; the overestimation is 9.1%; and the underestimation of the images is 1.1%. After the temporal filtering, these values were changed. Overall, the values of the overall degree of the agreement has not changed significantly, but the mean value of the underestimation was changed by 0.25%, and the mean value of the overestimation after the temporal filtering in the 1–3 day time step was changed by more than 1% – the misclassification of snow as land is increasing, but the misclassification of land as snow is approximately the same (Parajka – Blöschl 2008a, Marchane et al. 2014). In our future work, we expect higher values of the overall degree of the filtered satellite images by a combination of temporal and spatial filtering.

5 DISCUSSION AND CONCLUSIONS

Snow cover is a significant natural phenomenon; precipitation is accumulated during some months in the winter season and then is released in a very short time. This has quantitative and qualitative impacts on the water cycle.

The changes in the duration of the snow cover were evaluated in the period of the hydrological years of 1962–2010. This assessment was conducted using measured data from the five climate stations in the upper Hron River basin from different elevations. From the comparison, we can see a decreasing trend in the duration of the days with snow cover and, according to the Mann-Kendall statistical test.

We focused on an assessment of the changes in the snow water equivalent values in the upper Hron River basin in the period of 1961–2010. In the catchment we simulated the daily values of the SWE by the rainfall-runoff model Hron with lumped parameters. The period of 1961–2010 was divided into five decades; they were particularly calibrated, and the other years were used for the validation of the parameters of the model Hron. In this way we wanted to review the impact of the changed parameters of the simulated values of the SWE.

From the Nash-Sutcliffe (NS) values we can see higher values of NS in every calibrated decade than in the validated periods, except for the period of 1981–1990. No significant change of the model's parameters was detected over time. We assume that the state variables of the model obtained by simulating a shorter period are more reliable than the simulated values obtained with the simulated parameters calibrated for the entire period of 50 years.

From the comparison of the basic SWE statistics simulated from the whole period of 1961–2010 with the different sets of model parameters calibrated, we can state that the different sets of model parameters had an effect on the simulated SWE values in the individual months. Therefore, for the final analysis we selected the simulated SWE achieved from the simulations of the individual decades with each of their own calibrated parameters. These values of the "representative" simulated SWE were also consistent with the measured basin's values, which were estimated from the available measured SWE data from the climate stations in the basin.

The changes in the representative simulated SWE were evaluated by the trend analysis in the individual months, and the statistical significance of the trends was assessed by the Mann-Kendall statistical test. From the results it is possible to demonstrate a decrease in the SWE on the upper Hron River basin in the period of 1961–2010 in all the months of the winter season, and significant decreasing trends were indicated in months of December, January and February.

Finally, we evaluated and validated the MODIS satellite images and evaluated the accuracy of the MODIS snow data. These data were compared with the measured data in the area of interest, and the index of the accuracy, the overall degree of the agreement, and the misclassifications of the sensor were determined. The mean value of the overall degree of agreement of the original satellite images for the winter seasons was 85.4%; the overestimation was 9.1%; and the underestimation of the images was 1.1%. After the temporal filtering, the misclassification of snow as land was increased, but the misclassification of land as snow was approximately the same.

Acknowledgement: This work was supported by the Slovak Research and Development Agency under Contract No. APVV-0303-11 and by the VEGA No. 1/0908/11 research project.

REFERENCES

ARTAN, G. A. – VERDIN, J. P. – LIETZOW, R. (2013): Large scale snow water equivalent status monitoring: comparison of different snow water products in the upper Colorado Basin, Hydrology and Earth System Sciences, Vol. 17, 5127–5139, doi:10.5194/hess-17-5127-2013

BERGSTRÖM, S. (1976): Development and application of a conceptual runoff model for Scandinavian catchments, SMHI Report RHO 7, Norrköping.

BERGSTRÖM, S. (1992): The HBV model – its structure and applications. SMHI Reports RH, No. 4, Norrköping.

DANKO, M. – HLAVČOVÁ, K. – KOHNOVÁ, S. – SZOLGAY, J. (2010): Posúdenie extrémneho odtoku z topenia snehu v povodí Račianskeho potoka (Estimation of extreme runoff from snow melt in the Račiansky potok basin). Acta Hydrologica Slovaca, Vol. 11, No. 1, IH SAS, Bratislava, Slovakia (in Slovak)

GAÁL, L. – SZOLGAY, J. – KOHNOVÁ, S. – PARAJKA, J. – MERZ, R. – VIGLIONE, A. – BLÖSCHL, G. (2012): Flood timescales: Understanding the interplay of climate and catchment processes through comparative hydrology. Water Resources Research, Vol. 48, W04511, doi:10.1029/2011WR011509.

HALL, D. K., RIGGS, G., A. (2007): Accuracy assessment of the MODIS snow products. Hydrological Processes, 21, pp. 1534–1547.

HALMOVÁ, D. – MÉSZÁROŠ, I. – MIKLÁNEK, P. – MITKOVÁ, V. – PEKÁROVÁ, P. (2006): Simulácia vodnej hodnoty snehu v experimentálnom mikropovodí Rybárik semi-distribuovaným zrážkovo-odtokovým modelom (Snow water equivalent simulation in experimental microbasin Rybárik with semi-distributed rainfall-runoff model). Acta Hydrologica Slovaca, Vol. 7, No.1, IH SAS, Bratislava, Slovakia (in Slovak)

HOLKO, L. (2000): Vyhodnotenie dlhodobých meraní parametrov snehovej pokrývky v horskom povodí (Evaluation of long-term snow cover data in a mountain catchment). Acta Hydrologica Slovaca, Vol. 1, No.1, IH SAS, Bratislava, Slovakia (in Slovak)

HOLKO, L. – GORBACHOVÁ, L. – KOSTKA, Z. (2011): Snow Hydrology in Central Europe. Geography Compass, Vol. 5, No. 4, 200-218, doi: 10.1111/j.1749-8198.2011.00412.x

HOLKO L. – KOSTKA, Z. – PECUŠOVÁ, Z. (2005): Sneh (Snow). In Scenáre zmien vybraných zložiek hydrosféry a biosféry v povodí Hrona a Váhu v dôsledku klimatickej zmeny (Scenarios of changes in selected components of the hydrosphere and biosphere in the Hron River Basin and the balance due to climate change), Eds. P. Pekárová and J. Szolgay, Veda Bratislava, Slovakia, 105–167 [in Slovak]

HOOD, J. L. – HAYASHI, M. (2010): Assessing the application of a laser rangefinder for determining snow depth in inaccessible alpine terrain, Hydrology and Earth System Sciences, Vol. 14, 901–910, doi:10.5194/hess-14-901-2010

JURIČEKOVÁ, K. – HLAVČOVÁ, K. – SZOLGAY, J. – BARTÓKOVÁ, L. – SZÁSZ, V. (2013): Posúdenie zmeny simulovanej vodnej hodnoty snehu na povodí horného Hrona (Evaluating changes in simulated snow water equivalent in the upper Hron River basin). Acta Hydrologica Slovaca, Vol. 14, No.1, IH SAS, Bratislava, Slovakia (in Slovak)

KUBEŠ, R. (2007): Návrh koncepčného zrážkovo-odtokového modelu pre hydrologické predpovede (Proposal for a conceptual rainfall-runoff model for hydrological forecasting). Bratislava, Slovakia (in Slovak)

KUBEŠ, R. – HLAVČOVÁ, K. (2002): Simulácia extrémnej zrážkovo-odtokovej situácie na povodí Hrona. (Simulation of extreme rainfall-runoff situation in the Hron River basin) In: X. international poster day "Transport of Water, Chemicals and Energy in the System Soil – Crop Canopy – Atmosphere". Bratislava, Slovakia: Institute of Hydrology SAS, Geophysical Institute SAS. ISBN 80-968480-9-7.

KUCHMENT, L. S. – ROMANOV, P. – GELFAN, A. N. – DEMIDOV, V. N. (2010): Use of satellite-derived data for characterization of snow cover and simulation of snowmelt runoff through a distributed physically based model of runoff generation, Hydrology and Earth System Sciences, Vol. 14, doi:10.5194/hess-14-339-2010

LAPIN, M. – MELO, M. – FAŠKO, P. – PECHO, J. (2007): Snow cover changes scenarios for the Tatra Mountains in Slovakia. Proceedings of the 29th International Conference on Alpine Meteorology, 4. – 8. 6. 2007, Chambéry, France

MARCHANE, A. – JARLAN, L. – HANICH, L. – BOUDHAR, A. – GASCOIN, S. – LE PAGE, M. – TAVERNIER, A. – FILALI, N. – BERJAMY, B. – KHABBA, S. – CHEHBOUNI, G. (2014): Snow cover dynamic in the Atlas Chain (Morocco) using daily MODIS products over the last decade. Geophysical Research Abstracts, Vol. 16/2014: EGU General Assembly 2013.

MAURER, E.P. – RHOADS, J.D. – DUBAYAH, R.O. – LETTENMAIER, D.P. (2003): Evaluation of the snow covered area data product from MODIS. Hydrological Processes, 17, 59–71.

NATIONAL SNOW AND ICE DATA CENTER, http://nsidc.org/

PARAJKA, J. (2001): UEB EHZ – Distribuovaný energeticky založený model akumulácie a topenia snehovej pokrývky (UEB EHZ – distributed energy based snow accumulation and melt model). Acta Hydrologica Slovaca, Vol. 2, No.2, IH SAS, Bratislava, Slovakia (in Slovak)

PARAJKA, J. – BLÖSCHL, G. (2006): Validation of MODIS snow cover images over Austria. Hydrology and Earth System Sciences, Vol. 10, doi: 10.5194/hess-10-679-2006

PARAJKA, J. – BLÖSCHL, G. (2008a): Spatio-temporal combination of MODIS images – potential for snow cover mapping. Water resources research, Vol. 40, doi: 10.1029/2007WR006204

PARAJKA, J. – BLÖSCHL, G. (2008b): The value of MODIS snow cover data in validating and calibrating conceptual hydrologic models. Journal of Hydrology, 358, 240–258.

PARAJKA, J. – HOLKO, L. – KOSTKA, Z. – BLÖSCHL, G. (2012): MODIS snow cover mapping accuracy in a small mountain catchment – comparison between open and forest sites. Hydrology and Earth System Sciences, Vol. 16, 2365–2377, doi: 10.5194/hess-16-2365-2012

PARAJKA, J. – MERZ, R. – BLÖSCHL, G. (2003) Estimation of daily potential evapotranspiration for regional water balance modeling in Austria. In: Proceedings of the 11th International Poster Day and Institute of Hydrology. Transport of Water, Chemicals and Energy in the Soil – Crop - Canopy - Atmosphere System, Bratislava, Slovak Academy of Sciences, Bratislava, Slovakia

PEKÁROVÁ, P. – MIKLÁNEK, P. (2006): Predpoveď odtoku z topenia snehu z malého povodia (Snowmelt runoff forecast in small basin). Acta Hydrologica Slovaca, Vol. 7, No.1, IH SAS, Bratislava, Slovakia (in Slovak)

PEKÁROVÁ, P. – MIKLÁNEK, P. – ONDERKA, M. – KOHNOVÁ, S. (2009): Water balance comparison of two small experimental basins with different vegetation cover. Biologia, Vol. 64, No. 3, ISSN 0006-3088, 487-491.

PEKÁROVÁ, P. – SZOLGAY, J. (2005): Scenáre zmien vybraných zložiek hydrosféry a biosféry v povodí Hrona a Váhu v dôsledku klimatickej zmeny (Scenarios of changes in selected components of the hydrosphere and biosphere in the Hron River Basin and the balance due to climate change), Veda Bratislava, Slovakia (in Slovak)

VALENT, P. – DANEKOVÁ, J. – RIVERSO, C. (2011): Neistoty pri kalibrácii zrážkovo-odtokového modelu HBV (Uncertainties in the HBV model calibration). Acta Hydrologica Slovaca, Vol. 12, No. 2, IH SAS, Bratislava, Slovakia (in Slovak)

DE GRUYTER OPEN DOI: 10.2478/aslh-2014-0012 Acta Silv. Lign. Hung., Vol. 10, Nr. 2 (2014) 161–174

Alternative Approaches to a Calibration of Rainfall-Runoff Models for a Flood Frequency Analysis

Peter VALENT * – Ján SZOLGAY – Roman VÝLETA

[a] Department of Land and Water Resources Management, Faculty of Civil Engineering, Slovak University of Technology, Bratislava, Slovakia

Abstract – One of the tools which are currently being used in flood frequency analysis (FFA) is rainfall-runoff (RR) modelling. Its use in FFA often confronts the problem of how to correctly calibrate RR models to extreme flows. Since FFA only deals with extreme flows, traditional calibration techniques using simple objective functions such as the Nash-Sutcliffe model's efficiency criterion are not sufficient. In this paper we have focused on proposing alternative approaches for calibration techniques of RR models in order to enhance the description of extreme flows. We have selected the HBV type conceptual, lumped model HRON as an RR model. We have suggested two alternative calibration approaches: 1) the use of a new optimization function that compares only values higher than the 95th percentile of observed flows and 2) using two sets of parameters to separately simulate low and high flows. Each of these improvements has enhanced the simulation of extreme flows, which has been demonstrated in the empirical cumulative distribution function calculated for the simulated and observed annual maximum series of flows. The results of this paper show that improvement can be obtained by both approaches, which give good agreement between observed and simulated extreme flows, while preserving a good simulation of low and medium flows.

rainfall-runoff model / calibration / annual maximum series of flows / flood frequency analysis

Kivonat – Gyakoriság-tartóssági vizsgálatra használt csapadék lefolyási modellek kalibrációjának alternatív megközelítései. Az árhullámok gyakoriság-tartóssági vizsgálatára (FFA) a napjainkban használt eszközök egyike a csapadék-lefolyás (RR) modellezés. Ennek használata során gyakran kerülünk szembe avval a problémával, hogy hogyan tudjuk korrekt módon kalibrálni a RR modelleket az extrém vízhozamokra. Mivel az FFA csak az extrém vízhozamokra koncentrál az olyan egyszerű, objektív függvényekkel dolgozó, klasszikus kalibrációs módszerek, mint a Nash-Sutcliffe féle kritérium nem megfelelőek. Jelen tanulmány alternatív megközelítéseket javasol a RR modellek kalibrálására, abból a célból, hogy az extrém vízhozamok elemzését javítsa. A vizsgálatra a HBV típusú koncepcionális, koncentrált paraméterű HRON modellt, mint RR modellt választottuk ki. Két alternatív kalibrációs megközelítést javasoltunk: 1) új optimalizációs függvény használata, amely csak a vizsgált vízhozamok 95. percentilisénél nagyobb értékeket hasonlítja össze és 2) két paraméter készlet használata külön a kis és a nagy vízhozamok szimulációjára. Mindkét új fejlesztési megközelítés javítja az extrém vízhozamok szimulációját, a fejlesztések hatását a szimulált és mért eves maximális vízhozam idősorok empirikus tartóssági görbéinek segítségével mutatjuk be. A tanulmány szerint mindkét megközelítés javulást eredményezhet, amely a vizsgált és szimulált extrém vízhozamok közötti jó egyezéssel igazolható, az alacsony és közepes vízhozamok tartományában való jó szimuláció megtartása mellett.

csapadék lefolyás modell / modellillesztés / évi maximális vízhozam idősorok/ gyakoriság-tartósság vizsgálat

* Corresponding author: peter_valent@stuba.sk; Radlinského 11, 813 68 Bratislava, Slovakia

1 INTRODUCTION

In derived flood frequency analysis (FFA), rainfall-runoff (RR) models are commonly used to continually simulate runoff from a catchment. One of the strongest motivations for the use of RR models in FFA is that, together with stochastic rainfall models, they enable the easy simulation of arbitrarily long series of river flows containing unobserved combinations of extreme values. Such a long series of river flows can be subsequently used to extract various flood characteristics such as peak flow, flood volume or flood duration. One of the advantages of continuous simulation compared to event-based RR models is that these models can also simulate different variables representing the state of the catchment (e.g., soil moisture, evapotranspiration, the amount of water in any snow cover). This enables avoiding the making of estimates about the initial conditions of the catchment's state (see, e.g., Lamb 1999, Boughton – Droop 2003, Hoes – Nelen 2005, Pathiraja et al. 2012). However, the greatest advantage of a continuous simulation is that it can be linked with stochastic weather generators, which enable the generation of various inputs (most often, rainfall amounts and temperatures) of arbitrary lengths. Weather generators preserve the statistical characteristics of observed time series of input variables (see, e.g., Racsko et al. 1991, Chen et al. 2010, Výleta 2013). The RR model can then transform the generated weather data into a time series of generated catchment runoff. Despite the fact that the generated time series preserves the statistical characteristics of the observed time series, they can contain rare combinations of subsequent rainfall events that only occur with a very small degree of probability, thereby causing extreme floods, which are not present in the observed time series of the catchment runoff (Valent 2012a).

In the FFA, which is often used for the estimation of design floods, annual maximum (AM) series of flows or flows above a certain threshold (POT) are used in practise. Therefore, the RR model must be mainly able to satisfactorily simulate extremely high flows. This can be achieved by calibrating the RR model for extreme flows while the proper simulation of low and medium flows is neglected. However, this solution is not suitable, since it does not enable a good simulation of the catchment conditions preceding the flood event. Despite considerable efforts in this area, there is not a united methodology for calibrating RR models to extreme flows. The literature contains several studies dealing with this problem (see, e.g., Paquet et al. 2013, Viney et al. 2009, Tan et al. 2005, Lamb 1999).

This paper presents two new approaches to the calibration of RR models to extreme floods and compares them with traditionally used techniques utilizing the Nash-Sutcliffe criterion. In order to increase the credibility of the presented results, the methodology has been applied to two mountainous catchments situated in the central part of Slovakia (*Figure 1*). The approaches are tested on two nested Slovak mountainous catchments: 1) the Hron at Banská Bystrica (BB) and 2) the Hron at Brezno.

2 DATA

The first catchment is a catchment of the River Hron with an outlet at the Banská Bystrica station. The catchment drains an area of 1768.2 km^2 and flows in a relatively narrow valley with high mountains on each side. The mean altitude of the catchment is 845.1 mASL with the highest peak at 2030.1 mASL. The average annual precipitation amount calculated for the period between 1961 and 2010 from the area precipitation was 846 mm. A high percentage of the catchment is a national park and is covered with coniferous and deciduous forests. The regime of the catchment runoff has a strong seasonal effect with the highest flows in April and the lowest in the winter. The mean annual runoff calculated for the period between 1961 and 2010 is 25.1 m^3/s (447 mm) with minimum and maximum values of 4.9 and 515 m^3/s respectively. The flow data were collected for the period between 1.1.1961 and 31.12.2010.

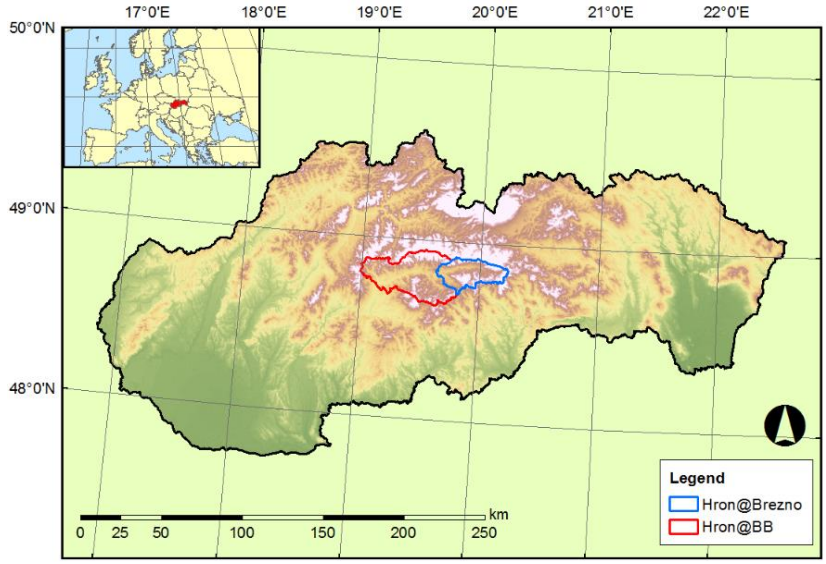

Figure 1. Position of the two catchments:
the Hron at Brezno and the Hron at Banská Bystrica in Slovakia (b)

a)

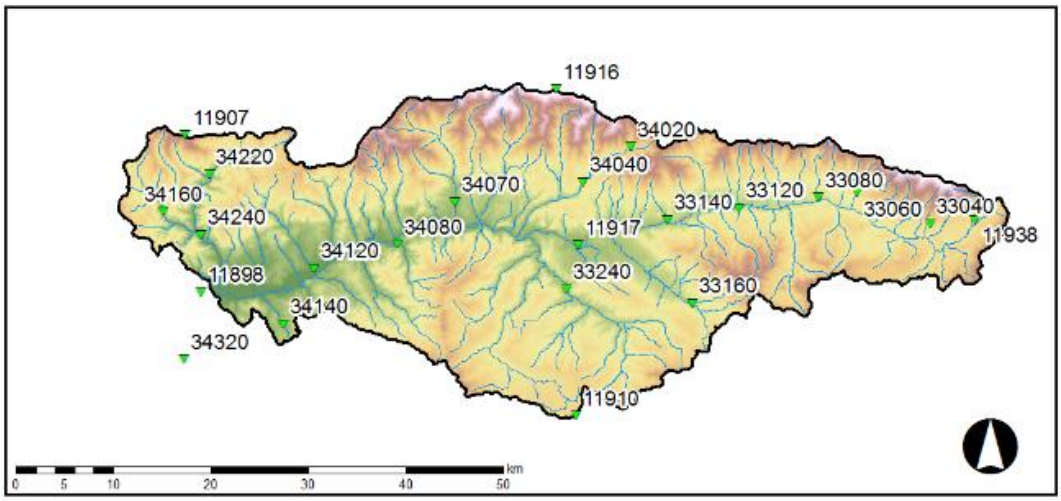

b)

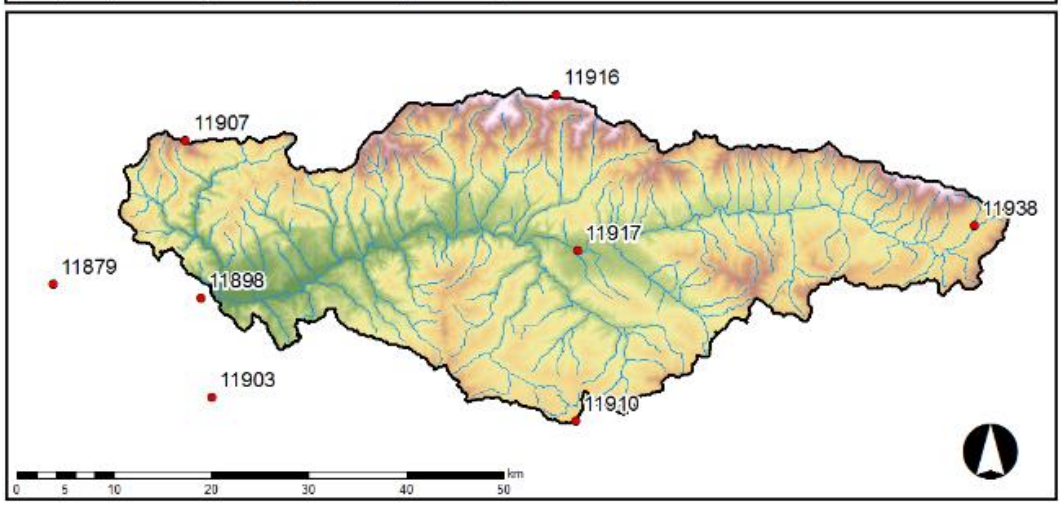

Figure 2. Location of measurement stations in the Hron catchment with the outlet at Banska Bystrica a) 24 rain gauges, b) 7 climatic stations measuring temperatures

The precipitation data were collected from 24 stations (*Figure 2a*) and processed using the inverse distance weighting interpolation method to obtain the catchment's average daily precipitation amounts. The temperature data were collected from 7 climatic stations (*Figure 2b*) and processed using the temperature gradient method to obtain an average daily air temperature for the catchment.

The second catchment is a nested catchment of the River Hron with an outlet at the Brezno station. The catchment drains an area of 578.6 km^2 and is situated in the upper part of the Hron catchment. The mean altitude of the catchment is 916 mASL with the highest peak of Kráľová Hoľa at an altitude of 1946 mASL. The mean annual precipitation amount calculated for the period between 1961 and 2010 from the area precipitation was 830 mm. The flow regime of the catchment is identical to the regime of the first catchment with the highest flows in April and the lowest in January. The mean annual runoff calculated for the period between 1961 and 2010 is 7.6 m^3/s (414 mm) with minimum and maximum values of 1.2 and 178 m^3/s respectively. The flows here were also collected for the period between 1.1.1961 and 31.12.2010.

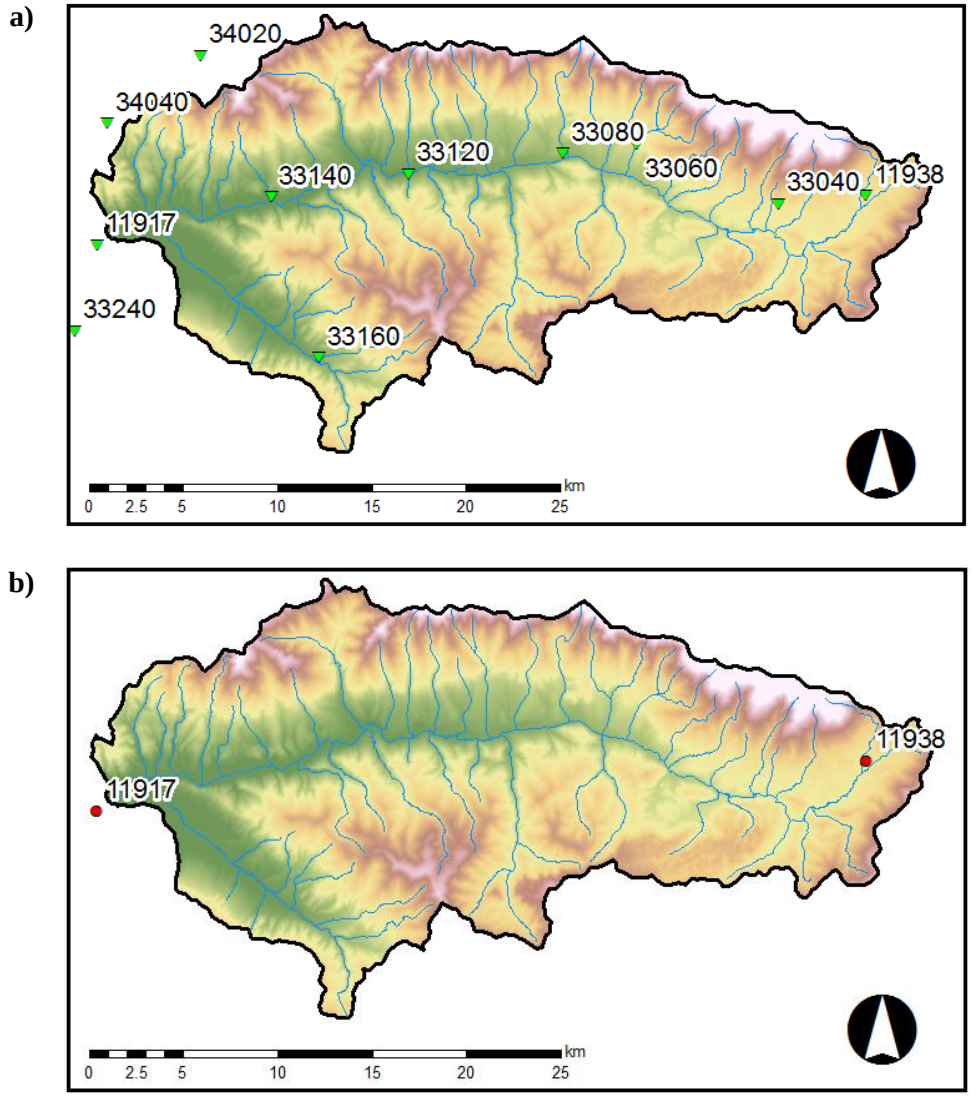

Figure 3. Location of measurement stations in the Hron catchment with the outlet at Brezno a) 11 rain gauges, b) 2 climatic stations measuring temperatures

The precipitation data were collected from 11 stations (*Figure 3a*) and processed in the same way as for the first catchment. The temperature data were collected from 2 climatic stations (*Figure 3b*) and processed using the temperature gradient method to obtain an average temperature for the catchment.

3 METHODOLOGY

This work is focused on the improvement of the calibration procedure of the HRON rainfall-runoff model to better simulate extreme flows. The HRON model is a conceptual lumped model, which works mainly in a daily time-step. It was developed at the Department of Land and Water Resources Management of the Slovak University of Technology and is based on the Swedish HBV model (Bergstrom 1976). The model comprises 3 submodels, each of which represents a different runoff generation process (for the scheme of the model, see *Figure 4*). The model has 14 parameters, which were calibrated using a harmony search algorithm (see, e.g., Valent 2012b or Geem 2009).

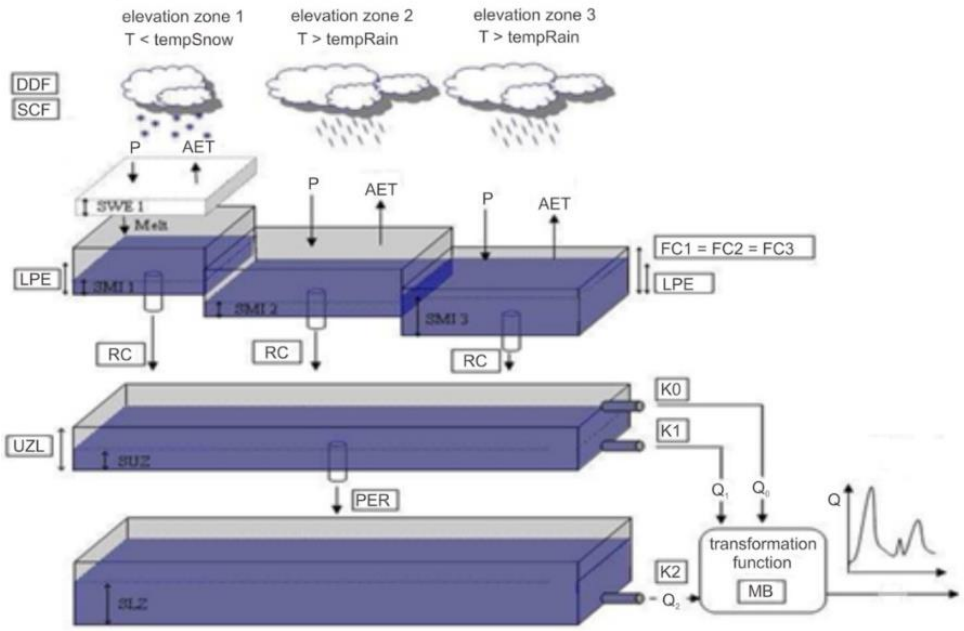

Figure 4. Scheme of the HRON rainfall-runoff model (Valent et al. 2011)

The paper compares the traditionally used calibration technique, utilizing a Nash-Sutcliffe (NS) criterion as the objective function (1) (Nash – Sutcliffe 1970), with two new approaches focused on the calibration to extreme flows. The NS criterion can be written as:

$$NS = 1 - \frac{\sum_{i=1}^{n}\left(Q_{sim,i} - Q_{obs,i}\right)^2}{\sum_{i=1}^{n}\left(Q_{sim,i} - \bar{Q}_{obs}\right)^2} \quad (1)$$

where $Q_{obs,i}$ and $Q_{sim,i}$ are observed and simulated flows in day i and $\bar{Q}_{obs}$ is the average observed flow.

The first approach is based on the selection of a different objective function. In order to improve the simulation of extreme flows, a new objective function has been proposed. The new objective function takes into account only values that are higher than the 95th percentile of the flows observed. The proposed objective function can be written as

$$f(x) = \frac{\left(Q_{obs,p95} - Q_{sim,p95}\right)^2}{\left(Q_{obs,p95} - Q_{p95}\right)^2} \quad (2)$$

where $Q_{obs,p95}$ are all the observed flows that are higher than the 95th percentile calculated from the observed flows; $Q_{sim,p95}$ are simulated flows corresponding to the $Q_{obs,p95}$, and Q_{p95} is the value of the 95th percentile of the flows observed.

The second approach is based on separate simulations of low and high flows. In this approach the HRON RR model utilizes two sets of parameters (the regime switching version of the model). The first set of parameters was used to simulate low flows and was obtained through a traditionally used calibration technique utilizing the NS coefficient (1). The second set of parameters was used to simulate high flows and was estimated by calibrating the model only to the annual maximum floods, where each flood is comprised of the flood peak and two days surrounding it (flood peak ± 2 days). In order to focus the optimization algorithm on the very extreme flows, an optimization function minimizing the NS criterion for both time and rank-ordered flows was used. The function can be written as

$$f(x) = NS\left(Q_{T,ord}\right) + w \cdot NS\left(Q_{R,ord}\right) \quad (3)$$

where $NS\left(Q_{T,ord}\right)$ and $NS\left(Q_{R,ord}\right)$ are Nash-Sutcliffe criteria calculated for time and rank-ordered flows, and *w* is a weight (with a value of 2 in this case), which gives the balance between the time (calibration to low and medium flows) and rank-ordered (calibration to high flows) NS criteria (Paquet et al. 2013). Both of the parameter sets were then combined into the switching version of the HRON RR model. The decision as to whether the current flow is considered low or high is taken based on the threshold value of the simulated flow from the previous day (the first flow is calculated as low). The threshold for determining whether the flow is low or high was also calibrated for each catchment individually.

4 RESULTS

In the first step the HRON RR model was calibrated by the traditional approach using the NS criterion as an objective function. In both cases the model was calibrated for the whole period between 1961 and 2010. The overall quality of the simulation was assessed by calculating the NS criterion values (0.744 for the Hron at BB and 0.780 for the Hron at Brezno) and by comparing the observed and simulated interannual flow regimes *(Figure 5)*. The quality of the simulation of the extreme flows was assessed by comparing the empirical cumulative distribution functions (ECDF), which were calculated for the observed and simulated series of the annual maximum (AM) flows (*Figure 6*). *Figure 6* shows that both models underestimate extreme flows, which is not acceptable in the FFA. The main reason for this is the NS criterion, which takes into account the flows (low and medium ones) which are the most frequent and thus have the largest impact on the NS value.

a)

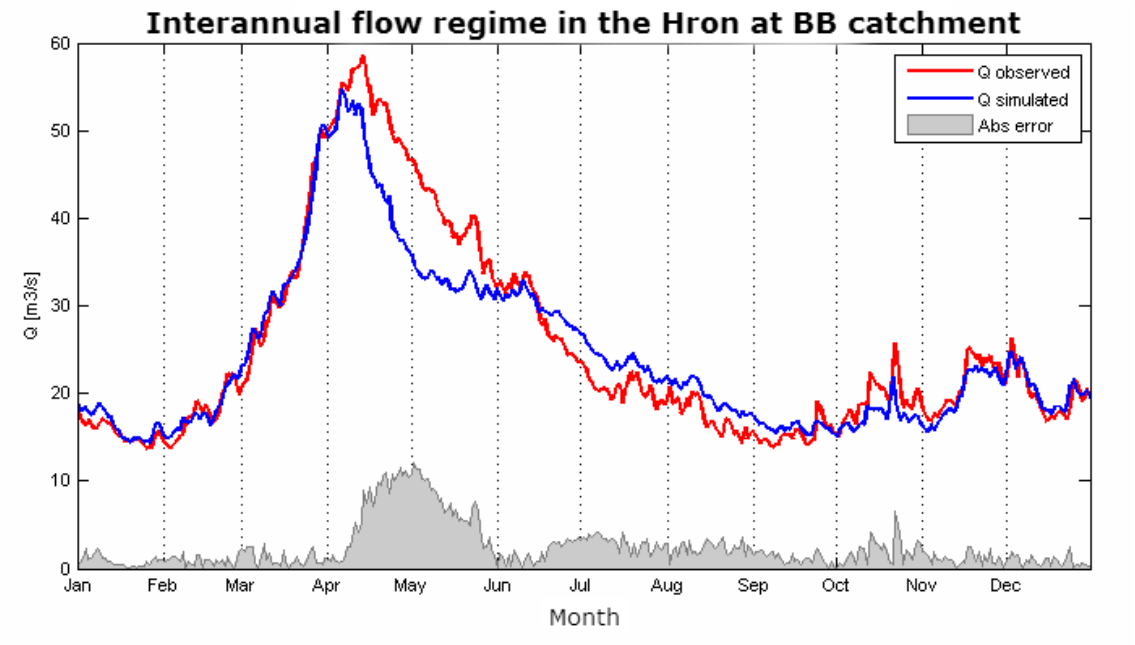

b)

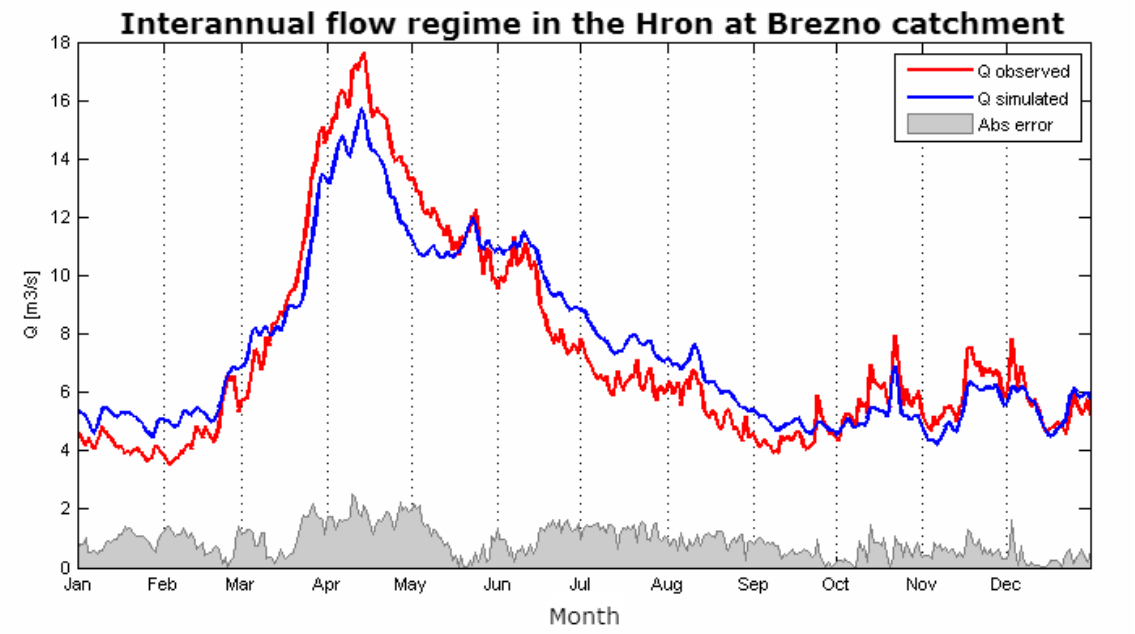

Figure 5. Comparison of observed and simulated interannual flow regimes for the Hron catchments at BB (a) and at Brezno (b). Calculated by the HRON model using the NS criterion (1) as an objective function

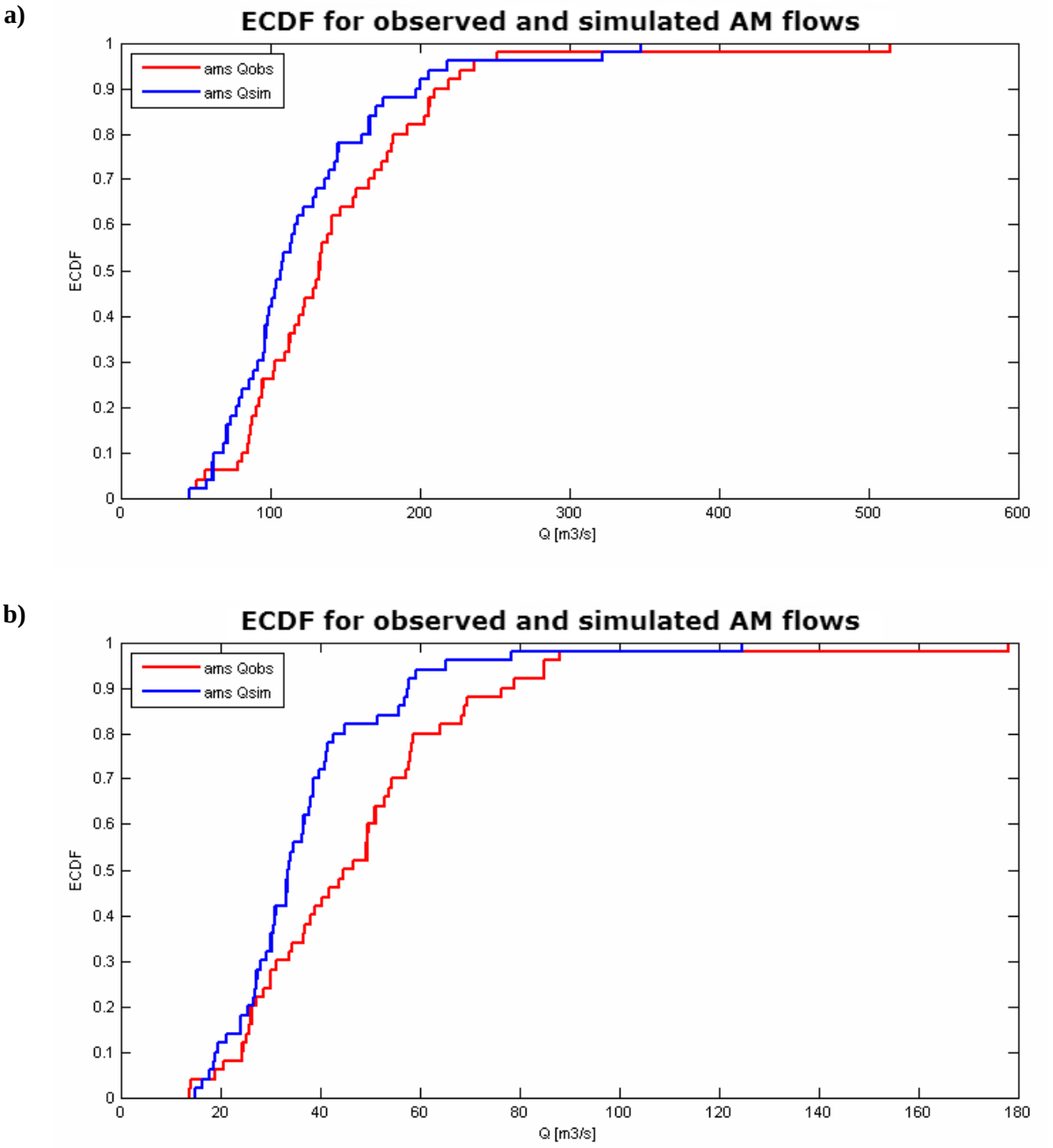

Figure 6. Comparison of the ECDF calculated for the observed and simulated AM flows for the Hron at BB (a) and the Hron at Brezno (b). Calculated by the HRON model using the NS criterion (1) as an objective function

In the next step a new optimization function has been used to improve the simulation of extreme flows. The use of the proposed optimization function (2) had a positive effect on the simulation of extreme flows, especially in the case of the Hron catchment at Brezno (*Figure 7b*). However, the calibration of the model to the values higher than the 95th percentile of the observed flows resulted in the model not being able to reproduce the low and medium flows (*Figure 8*); thus its application is very limited to FFA, when it does not enable correct the simulation of conditions preceding flood events.

a)

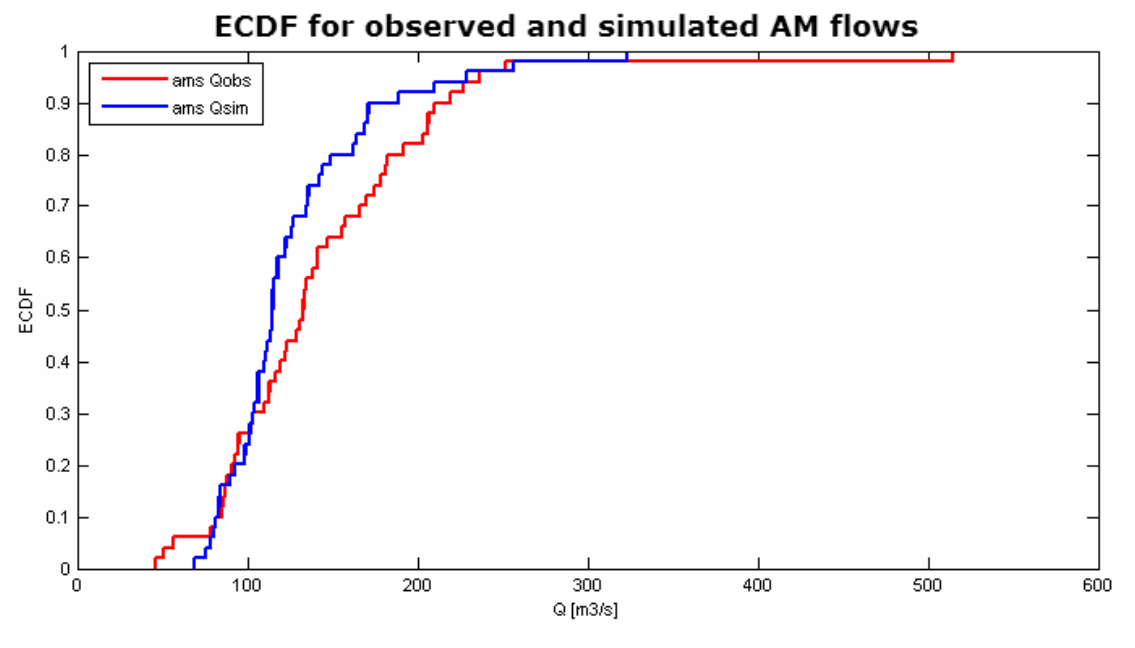

b)

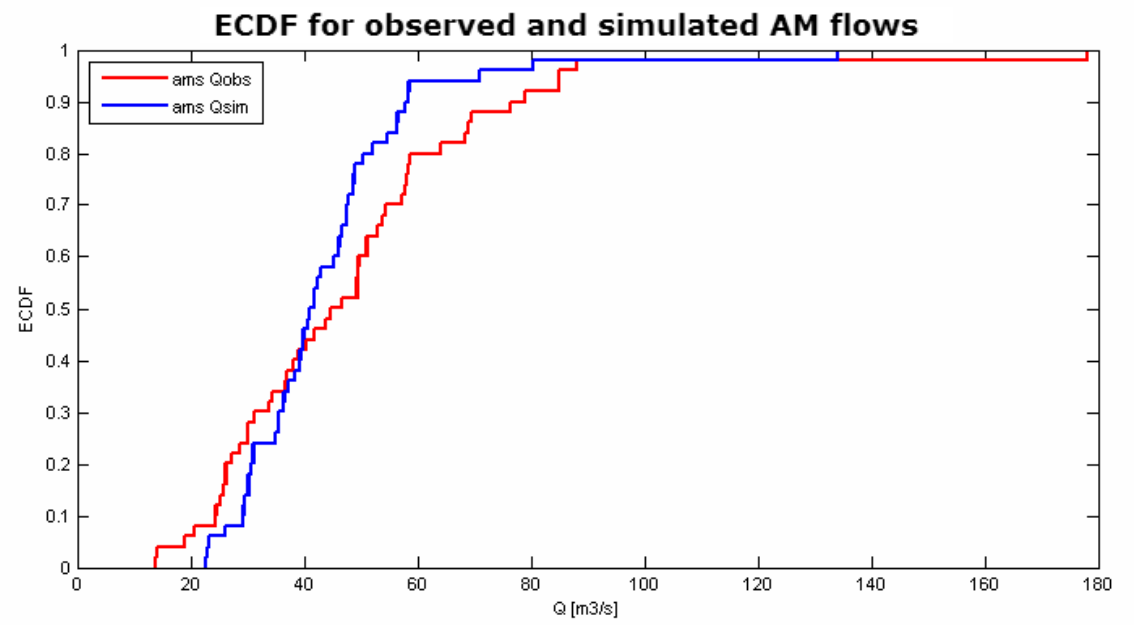

Figure 7. Comparison of the ECDF calculated for the observed and simulated AM flows for the Hron at BB (a) and the Hron at Brezno (b). Calculated by the HRON model using the objective function, which compared only the values higher than the 95th percentile of the observed flows (2)

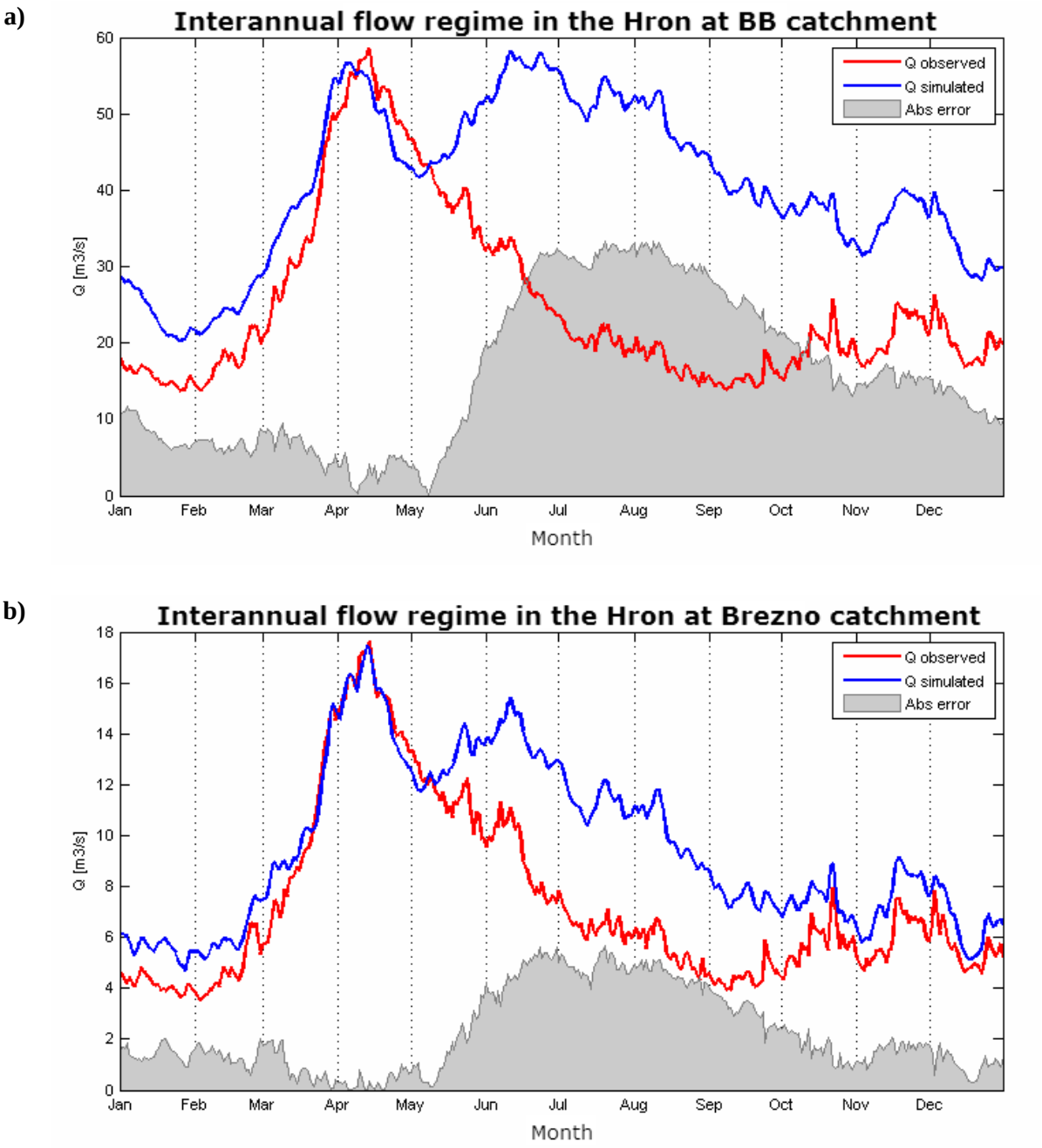

Figure 8. Comparison of the observed and simulated interannual flow regimes for the Hron catchments at BB (a) and at Brezno (b). Calculated by the switching version of the HRON model using the objective function, which compared only the values higher than the 95th percentile of the observed flows (2)

The second approach focuses on improving the simulation of extreme flows while maintaining the good simulation of low and medium flows. It utilizes two sets of parameters to separately simulate low and high flows. The threshold determining whether the flow is low or high was calibrated and was set to be 70.25 and 20.78 m^3/s for the Hron at BB and the Hron at Brezno, respectively. By using separate simulations of the low and high flows, a significant improvement of the simulation of the extreme flows has been observed (*Figure 9*), while preserving the good simulation of the low and medium flows (*Figure 10*).

a)

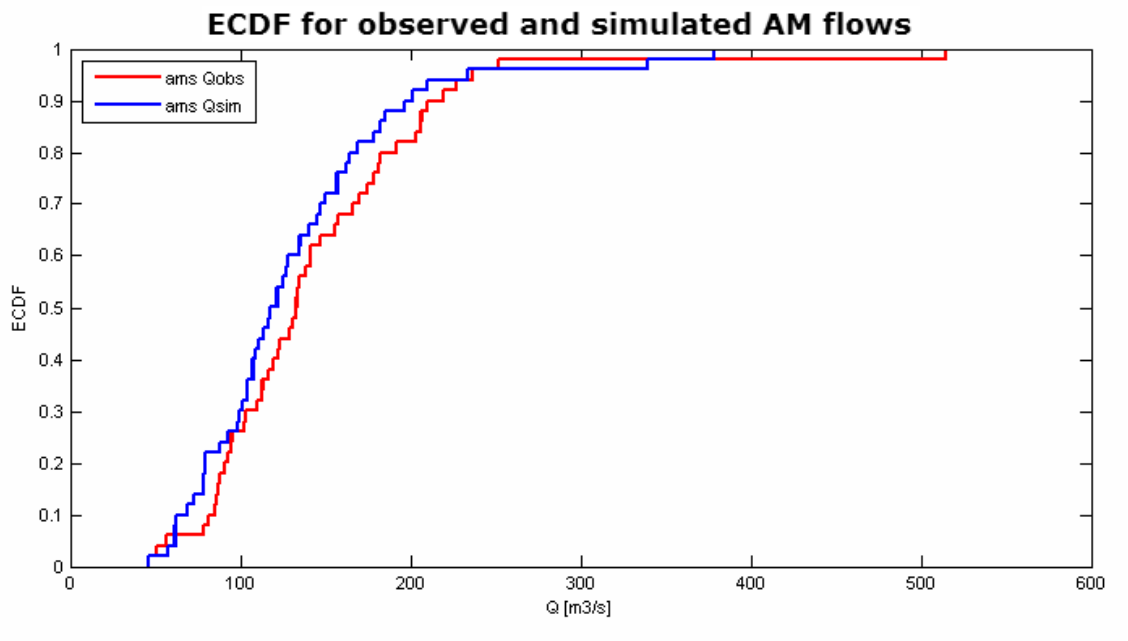

b)

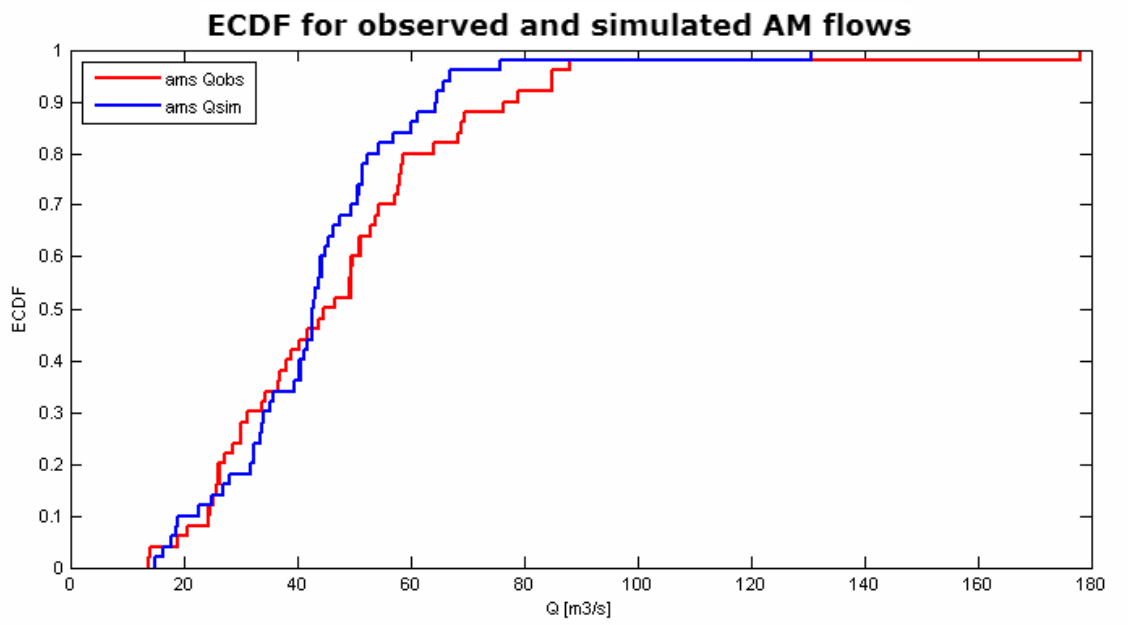

Figure 9. Comparison of the ECDF calculated for the observed and simulated AM flows for the Hron at BB (a) and the Hron at Brezno (b). Calculated by the switching version of the HRON model using the objective function (2) to calibrate parameters for the low flows and (3) for the high flows

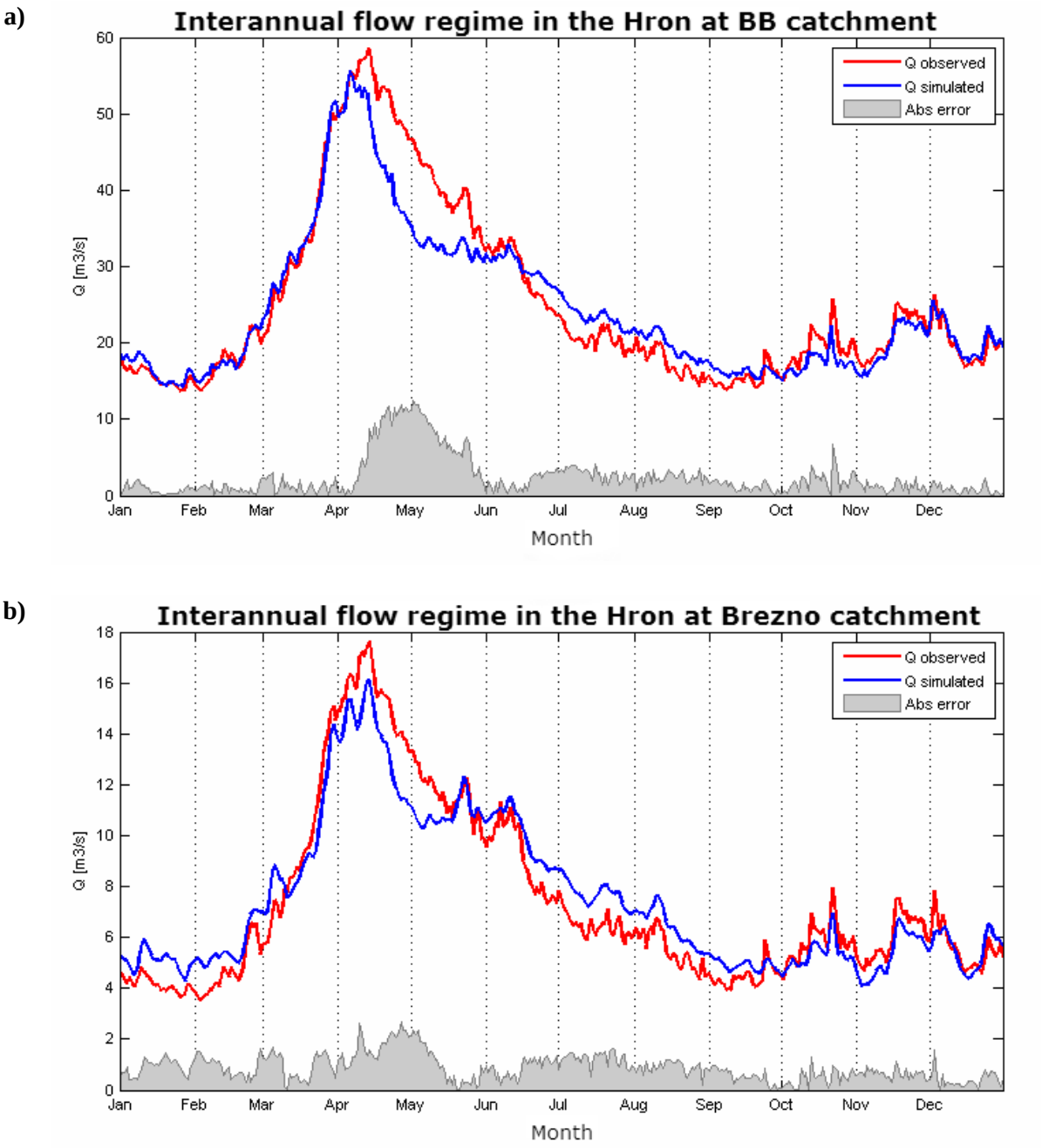

Figure 10. Comparison of the observed and simulated interannual flow regimes for the Hron catchments at BB (a) and at Brezno (b). Calculated by the switching version of the HRON model using the objective function (2) to calibrate parameters for the low flows and (3) for the high flows

5 SUMMARY AND CONCLUSIONS

The main objective of this paper was to improve the traditionally used calibration techniques of the RR models for use in FFA. Traditional approaches for the calibration of RR models are known for not being able to satisfactorily simulate extreme flows, which is caused by using optimization functions such as the Nash-Sutcliffe criterion or mean squared error. The correct

simulation of extreme flows is vital in FFA, since only the most extreme flows are used in the analysis (annual maximum series or peaks over threshold).

In the first case study of the paper a traditionally used method for calibrating an RR model was used. The method utilized a NS criterion as an objective function and, for both catchments, it proved to be good in maintaining the overall flow regime (*Figure 5*). The quality of the simulation of extreme flows was assessed by comparing the ECDFs calculated for both the observed and simulated AM flows (*Figure 6*). They proved that the simulation of extreme flows was unsatisfactory and that its use in the FFA is not recommended.

In the next part an alternative approach for calibrating RR models to extreme flows was proposed. The approach utilizes a new objective function, which compares only values higher than the 95^{th} percentile of the observed flows. The improvement of the simulation of the extreme flows was at the expense of the simulation of the low and medium flows. This makes this approach virtually unusable for tasks such as determining flood volumes or durations.

The second approach was comprised of separate simulations of the low and high flows. The low flows were simulated using the same set of parameters calibrated using the traditional approach, while the high flows were simulated using the parameters calibrated to the annual maximum floods (peak ± 2 days) and an objective function minimizing the NS criterion for both the time and rank-ordered flows. The thresholds determining whether a flow is low or high were estimated for each catchment and were set at 70.25 and 20.78 m^3/s for the Hron at BB and the Hron at Brezno, respectively. Using this approach the best simulation of the extreme flows was observed (*Figure 9*), while preserving a good simulation of the low and medium flows (*Figure 10*).

The results of this work show that further work in the calibration of RR models for the needs of FFA should focus not only on the development of new objective functions, but also on investigating the effects and possibilities of using RR models with multiple regimes.

Acknowledgements: This work was supported by the Agency for Research and Development under Contract Nos. APVV-0496-10 and VEGA Agency 1/0776/13. The authors thank the agencies for their research support.

REFERENCES

BERGSTROM, S. (1976): Development and application of a conceptual runoff model for Scandinavian catchments. SHMI RHO 7. Norrkoping. Sweden.

BOUGHTON, W. – DROOP, O. (2003): Continuous simulation for design flood estimation – a review. Environmental Modelling & Software 18 (4): 309–318.

GEEM, Z.W. (2009): Music-inspired harmony search algorithm: theory and applications. Springer. Berlin.

HOES, O. – NELEN, F. (2005): Continuous simulation or event-based modelling to estimate flood probabilities? WIT Transactions on Ecology and the Environment 80 (3–10).

CHEN, J. – BRISSETTE, F.P. – LECONTE, R. (2010): A daily stochastic weather generator for preserving low-frequency of climate variability. Journal of Hydrology 388 (3–4): 480–490.

LAMB, R. (1999): Calibration of a conceptual rainfall-runoff model for flood frequency estimation by continuous simulation. Water Resources Research 35 (10): 3103–3114.

NASH, J.E. – SUTCLIFFE, J.V. (1970): River flow forecasting through conceptual models, part 1 – a discussion of principles. Journal of Hydrology 10: 282–290.

PAQUET, E. – GARAVAGILA, F. – GARCON, R. – GAILHARD, J. (2013): The SCHADEX method: A semi-continuous rainfall–runoff simulation for extreme flood estimation. Journal of Hydrology 495: 23–37.

PATHIRAJA, S. – WESTRA, S. – SHARMA, A. (2012): Why continuous simulation? The role of antecedent moisture in design flood estimation. Water Resources Research 48 (6).

RACSKO, P. – SZEIDL, L. – SEMENOV, M. (1991): A serial approach to local stochastic weather models. Ecological Modelling 57 (1–2): 27–41.

TAN, K.S. – CHIEW, F.H.S. – GRAYSON, R.B. – SCANLON, P.J. – SIRIWARDENA, L. (2005): Calibration of a daily rainfall-runoff model to estimate high daily flows. Congress on Modelling and Simulation (MODSIM 2005). Melbourne. Australia. 2960–2966.

VALENT, P. – DANEKOVA, J. – RIVERSO, C. (2011): Neistoty pri kalibrácii zrážkovo-odtokového modelu HBV [Uncertainties in the HBV model calibration]. Acta Hydrologica Slovaca 12 (2), IH SAS, Bratislava, Slovakia (in Slovak).

VALENT, P. (2012a): Hydrologické simulačné modely pre frekvenčné analýzy [Hydrological simulation models for flood frequency analysis], Faculty of Civil Engineering. Slovak University of Technology in Bratislava (in Slovak).

VALENT, P. – SZOLGAY, J. – RIVERSO, C. (2012b): Assessment of the Uncertainties of a Conceptual Hydrologic Model by Using Artificially Generated Flows. Slovak Journal of Civil Engineering 20 (4): 1–10.

VINEY, N.R. – PERRAUD, J. – VAZE, J. – CHIEW, F.H.S. – POST, D.A. – YANG, A. (2009): The usefulness of bias constraints in model calibration for regionalisation to ungauged catchments. 18th World IMACS / MODSIM Congress. 13–17 July 2009. Cairns. Australia.

VYLETA, R. (2013): Simulácia denných úhrnov zrážok na povodí rieky Váh pomocou jednoduchého Markovovho modelu prvého rádu [Simulation of daily precipitation amounts on the River Vah catchment using a simple first order Markov]. Juniorstav 2013: 15. Odborná konference doktorského studia s mezinárodní účastí [Juniorstav 2013: 15th International Conference of Postgraduate Students]. 7.2.2013. Brno. VUT (in Slovak).

Guide for Authors

Acta Silvatica et Lignaria Hungarica publishes original reports and reviews in the field of forest, wood and environmental sciences. ASLH is published twice a year (Nr. 1 and 2) in serial volumes. It is online accessible under: http://aslh.nyme.hu

Submission of an article implies that the work has not been published previously (except in the form of an abstract or as part of a published lecture or academic thesis), that it is not under consideration for publication elsewhere. Articles should be written in English. All papers will be reviewed by two independent experts.

Authors of papers accepted for publication should sign the Publishing Agreement that can be downloaded from the homepage (http://aslh.nyme.hu).

All instructions for preparation of manuscripts can be downloaded from the homepage.

Contents and Abstracts of the Bulletin of Forest Science

Bulletin of Forest Science (Erdészettudományi Közlemények) is a new journal supported by the Hungarian Forest Research Institute and by the Faculty of Forestry of the University of West Hungary. The papers are in Hungarian, with English summaries. The recent issue (Vol. 4, Nr. 1 and Nr. 2, 2014) contains the following papers (with page numbers). The full papers can be found and downloaded in *pdf* format from the journal's webpage (www.erdtudkoz.hu).

Vol. 4, Nr. 1, 2014

Abstract – Results of nationwide analysis of Hungarian Forest Stand Database (date 01. 01. 2012) have been presented in this publication. We defined the potential natural forest communities of all forest compartments by the method of site evaluation. Comparison of potential natural forest communities and current forest stands makes it possible the analyses of relationship between the potential and current forest communities nationwide. This study makes an attempt to discover the background of current forest communities surveying the site conditions and former landscape use of forest compartments.

Abstract – This paper presents the four-year results of studies on 33, artificially created forest gaps of sessile oak-hornbeam forest in transform forest management subcompartments (Sopron Mts, Hungary). During the study the forest gaps have been divided into five segments: central circle and four sectors according to the point of compass; dominance of occurring plant species and number of specimens of natural regrowth has been recorded in five segments of gaps. During the study plentiful and species rich woody regrowth appeared in the studied forest gaps. Regrowth of Quercus petraea and Quercus cerris were the most prominent, although the renewal of Carpinus betulus, Tilia cordata and Cerasus avium were also considerable. The most specimens of woody regrowth occurred in the northern segment, followed by western, southern and eastern ones respectively; while the fewest specimens were experienced in the central circle. As our results demonstrated, the elongated elliptic and smaller, 250 m^2 > sized gaps proved to be the most optimal in regard to appearance and survival of woody regrowth in the studied forest subcompartment.

Abstract – The paper presents and discusses the relations of stand structure, richness of the herb layer and macrofungi occurrences in a submontane beech selection forest stand. Due to the selection system, the associate tree species are lacking in younger age classes, and the stand progressively develops to a pure beech forest. Ratio of coarse-limbed trees is significantly higher than in the case of a traditional rotation system. The understory vegetation is dominated by forest herbs, whereas role of non-forest weeds and invaders is neglilible. In case of increasing canopy cover the number and the cover of herbs tends to decrease; however, the reduction rate of forest herbs is significantly smaller. The microhabitat-rich stand structure and the remarkable deadwood proportion favour the occurrence of macrofungi.

Abstract – The aim of this study was the morphological analyses of generative organs of two native Fraxinus species. Fraxinus samples were taken mostly from populations of Rábaköz – Répce-sík and analysed with multivariate statistics separating the qualitative and quantitative morphological characteristics. Hierarchical clustering, Principal Component Analysis (PCA), Principal Coordinates Analysis (PCoA) and Non-metric Multidimensional Scaling (NMDS) have been applied to demonstrate the correspondences between morphological characteristics and specimens. Specimens of two different taxa could not be distinctive through quantitative characteristics; however they separated considerable during the analyses of qualitative characteristics. Our results draw attention to the significance of inflorescence structure as an important distinctive morphological characteristic, although specimens with atypical inflorescence have been analysed as well.

Abstract – The paper analyses the stand structure and yield of black locust (*Robinia pseudoacacia*) stands mixed with grey poplar (*Populus* × *canescens*) in various proportions, partly applying a new methodological approach. The main stand structure and yield factors were determined separately for each species, measured stem by stem, using the volume functions prepared for each species. The ratio of the volumes of the species (RVA and RVB) was determined based on the particular yield tables. A close relationship has been found between the ratio of relative volume and the proportion of the species calculated by number of stems. The relative surplus in the volume of the mixed stands varied between l.32–1.80 at age 16 and 21 years compared to the control, i.e. the yield of pure stands of the species concerned. The investigations have also proven that if two species have a fast initial growth rate and a similar rotation age, they can be planted in mixed stands resulting in mutual growing advantages.

Abstract – Among the tree forest blocks managed with transformation silviculture system by Zselic Forestry, we have made full forest inventory in the Töröcskei-Block on 21.5 respectively 43.75 ha. We have analyzed the stand structure of European Beech, Hornbeam, Silver Lime, Sessile Oak and Turkey Oak. In the course of comparison, we experienced that the variety of height and the volume of hornbeam is different but in the case of the others we admixed the tree species and only the volume was different. In the face of the results we have made a D-test (Welch's-test) of height and volume of hornbeam, respectively the result of the T-test of all the other tree species. Based on the results (p=0.05) the height and volume of the two sampling plots equaled.

Abstract – A gas exchange based ecophysiological performance of five regrowth species has been investigated in a xero-mesophilous oak forest. Seasonal light responses, capacities and variability of assimilation, transpiration and water use efficiency under light saturated conditions are discussed to reveal ecophysiological characteristics of the species in gap-phase dynamics. Species present assimilation maximum in autumn, followed by a continuously increasing carbon-dioxide fixation rate through the seasons. Transpiration peak is manifested differentially in summer and autumn. Autumn maximum of photosynthetic water use efficiency as the ratio of carbon input and water output is detected for all studied species. Limitation of gas exchange parameters is highly indicated by low level of water use efficiency in the summer season in case of Fraxinus ornus, Quercus cerris and Q. petraea. Carpinus betulus turned out to be a source saving species by a moderate gas exchange rate in every season. According to the moderate rate of carbon assimilation and transpiration but the highest rate of water use efficiency, Rubus fruticosus can be the most effective species in the early stage of gap-phase dynamics. Assimilation to transpiration rate in spring and summer is strongly coordinated, water use efficiency is a species and season dependent aspect. Autumn and summer season water use efficiency can serve an appropriate tool for indicating environmental limitation and scaling habitat suitability of the species in dry oak forests.

Abstract – We estimated the amount of carbon stored in the Hungarian harvested wood product pool, and the amount of annual inflow and outflow from the pool for the time period 1900–2020. We studied national and international data sources in order to find the best available and consistent data on production and trade. Because both the dataset and the methodology, i.e., the 2013 IPCC Supplementary Guidance that were used for this study differ from those in earlier studies, the results obtained are different as well. We now estimate that the carbon accumulation of the Hungarian HWP pool amounts to 9 million tonnes of carbon, and the average of annual net emissions from the pool is around ‑100,000 tonnes CO_2.

Abstract – The mini-rotation energy plantations are important on the one hand as a source of renewable energy, on the other hand, makes it useful the not suitable for agricultural use lands. We try to give an answer to the question, under what climate and soil conditions is the increase the most significant. Large number of variables, in the experiment was reduced to a minimum by means of multivariate statistics (principal component analysis and factor analysis). We found that the yields are affects primarily by temperature, by soil pH, by CaCO3 content and by Arany's value. As in the pilot areas significant difference in terms of rainfall was not, so the effect of this factor reduced the minimum.

Abstract – When constructing forest roads on cohesive soil, it is suitable to substitute sandy gravel sub-base course with lime stabilized subgrade. This solution reduces the volume of construction materials and at the same time moderates the unfavourable properties of cohesive soils. If the bearing capacity of the lime stabilized layer can be included in the bearing capacity of the pavement, then the costs of road construction can be reduced by reducing the thickness of the crushed stone course. To achieve this, the testing of the bearing capacity of the lime stabilized layer is necessary. It is suitable to complete the test on an experimental road-section practically in forest circumstances. Such an experimental road-section was constructed in cooperation between the Institute of Geomatics and Civil Engineering and the Zalaerdő Forestry Closed Company, within the frame of the Regional University Knowledge Centre of Forest and Wood Utilization. The results of this test clearly demonstrate that the local cohesive soil stabilized with suitable lime feeding can be the bearing layer of the pavement of forest roads.

Abstract – Most of the forest roads are used not only by forestry vehicles and staff, but by local inhabitants, tourists and others. Although heavy traffic is generated mostly by the vehicles connected to forestry operations. Different user groups have different needs against the geometry, the pavement type and the pavement condition of forest roads. To determine these needs, the traffic on the segments of a forest road network must be analysed. In this work, a traffic counting system and the obtained data are presented. The system consists of two retro-reflective photoelectric sensors, a safety camera and a control unit. A photo is taken whenever the light beam is interrupted. Combining the images with the data log of the sensors, the direction, the speed and the temporal distribution of the users of a particular forest road could be deduced. Based on this data, a proposal is made for the method of traffic analysis on whole road networks. As a result of this analysis the preferences of the forest road user groups could be determined. This information could be taken into account in the planning process of new forest road networks or the development of existing ones.

Abstract – In the last century the Wild T0 compass theodolite was the standard instrument of forest mapping and inventory. Nowadays this instrument is almost disappeared from the forestry surveying. Instead of theodolite we use GNSS instruments, which are easy to use even for not professionals. Data management is much faster with this instrument because of its compatibility with GIS software, but sometimes its accuracy is not so good as in the case of theodolite. In these days we can find digital surveying instruments, which can be operated by simple methods. The accuracy and efficiency of these instruments are suitable for today's engineers, and the processing of the data can be supported by geoinformatics. We examined the accuracy and effectiveness of the instrument, TruPulse 360B by test measurements. This instrument is a possible alternative of Wild T0, because we also can measure magnetic horizontal angle with it. We established a test field with surveying accuracy for the test measurements, where we can examine many kind of surveying methods. We found that the required accuracy can be achieved applying appropriate measuring mode and processing method. Therefore we can apply this instrument for engineer project.

Abstract – Coverage, richness and composition of bryophytes were compared between spruce and beech forest stands in the Sopron mountains. The highest coverage of bryophytes species in beech forests had *Hypnum cupressiforme*, which was followed by terricollous species like *Atrichum undulatum* and *Dicranella heteromalla*. The most dominant species in the spruce stands was *Brachythecium velutinum*; *Brachythecium rutabulum* and *Fissidens taxifolius* had slightly lower cover. The cover of bryophytes in beech stands was twice as high as in spruce stands. The total bryophyte coverage was very small in both forest types. The proportion of stands without bryophytes was the same in beech and spruce forest stands. Greater richness of bryophyte was found in beech stands than in spruce stands. The most frequent species were *Hypnum cupressiforme* and *Brachythecium velutinum* in both forest stands. The bryophyte flora was richer in native beech forests, than in spruce stands, which were planted on natural beech forests sites. However, the bryophyte composition of beech and spruce stands show considerable similarity. Generally, the older spruce plantations had unfavorable effect on the bryophyte diversity.

Abstract – In 2013, the ground beetle assemblageses of an artificial gap were studied in the field of Bálint-hegyi Erdőbirtokossági Társulat, in the subcompartment of Zánka 1B. We used 10 pitfall trapps filled with acetic acid solution. We collected altogether 4357 individuals of 20 carabid species. In our research, we examined the number of species and the number of individuals by dates and habitats. We trapped the highest number of species (16 species) on the 28th of June, while we trapped the highest number of specimens (1422 specimens) on the 31th of July. The number of species was the highest in the gap edge and in the mesic part of the forest (16 species each). The number of specimens was the highest in the gap edge (1308 specimens). We examined the dominance of the species and the distribution of the fauna elements. In all habitats *Carabus convexus* convexus had the highest dominance values. The

ground beetle fauna of the investigated locations (gap, gap edge, closed forest, mesic part of the forest) were compared with various ecological parameters (diversity, the level of consistency, similarity measures and hierarchical cluster analysis, based on Bray-Curtis).

Abstract – Macrolepidoptera communities and their diversity were compared in different age sessile oak-hornbeam forests, in the Sopron Mountains. The study was carried out in 2012-2013 from the end of March until early November each year, using portable light-traps. Our goal was to find any correlation between Lepidoptera diversity and the age of the forests. We used community and ecological characteristics to determine and compare Lepidoptera assemblages (Shannon and Simpson diversity indices, Pielou's evenness indices, Community dominance indices, Bray-Curtis similarity indices, Rényi's diversity ordering). Our result did not show a direct correlation between the Macrolepidoptera diversity and forests' age. However, our conclusions support the high influence the abundance of different vegetation layers on macromoth communities.

Abstract – During the hunting season 2012-13 we investigated occurrence of the Thorny-headed Worm Macracanthorhynchus hirudinaceus in 7 hunting areas. We dissected 618 wild boar (Sus scrofa) viscera. Worms were present in 4 areas, with a prevalence varying between 4.3-100%. M. hirudinaceus mostly occurred in areas characterised by sandy soils and a high density of cockchafers (Melolontha spp., Rhizotrogus spp.).

Contents and Abstracts of the Bulletin of Forest Science

Vol. 4, Nr. 2, 2014

Abstract – I show three relative brief episodes in relation to the history of Hungarian climate research. I investigate the peak of the climate controversy of the Great Hungarian Plain, i.e. the Kaán–Réthly debate, where not only two different personalities, but also two different imaginations of environmental or climate change faced with each other. Second, I show the effect of extreme weather on the media and public discourse through newspaper coverage, pointing out the similar attitude of the press compared to the present. Third, I recall the circumstances of the introduction of the global climate change theory in Hungary. I highlight that a representative of the old idea, i.e. stable climate with climatic fluctuations, raised the new theory first, but the new generation extended it with international impulses, partly with Soviet transmission in the background

Abstract – In this article we would like to give a picture of the characteristic features of sand-land forests concerning their water balance, and in relation to forest hydrology, that is we would like to outline how to apply those features in the course of nature conservation treatment. We based our survey both on special literature and on exchanges of practical experience with experts. More detailed investigation of the general hydrology of Duna-Tisza Sandrige started in the 1970s and expert opinions differ widely over the effects of crops on ground water level, that is, whether we can establish a connection between the growing afforestation in the area and the decrease in groundwater levels. This study confirms that we need to broaden our knowledge about this special field during forestry and nature protection management, and to explore the water management of sand-land sites, which are characterized by dry growing features, even more in the future. The local measurements and experiences must be determining in rational management and conservation treatment, because significant part of forests are in protected areas in Kiskunság.

Abstract – Today the Hungarian forest-steppe oak stands are grown mainly on unfavourable sandy sites. On these areas both the precipitation distribution and the water regime are unfavourable and the groundwater is in inaccessible depth for stands. In spite of that a lot of old high quality stem can be found in the investigated forest associations according to our experience the associations' regenerations sometimes encounter insolvable difficulties. In spite of that the rate of growth of the present stand relates to sufficient water quantity the growing of the planted seedlings and sowings is slow in the different forest regenerations. The state of health of the regrowth is bad, the stand becomes thinner and invasive weeds occupy on the area after a few years. We carried out root excavations to find out the reason of the different growth pattern between the regrowth and the original stand. On the area the investigated root systems of the three tree species – pedunculate oak (*Quercus robur*), white poplar (*Populus alba*) and common ash (*Fraxinus excelsior*) – show that the present old stand didn't evolve by means of dry sandy site but it developed due to the effect of the covered meadow soil.

Abstract – Considering the possible impacts of the climate change we investigated the time series of precipitation ranging from 1901 to 2013 at Nagykanizsa and Zalaegerszeg in Zala County. Firstly we aggregated seasonal sums from the monthly data according to the periods of the water cycle in the forest (storage: Nov-Apr, main consumption: May-July, maintenance: AugOct, hydrological year: Nov-Oct), then we studied the distributions and trends in time, and analysed the break points. We also carried out these analyses on the temperature data of Nagykanizsa (1972–2013). The results show great variety in the seasonal precipitation sums (CV is about 30%), while the CV of the seasonal mean of the temperature – except from the storage period – is smaller (5–7%). Depending on the station and the period, mostly a decreasing trend can be detected for precipitation and the seasonal means of the temperature are increasing significantly. Break points appear in the time series of the precipitation from 1941 till 2000, but they occur mostly in different years on the different stations, thus they are not valid for the whole region. In the time series of temperature there are break points in the recent past.

Abstract – Within the framework of AGRÁRKLÍMA project we prepared soil maps for both forest- and croplands of Zala County of Hungary. To achieve this we used a GIS database consisting of data on geology, relief, hydrology, (referred as environmental variables) and forestry, supported with data from the Digital Kreybig Soil Information System. The available set of site data from forestry and agricultural database was evaluated in relation to the environmental datasets. This process aimed at setting up signatures for all soil types by signature of the most strongly related environmental feature sets for each soil type. Using these signatures we trained hierarchical and non-hierarchical classification tools to identify the spatial extent of soils in Zala County. Neural networks were found to be the most effective

mapping tool. Making a validation with a data set of known soil characteristics we found 67% correct classification rate for the county. Additionally, we set up a joint soil type database for County Zala.

Abstract – Water balance of Zala County was analysed using remote-sensing based evapotranspiration maps for Hungary (Kovács 2011). Mean (1999–2008 period) annual evapotranspiration and runoff maps were evaluated in the context of land cover types (Corine Land Cover 2006). The mean annual evapotranspiration of Zala County (577 mm/year) was 88 percent of the mean annual precipitation (655.7 mm/year) in the examined period. The highest evapotranspiration values were determined for water bodies as well as forest and semi natural areas. For evaluating the effects of climate change on evapotranspiration we used the Budyko-type model (α-parameter), moreover a linear model with β-parameter was introduced for the extrawater affected pixels. Applying the two parameter maps and future data of climate models (mean annual temperature and precipitation) evapotranspiration and runoff predictions have been estimated by the end of the 21st century. According to the predictions, the mean annual evapotranspiration may increase by 5 percent while the runoff may decrease to the one third to the end of the century.

Abstract – One of the upcoming most severe issues in forestry in relation with climate change is set up a sound base for correct choice of applicable species. The current practice is unable to entirely solve this problem. Within the framework of AGRÁRKLÍMA project we investigated the site dependence of height growth for some species in County Zala. For the study we used data of different sources: forest management plans, long-term experimental plots of NARIC FRI for yield assessments, and site characteristics. We identified the factors from the dataset, which have main influence on height growth of the following species: beech, sessile oak, turkey oak, scots pine. Using multiple regressions we derived functions to assess height growth of above species. We found biologically high values of R-square between 0.65 and 0.87. Beside the age of the stands the most influencing factors were: forest aridity index, rootable depth, and soil texture. Using the regression equations and the new yield tables for the county we prepared maps showing the expected change in yield classes and growth-capacity according to the increase of aridity index due to climate change. This method makes us able to support yield based choice of tree species for future afforestations and regenerations.

Abstract – Out of the 1998 series of the international beech provenance trials, one experiment was established in Bucsuta, SW Hungary. The site is close to the low-elevation, xeric distributional limit of the species. The climatic conditions are the most extreme compared with other experiments. Bucsuta is therefore the most suitable site to model

responses of populations to sudden climatic changes, simulated by transfer. Plot averages of 15-year diameter, measured on the 5 largest trees per plot were analysed. Out of the climatic variables, the ones determined by summer temperatures (Tmax, TQW) and drought conditions (DMI, EQ) were significant. Not surprisingly, Ellenberg's drought index has shown the best correlation and was selected for the characterization of ecodistance. The climatic distance between the provenance origin and the test site, and the 15-year diameter data were used to establish a linear transfer function of high significance (p=0.0006). The regression (Fig. 3) indicates a monotonous decline which has no maximum value at "0" ecodistance, and may be used for the estimation of growth decline caused by changing climatic conditions.

Gábor VEPERDI:

Determination of site quality index based on the mean annual increment of the growing stock at or near the rotation age … 101–107

Abstract – Recent research activities have proven that in case of new local yield tables the mean annual increment of the total production cannot be used to determine site quality index as total production is not known in most cases. This paper suggests using the mean annual increment of the growing stock as a basis of determination of site quality index. On the other hand, this value is not comparable with site quality indices derived from existing global yield tables. The paper presents a new method of site classification where site quality index is derived from growing stock data in global yield tables. Both a graphical method and numeric values are presented.

Ernő FÜHRER, Imre CSIHA, Ildikó SZABADOS, Zoltán PÖDÖR and Anikó JAGODICS:

Aboveground and belowground dendromass in a stand of Turkey oak … 109–119

Abstract – In general view, the role of forests in carbon cycle is considered to be positive in reference to the impacts and mitigation of climate change. To verify this by results in Hungary, we have to assess the amount of carbon stored in forests in Hungary as a basis for comparison. Expecting warmer and drier climate as an effect of the climate change, we have to prefer the native tree species that are able to survive and maintain vitality under the new conditions. Therefore in a stand of Turkey oak we investigated the compartments of aboveground and belowground dendromass in terms of carbon equivalent. According to the results, 70% of the total dendromass was above and 30% of it was below the ground. Percentage of the compartments in descending order are as follows: stems: 55%, roots 24%, branches 13%, trunks 6% and foliage 2%. The ratio of aboveground (without foliage) and belowground carbon stock is 2.3. Taking our previous results of other forest stands into account, we could determine the correlation of Forestry Aridity Index (FAI) and this ratio. Hence the carbon amount in belowground dendromass can be estimated based on the stand volume and this climate-dependent ratio.

András BIDLÓ, Péter SZŰCS, Adrienn HORVÁTH, Éva KIRÁLY, Eszter NÉMETH and Zoltán SOMOGYI:

The effect of afforestations on the carbon stock of soil in Transdanubian Region (Hungary) … 121–133

Abstract – Forest ecosystems are the most important carbon sinks, and the forest soils play an important role in the global carbon cycle. We have little data on the carbon stock of soils and its change due to human activities, which have similar value to carbon content of biomass. In our investigation we measured the carbon stock of soil in six stands of *Quercus*

petrea and six stands of *Robinia pseudoacacia* after afforestations. We compared the carbon stock of forests with that of neighboring arable lands of the same soil conditions. We found larger quantity of carbon under the forest stands than in the arable lands (including the forest litter). However, differences were less clear in case of soil layers. In any event, the afforestations increase the carbon stock of soil (including the forest litter), and contribute to the mitigation of atmospheric carbon-dioxide

Abstract – We have analysed the genetic pattern of oak decline through the comparison of subpopulations composed viable and declined trees growing close to each other on various stands. The applied sampling method excluded most of the site effects influencing viability. For the genetic investigation 6 nuclear microsatellite loci (ZAG1/5, ZAG96, ZAG110, ZAG9, ZAG11, ZAG112) and 7 isoenzyme loci (IDH_B, PGI_B, AAP_A, AAT_B, ADH_A, SKDH_A, PGM_B) were applied. The genetic diversity of the analysed subpopulations were evaluated by different indices, such as number of alleles, effective number of alleles, Shannon diversity index, number of private allele, expected- and observed heterozygosity, fixation index. The different tendency of results regarding isoenzyme markers in case of pedunculate and sessile oaks was a conspicuous speciality of the study. Higher allele diversity was detected in the declined pedunculate oak subpopulation, while in case of the sessile oaks the viable subpopulation showed higher values. A very similar tendency could be revealed with the calculation of fixation index based on the heterozygosity values. In case of the microsatellite markers the outstanding allelic diversity of the viable pedunculate oak subpopulation was remarkable. Based on the genetic distance among the analysed subgroups the two oak species compose two distinct clusters, and also the viable and declined subpopulations separate within the two main clusters.

Abstract – The drought induced oak decline has been continuously observed for more than three decades in Hungary. We introduced a novel health assessment method based on the evaluation of the decline of stand density (compared to the density of the fully stocked stand) caused by drought-induced tree mortality. The health condition of the stand can only be assessed, if the decreased relative stand density due to the mortality is further reduced through concerning the health condition of the survived trees. Stands for the assessment were selected along a climatic gradient from the humid region in SW-Hungary to the continental-semiarid region in NE Hungary where no forest intervention was applied during the last decades. Results outline that the health status of the stands in SW Hungary is between 70–80% while near to its xeric limit around 50%.